

최종보고서

해양쓰레기 선별선 내항성능 평가를 위한  
운동실험 및 운동해석 연구

2021.10.

창원대학교 산학협력단  
(조선해양공학과)

제 출 문

부산대학교 산학협력단장 귀하

본 보고서를 부산대학교 산학협력단 용역과제 “해양쓰레기 선별선 내항성능 평가를 위한 운동실험 및 운동해석 연구”에 관한 최종보고서로 제출합니다.

2021년 10월

## Table of Contents

<b>1. Introduction .....</b>	<b>1</b>
1.1 Test model .....	1
1.2 Coordinate system .....	2
1.3 Objectives .....	2
<b>2. Numerical Simulation .....</b>	<b>4</b>
2.1 Theoretical background .....	4
2.1.1 3D panel method .....	4
2.1.2 Response Amplitude Operator (RAO) .....	5
2.1.3 Phase of Motion .....	6
2.1.4 Natural frequency .....	6
2.1.5 Roll damping estimation .....	7
2.2 Simulation .....	9
2.2.1 Simulation modelling .....	9
2.2.2 Correction of roll damping coefficient .....	10
2.2.3 Simulation results .....	12
<b>3. Seakeeping Test .....</b>	<b>21</b>
3.1 Overview .....	21
3.1.1 Test facility .....	21
3.1.2 Model ship .....	22
3.1.3 Test equipment .....	23
3.1.4 Test condition .....	25
3.2 Pre-test .....	27
3.2.1 Wave probe calibration .....	27
3.2.2 Wave maker calibration .....	28
3.2.3 Ballasting test .....	33
3.2.4 Inclining test .....	33
3.2.5 Free roll decay test .....	35
3.2.6 Inertia tests for $I_{xx}$ , $I_{yy}$ and $I_{zz}$ .....	36
3.2.7 Tension gauge calibration .....	40
3.2.8 Accelerometer .....	41
3.3 Experimental setup .....	42
3.3.1 Model ship .....	42
3.3.2 Measurement sensors .....	45
3.4 Data acquisition .....	46
3.5 Decay test .....	49
3.5.1 Spring selection .....	49

3.5.2 Free ship decay .....	49
3.5.3 Ship decay with soft mooring .....	50
3.6 Seakeeping performance in regular waves .....	56
3.6.1 Wave drift force .....	59
3.6.2 First-order wave force .....	64
3.6.3 Vertical acceleration .....	68
3.6.4 RAO and phase .....	70
3.6.5 Comparison of ship motion .....	83
3.6.6 Spring effect to ship motion .....	91
<b>4. Seakeeping of the Ship in Irregular Waves .....</b>	<b>96</b>
4.1 Wave spectrum .....	96
4.2 Root-Mean-Square (RMS) motion .....	99
4.2.1 Sinan .....	99
4.2.2 Tongyeong .....	111
4.3 Significant Single Amplitude (SSA) .....	122
4.3.1 Sinan .....	122
4.3.2 Tongyeong .....	133
<b>5. Conclusion .....</b>	<b>144</b>
<b>6. Reference .....</b>	<b>146</b>

## List of tables

Table 1.1 Principal dimensions of the barge .....	1
Table 2.1 Natural frequency .....	7
Table 2.2 Roll damping coefficient .....	12
Table 3.1 Specifications of 3D wave tanker .....	22
Table 3.2 Wave test condition .....	26
Table 3.3 Target wave height and input wave maker stroke .....	30
Table 3.4 Measured period of free roll decay test .....	36
Table 3.5 Inertia swing results .....	38
Table 3.6 Inertia table results .....	40
Table 3.7 Data acquired by the sensors .....	46
Table 3.8 Definition of accelerometer coordinate system .....	48
Table 3.9 Definition of OptiTrack coordinate system .....	48
Table 3.10 Decay results for two spring .....	49
Table 3.11 Period of free ship decay .....	50
Table 3.12 Period of ship decay for translational motion with soft mooring	55
Table 3.13 Period of ship decay for rotational motion with soft mooring	56
Table 4.1 Irregular wave conditions in Sinan .....	97
Table 4.2 Irregular wave conditions in Tongyeong .....	97
Table 4.3 RMS value for surge based on ITTC spectrum in Sinan (m) ....	103
Table 4.4 RMS value for surge based on TMA spectrum in Sinan (m) ....	103
Table 4.5 RMS value for sway based on ITTC spectrum in Sinan (m) ....	103
Table 4.6 RMS value for sway based on TMA spectrum in Sinan (m) ....	104
Table 4.7 RMS value for heave based on ITTC spectrum in Sinan (m) ....	106
Table 4.8 RMS value for heave based on TMA spectrum in Sinan (m) ....	106
Table 4.9 RMS value for roll based on ITTC spectrum in Sinan (°) .....	107
Table 4.10 RMS value for roll based on TMA spectrum in Sinan (°) .....	107
Table 4.11 RMS value for pitch based on ITTC spectrum in Sinan (°) ....	109
Table 4.12 RMS value for pitch based on TMA spectrum in Sinan (°) ....	110
Table 4.13 RMS value for yaw based on ITTC spectrum in Sinan (°) .....	110
Table 4.14 RMS value for yaw based on TMA spectrum in Sinan (°) .....	110
Table 4.15 RMS value for surge based on ITTC spectrum in Tongyeong (m) ..	114
Table 4.16 RMS value for surge based on TMA spectrum in Tongyeong (m) ..	114
Table 4.17 RMS value for sway based on ITTC spectrum in Tongyeong (m) ....	114
Table 4.18 RMS value for sway based on TMA spectrum in Tongyeong (m) ....	115
Table 4.19 RMS value for heave based on ITTC spectrum in Tongyeong (m) ..	117
Table 4.20 RMS value for heave based on TMA spectrum in Tongyeong (m) ..	117

Table 4.21 RMS value for roll based on ITTC spectrum in Tongyeong (°) .....	118
Table 4.22 RMS value for roll based on TMA spectrum in Tongyeong (°) .....	118
Table 4.23 RMS value for pitch based on ITTC spectrum in Tongyeong (°) .....	120
Table 4.24 RMS value for pitch based on TMA spectrum in Tongyeong (°) .....	121
Table 4.25 RMS value for yaw based on ITTC spectrum in Tongyeong (°) .....	121
Table 4.26 RMS value for yaw based on TMA spectrum in Tongyeong (°) .....	121
Table 4.27 SSA value for surge based on ITTC spectrum in Sinan (m) ....	125
Table 4.28 SSA value for surge based on TMA spectrum in Sinan (m) ....	125
Table 4.29 SSA value for sway based on ITTC spectrum in Sinan (m) ....	125
Table 4.30 SSA value for sway based on TMA spectrum in Sinan (m) ....	126
Table 4.31 SSA value for heave based on ITTC spectrum in Sinan (m) ...	128
Table 4.32 SSA value for heave based on TMA spectrum in Sinan (m) ...	128
Table 4.33 SSA value for roll based on ITTC spectrum in Sinan (°) .....	129
Table 4.34 SSA value for roll based on TMA spectrum in Sinan (°) .....	129
Table 4.35 SSA value for pitch based on ITTC spectrum in Sinan (°) .....	131
Table 4.36 SSA value for pitch based on TMA spectrum in Sinan (°) .....	132
Table 4.37 SSA value for yaw based on ITTC spectrum in Sinan (°) .....	132
Table 4.38 SSA value for yaw based on TMA spectrum in Sinan (°) .....	132
Table 4.39 SSA value for surge based on ITTC spectrum in Tongyeong (m) ....	136
Table 4.40 SSA value for surge based on TMA spectrum in Tongyeong (m) ....	136
Table 4.41 SSA value for sway based on ITTC spectrum in Tongyeong (m) ....	136
Table 4.42 SSA value for sway based on TMA spectrum in Tongyeong (m) ....	137
Table 4.43 SSA value for heave based on ITTC spectrum in Tongyeong (m) ...	139
Table 4.44 SSA value for heave based on TMA spectrum in Tongyeong (m) ....	139
Table 4.45 SSA value for roll based on ITTC spectrum in Tongyeong (°) .....	140
Table 4.46 SSA value for roll based on TMA spectrum in Tongyeong (°) .....	140
Table 4.47 SSA value for pitch based on ITTC spectrum in Tongyeong (°) .....	142
Table 4.48 SSA value for pitch based on TMA spectrum in Tongyeong (°) .....	143
Table 4.49 SSA value for yaw based on ITTC spectrum in Tongyeong (°) .....	143
Table 4.50 SSA value for yaw based on TMA spectrum in Tongyeong (°) .....	143

## List of Figures

Fig. 1.1 Test model .....	1
Fig. 1.2 Coordinate system for 6-DOF ship motion .....	2
Fig. 2.1 Definition of phase .....	6
Fig. 2.2 Mesh generation .....	10
Fig. 2.3 Roll decay test result compared with simulation data .....	10
Fig. 2.4 Estimation of roll damping coefficient .....	11
Fig. 2.5 Surge RAO (Simulation) .....	13
Fig. 2.6 Sway RAO (Simulation) .....	14
Fig. 2.7 Heave RAO (Simulation) .....	15
Fig. 2.8 Roll RAO (Simulation) .....	17
Fig. 2.9 Pitch RAO (Simulation) .....	18
Fig. 2.10 Yaw RAO (Simulation) .....	19
Fig 3.1 CWNU Model Basin .....	21
Fig 3.2. Wave maker and wave absorber .....	21
Fig 3.3 Hull model .....	22
Fig 3.4 Barge model .....	23
Fig 3.5 Wave probe .....	23
Fig 3.6 OptiTrack .....	23
Fig 3.7 IMU .....	24
Fig 3.8 Tension gauge .....	24
Fig 3.9 Accelerometer and connector .....	24
Fig. 3.10 A/D converter .....	25
Fig. 3.11 Definition of wave direction .....	26
Fig. 3.12 Carriage moving with respect to wave directions .....	27
Fig. 3.13 Wave probe calibration setup .....	27
Fig. 3.14 Results of wave probe calibration .....	28
Fig. 3.15 Results of wave maker calibration .....	28
Fig. 3.16 Time series of measured wave height .....	30
Fig. 3.17 Ballasting test .....	33
Fig. 3.18 Definition of an inclining test .....	34
Fig. 3.19 Results of inclining test .....	35
Fig. 3.20 Time series of free roll decay test .....	35
Fig. 3.21 Inertia swing test .....	36
Fig. 3.22 Time series of inertia swing w.r.t. x .....	37
Fig. 3.23 Time series of inertia swing w.r.t. y .....	38
Fig. 3.24 Inertia table test .....	38

Fig. 3.25 Calibration results .....	39
Fig. 3.26 Inertia test results .....	39
Fig. 3.27 Tension gauge calibration .....	40
Fig. 3.28 Tension gauge calibration results .....	41
Fig. 3.29 Accelerometer raw signal. ....	42
Fig. 3.30 Accelerometer installed on the model ship .....	42
Fig. 3.31 Model ship installation .....	43
Fig. 3.32 Model ship installation schematic plan .....	44
Fig. 3.33 Wave probe installation .....	45
Fig. 3.34 OptiTrack installation .....	45
Fig. 3.35 Camera installation .....	46
Fig. 3.36 Setup of data acquisition of measurement sensor .....	46
Fig. 3.37 Data acquisition SW .....	47
Fig. 3.38 Accelerometer coordinate system .....	47
Fig. 3.39 OptiTrack coordinate system .....	48
Fig. 3.40 Time series of free roll decay test .....	50
Fig. 3.41 Time series of free pitch decay test .....	50
Fig. 3.42 Time series of surge decay .....	51
Fig. 3.43 Time series of sway decay .....	52
Fig. 3.44 Time series of heave decay .....	53
Fig. 3.45 Time series of roll decay .....	53
Fig. 3.46 Time series of pitch decay .....	54
Fig. 3.47 Time series of yaw decay .....	55
Fig. 3.48 Time series of wave force measured by tension gauges .....	57
Fig. 3.49 Time series of vertical acceleration measured by accelerometers ..	58
Fig. 3.50 Time series of 6-DOF motion measured by OptiTrack .....	58
Fig. 3.51 Wave force analysis scheme .....	59
Fig. 3.52 Additional resistance by speed and incident wave direction .....	60
Fig. 3.53 Lateral wave-induced force by speed and incident wave direction ..	61
Fig. 3.54 Yaw waves-induced moment by speed and incident wave direction ..	63
Fig. 3.55 First-order surge force by speed and incident wave direction .....	64
Fig. 3.56 First-order sway force by speed and incident wave direction .....	65
Fig. 3.57 First-order yaw moment by speed and incident wave direction ..	67
Fig. 3.58 Vertical acceleration .....	69
Fig. 3.59 Definition of phase parameter .....	71
Fig. 3.60 Surge RAO (Experiment) .....	75
Fig. 3.61 Sway RAO (Experiment) .....	76

Fig. 3.62 Heave RAO (Experiment) .....	77
Fig. 3.63 Roll RAO (Experiment) .....	79
Fig. 3.64 Pitch RAO (Experiment) .....	80
Fig. 3.65 Yaw RAO (Experiment) .....	81
Fig. 3.66 Comparison of surge RAO .....	83
Fig. 3.67 Comparison of sway RAO .....	85
Fig. 3.68 Comparison of heave RAO .....	86
Fig. 3.69 Comparison of roll RAO .....	87
Fig. 3.70 Comparison of pitch RAO .....	89
Fig. 3.71 Comparison of yaw RAO .....	90
Fig. 3.72 Spring effect of zero speed at wave direction 180° .....	92
Fig. 3.73 Spring effect of zero speed at wave direction 150° .....	93
Fig. 3.74 Spring effect of zero speed at wave direction 120° .....	94
Fig. 3.75 Spring effect of zero speed at wave direction 90° .....	95
Fig. 4.1 Comparison of ITTC and TMA spectrum in various sea states .....	98
Fig. 4.2 RMS surge in case of sea state 2 in Sinan (m) .....	101
Fig. 4.3 RMS surge in case of sea state 3 in Sinan (m) .....	101
Fig. 4.4 RMS surge in case of sea state 4 in Sinan (m) .....	101
Fig. 4.5 RMS sway in case of sea state 2 in Sinan (m) .....	102
Fig. 4.6 RMS sway in case of sea state 3 in Sinan (m) .....	102
Fig. 4.7 RMS sway in case of sea state 4 in Sinan (m) .....	102
Fig. 4.8 RMS heave in case of sea state 2 in Sinan (m) .....	104
Fig. 4.9 RMS heave in case of sea state 3 in Sinan (m) .....	104
Fig. 4.10 RMS heave in case of sea state 4 in Sinan (m) .....	105
Fig. 4.11 RMS roll in case of sea state 2 in Sinan (°) .....	105
Fig. 4.12 RMS roll in case of sea state 3 in Sinan (°) .....	105
Fig. 4.13 RMS roll in case of sea state 4 in Sinan (°) .....	106
Fig. 4.14 RMS pitch in case of sea state 2 in Sinan (°) .....	107
Fig. 4.15 RMS pitch in case of sea state 3 in Sinan (°) .....	108
Fig. 4.16 RMS pitch in case of sea state 4 in Sinan (°) .....	108
Fig. 4.17 RMS yaw in case of sea state 2 in Sinan (°) .....	108
Fig. 4.18 RMS yaw in case of sea state 3 in Sinan (°) .....	109
Fig. 4.19 RMS yaw in case of sea state 4 in Sinan (°) .....	109
Fig. 4.20 RMS surge in case of sea state 2 in Tongyeong (m) .....	112
Fig. 4.21 RMS surge in case of sea state 3 in Tongyeong (m) .....	112
Fig. 4.22 RMS surge in case of sea state 4 in Tongyeong (m) .....	112
Fig. 4.23 RMS sway in case of sea state 2 in Tongyeong (m) .....	113

Fig. 4.24 RMS sway in case of sea state 3 in Tongyeong (m) .....	113
Fig. 4.25 RMS sway in case of sea state 4 in Tongyeong (m) .....	113
Fig. 4.26 RMS heave in case of sea state 2 in Tongyeong (m) .....	115
Fig. 4.27 RMS heave in case of sea state 3 in Tongyeong (m) .....	115
Fig. 4.28 RMS heave in case of sea state 4 in Tongyeong (m) .....	116
Fig. 4.29 RMS roll in case of sea state 2 in Tongyeong (°) .....	116
Fig. 4.30 RMS roll in case of sea state 3 in Tongyeong (°) .....	116
Fig. 4.31 RMS roll in case of sea state 4 in Tongyeong (°) .....	117
Fig. 4.32 RMS pitch in case of sea state 2 in Tongyeong (°) .....	118
Fig. 4.33 RMS pitch in case of sea state 3 in Tongyeong (°) .....	119
Fig. 4.34 RMS pitch in case of sea state 4 in Tongyeong (°) .....	119
Fig. 4.35 RMS yaw in case of sea state 2 in Tongyeong (°) .....	119
Fig. 4.36 RMS yaw in case of sea state 3 in Tongyeong (°) .....	120
Fig. 4.37 RMS yaw in case of sea state 4 in Tongyeong (°) .....	120
Fig. 4.38 SSA surge in case of sea state 2 in Sinan (m) .....	123
Fig. 4.39 SSA surge in case of sea state 3 in Sinan (m) .....	123
Fig. 4.40 SSA surge in case of sea state 4 in Sinan (m) .....	123
Fig. 4.41 SSA sway in case of sea state 2 in Sinan (m) .....	124
Fig. 4.42 SSA sway in case of sea state 3 in Sinan (m) .....	124
Fig. 4.43 SSA sway in case of sea state 4 in Sinan (m) .....	124
Fig. 4.44 SSA heave in case of sea state 2 in Sinan (m) .....	126
Fig. 4.45 SSA heave in case of sea state 3 in Sinan (m) .....	126
Fig. 4.46 SSA heave in case of sea state 4 in Sinan (m) .....	127
Fig. 4.47 SSA roll in case of sea state 2 in Sinan (°) .....	127
Fig. 4.48 SSA roll in case of sea state 3 in Sinan (°) .....	127
Fig. 4.49 SSA roll in case of sea state 4 in Sinan (°) .....	127
Fig. 4.50 SSA pitch in case of sea state 2 in Sinan (°) .....	129
Fig. 4.51 SSA pitch in case of sea state 3 in Sinan (°) .....	130
Fig. 4.52 SSA pitch in case of sea state 4 in Sinan (°) .....	130
Fig. 4.53 SSA yaw in case of sea state 2 in Sinan (°) .....	130
Fig. 4.54 SSA yaw in case of sea state 3 in Sinan (°) .....	131
Fig. 4.55 SSA yaw in case of sea state 4 in Sinan (°) .....	131
Fig. 4.56 SSA surge in case of sea state 2 in Tongyeong (m) .....	134
Fig. 4.57 SSA surge in case of sea state 3 in Tongyeong (m) .....	134
Fig. 4.58 SSA surge in case of sea state 4 in Tongyeong (m) .....	134
Fig. 4.59 SSA sway in case of sea state 2 in Tongyeong (m) .....	135
Fig. 4.60 SSA sway in case of sea state 3 in Tongyeong (m) .....	135

Fig. 4.61 SSA sway in case of sea state 4 in Tongyeong (m) .....	135
Fig. 4.62 SSA heave in case of sea state 2 in Tongyeong (m) .....	137
Fig. 4.63 SSA heave in case of sea state 3 in Tongyeong (m) .....	137
Fig. 4.64 SSA heave in case of sea state 4 in Tongyeong (m) .....	138
Fig. 4.65 SSA roll in case of sea state 2 in Tongyeong ( $^{\circ}$ ) .....	138
Fig. 4.66 SSA roll in case of sea state 3 in Tongyeong ( $^{\circ}$ ) .....	138
Fig. 4.67 SSA roll in case of sea state 4 in Tongyeong ( $^{\circ}$ ) .....	139
Fig. 4.68 SSA pitch in case of sea state 2 in Tongyeong ( $^{\circ}$ ) .....	140
Fig. 4.69 SSA pitch in case of sea state 3 in Tongyeong ( $^{\circ}$ ) .....	141
Fig. 4.70 SSA pitch in case of sea state 4 in Tongyeong ( $^{\circ}$ ) .....	141
Fig. 4.71 SSA yaw in case of sea state 2 in Tongyeong ( $^{\circ}$ ) .....	141
Fig. 4.72 SSA yaw in case of sea state 3 in Tongyeong ( $^{\circ}$ ) .....	142
Fig. 4.73 SSA yaw in case of sea state 4 in Tongyeong ( $^{\circ}$ ) .....	142

# 1. Introduction

## 1.1 Test model

The test model is a garbage barge and it has a wide and flat bottom. Hull shape is symmetrical and two stern tabs are installed as shown in Fig. 1.1. Principal dimensions of the barge at full and model scale are described in Table 1.1. The scale ratio and the test condition were decided in consideration of the size of the water tank at Changwon National University.

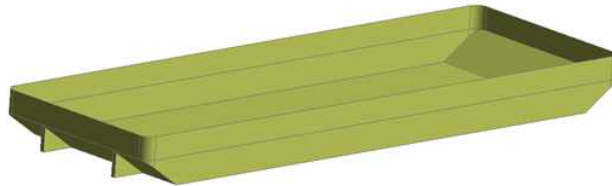


Fig. 1.1 Test model

Table 1.1. Principal dimensions of the barge

Principal dimension	Full-scale	Model-scale
Scale ratio	1	1/49
Length between perpendicular, Lpp (m)	39.2	0.8
Breadth, B (m)	13.0	0.265
Depth, D (m)	3.3	0.0673
Draft, T (m)	1.523	0.0311
Displacement weight, W (kgf)	735,000	6.249
LCG from AP (m)	19.6	0.4
VCG from BL (m)	2.713	0.0554
GMt (m)	7.794	0.1589
$C_b$ (-)		0.942
$k_{xx}/B$ (-)		0.348
$k_{yy}/L_{pp}$ (-)		0.25
$k_{zz}/L_{pp}$ (-)		0.25
Speed, U (m/s)	0, 1.030, 3.086	0, 0.147, 0.441
Speed, U (knots)	0, 2, 6	
Wave direction, $\mu$ (deg.)	180, 150, 120, 90, 60, 30, 0	

## 1.2 Coordinate system

Fig. 1.2 shows the employed coordinate system where the translational displacements in the x, y and z directions are surge, sway and heave, and the angular displacements of rotational motion about the x, y and z axes are roll, pitch and yaw, respectively. The O-xyz is a body-fixed coordinate system with a origin O located at the center of gravity. X-axis is parallel to centerline of the ship pointing to the bow, Z-axis is vertical to the waterline and Y-axis points to the port side of the ship.

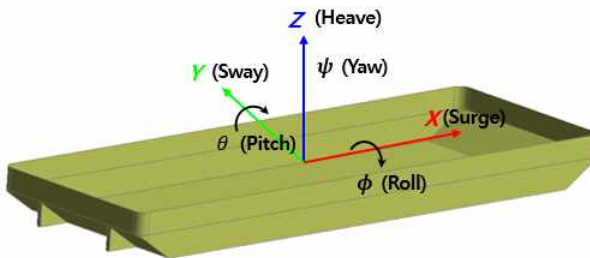


Fig. 1.2 Coordinate system for 6-DOF ship motion

## 1.3 Objectives

In order to evaluate the seakeeping performance for garbage barge in regular and irregular waves, numerical simulation at full-scale using Ansys AQWA and model tests in 3D wave tank were carried out. Details of this study are described as follows.

- Chapter 2 presents results from the numerical simulation of estimating the motion RAO and phase at various wave directions and speed conditions at full-scale using the 3D panel method in Ansys AQWA. Estimation methods for roll damping coefficient using roll decay test results are also discussed. Experimental data are used in Ansys AQWA to correct the roll amplitude in natural frequency.
- Chapter 3 describes the model test results at the 3D wave tank in regular waves. Ship motions and force were measured using tension gauge, accelerometer and OptiTrack. Test results are compared with the data from the numerical simulation. In addition, the effect of spring stiffness on experiments were examined.

- Chapter 4 shows the seakeeping analysis results in irregular waves. The sea state 2, 3, and 4 were applied to calculate Root Mean Square value and Significant Single Amplitude (SSA) at various wave directions and speed conditions. In addition, the results of applying the ITTC and TMA spectrum at Sinan and Tongyeong were compared and evaluated.

## 2. Numerical Simulation

### 2.1 Theoretical background

#### 2.1.1 3D panel method

Assuming incompressible, inviscid and irrotational flow, the governing equation and boundary conditions of the flow field can be expressed using the velocity potential  $\phi$ , as follows.

- Governing equation:  $\nabla^2\phi = 0$  for  $x \in R$  (2.1)

- Free surface boundary condition:  $-\omega^2\phi + g \frac{\partial\phi}{\partial z} = 0$  on  $z = 0$  (2.2)

- Bottom boundary condition:  $\frac{\partial\phi}{\partial z} = 0$  on  $z = -h$  (2.3)

- Body boundary condition:  $\frac{\partial\phi}{\partial h} = U_n$  on  $S$  (2.4)

Velocity potential can be subdivided into incident potential  $\phi_I$ , diffraction potential  $\phi_D$  and radiation potential  $\phi_j$  by Eq. (2.5).

$$\phi = \phi_I + \phi_D + \phi_j = Re\left\{ [\phi_I(x, y, z) + \phi_D(x, y, z) + \phi_R(x, y, z)e^{-i\omega t}] \right\} \quad (2.5)$$

Boundary conditions for diffraction and radiation velocity are given by Eqs. (2.6) and (2.7). The potential for undisturbed incident wave field at a point  $(x, y, z)$  in fluid domain and incident wave potential is estimated in Eq. (2.8)

$$\frac{\partial\phi_D}{\partial n} = -\frac{\partial\phi_I}{\partial n} \text{ on } S \quad (2.6)$$

$$\frac{\partial\phi_j}{\partial n} = -i\omega n_j \text{ on } S \quad (2.7)$$

$$\phi_I = -\frac{\omega}{k} \frac{\cosh(z+h)}{\sinh kh} e^{ik(x\cos\mu + y\sin\mu)} \quad (2.8)$$

where  $n_j$  is the generalized normal vector and  $\mu$  is wave direction. Radiation for diffraction velocity potential located inside the fluid domain can be expressed in Eq. (2.9)

$$\phi(x, y, z) = \frac{1}{4\pi} \iint_S \sigma(P) G(x, y, z, P) dS \quad (2.9)$$

Here,  $P$  is located in the source on surface  $S$  and  $G(x,y,z,P)$  is the Green function which describes the flow at  $(x,y,z)$ . The Green function satisfies Laplace equation and the boundary condition everywhere except body surface, and the boundary condition on surface as

$$\frac{\phi(x,y,z)}{\partial n} = v_n \text{ on } S \quad (2.10)$$

The source strength on the body surface is set by Eq. (2.11)

$$G(x,y,z,P) = \frac{1}{r_{PQ}} \quad (2.11)$$

where  $r_{PQ}$  is the distance between source point  $P$  and field point  $Q$ . By application of panel method introduced by Hess and Smith (1968), the solution of three dimensional velocity potential for ship motion with specified motion can be obtained.

$$2\pi\sigma(P) + \iint_S \sigma(P) \frac{\partial}{\partial n} \frac{1}{r_{PQ}} dS = \iint_S \frac{1}{r_{PQ}} \frac{\partial\sigma(P)}{\partial n} dS \quad (2.12)$$

### 2.1.2 Response Amplitude Operator (RAO)

Three translations and three rotations of the ship's center of gravity in the direction of the  $x$ ,  $y$  and  $z$  axes are defined as follows.

$$\text{Surge: } x = x_a \cos(\omega_e t + \varepsilon_x \zeta) \quad (2.13)$$

$$\text{Sway: } y = y_a \cos(\omega_e t + \varepsilon_y \zeta) \quad (2.14)$$

$$\text{Heave: } z = z_a \cos(\omega_e t + \varepsilon_z \zeta) \quad (2.15)$$

$$\text{Roll: } \phi = \phi_a \cos(\omega_e t + \varepsilon_\phi \zeta) \quad (2.16)$$

$$\text{Pitch: } \theta = \theta_a \cos(\omega_e t + \varepsilon_\theta \zeta) \quad (2.17)$$

$$\text{Yaw: } \psi = \psi_a \cos(\omega_e t + \varepsilon_\psi \zeta) \quad (2.18)$$

where  $\varepsilon$  is the phase difference between motion and incident wave. The non-dimensional translation and rotation responses can be determined as

$$\text{For translations: } RAO = \frac{x, y, z}{\zeta_a} \quad (2.19)$$

$$\text{For rotations: } RAO = \frac{\phi, \theta, \psi}{k\zeta_a} \quad (2.20)$$

Here,  $\zeta_a$  is the wave amplitude and  $k$  is the wave number.

### 2.1.3 Phase of Motion

The phase angle of parameters such as the surge RAO or wave exciting force is defined according to the difference from the time when the regular wave crest is at the center of gravity of a structure to the time when this parameter reaches its peak value. The time histories of an incident wave elevation and the corresponding force or response parameter are represented as follows.

$$\zeta = \zeta_a \cos(-\omega t + \varepsilon) \quad (2.21)$$

$$p = a_p \cos(-\omega t + \varepsilon + \xi) \quad (2.22)$$

where  $\zeta_a$ ,  $\varepsilon$ ,  $a_p$  and  $\xi$  are regular wave amplitude, wave phase angle relative to the origin of the fixed reference axes, the amplitude of the motion and the phase angle of the motion, respectively.

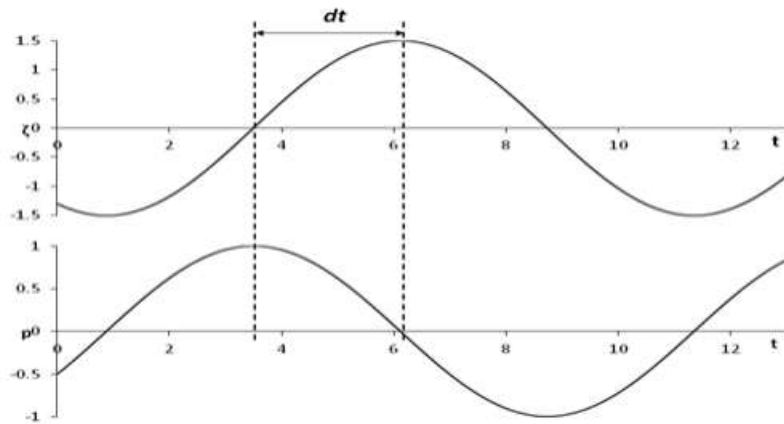


Fig. 2.1 Definition of phase

### 2.1.4 Natural frequency

Three motion modes have restoring force, so natural frequencies, too.

$$\text{Heave: } \omega_n = \sqrt{\frac{\rho g A_w}{m + m_a}} \quad (2.23)$$

$$\text{Roll: } \omega_\phi = \sqrt{\frac{mg GM_T}{I_{xx} + J_{xx}}} \quad (2.24)$$

$$\text{Pitch: } \omega_\theta = \sqrt{\frac{mg GM_L}{I_{yy} + J_{yy}}} \quad (2.25)$$

where  $\rho$ ,  $g$  and  $m$  are the water density, gravitational acceleration and mass of ship, respectively.  $m_a$  is the added mass,  $A_w$  is denotes the water plane area,  $GM_T$  and  $GM_L$  are the transverse and longitudinal metacentric heights,  $I_{xx}$  and  $I_{yy}$  are the mass moment of inertias with respect to x-axis and y-axis,  $J_{xx}$  and  $J_{yy}$  are the added mass moment of inertia of roll and pitch. Based on given parameters of the ship, the natural frequency of heave, roll, and pitch can be calculated as shown in Table 2.1 for the garbage barge at full scale and model scale.

Table 2.1. Natural frequency

Motion	Unit	Full-scale	Model-scale
Heave	rad/s	1.823	12.762
Roll		1.503	10.521
Pitch		2.037	14.259

### 2.1.5 Roll damping estimation

The ship motion in waves can be calculated using a potential code like Ansys AQWA. However, roll damping is significantly affected by viscous effects. Therefore, a result calculated using potential theory can overestimate the roll amplitude in natural frequency. It is necessary for the calculation of roll damping to use estimation methods in order to consider the viscosity effects. The roll damping coefficients can be estimated using roll decay test results. The estimation procedure is described here. First of all, the roll decay motion of a ship in calm water can be expressed as 1-DOF(Degree Of Freedom) equation given by

$$(I_{44} + a_{44})\ddot{\phi}(t) + b_{44}(\phi)(\dot{\phi}(t)) + c_{44}\phi(t) = 0 \quad (2.26)$$

where  $\phi(t)$  represents the instantaneous roll motion,  $I_{44}$  is the mass moment of inertia,  $a_{44}$  and  $c_{44}$  denote added mass moment of inertia and hydrostatic restoring coefficients, respectively.  $b_{44}(\phi)$  is the damping coefficient, which can be considered dependent on roll amplitude. Eq. (2.26) can be rewritten as

$$\ddot{\phi} + p(\phi)\dot{\phi} + \omega_n^2\phi = 0 \quad (2.27)$$

Here,

$$\omega_n^2 = \frac{mgGM_T}{I_{44} + a_{44}} \quad (2.28)$$

$$p(\phi) = \frac{b_{44}(\phi)}{I_{44} + a_{44}} \quad (2.29)$$

The damping moment can be expressed in terms of linear and quadratic contributions.

$$p(\phi)\dot{\phi} = p_1\dot{\phi} + p_2\dot{\phi}|\dot{\phi}| \quad (2.30)$$

Assuming harmonic roll motion and equivalent dissipated energy for both damping representations, an additional relationship between the coefficients  $p$ ,  $p_1$ , and  $p_2$  can be established.

$$p(\phi_a) = p_1 + p_2 \frac{16}{3T_k} \phi_a \quad (2.31)$$

where the roll amplitude is  $\phi_a = (\phi_k + \phi_{k+1})/2$ ,  $\phi_k$  and  $\phi_{k+1}$  denote two successive peaks in the roll decay motion and  $T_k$  is the roll period. The roll damping coefficients  $p$ ,  $p_1$ , and  $p_2$  are obtained from the roll decay time records. In this study, Froude energy method was used to analyze the roll decay time records. This approach is based on the energy loss balance in each half cycle. The energy dissipated by the damping term is equal to the variation of the potential energy (work done by the restoring moment) when the kinetic energy at the initial and final positions are zero. Assuming the linear plus quadratic damping form and linear restoring moment in the roll decay equation, the energy balance gives

$$\int_{\phi_k}^{\phi_{k+1}} [\ddot{\phi} + p_1\dot{\phi} + p_2\dot{\phi}|\dot{\phi}|] d\phi = \int_{\phi_k}^{\phi_{k+1}} \omega_n^2 \phi d\phi \quad (2.32)$$

with  $d\phi = \dot{\phi}dt$

$$\int_0^{T_{k/2}} [\ddot{\phi} + p_1\dot{\phi} + p_2\dot{\phi}|\dot{\phi}|] \dot{\phi} dt = \int_{\phi_k}^{\phi_{k+1}} \omega_n^2 \phi d\phi \quad (2.33)$$

The integration of each term gives

$$\int_0^{T_k/2} \ddot{\phi}(t) \dot{\phi}(t) dt = 0, \quad (2.34)$$

$$\int_0^{T_k/2} p_1 \dot{\phi}(t) \dot{\phi}(t) dt = p_1 \frac{\pi^2}{T_k} \phi_a^2,$$

$$\int_0^{T_k/2} p_2 \dot{\phi}(t) |\dot{\phi}(t)| \dot{\phi}(t) dt = p_2 \frac{16\pi^2}{3T_k^2} \phi_a^3$$

where  $\phi_a = \frac{(\phi_k + \phi_{k+1})}{2}$  and  $\omega_n = \frac{2\pi}{T_k}$

$$p_1 \frac{\pi^2}{T_k} \phi_a^2 + p_2 \frac{16\pi^2}{3T_k^2} \phi_a^3 = \omega_n^2 (\phi_{k+1} - \phi_k) \phi_a \quad (2.35)$$

Denoting  $\delta\phi = (\phi_k - \phi_{k+1})$

$$\delta_\phi = p_1 \frac{T_k}{4} \phi_a + p_2 \frac{4}{3} \phi_a^2 \quad (2.36)$$

Eq. (2.36) represents a quadratic function for  $\delta\phi$  against  $\phi_a$ , where  $p_1$  and  $p_2$  can be obtained by a regression procedure. In this approach,  $k$  refers to a positive peak while the successive  $k+1$  peak refers to a negative one. The non-dimensionalized roll damping coefficient is expressed as

$$\hat{B}_{44} = \frac{B_{44}}{\rho \nabla B^2} \sqrt{\frac{B}{2g}} \quad (2.37)$$

Based on Eq. (2.37), the roll damping coefficients can be estimated.

## 2.2 Simulation

### 2.2.1 Simulation modelling

The numerical simulation was carried out for full-scale ship. The regular waves were generated throughout the simulation for a range of frequency from 0.2~3.0 rad/s with interval 0.05 rad/s. The given speed conditions for the full scale ship are 0, 1.030, and 3.086 m/s (0, 2, and 6 knots).

Numerical simulations were carried out in a range of wave direction from 0~180 degrees with interval 30 degrees. Fig. 2.2 shows the mesh generation for the simulation.

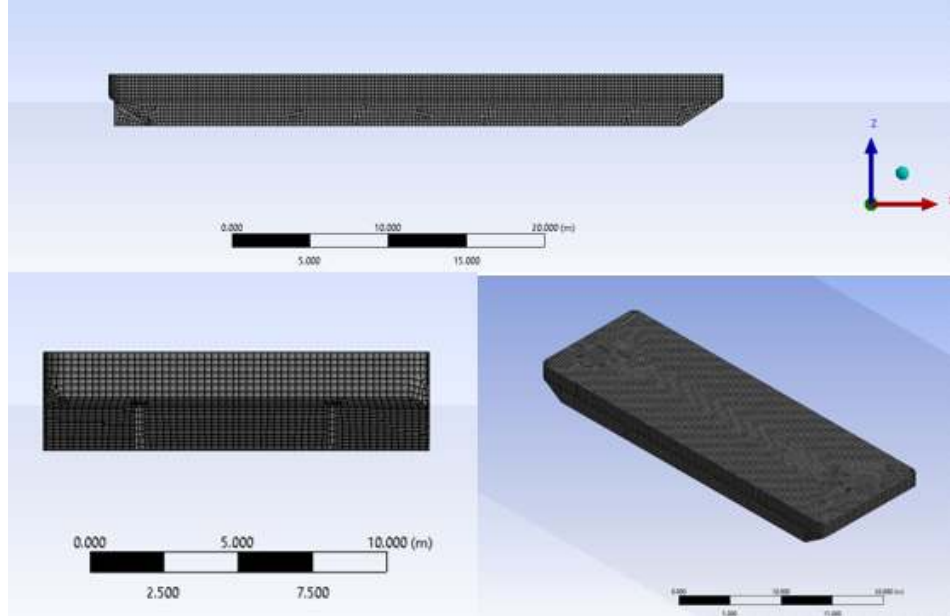
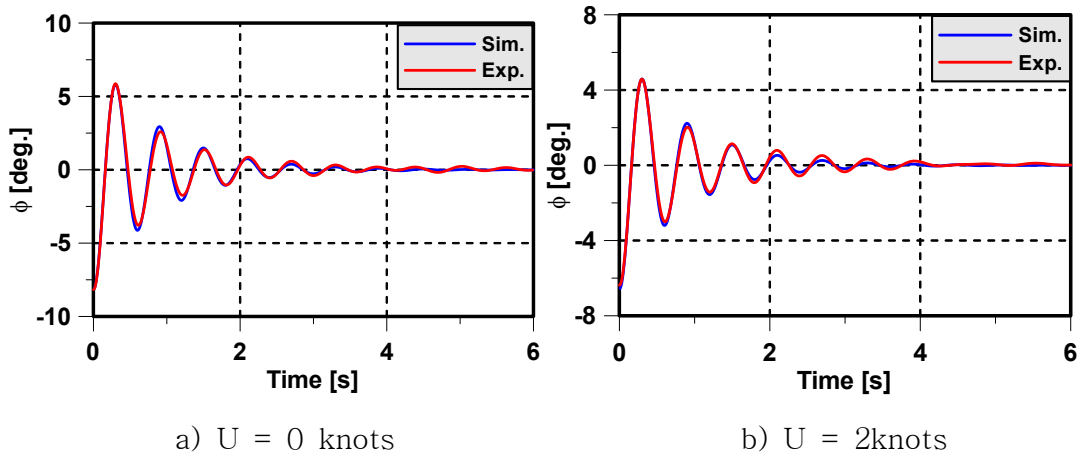
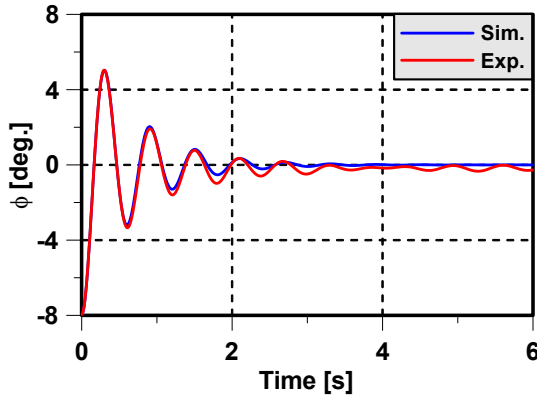


Fig. 2.2 Mesh generation

### 2.2.2 Correction of roll damping coefficient

The roll damping coefficients were estimated from the roll decay test results of the model ship in the water tank. Roll decay test was conducted at three speed conditions (0, 2, and 6 knots at full scale). Fig. 2.3 shows the experimental results of roll decay test for model ship at 0, 2, and 6 knots. Comparing with the experimental data at given initial condition, numerical results are well matched with the experimental results.

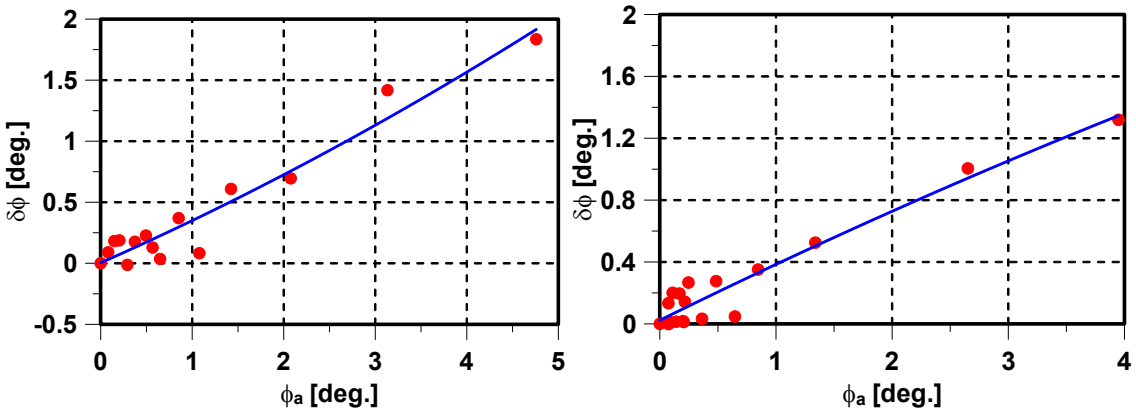




c)  $U = 6$  knots

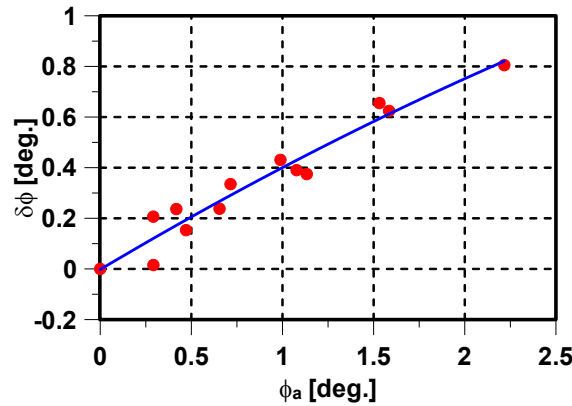
Fig. 2.3 Roll decay test result compared with simulation data

By analyzing roll decay test results using Froude energy method, the linear coefficients of the parabolic regression function provides  $p_1$  and the quadratic term delivers  $p_2$ . Fig. 2.4 shows the plots corresponding to the analyses for 0, 2, and 6 knots.



a)  $U = 0$  knots

b)  $U = 2$  knots



c)  $U = 6$  knots

Fig. 2.4 Estimation of roll damping coefficient

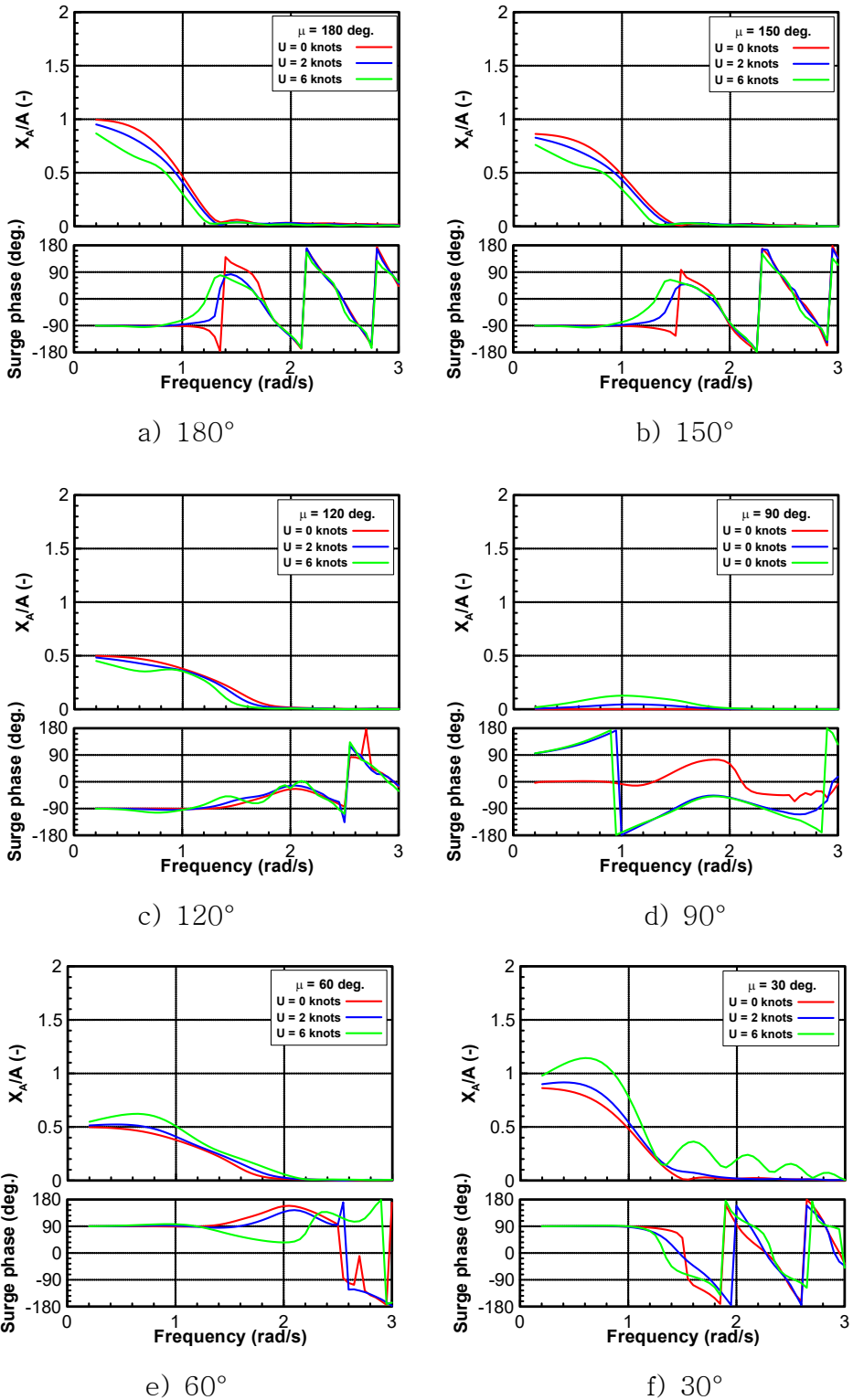
The roll damping coefficients are given in Table 2.2. It is applied to potential code to consider viscosity effects and correct the roll amplitude in resonance frequency. The roll damping coefficients are given as shown in Table 2.2.

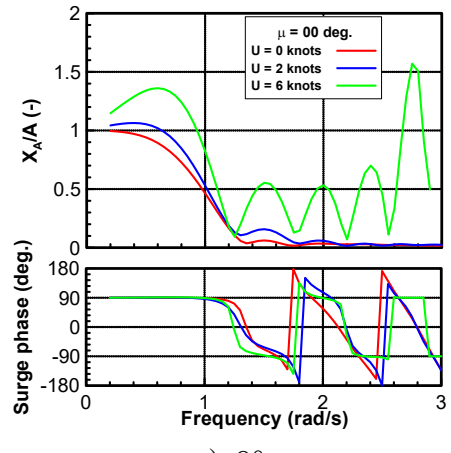
Table 2.2. Roll damping coefficient

Speed [knots]	$p_1$ [ $s^{-1}$ ]	$p_2$ [ $rad^{-1}$ ]	$\hat{B}_{44}$ [-]	$\hat{B}_{44}$ [ $kg \cdot m^2/s$ ]
0	2.4563	0.0077	0.0587	8,943,703
2	2.5800	0.0008	0.0617	9,393,930
6	3.1575	-0.0525	0.0755	11,496,613

### 2.2.3 Simulation results

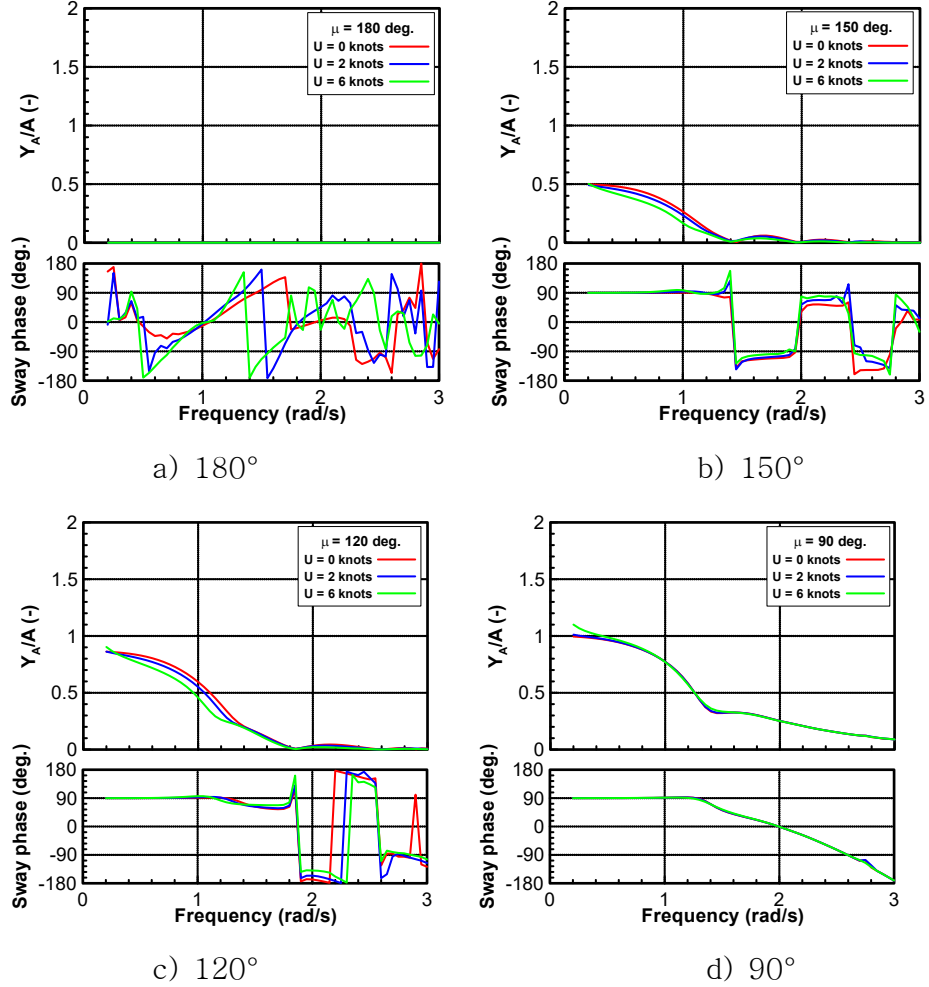
Figs. 2.5~2.9 plots 6-DOF motion RAOs and phases at multi-directions condition in regular waves. Fig. 2.5 shows the surge motion response at three speed condition. In general, the magnitude of the surge is larger in stern waves and largest at following waves. In the bow waves, the surge amplitude decreases at a higher speed, while the amplitude at higher speed is greater in stern waves. Corresponding to surge motion, sway amplitude at higher speed also decreases at bow waves and slightly greater at stern waves. Fig. 2.6 shows the sway amplitude and the largest response occurs in beam waves. Fig. 2.7 represents the heave motion. As the frequency decreases, mean wave length increases, the ship moves along the wave surface, so the RAO converges to 1 in the low frequency region. The difference of heave amplitude according to the speed is not noticeable. Roll motions are described in Fig. 2.8. The magnitude of roll RAO shows the largest at beam waves and decreases gradually to head waves and following waves. The difference of roll magnitude according to the speed is not noticeable at low frequency. However, the difference is noticeable around resonance frequency, the roll magnitude at high speed increases in bow waves and decreases in stern waves. Fig. 2.9 shows the pitch magnitude and its largest occurs at head waves and following waves and decreases to beam waves. It is clearly observed at zero speed condition. Fig. 2.10 shows yaw motion. Because the model ship is right and left and nearly fore and aft symmetrical, the yaw RAO is zero at head waves, beam waves and following waves.





g)  $0^\circ$

Fig. 2.5 Surge RAO (Simulation)



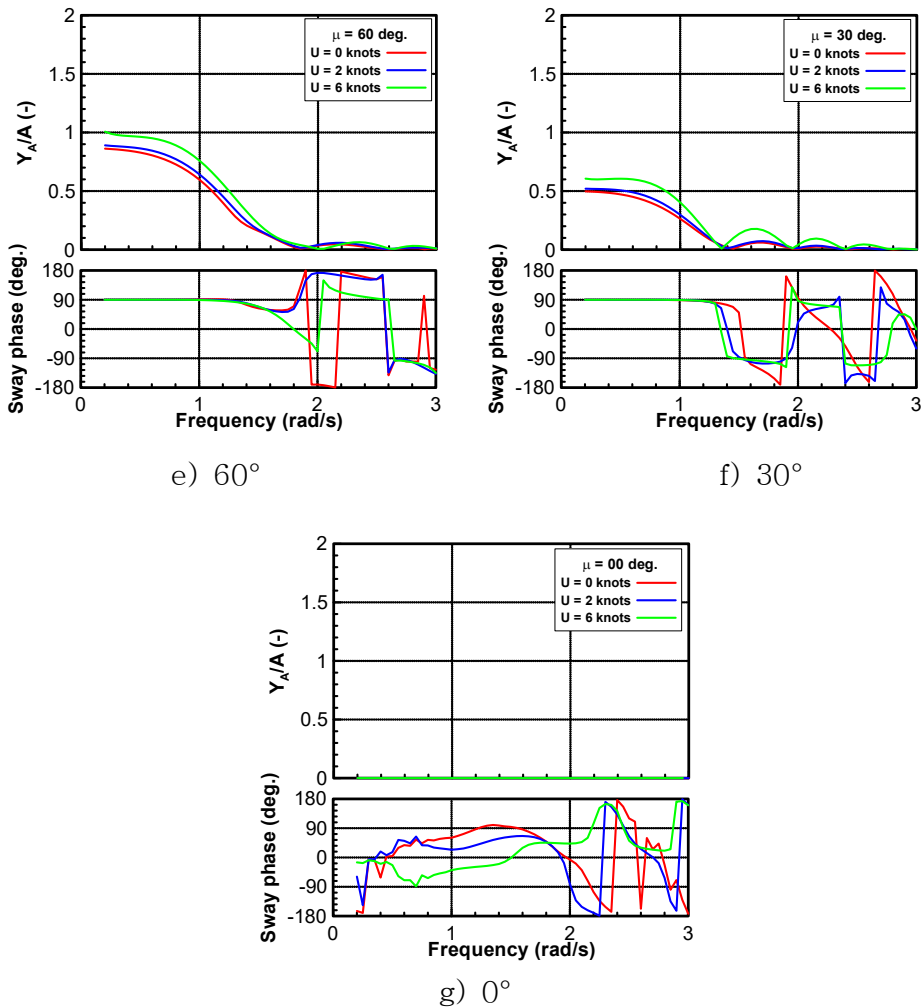
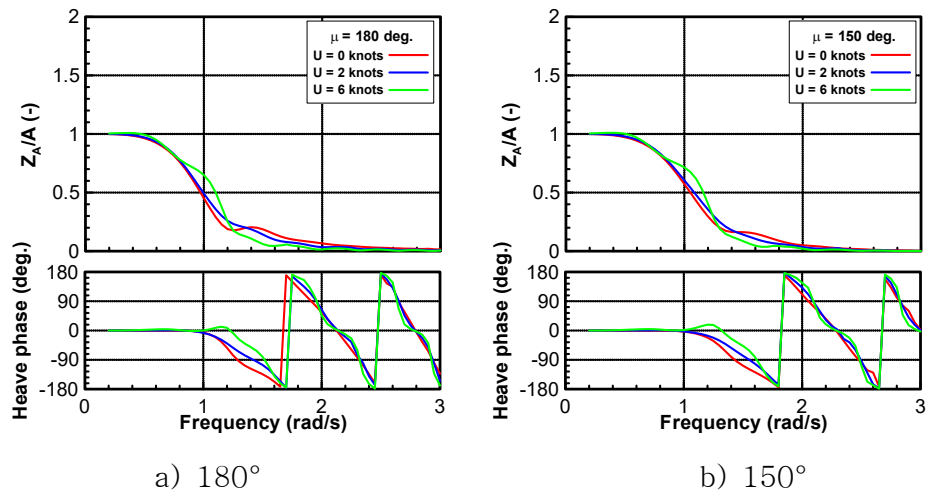


Fig. 2.6 Sway RAO (Simulation)



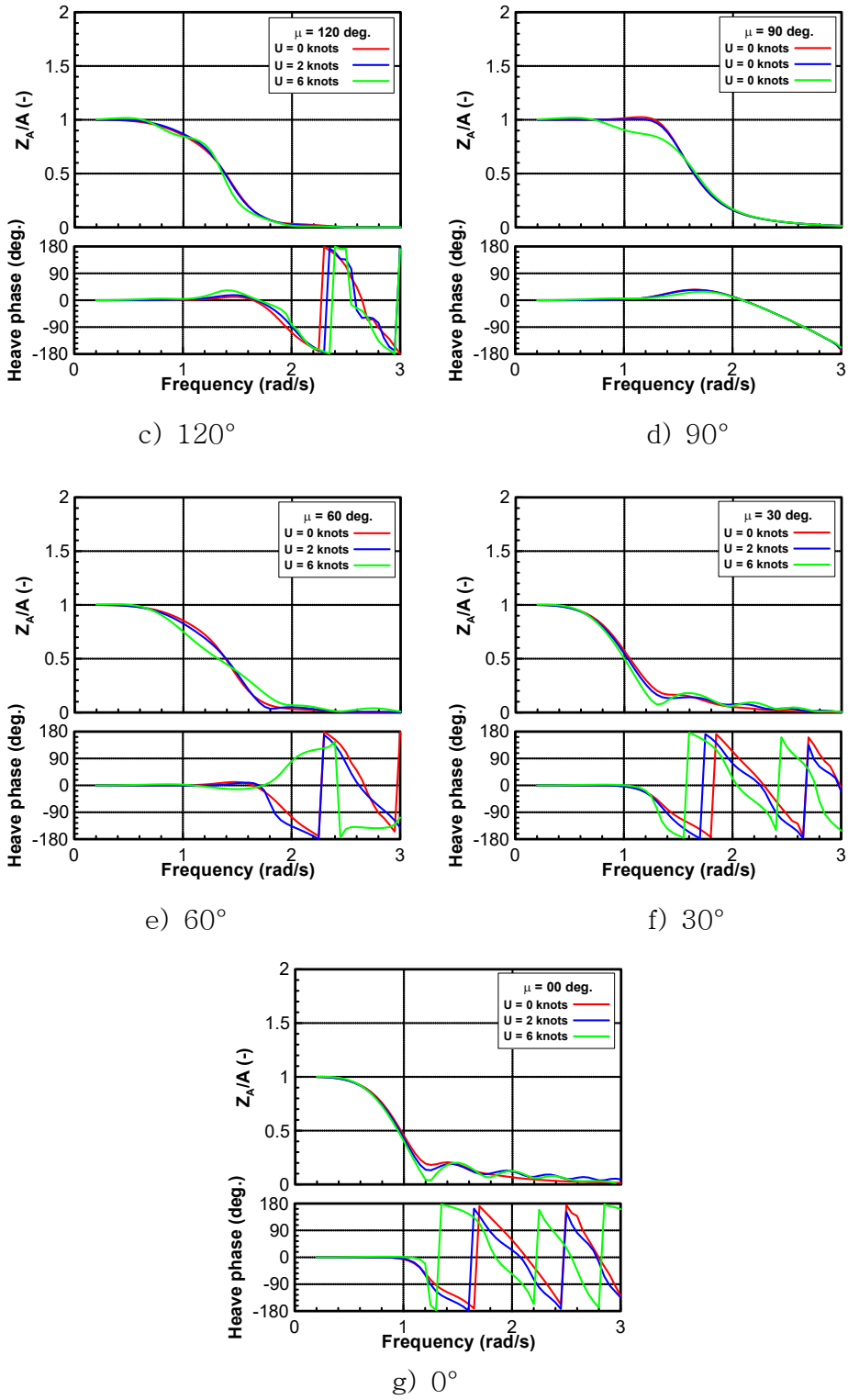
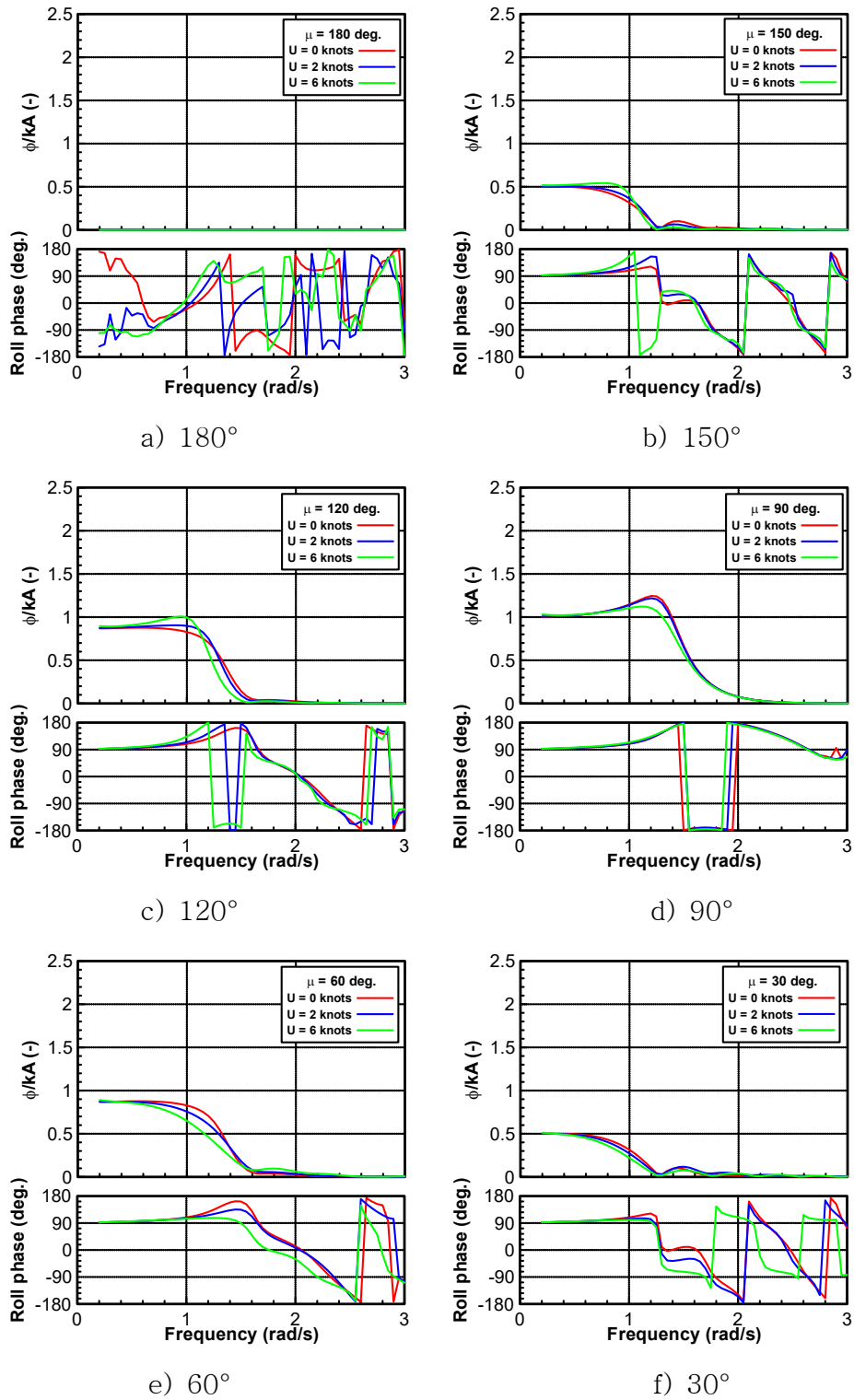
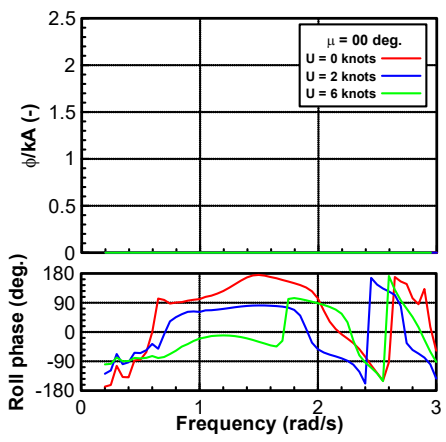


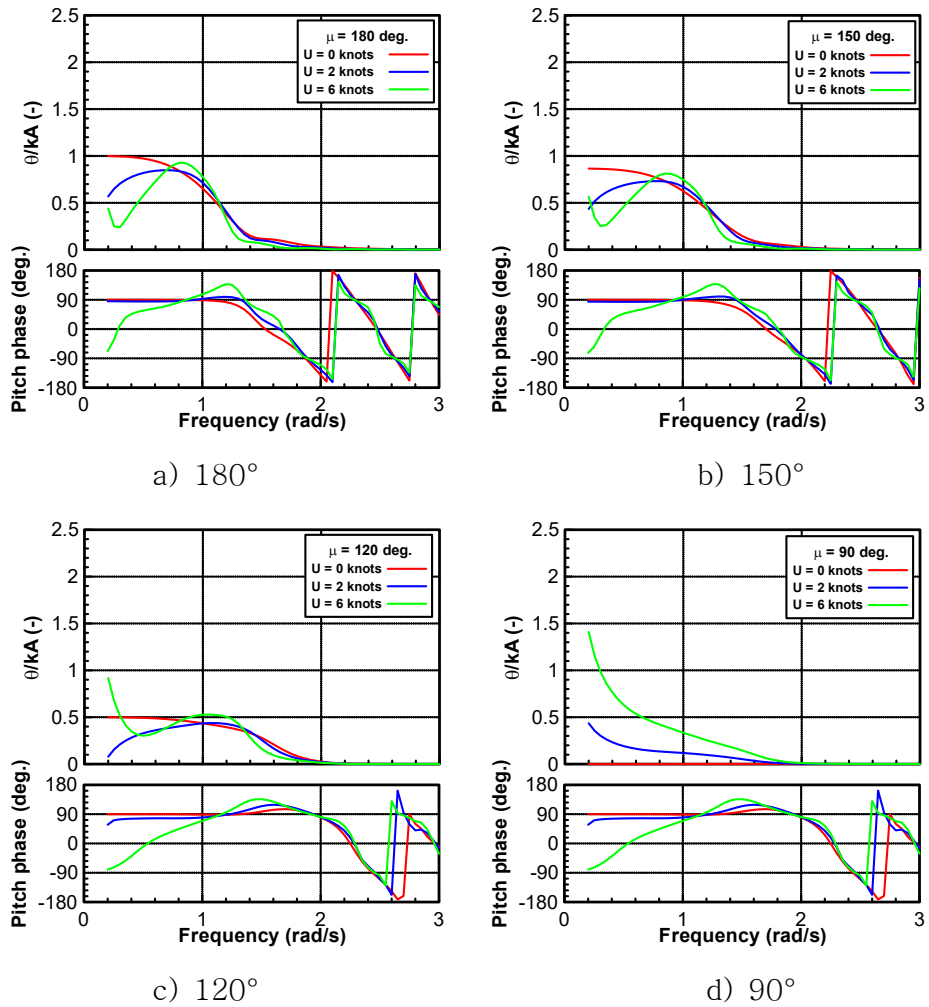
Fig. 2.7 Heave RAO (Simulation)





g)  $0^\circ$

Fig. 2.8 Roll RAO (Simulation)



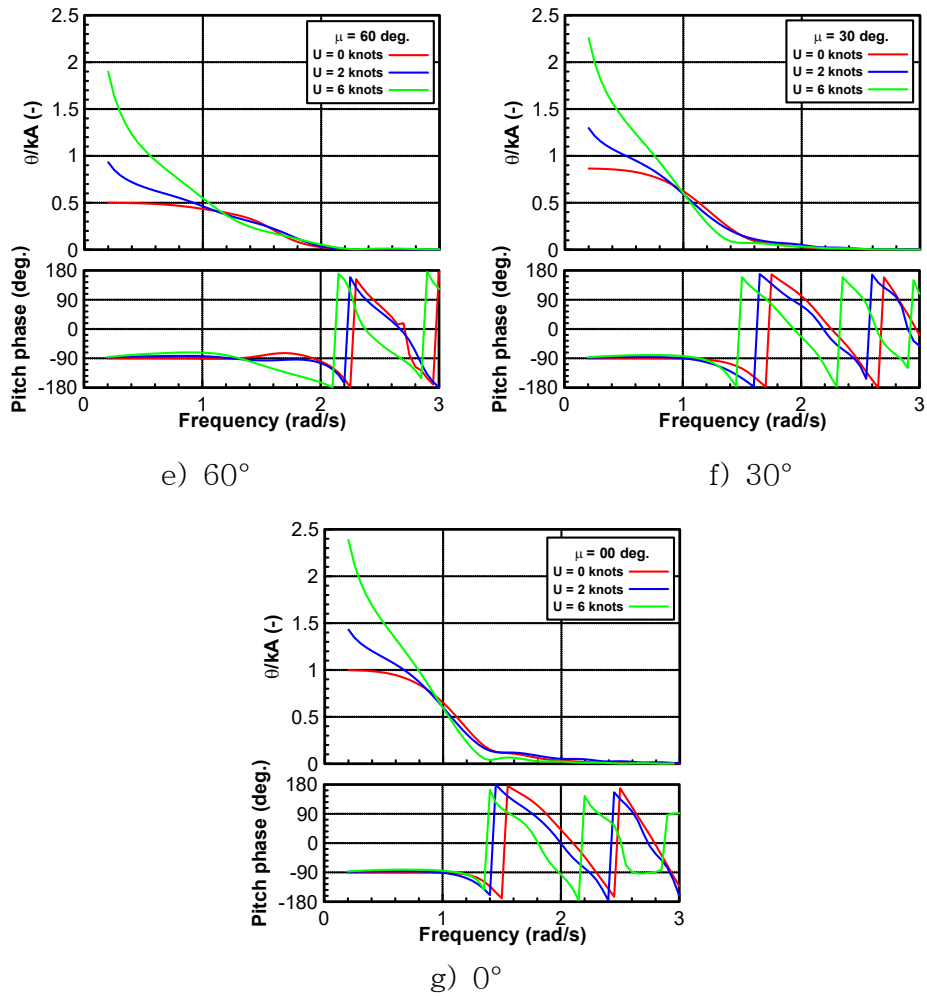
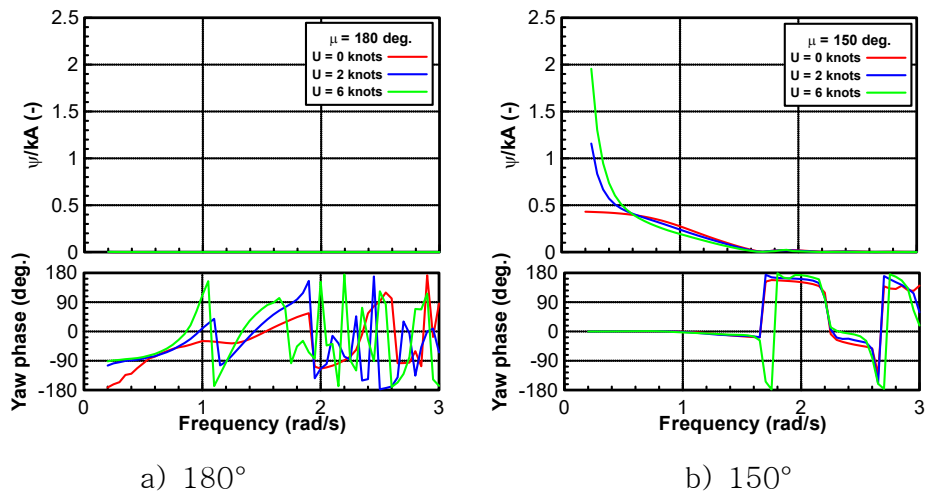


Fig. 2.9 Pitch RAO (Simulation)



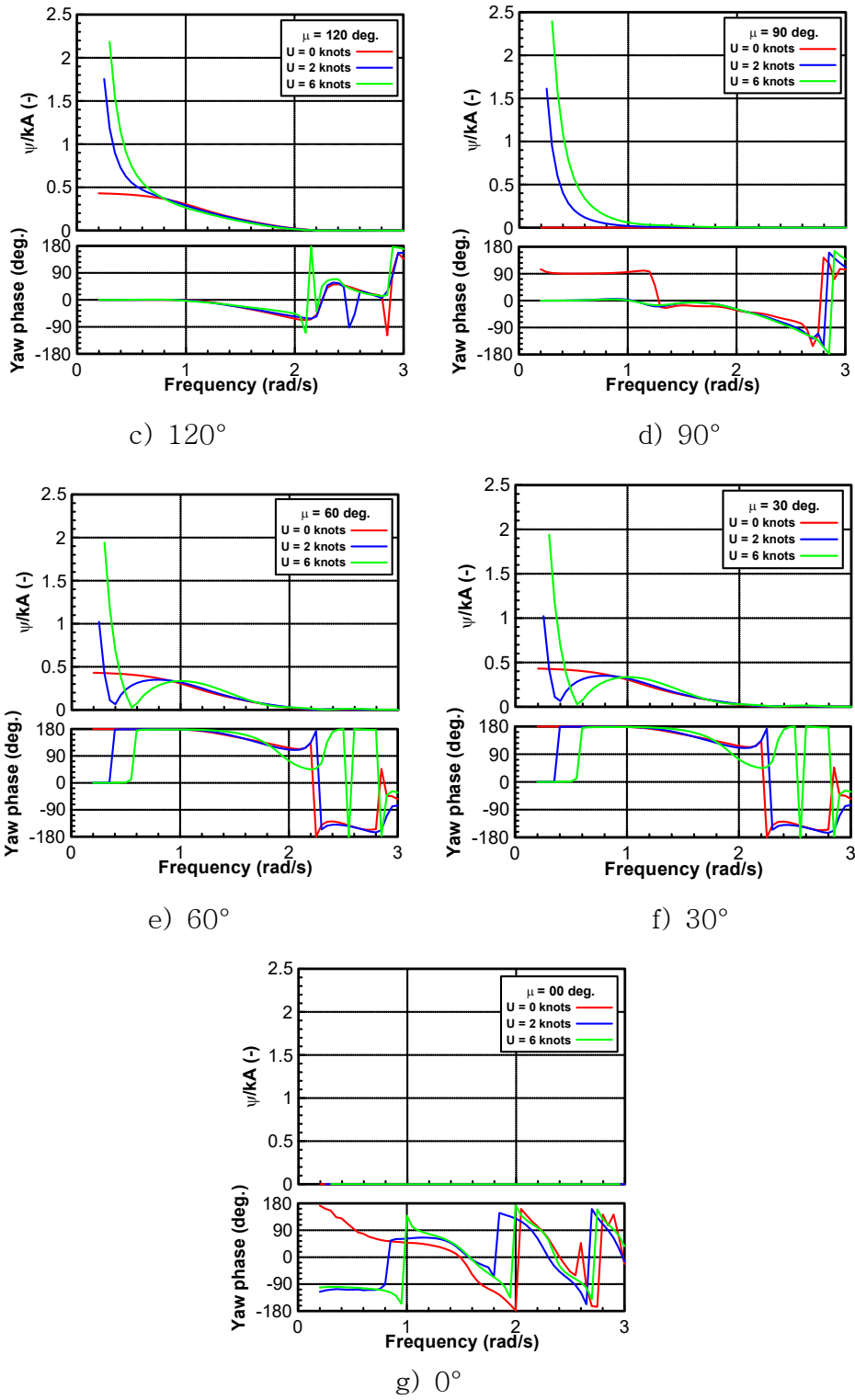


Fig. 2.10 Yaw RAO (Simulation)

### 3. Seakeeping Test

#### 3.1 Overview

##### 3.1.1 Test facility

The model test was performed in the 3D wave tank of Changwon National University shown in Fig. 3.1. The wave maker with 28 pistons is installed at the end of the tank to generate regular waves and irregular waves. As shown in Fig. 3.2, the wave absorbing device is installed in front of the end of the tank to effectively attenuate the generated wave. The main specifications of the tank are described in Table 3.1. The main scopes of application are ship seakeeping test, wave load measurement test for ship and offshore structure and captive model test.



Fig 3.1 CWNU Model Basin



Fig 3.2. Wave maker and wave absorber

Table 3.1. Specifications of 3D wave tank

Item	Value
Length (m)	20.0
Breadth (m)	14.0
Depth (m)	1.95
Maximum water depth (m)	1.85
Maximum towing speed (m/s)	1.0
Maximum length of a model ship (m)	1.5
Maximum wave length (m)	3.0
Maximum wave height (m)	0.3

### 3.1.2 Model ship

The model ship is shown in Fig. 3.3 and 3.4. Hull shape of garbage barge is symmetrical at bow and stern, starboard and port sides. Principal dimensions of the model ship are described in Table 1.1.



Fig 3.3 Hull model

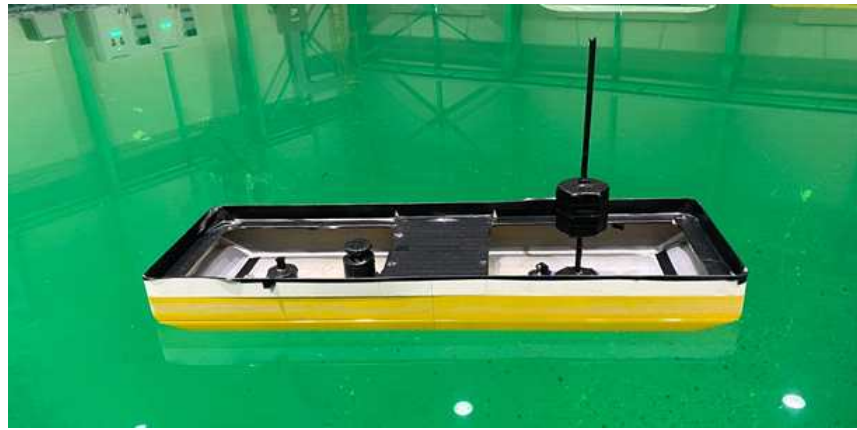


Fig 3.4 Barge model

### 3.1.3 Test equipment

Fig. 3.5 shows a capacity type wave probe and it is used as a sensor to measure the wave height during the wave calibration and seakeeping test.



Fig 3.5 Wave probe

The optic-based system, OptiTrack V120:TRIO, produced by NaturalPoint is used in this experiment to measure the 6-DOF motion. Fig. 3.6 shows the components of OptiTrack and it consists of markers, cameras, cable, and connector.



Fig 3.6 OptiTrack

Fig. 3.7 shows an inertial measurement unit (IMU) and it is used as a sensor to measure attitude, angular velocity and translational acceleration of the model ship in waves.



Fig 3.7 IMU

Fig. 3.8 shows the tension gauges and it is the sensor which can measure the wave force acting on the model test.



Fig 3.8 Tension gauge

The vertical and horizontal accelerations at bow and stern are measured by 3-axis accelerometer. Fig. 3.9 shows the accelerometers.



Fig 3.9 Accelerometer and connector

A/D converter NI USB-6212 is used to convert the electrical signal of the output data of tension gauge, wave probe and accelerometer into a digital signal for acquisition by a computer.



Fig. 3.10 A/D converter

### 3.1.4 Test condition

In order to carry out the seakeeping test for the model ship in regular waves, test conditions at full-scale should be converted to the one at model-scale. The speed condition at full scale is 0, 2, and 6 knots, respectively, and the Froude number should be the same for both full and model scale vessels. Therefore, speed conditions for model ship are 0, 0.147 and 0.441 m/s, respectively. The regular waves are generated throughout the seakeeping test. The range of wave frequency of 0.65~1.80 rad/s at full scale is given. According to scale ratio of 1/49, the wave frequency increases by the square root of the scale ratio, so the range of wave frequency for scale model is 4.55~12.60 rad/s. Table 3.2 describes the regular wave conditions of the model ship. According to ITTC recommendation for the seakeeping experiments (1974), the wave height should be under the condition of a small wave slope (wave height/ wave length < 1/50) to get a similar results to the linear surface wave theory. So, the wave height condition for each frequency can be decided. In addition, a model ship is symmetrical and it has the same seaworthiness performance for waves incident on the starboard and port side. Therefore, the experiment was performed only on the port side as shown in Fig. 3.11.

Table 3.2 Wave test condition

No.	Frequency (rad/s)	Wave length (m)	Wave length/ Ship length	Wave height (cm)
RW01	4.550	2.977	3.722	5.954
RW02	4.900	2.567	3.209	5.134
RW03	5.250	2.236	2.795	4.472
RW04	5.600	1.965	2.457	3.930
RW05	5.950	1.741	2.176	3.482
RW06	6.650	1.394	1.742	2.788
RW07	7.000	1.258	1.572	2.516
RW08	7.700	1.040	1.300	2.080
RW09	8.050	0.951	1.189	1.902
RW10	8.400	0.874	1.092	1.748
RW11	9.100	0.744	0.930	1.488
RW12	10.150	0.598	0.748	1.196
RW13	11.200	0.491	0.614	0.982
RW14	11.900	0.435	0.544	0.870
RW15	12.600	0.388	0.485	0.776

The wave incident on the bow is defined as 180 degrees and the wave incident on the stern is defined as 0 degrees. The interval of wave direction is 30 degrees. The waves are generated by the wave maker in the same direction. To simulate the multi-directional regular waves of the ship, the towing carriage is moved in tank forward, backward, left, and right simultaneously as shown in Fig. 3.12.

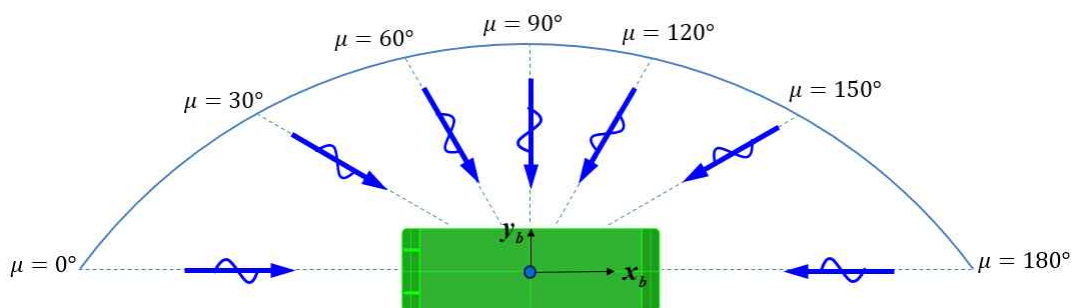


Fig. 3.11 Definition of wave direction



Fig. 3.12 Carriage moving with respect to wave directions

### 3.2 Pre-test

The pre-test was performed before the main test to calibrate the measurement system, set the ship state, and measure necessary values for the ship. The pre-test includes ballasting test, inclining test, decay test inertia test, and sensor calibration test such as tension gauge, wave probe and wave maker.

#### 3.2.1 Wave probe calibration

Fig. 3.13 shows the wave probe calibration setup including a capacity type wave probe, amplifier that amplifies measured signal, A/D converter to convert analog signal to digital signal and DAQ (Data AcQuisition) PC. Fig. 3.14 shows the results of the wave probe calibration test.

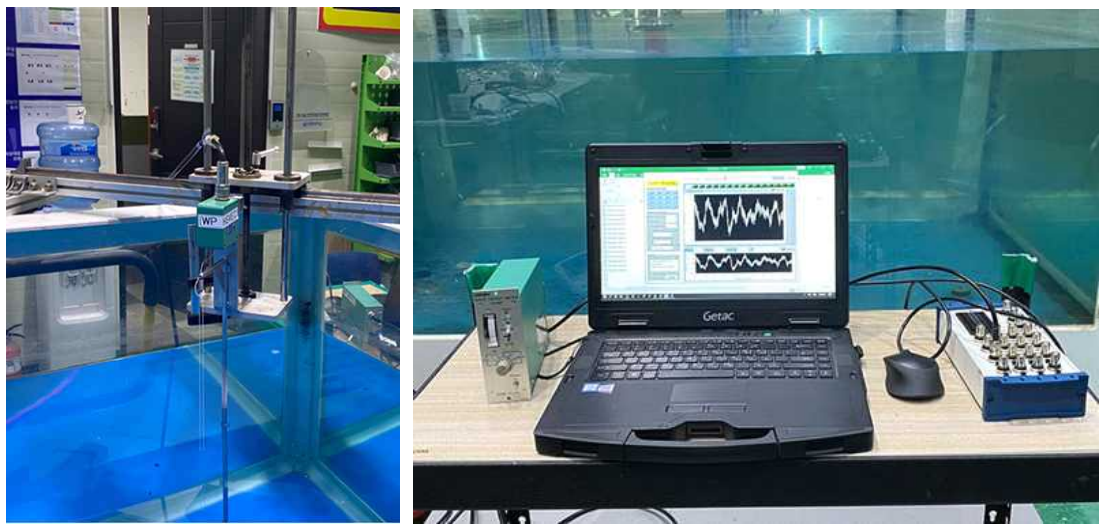


Fig. 3.13 Wave probe calibration setup

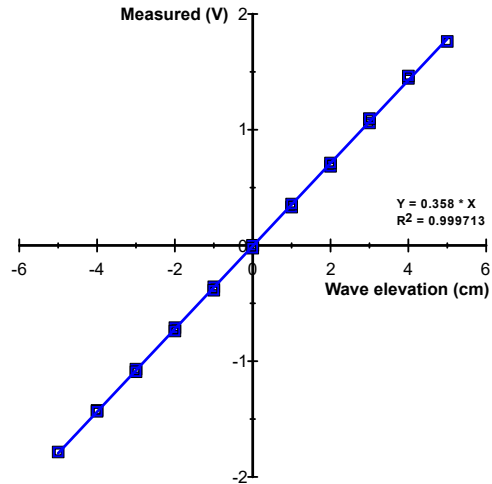
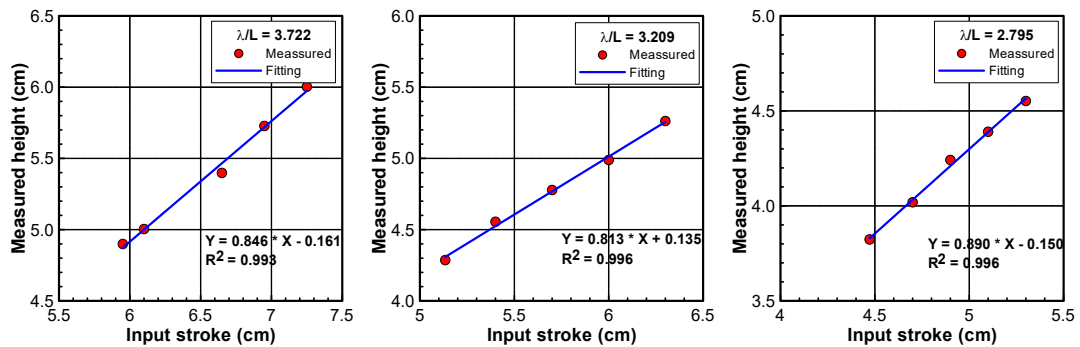


Fig. 3.14 Results of wave probe calibration

### 3.2.2 Wave maker calibration

After wave probe calibration, it was installed in the tank for wave maker calibration. The purpose of wave maker calibration test is to find the relationship between the wave height input in the wave generator program and the actual wave height to obtain the correction factor for the input wave height. The regular wave calibration was performed by inputting different wave heights for each frequency into wave generator program. The wave maker calibration test for 15 frequencies was carried out. Fig. 3.15 shows the relationship between input wave maker stroke and the measured wave height for RW01~RW15 of the regular wave described in Table 3.3. The time series of measured wave height is shown in Fig. 3.16 for each frequency.



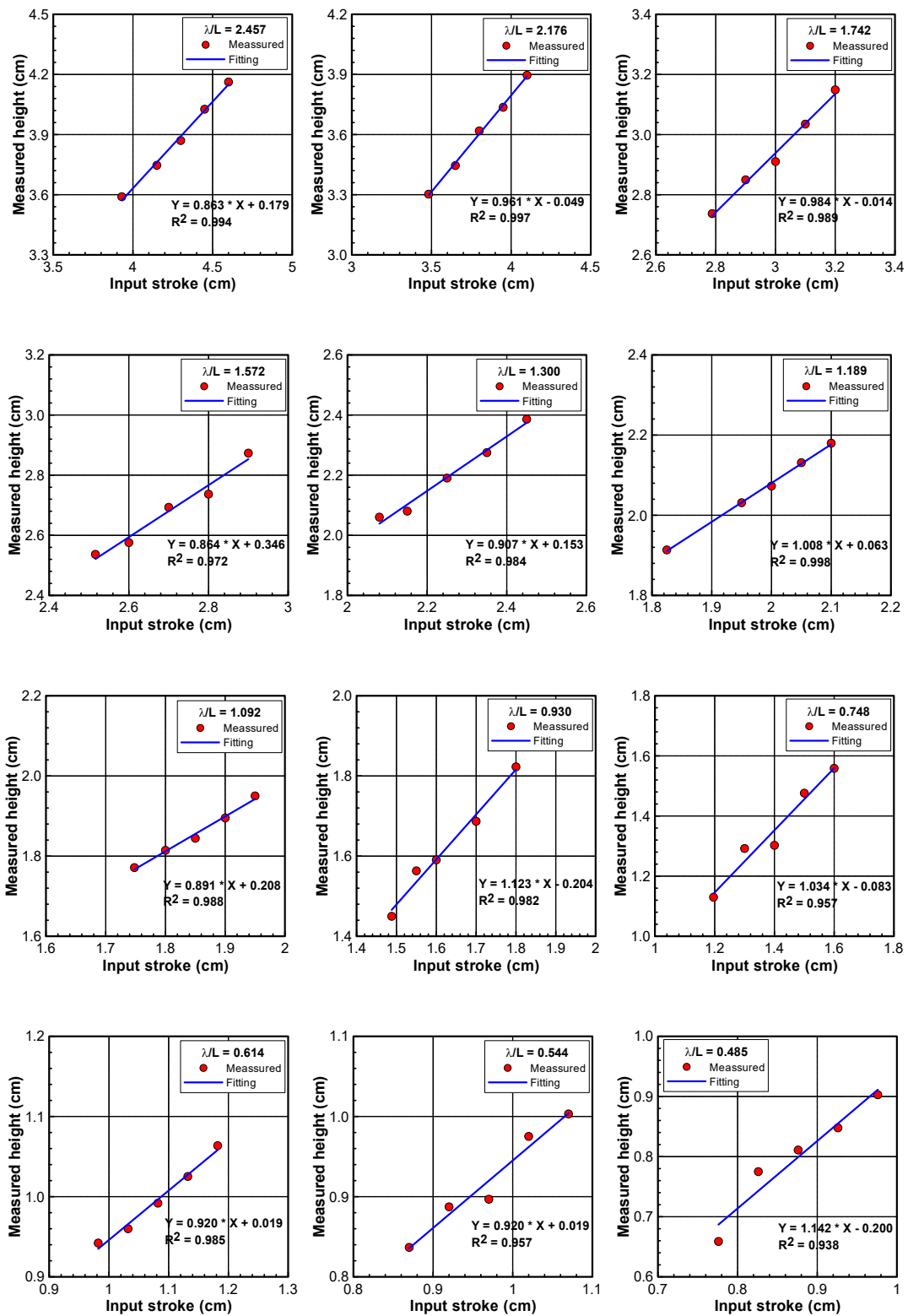
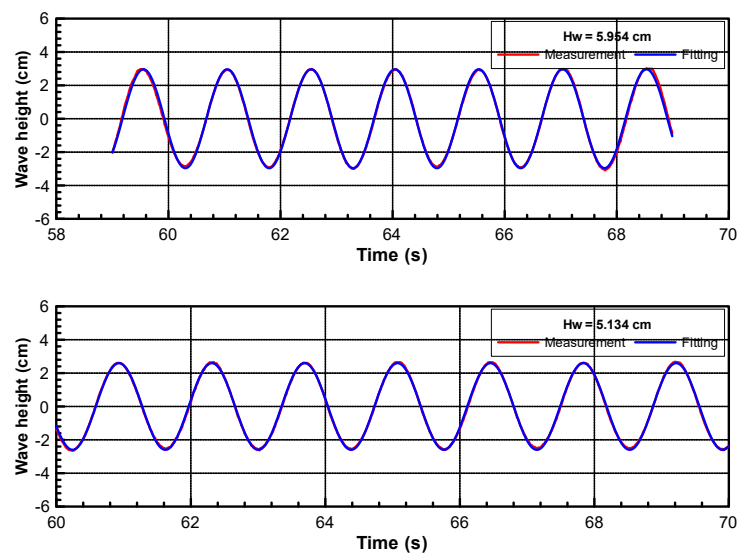
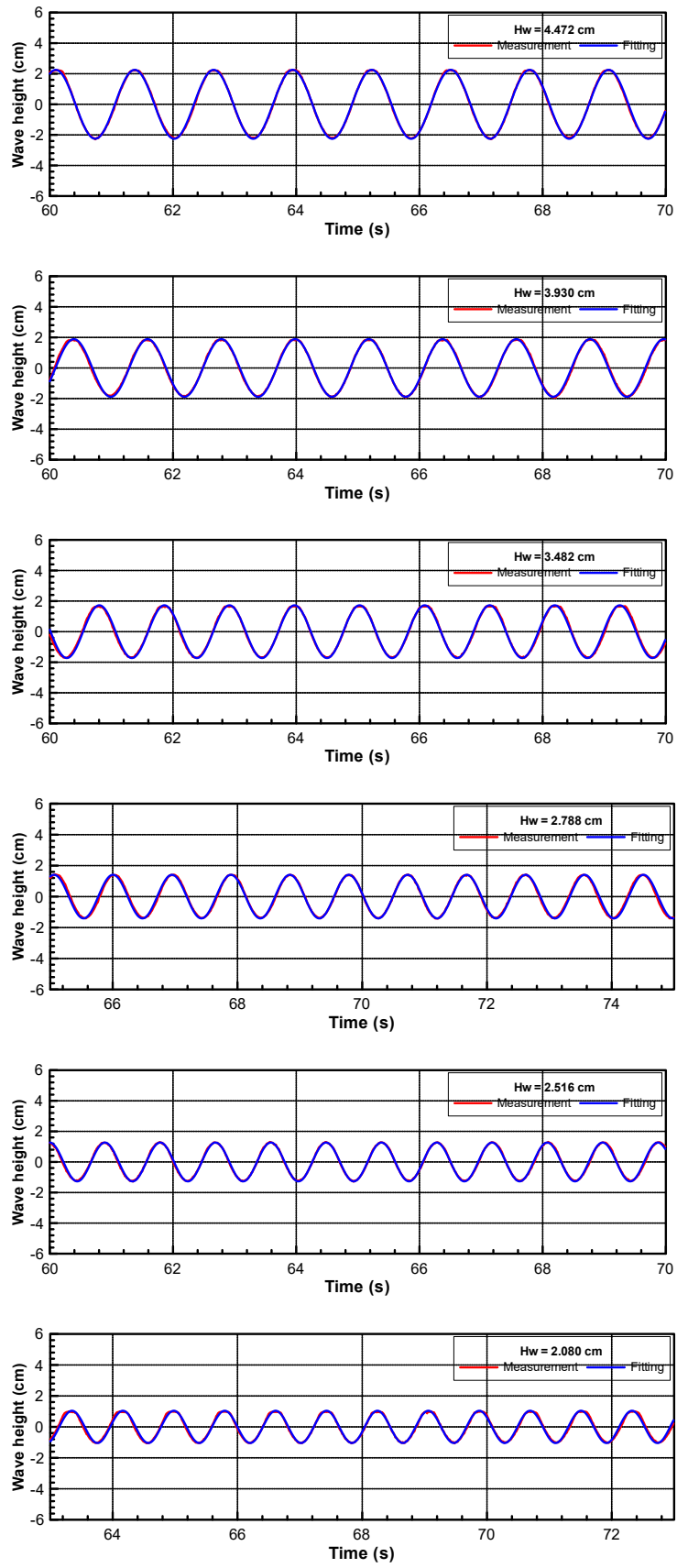


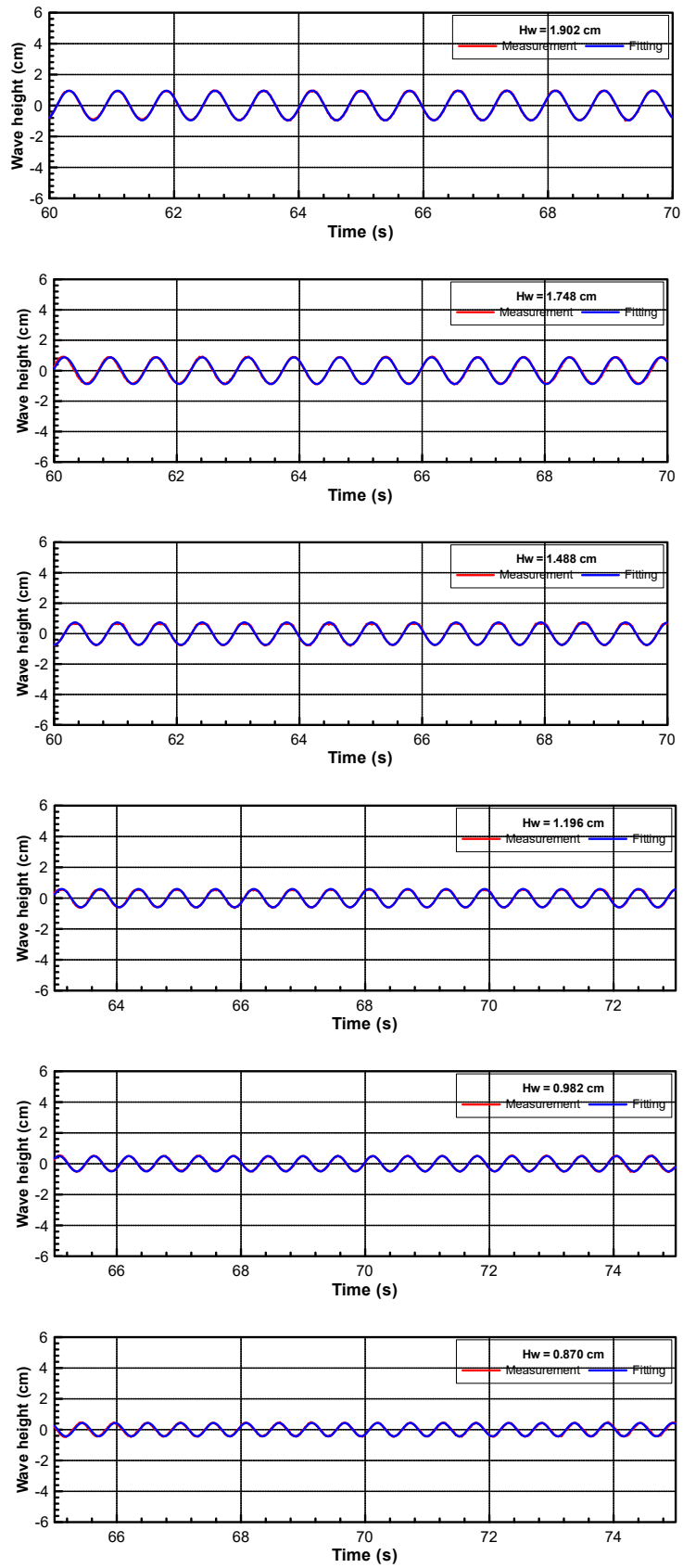
Fig. 3.15 Results of wave maker calibration

Table 3.3 Target wave height and input wave maker stroke

No.	Frequency (rad/s)	Target wave height (cm)	Input stroke (cm)	Measured wave height (cm)	Difference (%)
RW01	4.55	5.95	7.23	5.92	0.50
RW02	4.90	5.13	6.15	5.19	1.17
RW03	5.25	4.47	5.19	4.51	0.89
RW04	5.60	3.93	4.30	3.87	1.53
RW05	5.95	3.48	3.65	3.45	0.86
RW06	6.65	2.79	2.85	2.81	0.72
RW07	7.00	2.52	2.52	2.54	0.79
RW08	7.70	2.08	2.13	2.09	0.48
RW09	8.05	1.90	1.82	1.91	0.53
RW10	8.40	1.75	1.73	1.75	0.00
RW11	9.10	1.49	1.51	1.48	0.67
RW12	10.15	1.20	1.21	1.19	0.83
RW13	11.20	0.98	1.08	0.99	1.02
RW14	11.90	0.87	0.90	0.86	1.15
RW15	12.60	0.78	0.86	0.78	0.00







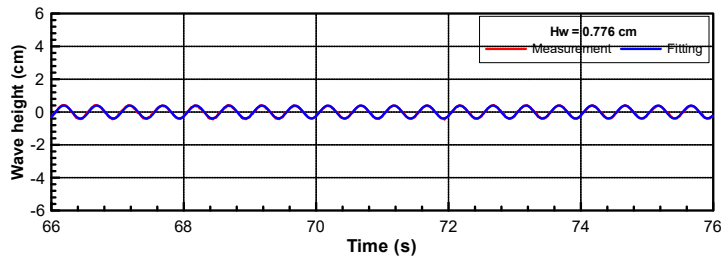


Fig. 3.16 Time series of measured wave height.

### 3.2.3 Ballasting test

Ballasting test for the model ship should be conducted to ensure that the mass and draft of the model ship are the same to the real ship.

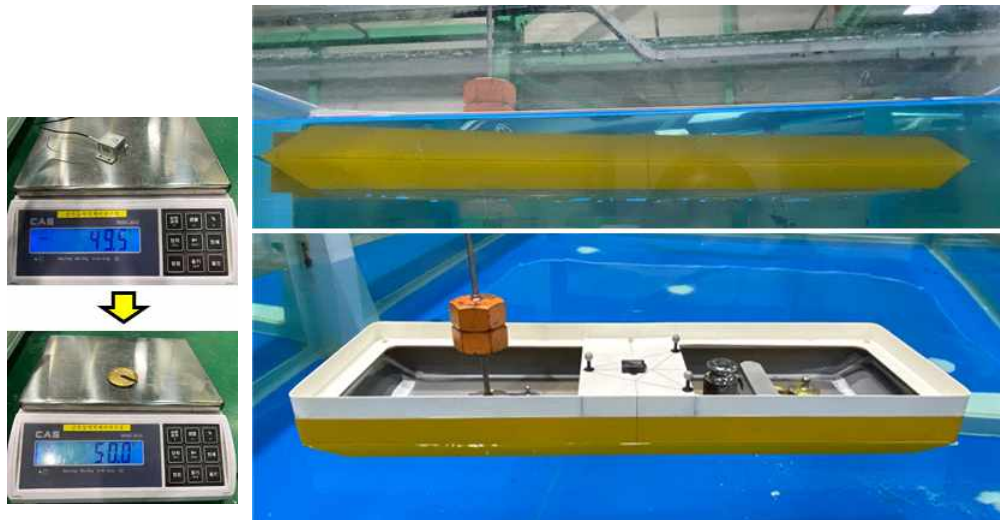


Fig. 3.17 Ballasting test

It was performed according to given draft ( $T = 0.0311 \text{ m}$ ) corresponding to the density of seawater. The mass includes additional weight and an inclinometer sensor in the ship. Because the sensor was attached to the electrical cables that were difficult for ballasting process, so it was replaced by a weight of the same mass. Fig. 3.17 shows the ballasting results for the model ship.

### 3.2.4 Inclining test

After ballasting test was completed, an inclining test was carried out to check the transverse metacenter height ( $GM_T$ ). The inclining test confirms

the inclination angle when the mass in the model ship is moved in the horizontal direction and adjusts the height of the weight attached to the stern side of ship. During ballasting test of the model ship, it is convenient to attach the digital protractor(inclinometer sensor) to the model ship and perform ballasting together. As shown in Fig. 3.18, the position of the  $GM_T$  is determined by the displaced hull shape of the hull, and buoyancy center ( $B$ ) is determined by the displacement of the ship.  $GM_T$  is the distance from the ship's center of gravity ( $G$ ) to the metacenter height ( $M$ ) and the case where the  $M$  is above  $G$  is defined as a positive value. The formula for estimating the transverse metacenter height  $GM_T$  using the heel angle generated by changing the weight distribution as Eq. (3.1)

$$GM_T = \frac{w \cdot l_y}{W \cdot \tan\phi} \quad (3.1)$$

Here,  $w$  is moving weight,  $W$  means displacement of the model,  $l_y$  represents the lateral distance of the moving weight and  $\phi$  is heel angle.

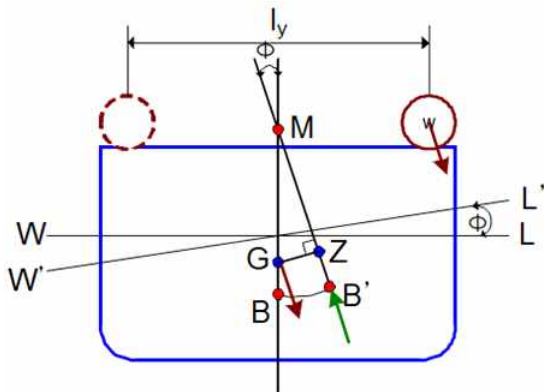
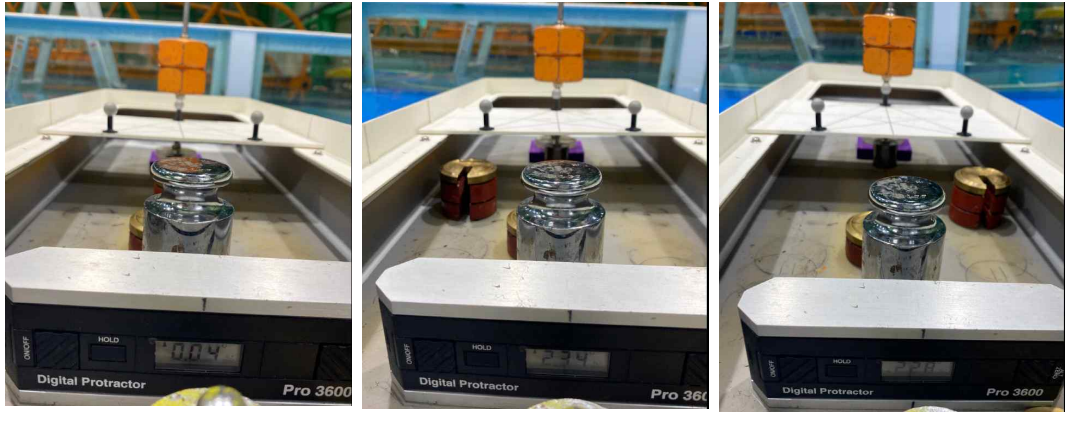


Fig. 3.18 Definition of an inclining test

To calculate the target heel angle that occurs when the weight is moved in the horizontal direction, we selected the weight with 0.5 kgf. Lateral moving distance is 0.08 m and is limited by the ship's breadth. Applying Eq. (3.1), the target heel angle should be 2.306°. Fig. 3.19 shows the results of inclining test. 2.30° and 2.32° are results when the weight is moved to starboard and port side, respectively. The difference values are 0.280% and 0.587% compared with target heel angle for starboard and port side, respectively.



a) Initial state      b) Move weight to STBD      c) Move weight to Port

Fig. 3.19 Results of inclining test

### 3.2.5 Free roll decay test

Free roll decay test was performed to check the virtual mass moment of inertia with respect to x direction ( $I_{xx}$ ). It was performed using IMU located at midship in the ballasting tank. Fig. 3.20 shows the time series data of free roll decay test. Table 3.4 describes the measured period. It can be seen that the measured value is similar to the target value with a small difference. It was also confirmed that the mass distribution was reasonable. Ballasting test, inclining test, and free roll decay test should be performed concurrently to ensure the mass distribution on the ship model. If any test deviation is over 5 % compared with target value, ballasting test, inclining test, and free roll decay test should be repeated until the deviation decreases.

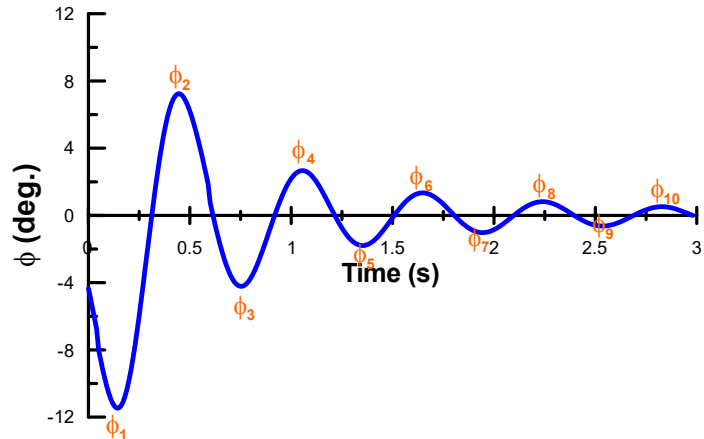


Fig. 3.20 Time series of free roll decay test

Table 3.4 Measured period of free roll decay test

Period	Target (s)	Measured (s)	Difference (%)
$T_1 (\phi_2 - \phi_4)$	0.597	0.610	2.178
$T_2 (\phi_4 - \phi_6)$	0.597	0.590	1.173
$T_3 (\phi_6 - \phi_8)$	0.597	0.590	1.173
$T_4 (\phi_8 - \phi_{10})$	0.597	0.580	2.848
Mean	0.597	0.5925	0.754

### 3.2.6 Inertia tests for $I_{xx}$ , $I_{yy}$ and $I_{zz}$

After mass distribution of the model ship was determined, the inertia tests were performed to confirm with estimated mass moment of inertia with respect to x, y, and z without changing the center of gravity.

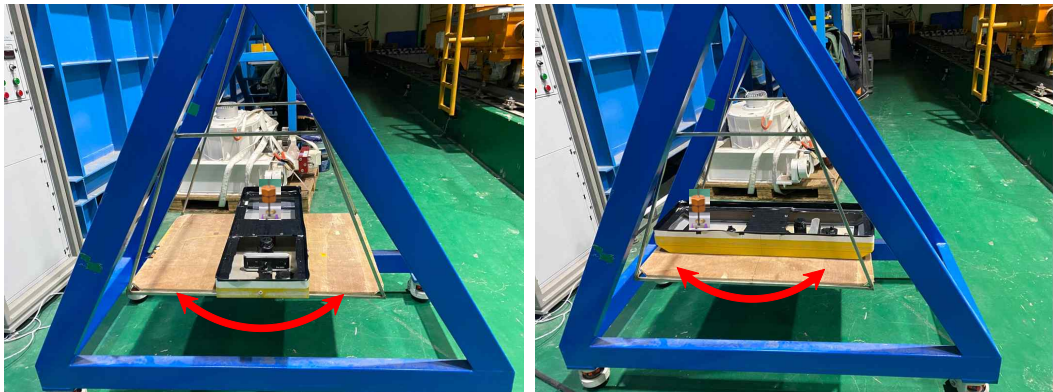


Fig. 3.21 Inertia swing test

First, the inertia of the model ship is measured using the inertia swing as shown in Fig. 3.21 to estimate the mass moment of inertia with respect to x ( $I_{xx}$ ) and y ( $I_{yy}$ ), respectively. A potentiometer is attached to the inertia swing and it measures the displacement of the swing. The mass moment of inertia of the model ship can be calculated by checking the swing period. Since the swing has its own inertia, it is necessary to measure the value in advance and correct it later. The 1-DOF equation of motion about the axis of rotation of the inertia swing is as follow.

$$(I + ml^2)\ddot{\theta} + b\dot{\theta} + mlg\theta \approx (I + ml^2)\ddot{\theta} + mlg\theta \quad (3.2)$$

It is supposed that the inertia swing is free-damped and oscillated with respect to the small initial angular displacement. In that case, the following algebraic equations can be obtained for the mass moment of inertia, and the weight of the inertia swing.

$$I_0 + m_0 l_0^2 + m_1 l_1^2 = \frac{(m_0 l_0 + m_1 l_1)g}{\omega_1^2} \rightarrow I_0 + m_0 l_0^2 + m_1 l_1^2 = \frac{T_1^2}{4\pi^2} (m_0 l_0 + m_1 l_1)g \quad (3.3)$$

If  $A$ ,  $B$ ,  $C$  are set as  $-m_0 l_0 g$ ,  $I_0 + m_0 l_0^2$ ,  $m l g T^2 - 4\pi^2 m l^2$ , respectively, and a known weight is set differently from  $l$  and the period is measured while performing the test, the following expression for  $A$  and  $B$  can be obtained

$$\begin{aligned} A T_1^2 + 4\pi^2 B &= C_1 \\ A T_2^2 + 4\pi^2 B &= C_2 \end{aligned} \quad (3.4)$$

$$A = \frac{C_1 - C_2}{T_1^2 - T_2^2}, \quad B = \frac{T_1^2 C_2 - T_2^2 C_1}{4\pi^2 (T_1^2 - T_2^2)}, \quad C = m l g T^2 - 4\pi^2 m l^2 \quad (3.5)$$

$A$  and  $B$  are coefficients related to the mass moment of inertia of the inertia swing itself.

$$I_0 + m_0 l_0^2 + I_s + m_s l_s^2 = \frac{(m_0 l_0 + m_s l_s)g}{\omega_s^2} \rightarrow I_s = -m_s l_s^2 - B + \frac{T_s^2}{4\pi^2} (m_s l_s g - A) \quad (3.6)$$

Figs. 3.22 and 3.23 show the time series of inertia swing with respect to x and y, respectively.

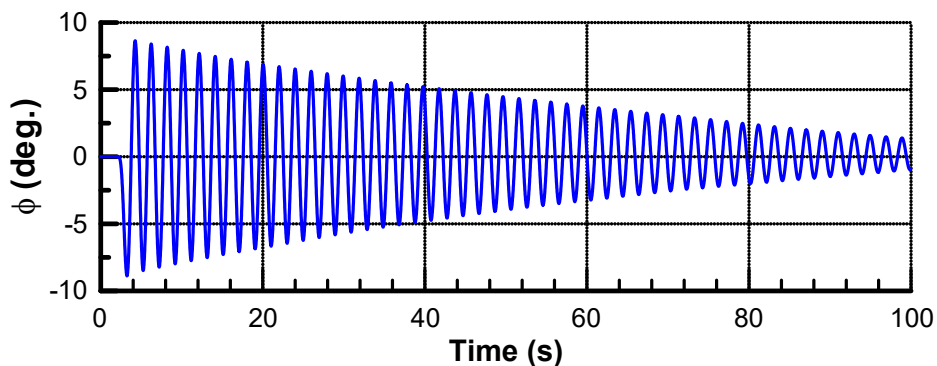


Fig. 3.22 Time series of inertia swing w.r.t. x

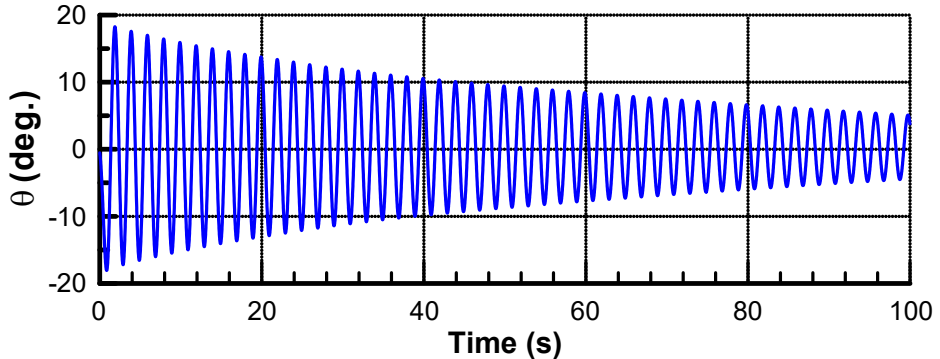


Fig. 3.23 Time series of inertia swing w.r.t. y

The total periods counted for the model ship including the swing table are 1.975 s and 2.005 s for roll and pitch, respectively. By subtracting the period of the swing table, the period of the model ship can be estimated. Table 3.5 depicts the mass moment of inertias measured by the inertia swing. The difference between target value estimated by theory and measurement values seems small.

Table 3.5 Inertia swing results

Moment of inertia	Target ( $\text{kg}\cdot\text{m}^2$ )	Measured ( $\text{kg}\cdot\text{m}^2$ )	Difference (%)
$I_{xx}$	0.0704	0.0671	4.690
$I_{yy}$	0.250	0.265	5.078

Mass moment of inertia with respect to z ( $I_{zz}$ ) is measured by inertia table.



Fig. 3.24 Inertia table test

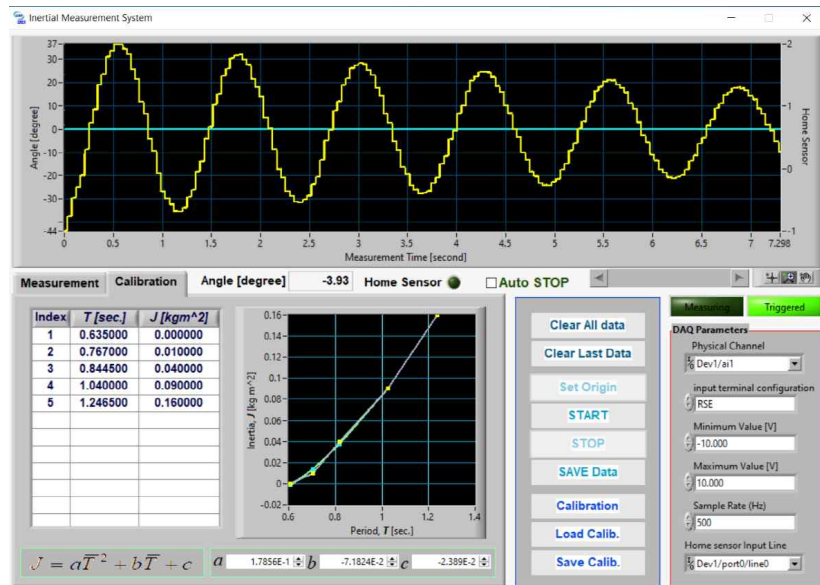


Fig. 3.25 Calibration results

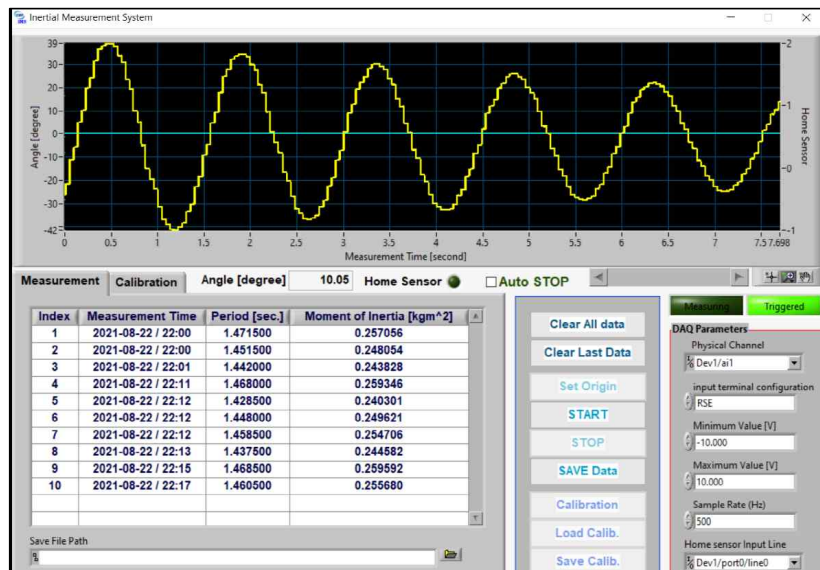


Fig. 3.26 Inertia test results

Fig. 3.24 shows a setup for the model ship in inertia table. Before measuring the moment of inertia, the calibration was performed by changing the distance of the weights. Fig. 3.25 depicts the calibration results. The moment of inertia for the model ship was measured with a repeat 10 times and an average of results was taken. Table 3.6 shows the inertia test results and it can be seen that there are very small difference (0.511 %) between the target value and the measured value.

Table 3.6 Inertia table results

Moment of inertia	Target ( $\text{kg}\cdot\text{m}^2$ )	Measured ( $\text{kg}\cdot\text{m}^2$ )	Difference (%)
$I_{zz}$	0.250	0.251	0.511

The small difference between target value and measured value in inertia test means that the mass distribution in the model ship is well matched to the real ship. We can fix the weight and use this state for further tests.

### 3.2.7 Tension gauge calibration

It is necessary to calibrate other sensors to measure physical quantities during the model test after distributing the mass of the model ship such as ballasting test, inclining test and inertia test. The tension gauges were used to measure the wave force acting on the ship model. It is connected to the ship at four angle positions of the support frame to ensure the balance of the ship. As shown in Fig. 3.27 for tension gauge calibration, an analog signal is measured by placing a weight in the vertical direction. The output signal is amplified by an amplifier, an analog signal is converted to a digital signal using A/D converter, and digital signal is then displayed in PC. Fig. 3.28 depicts the calibration results for four tension gauges. It gives the approximation results of the tension gauges. Eq. (3.7) expresses the calibration coefficient matrix for the tension gauges.



Fig. 3.27 Tension gauge calibration

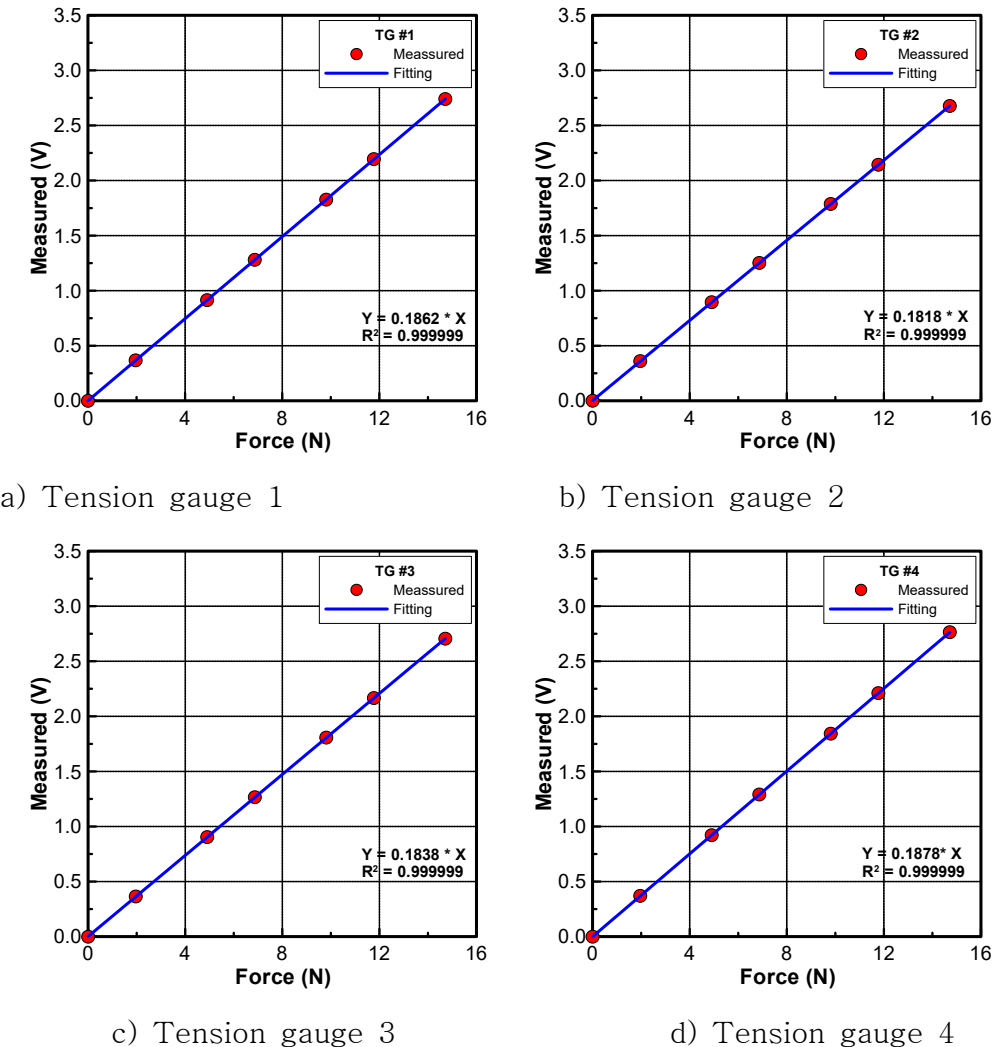


Fig. 3.28 Tension gauge calibration results

$$\begin{bmatrix} T_1 \\ T_2 \\ T_3 \\ T_4 \end{bmatrix} (N) = \begin{bmatrix} 5.370 & 0 & 0 & 0 \\ 0 & 5.499 & 0 & 0 \\ 0 & 0 & 5.439 & 0 \\ 0 & 0 & 0 & 5.324 \end{bmatrix} \begin{bmatrix} T_1 \\ T_2 \\ T_3 \\ T_4 \end{bmatrix} (V) \quad (3.7)$$

### 3.2.8 Accelerometer

The 3-axis accelerometer is used to measure vertical and horizontal acceleration in waves. We checked the calibration coefficients for the gravitational acceleration and analog signal. Fig. 3.29 shows the raw signal from the accelerometer. According to ITTC recommendation, the accelerometer was installed at 10 % of bow and 10 % of stern as shown in Fig. 3.30.

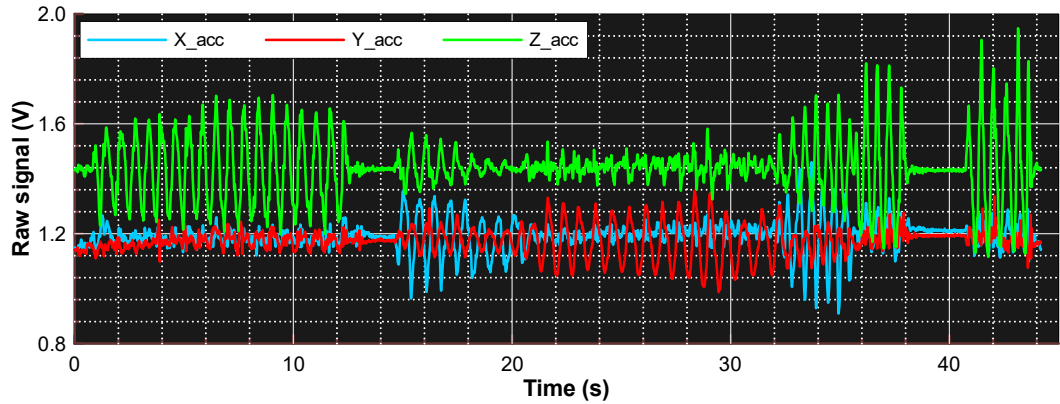


Fig. 3.29 Accelerometer raw signal

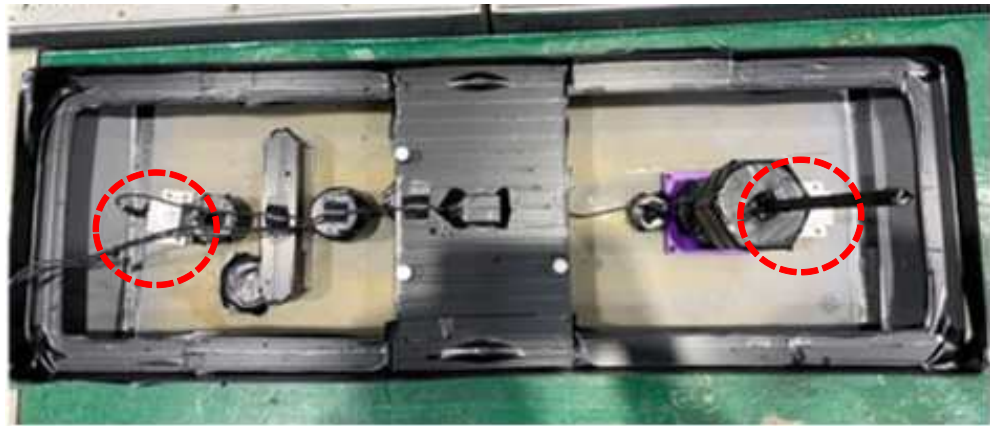


Fig. 3.30 Accelerometer installed on the model ship

### 3.3 Experiment Setup

#### 3.3.1 Model ship

The model ship was installed in the 3D wave tank after various calibration tests for the model ship and measurement sensor were completed. As shown in Fig. 3.31, the model ship is installed in a state where 6-DOF motion is free by applying the soft mooring spring. After installing the tension gauges at four angle points, tension gauges, mooring lines and springs should be connected to the model ship. At this time, it is necessary to check the pretension to the tension gauge and measure the force when the model ship shakes by giving a force to the tension gauge. Fig. 3.32 describes the model ship installation schematic plan with sensors, soft mooring and dimensions.

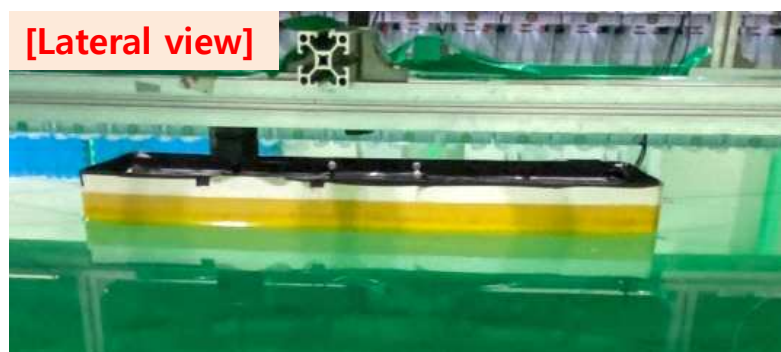
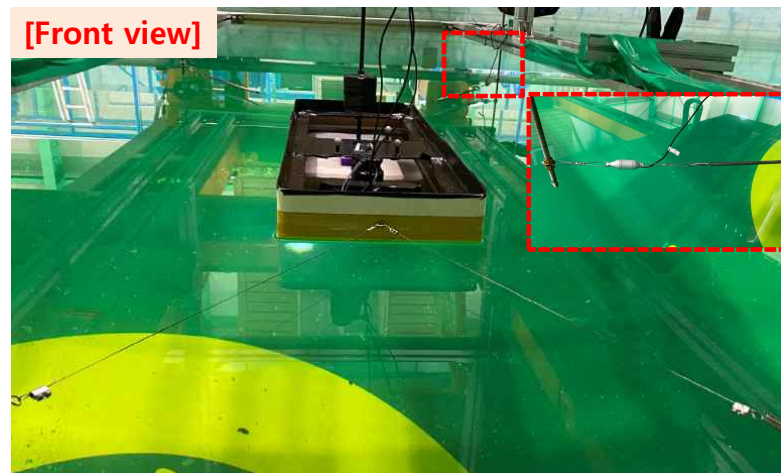


Fig. 3.31 Model ship installation

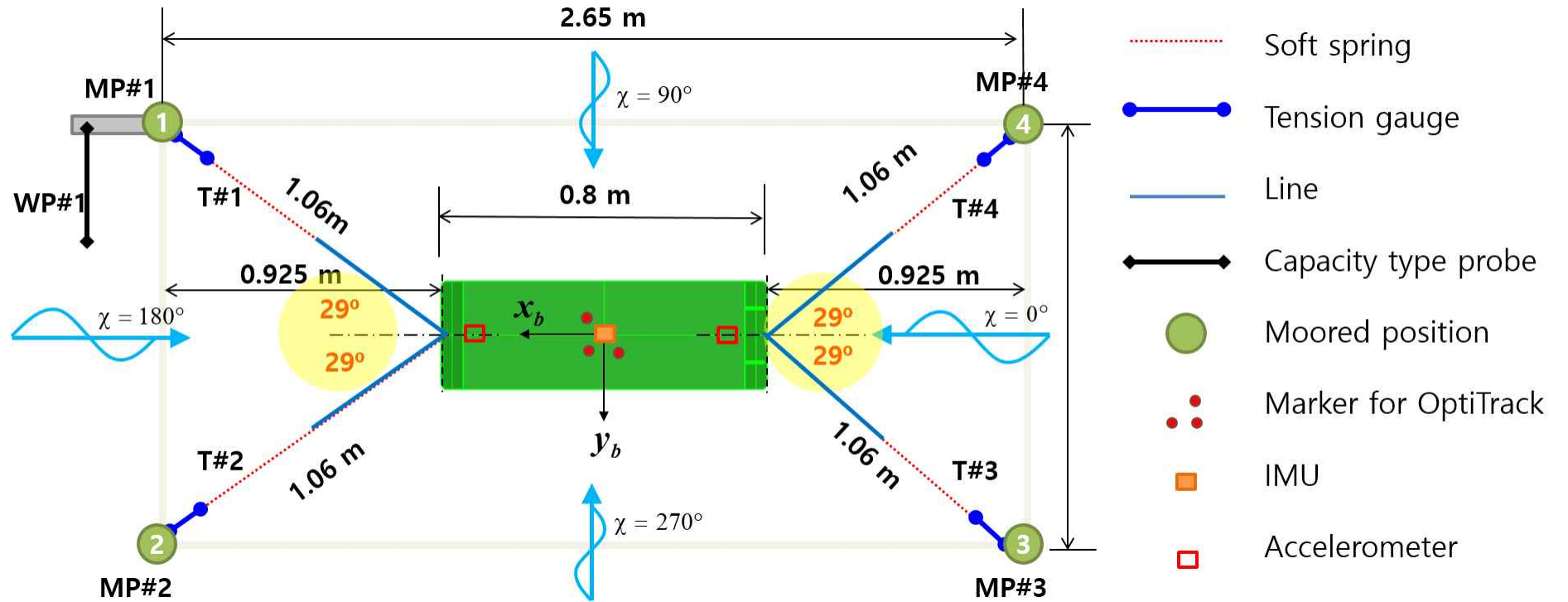


Fig. 3.32 Model ship installation schematic plan

### 3.3.2 Measurement sensors

Fig. 3.33 shows the wave probe installation in the 3D wave tank. It is placed at the support structure and front of the model ship. Fig. 3.34 shows the OptiTrack installation with the camera unit and makers in the model ship. The camera unit is installed with the distance so that it can catch the makers well. Besides, the black tape covers the model to remove the unwanted optical noise because the camera unit would identify any white color as a maker. On the other hand, two GoPro cameras are installed at front and lateral to record the ship's motion as shown in Fig. 3.35. And, Fig. 3.36 is data acquisition configuration of the measurement sensors installed on the carriage.

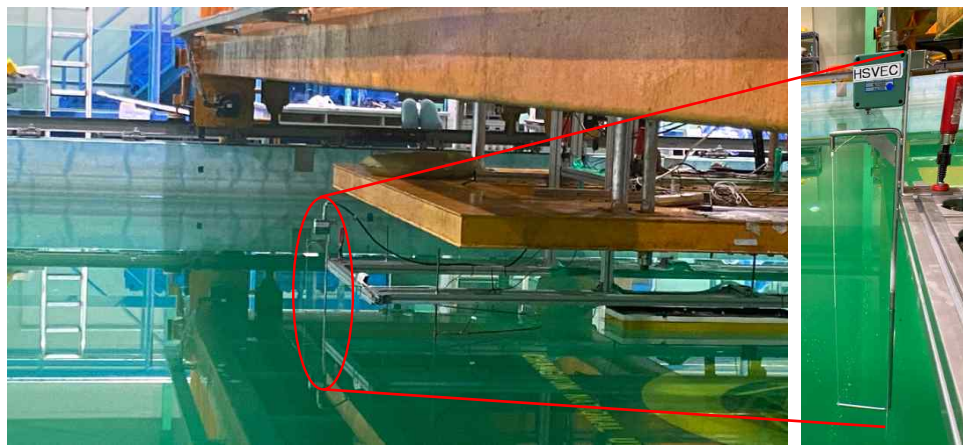


Fig. 3.33 Wave probe installation



Fig. 3.34 OptiTrack installation

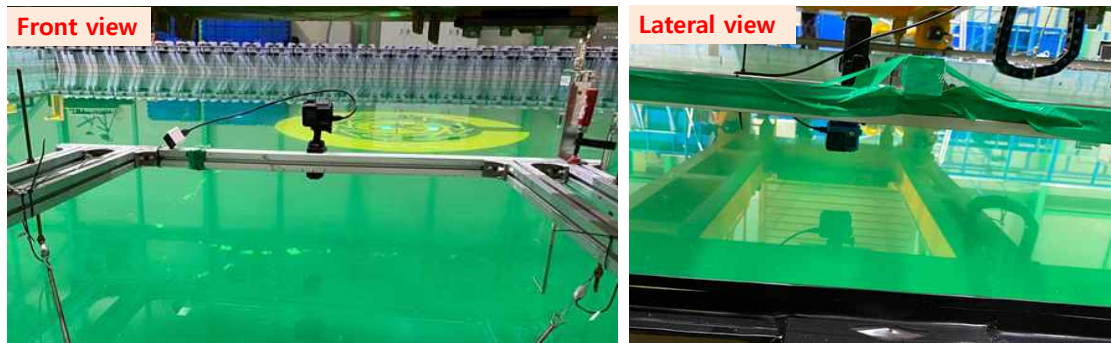


Fig. 3.35 Camera installation

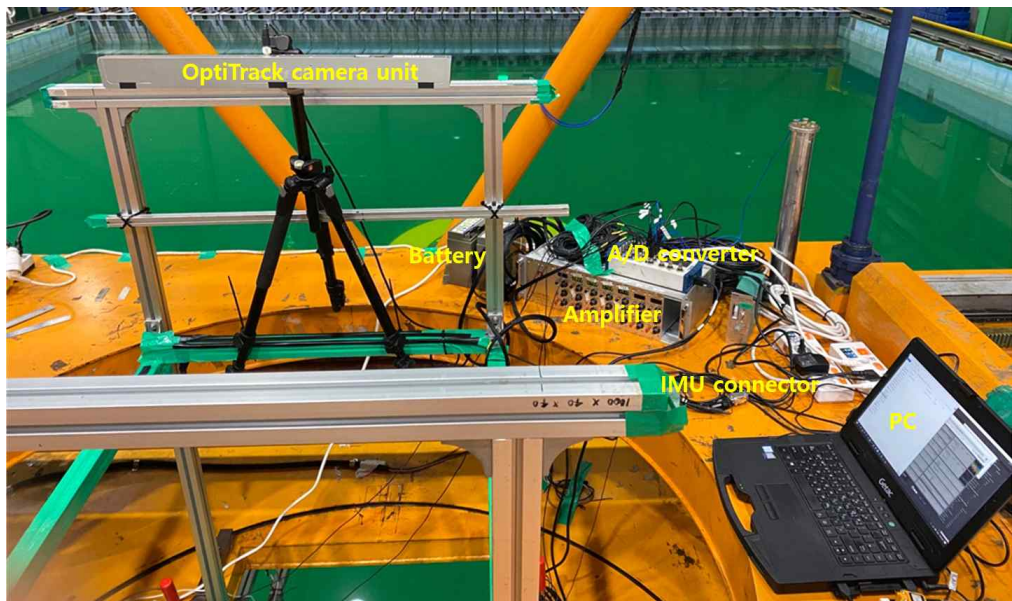


Fig. 3.36 Setup of data acquisition of measurement sensor

### 3.4 Data acquisition

The data acquired by the sensors are listed in Table 3.7.

Table 3.7 Data acquired by the sensors

Sensor	Data type
Wave probe	$\zeta$
OptiTrack	$x, y, z, \phi, \theta, \psi$
IMU	$\phi, \theta, \psi, p, q, r, \ddot{x}, \ddot{y}, \ddot{z}$
Tension gauge	$T_1, T_2, T_3, T_4$
Accelerometer	$\ddot{x}_{bow}, \ddot{y}_{bow}, \ddot{z}_{bow}, \ddot{x}_{stern}, \ddot{y}_{stern}, \ddot{z}_{stern}$

The data acquired by the wave probe, tension gauge, and accelerometer are taken in the data acquisition system with ten channels, as shown in Fig. 3.37. The signal from IMU is recorded in the MIP Monitor software and the signal from OptiTrack is given based on the recording the motion of the markers. During the installation, the coordinate systems of the accelerometer and OptiTrack could be different. Fig. 3.38 defines the coordinate system of the accelerometers at bow and stern. Fig. 3.39 describes the coordinate system of the OptiTrack. Based on this definition, the coordinate systems are redefined in Tables 3.8 and 3.9 for accelerometer and OptiTrack, respectively.

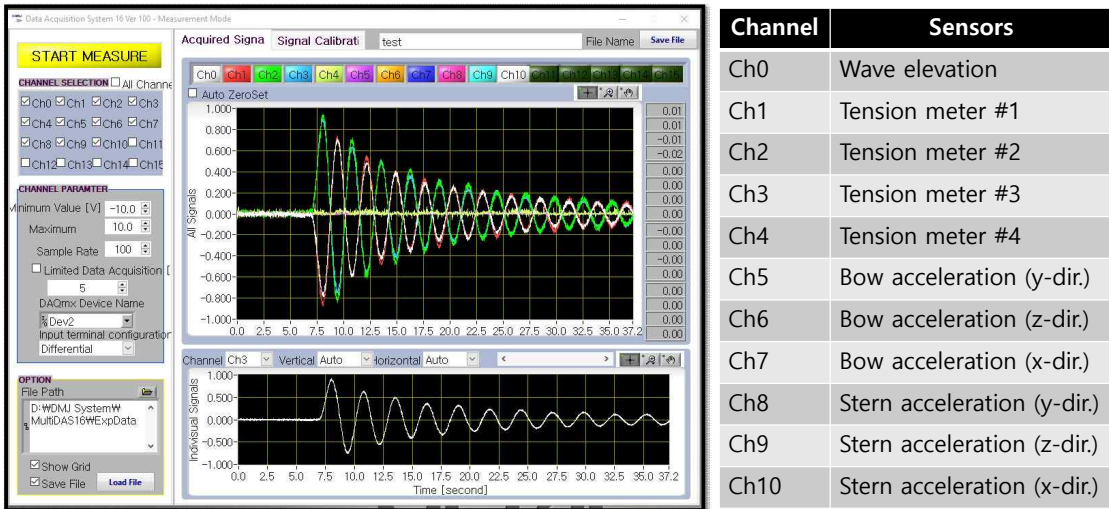


Fig. 3.37 Data acquisition SW

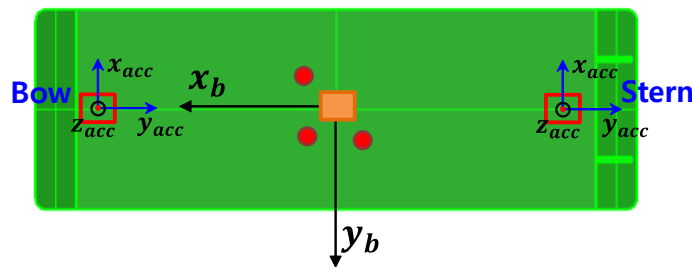


Fig. 3.38 Accelerometer coordinate system

Table 3.8 Definition of accelerometer coordinate system

Seakeeping	Accelerometer at bow	Accelerometer at stern
$x_b$	$-y_{acc}$	$-y_{acc}$
$y_b$	$-x_{acc}$	$-x_{acc}$
$z_b$	$z_{acc}$	$z_{acc}$

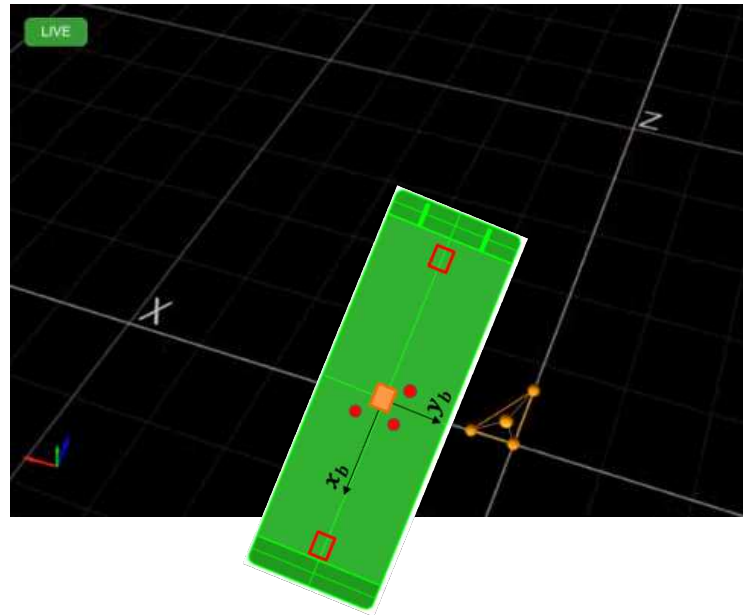


Fig. 3.39 OptiTrack coordinate system

Table 3.9 Definition of OptiTrack coordinate system

Seakeeping	OptiTrack
$x_b$	$-z_{OT}$
$y_b$	$-x_{OT}$
$z_b$	$y_{OT}$

On the other hand, the signal of rotation angle from OptiTrack is the quaternions. It is necessary to convert from quaternions to Euler angles. Then the process for transformation as follows.

- A unit quaternion

$$e = [\varepsilon_1 \varepsilon_2 \varepsilon_3 \eta]^T \quad (3.8)$$

- This parameterization implies that the Euler parameters satisfy the constraint  $e^T e = 1$

$$\varepsilon_1^2 + \varepsilon_2^2 + \varepsilon_3^2 + 1 = 1 \quad (3.9)$$

- The transformation matrix is expressed as follows,

$$E_1(e) = \begin{bmatrix} 1 - 2(\varepsilon_2^2 + \varepsilon_3^2) & 2(\varepsilon_1\varepsilon_2 - \varepsilon_3\eta) & 2(\varepsilon_1\varepsilon_3 + \varepsilon_2\eta) \\ 2(\varepsilon_1\varepsilon_2 + \varepsilon_3\eta) & 1 - 2(\varepsilon_1^2 + \varepsilon_3^2) & 2(\varepsilon_2\varepsilon_3 - \varepsilon_1\eta) \\ 2(\varepsilon_1\varepsilon_3 - \varepsilon_2\eta) & 2(\varepsilon_2\varepsilon_3 + \varepsilon_1\eta) & 1 - 2(\varepsilon_1^2 + \varepsilon_2^2) \end{bmatrix} \quad (3.10)$$

### 3.5 Decay test

#### 3.5.1 Spring selection

According to ITTC recommendation, the model ship can be restrained in surge or towed with a spring system. Spring should be selected resulting in a resonance frequency at least a factor 2 lower than the lowest wave encounter frequency. We opt for two springs with 9 N/m and 15 N/m stiffness to perform decay test at zero speed in calm water for horizontal motion based on this recommendation. The frequencies of each spring are taken to compare with a factor 2 lower than lowest wave encounter frequency. Table 3.10 shows the decay test results for two springs and it can be seen that spring stiffness 9 N/m satisfies surge and sway motion, while spring stiffness 15 N/m does not satisfy surge motion compared with reference encounter frequency. Therefore, spring stiffness 9 N/m was selected for further test.

Table 3.10 Decay results for two spring

Motion	$k = 9 \text{ N/m}$		$k = 15 \text{ N/m}$		$0.5\omega_e$ (reference freq.)
	Period (s)	Freq. (rad/s)	Period (s)	Freq. (rad/s)	
Surge	3.020	2.081	2.382	2.638	2.100
Sway	4.520	1.390	3.645	1.724	2.100
Yaw	1.500	4.189	1.228	5.116	2.100

#### 3.5.2 Free ship decay

Free ship decay is performed without a mooring system for three motions

that can recover in calm water. We performed free decay for heave, roll, and pitch with three times repeatedly. Figs. 3.40 and 3.41 show the time series of free roll and pitch decay test, respectively. Table 3.11 depicts the period of free ship decay for heave, roll, and pitch.

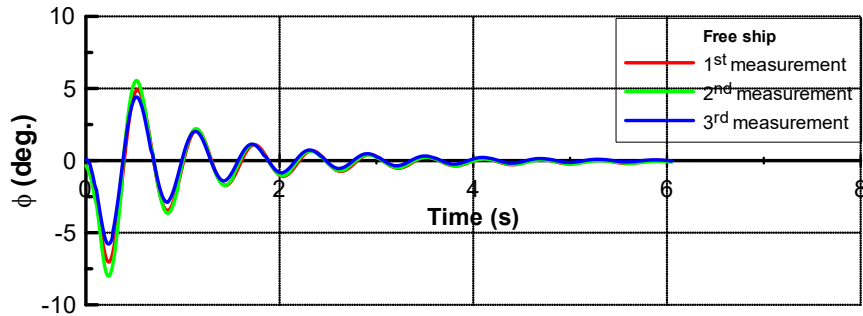


Fig. 3.40 Time series of free roll decay test

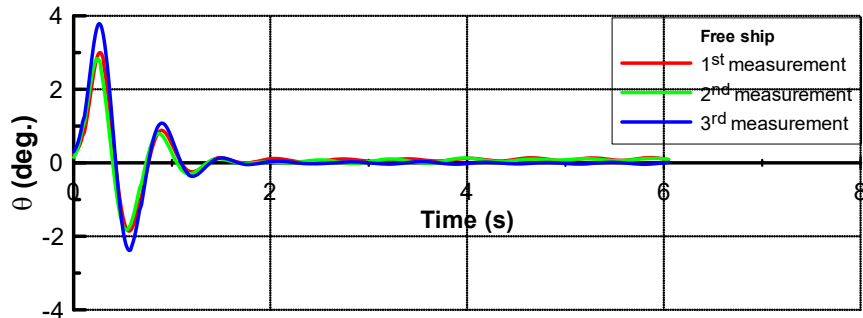


Fig. 3.41 Time series of free pitch decay test

Table 3.11 Period of free ship decay

No.	Heave (s)	Roll (s)	Pitch (s)
1	0.670	0.603	0.630
2	0.660	0.603	0.620
3	0.670	0.600	0.630
Mean	0.667	0.602	0.627

### 3.5.3 Ship decay with soft mooring

After selecting the spring stiffness 9 N/m in section 3.5.1, the ship decay tests were performed for 6-DOF motion with the soft mooring system at various speed conditions. Measurements were performed three times in all motion and speed conditions. Figs. 3.42~3.47 show the time series of ship

decay tests for surge, sway, heave, roll, pitch, and yaw, respectively. Tables 3.12 and 3.13 depict the period of ship decay for translational and rotational motion. Because the mooring system affects the vertical motion, the periods of heave and pitch at zero speed are slightly slower than the case of free ship motion. However, the period of roll motion is not different between with and without the mooring system. According to speed condition, the period of all motion is slightly slower at higher speeds (6 knots), but it is slightly faster at very low speeds (2 knots) comparing with zero speed. This is clearly observed at surge, sway, heave, pitch, and yaw motion. The period of roll motion does not change due to speed condition.

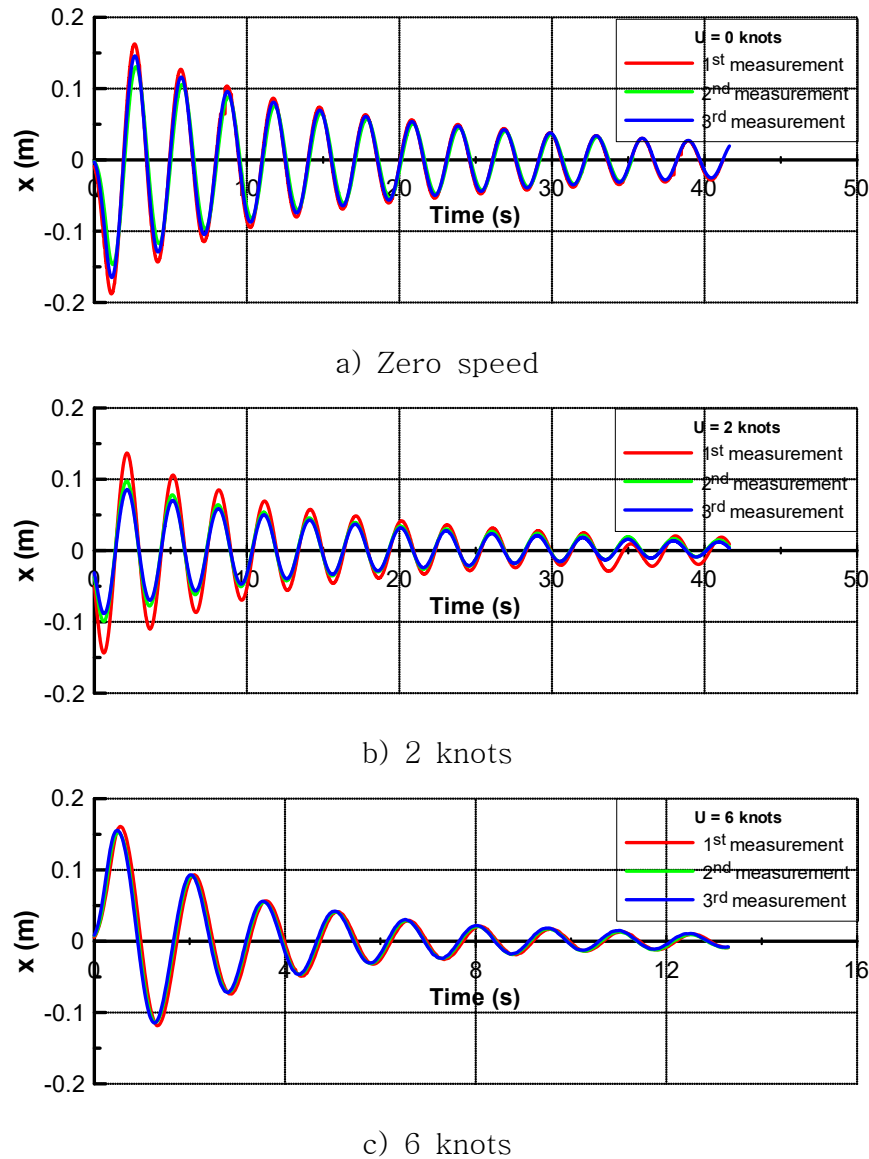
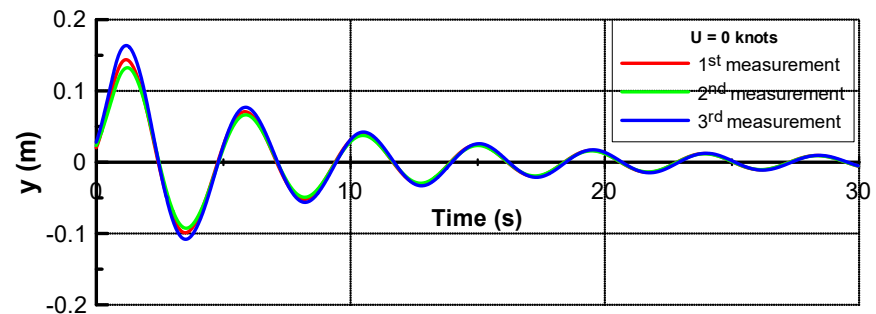
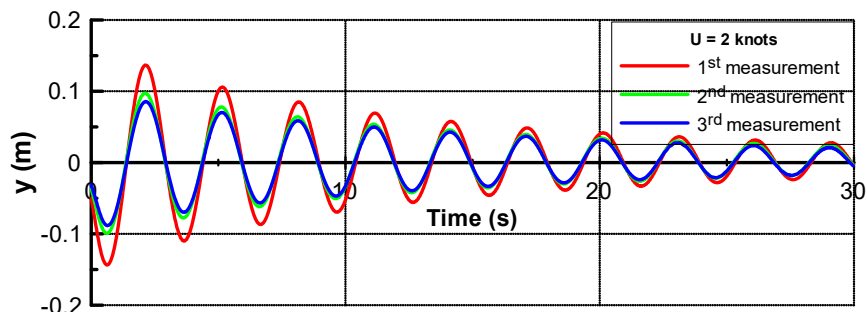


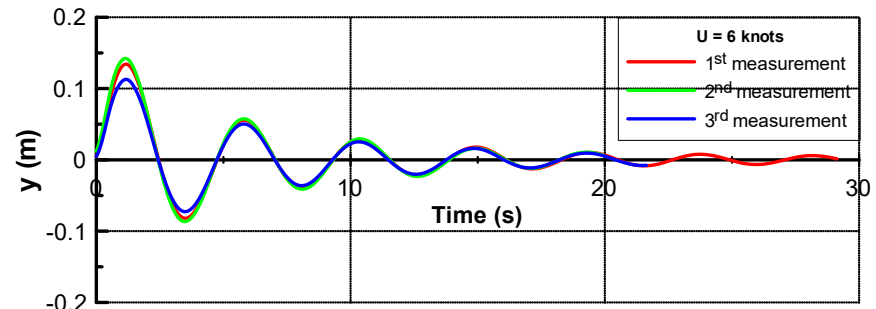
Fig. 3.42 Time series of surge decay



a) Zero speed

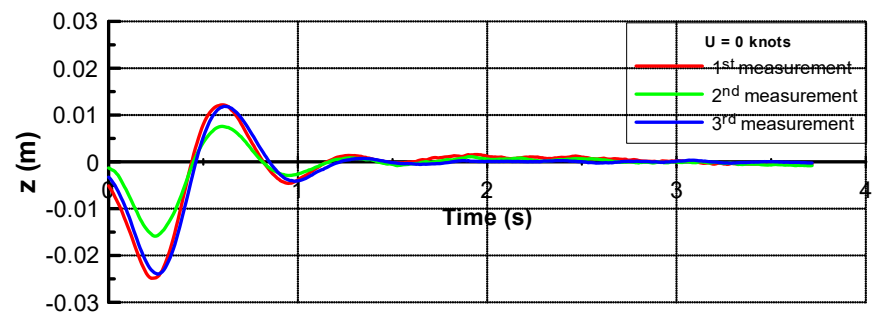


b) 2 knots

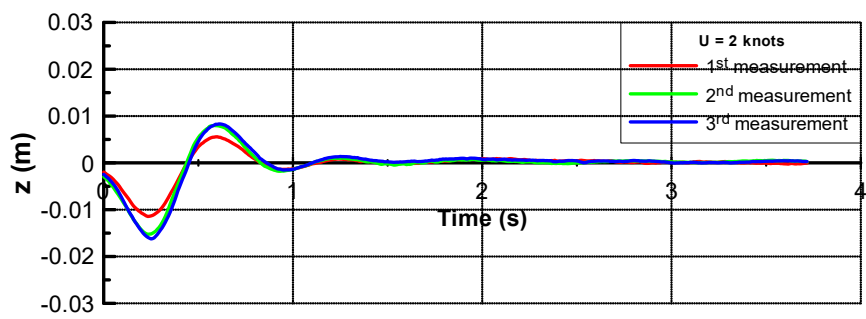


c) 6 knots

Fig. 3.43 Time series of sway decay



a) Zero speed



b) 2 knots

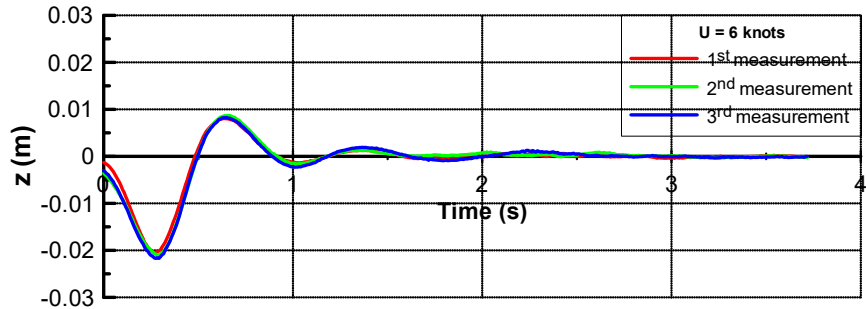
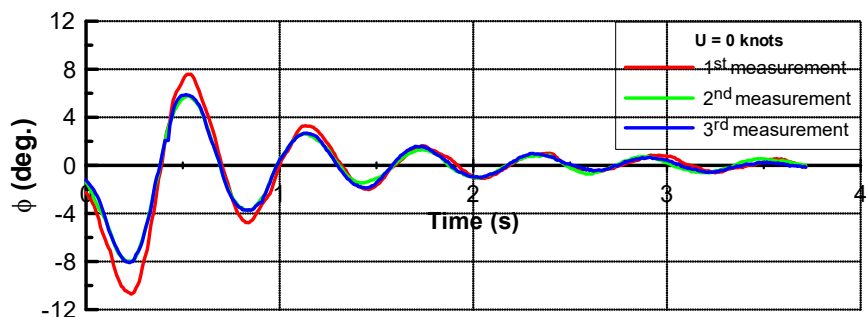
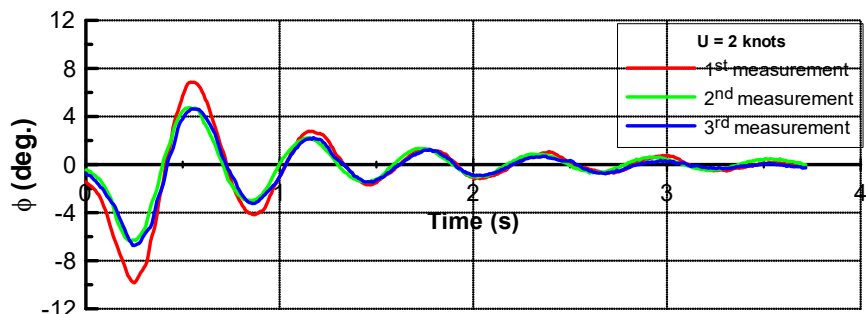
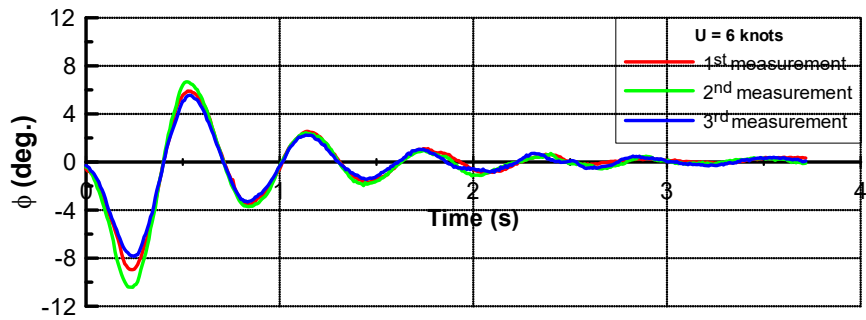


Fig. 3.44 Time series of heave decay



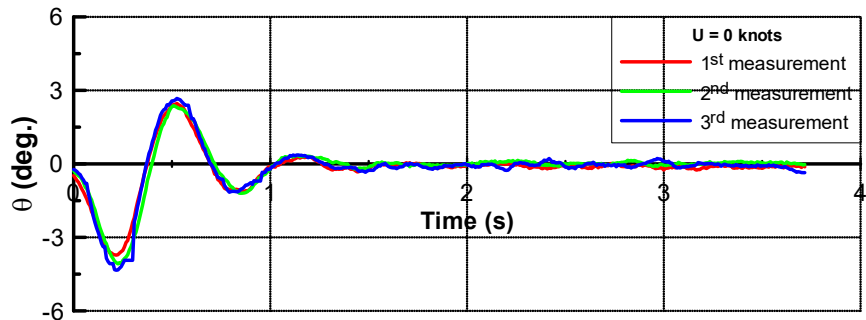
a) Zero speed



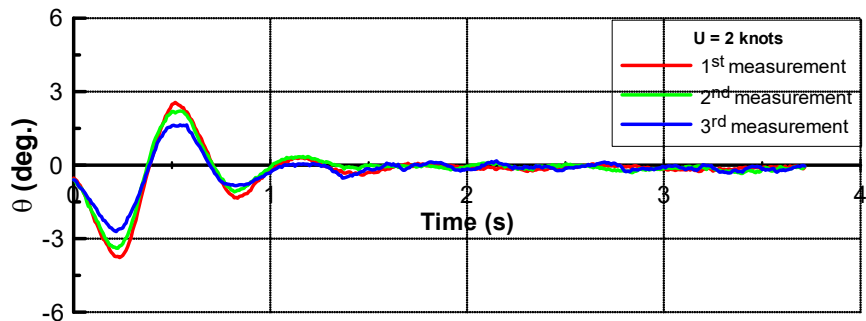


c) 6 knots

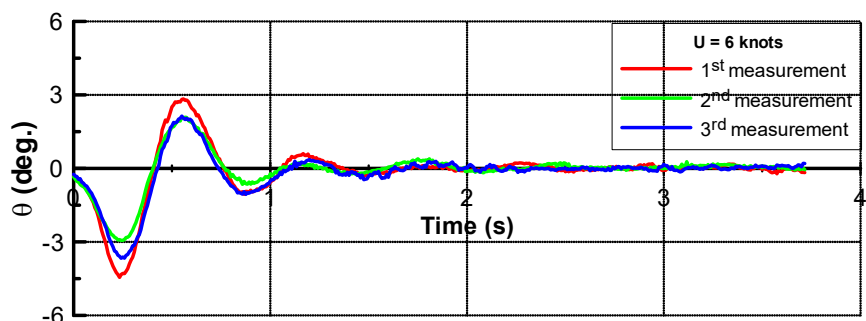
Fig. 3.45 Time series of roll decay



a) Zero speed



b) 2 knots



c) 6 knots

Fig. 3.46 Time series of pitch decay

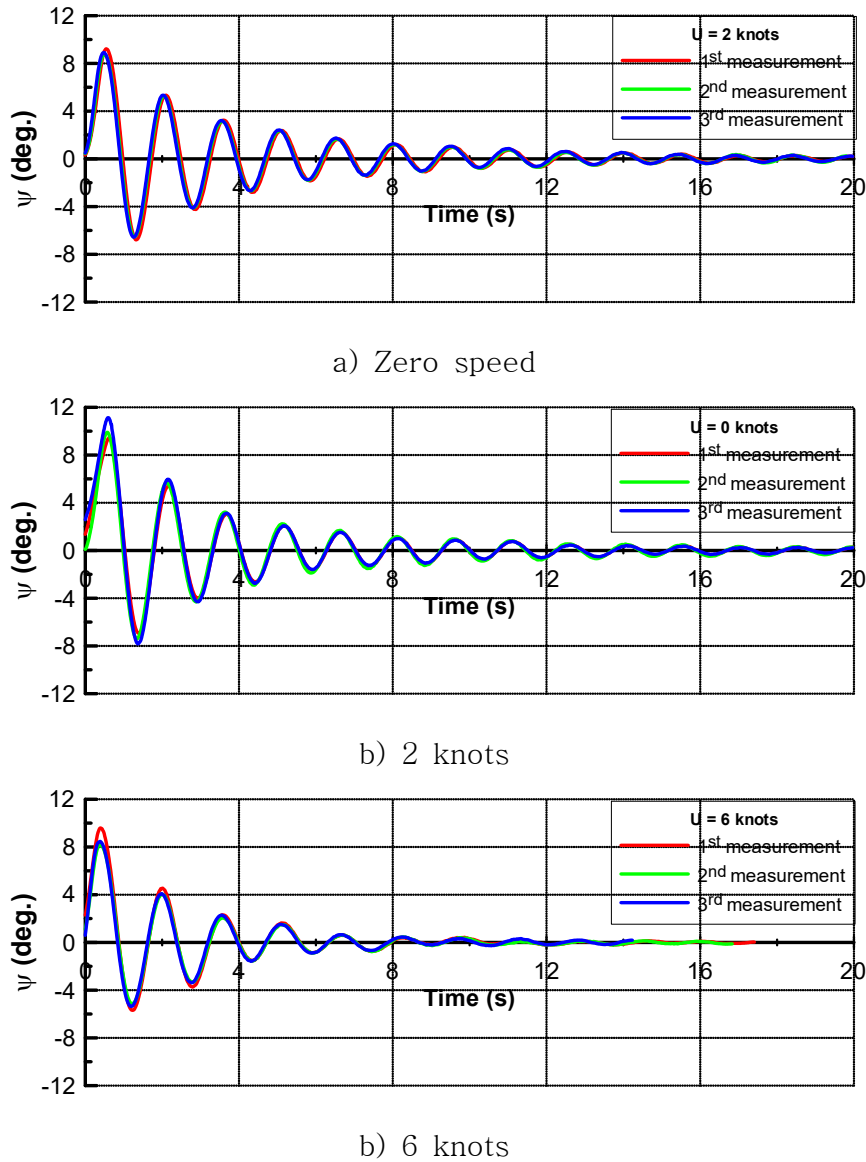


Fig. 3.47 Time series of yaw decay

Table 3.12 Period of ship decay for translational motion with soft mooring

No.	Surge (s)			Sway (s)			Heave (s)		
	0 knots	2 knots	6 knots	0 knots	2 knots	6 knots	0 knots	2 knots	6 knots
1	3.018	3.000	3.123	4.540	4.493	4.533	0.683	0.642	0.725
2	3.020	2.992	3.097	4.520	4.493	4.535	0.675	0.675	0.742
3	3.023	2.992	3.126	4.500	4.517	4.542	0.682	0.642	0.708
Mean	3.020	2.995	3.115	4.520	4.501	4.537	0.680	0.653	0.725

Table 3.13 Period of ship decay for rotational motion with soft mooring

No.	Roll (s)			Pitch (s)			Yaw (s)		
	0 knots	2 knots	6 knots	0 knots	2 knots	6 knots	0 knots	2 knots	6 knots
1	0.600	0.603	0.603	0.600	0.585	0.620	1.500	1.500	1.563
2	0.593	0.598	0.600	0.600	0.590	0.620	1.500	1.500	1.567
3	0.603	0.592	0.595	0.607	0.590	0.613	1.500	1.500	1.556
Mean	0.598	0.598	0.599	0.602	0.588	0.618	1.500	1.500	1.562

### 3.6 Seakeeping performance in regular waves

Ship motion tests in regular waves were carried out in the 3D wave tank to measure the wave force acting on the model ship, vertical acceleration, and 6-DOF motion. The seakeeping tests for model ship were performed for seven wave directions at zero speed, 0.147 m/s, and 0.441 m/s according to the full-scale ship speed 0, 2, and 6 knots. The motions in regular waves were analyzed using Fourier analysis. The Fourier coefficients for harmonic motion can be obtained through the least squares method. Figs. 3.48~3.50 are the examples of the result of frequency fitting of time series for wave force, vertical acceleration, and 6-DOF motion measured by tension gauge, accelerometer, and OptiTrack for different speed conditions.

- The definition of harmonic motion is expressed as Eq. (3.11),

$$z(t) = a_0 + a_1 \cos(\omega t) + a_2 \sin(\omega t) \quad (3.11)$$

- Fourier coefficients are calculated as Eq. (3.12),

$$\underline{\beta} = [a_1 \ a_2 \ a_3]^T \quad (3.12)$$

- Fourier coefficient vector can be obtained as Eq. (3.13).

$$\underline{\beta} = (H^T H)^{-1} H^T \underline{Z} \quad (3.13)$$

$$H = \begin{bmatrix} 1 & \cos\omega t_1 & \sin\omega t_1 \\ 1 & \cos\omega t_2 & \sin\omega t_2 \\ \vdots & \vdots & \vdots \\ 1 & \cos\omega t_n & \sin\omega t_n \end{bmatrix} \quad (3.14)$$

$$Z = [z(t_1) \ z(t_2) \ \dots \ z(t_n)]^T \quad (3.15)$$

On the other hand, wave force is analyzed using Fourier analysis in the form of a fourth harmonic function as Eq. (3.16)

$$f(t) = f_0 + f_1 \cos(\omega_e t + \varepsilon_1) + f_2 \cos(2\omega_e t + \varepsilon_2) + f_3 \cos(3\omega_e t + \varepsilon_3) + f_4 \cos(4\omega_e t + \varepsilon_4) \quad (3.16)$$

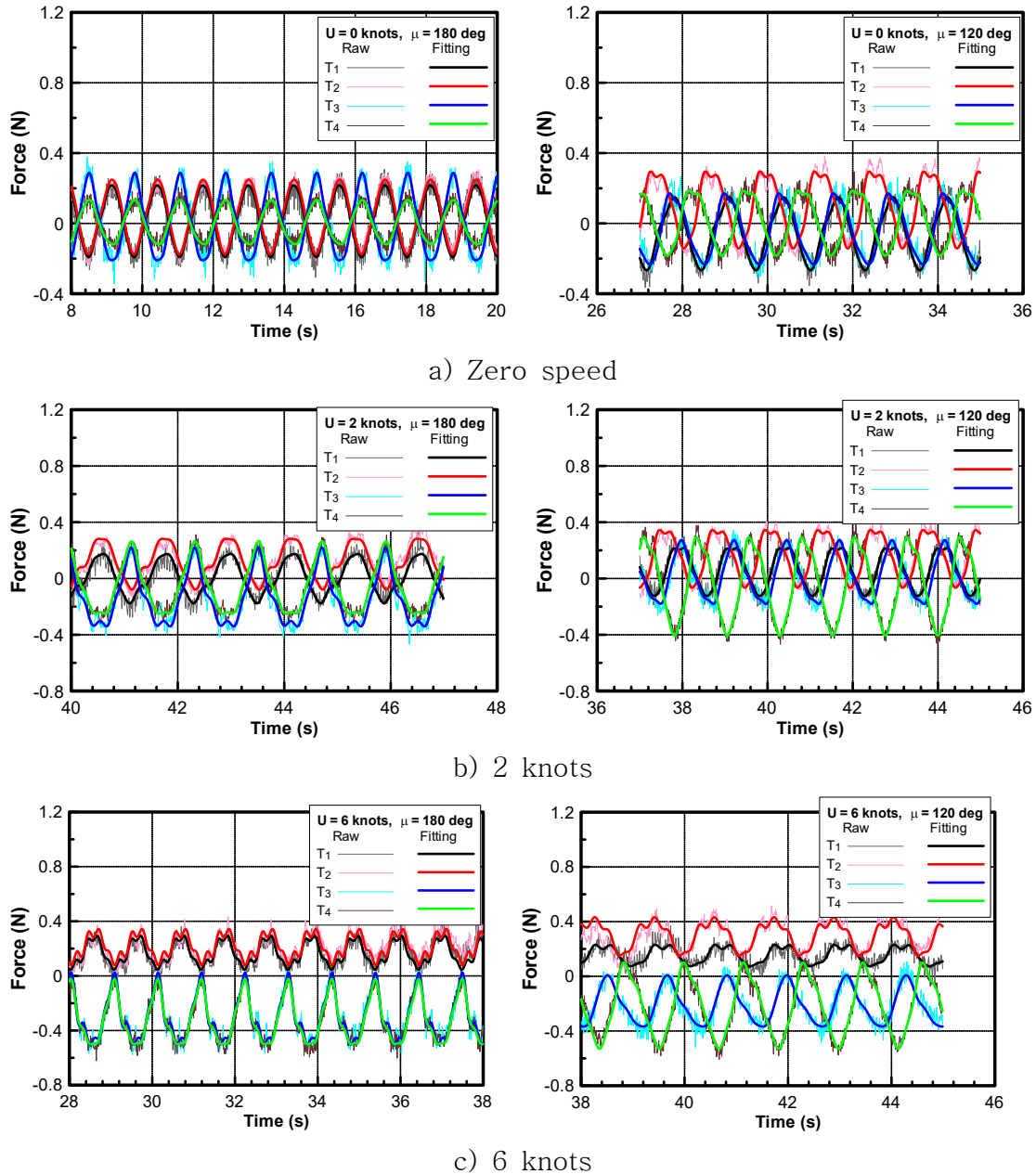
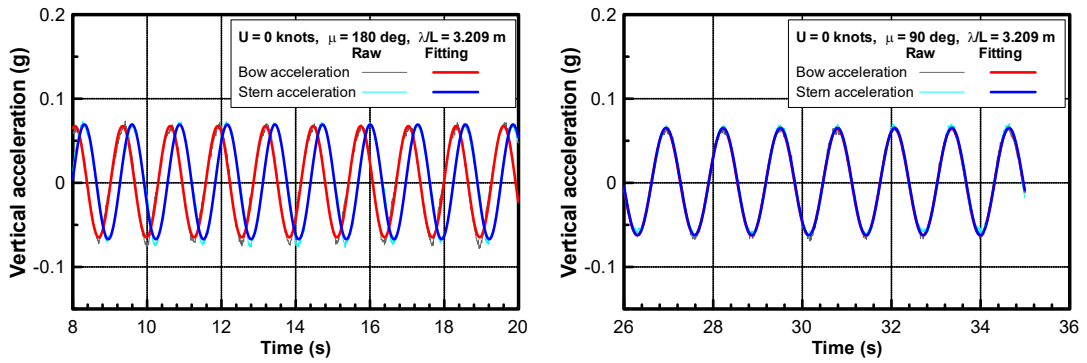
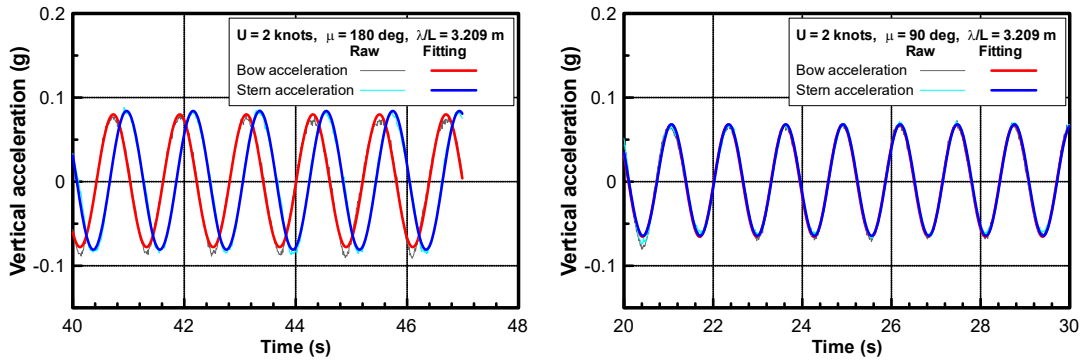


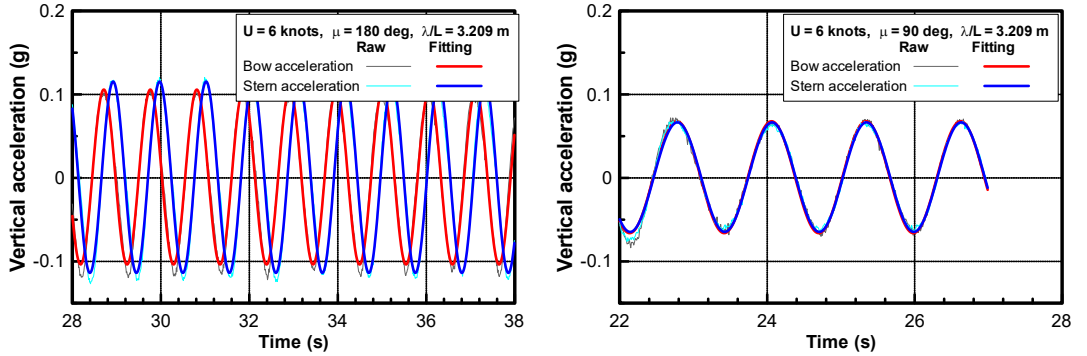
Fig. 3.48 Time series of wave force measured by tension gauges



a) Zero speed

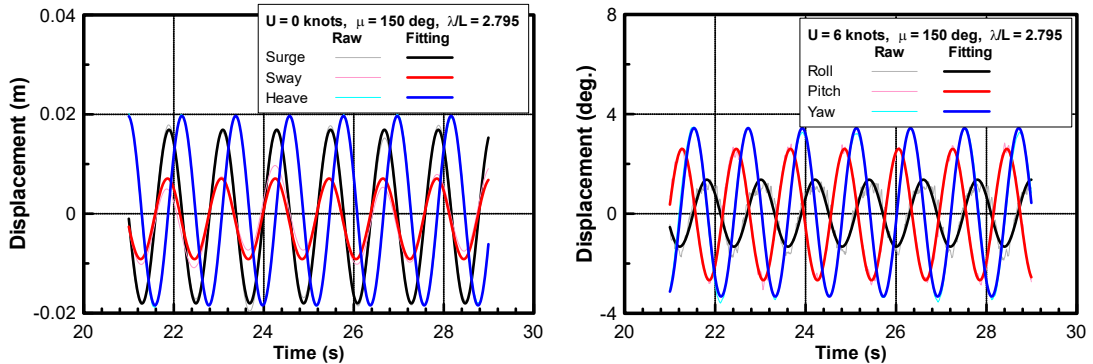


b) 2 knots



c) 6 knots

Fig. 3.49 Time series of vertical acceleration measured by accelerometers



a) Zero speed

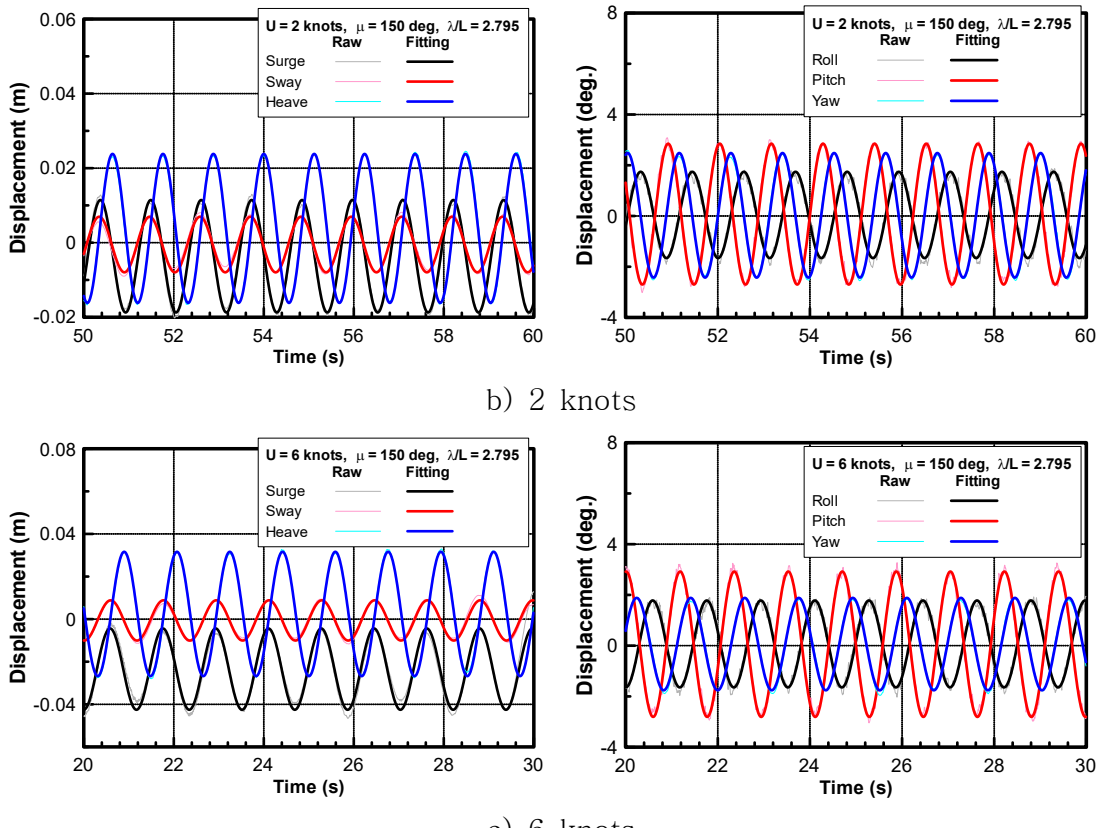


Fig. 3.50 Time series of 6-DOF motion measured by OptiTrack

### 3.6.1 Wave drift force

Wave force was measured using four tension gauges located at four mooring line angles connecting to the support structure. Fig. 3.51 shows the wave force analysis scheme. Then, the surge force, sway force and yaw moment of the model ship in waves are calculated by Eq. (3.17). Eq. (3.18) expresses the non-dimensional wave drift force acting on the ship.

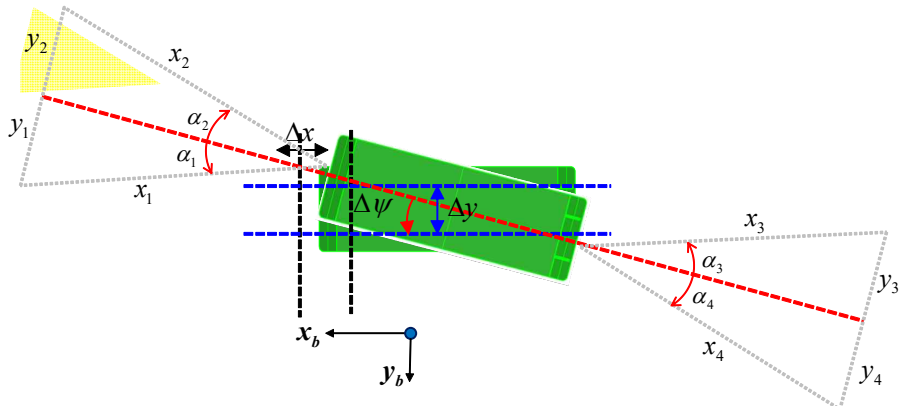


Fig. 3.51 Wave force analysis scheme

- Calculation of wave drift force:

$$\bar{X}_w = T_1 \cos \alpha_1 + T_2 \cos \alpha_2 - T_3 \cos \alpha_3 - T_4 \cos \alpha_4 \quad (3.17)$$

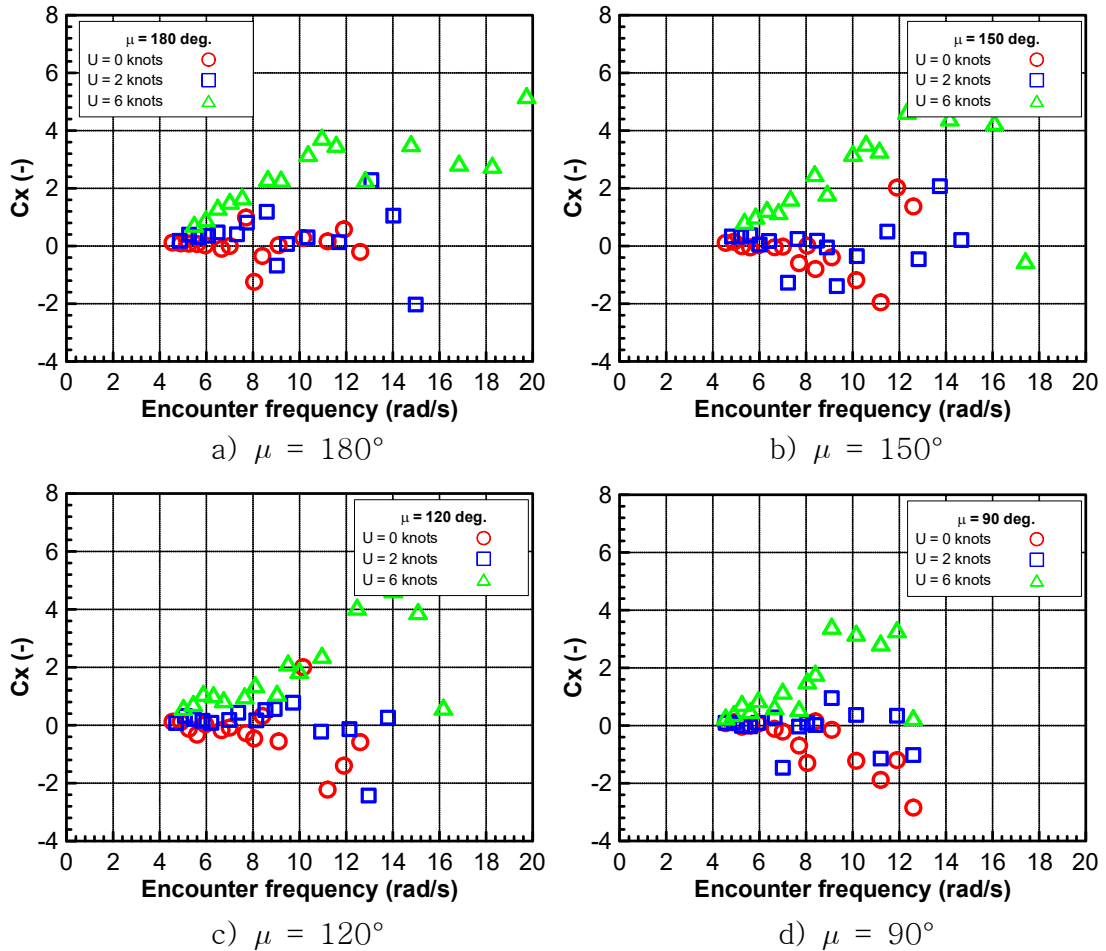
$$\bar{Y}_w = T_1 \sin \alpha_1 - T_2 \sin \alpha_2 - T_3 \sin \alpha_3 + T_4 \sin \alpha_4$$

$$\bar{N}_w = x_{Tf} (T_1 \sin \alpha_1 - T_2 \sin \alpha_2) + x_{Ta} (-T_3 \sin \alpha_3 + T_4 \sin \alpha_4)$$

- Non-dimensional wave drift force:

$$\begin{cases} C_x = \frac{X_w - R_{calm}}{\rho g h_a^2 B^2 / L} \\ C_y = \frac{Y_w}{\rho g h_a^2 B^2 / L} \\ C_n = \frac{N_w}{\rho g h_a^2 B^2} \end{cases} \quad (3.18)$$

Figs. 3.52~3.54 show wave drift force and moment depending on speed and incident wave direction with respect to encounter frequency. It can be seen that wave drift force increases following speed. However, the results at zero speed and 2 knots show comparatively different aspect.



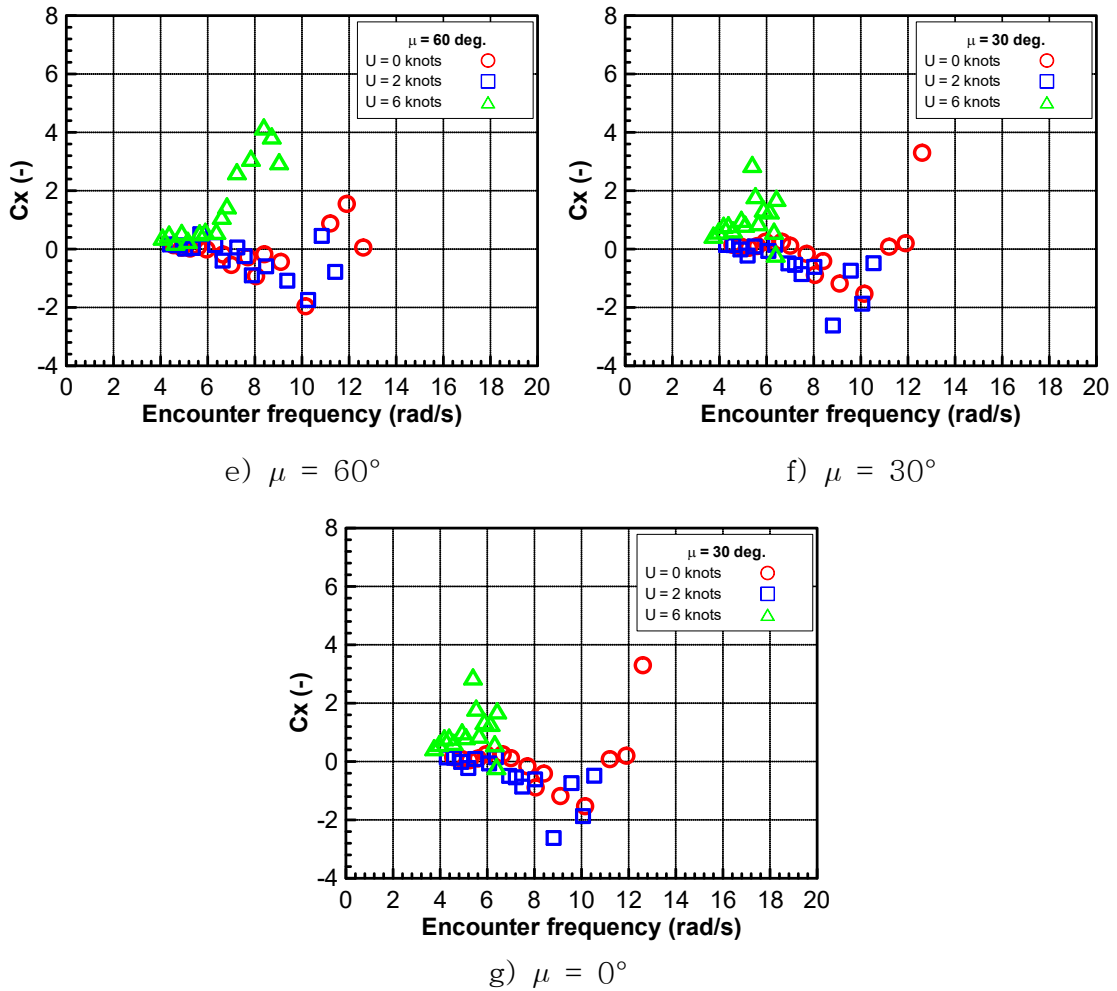
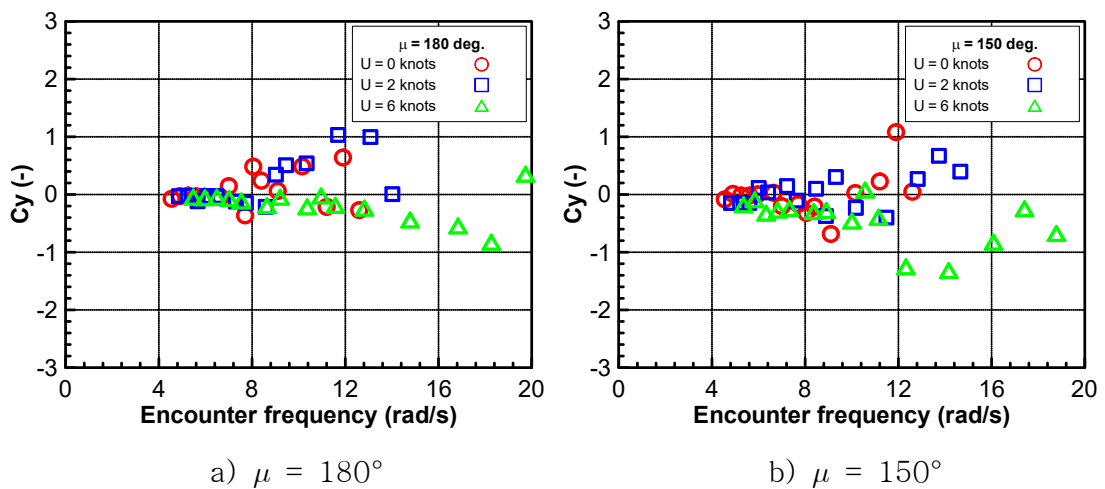


Fig. 3.52 Additional resistance by speed and incident wave direction



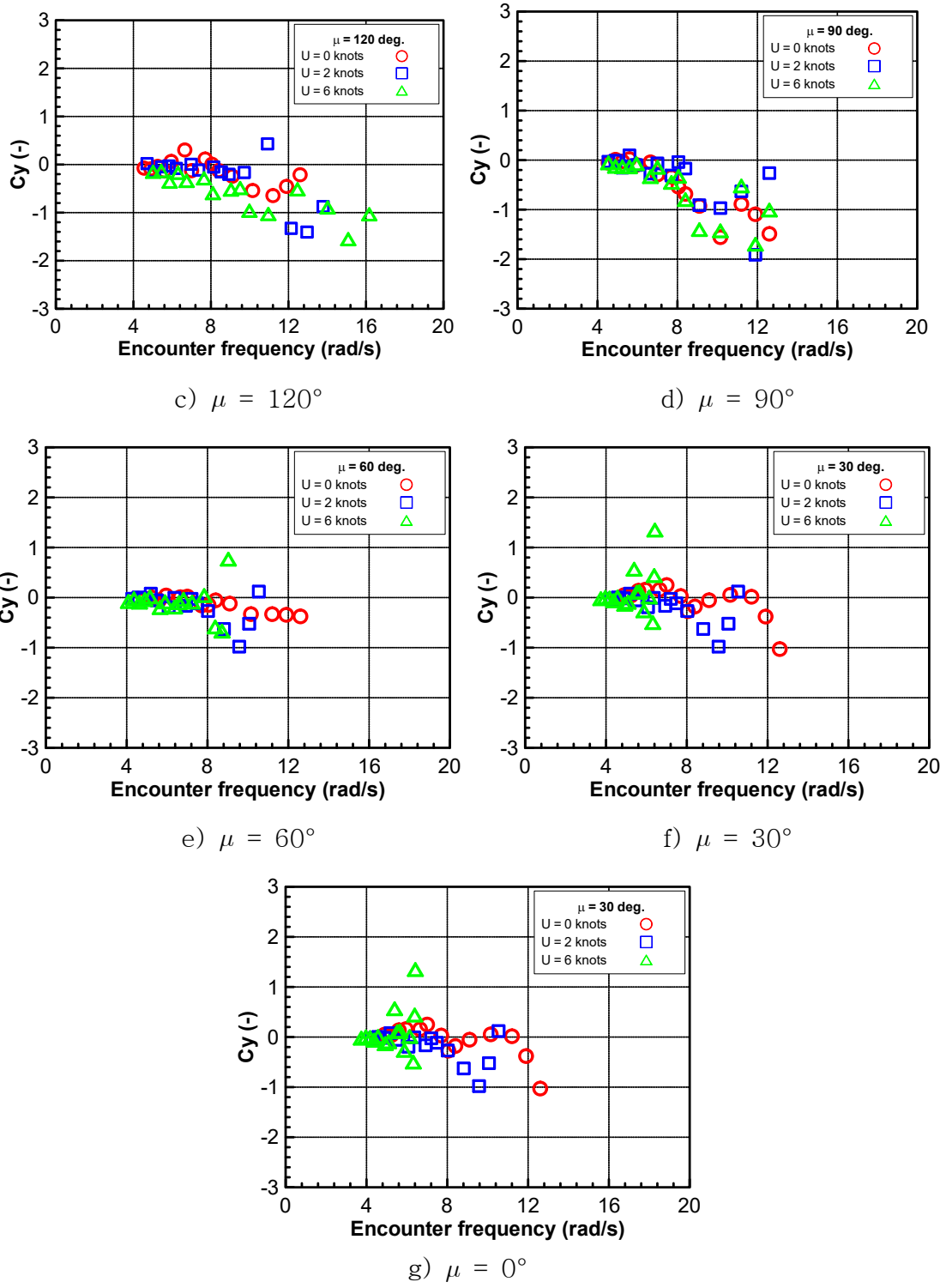
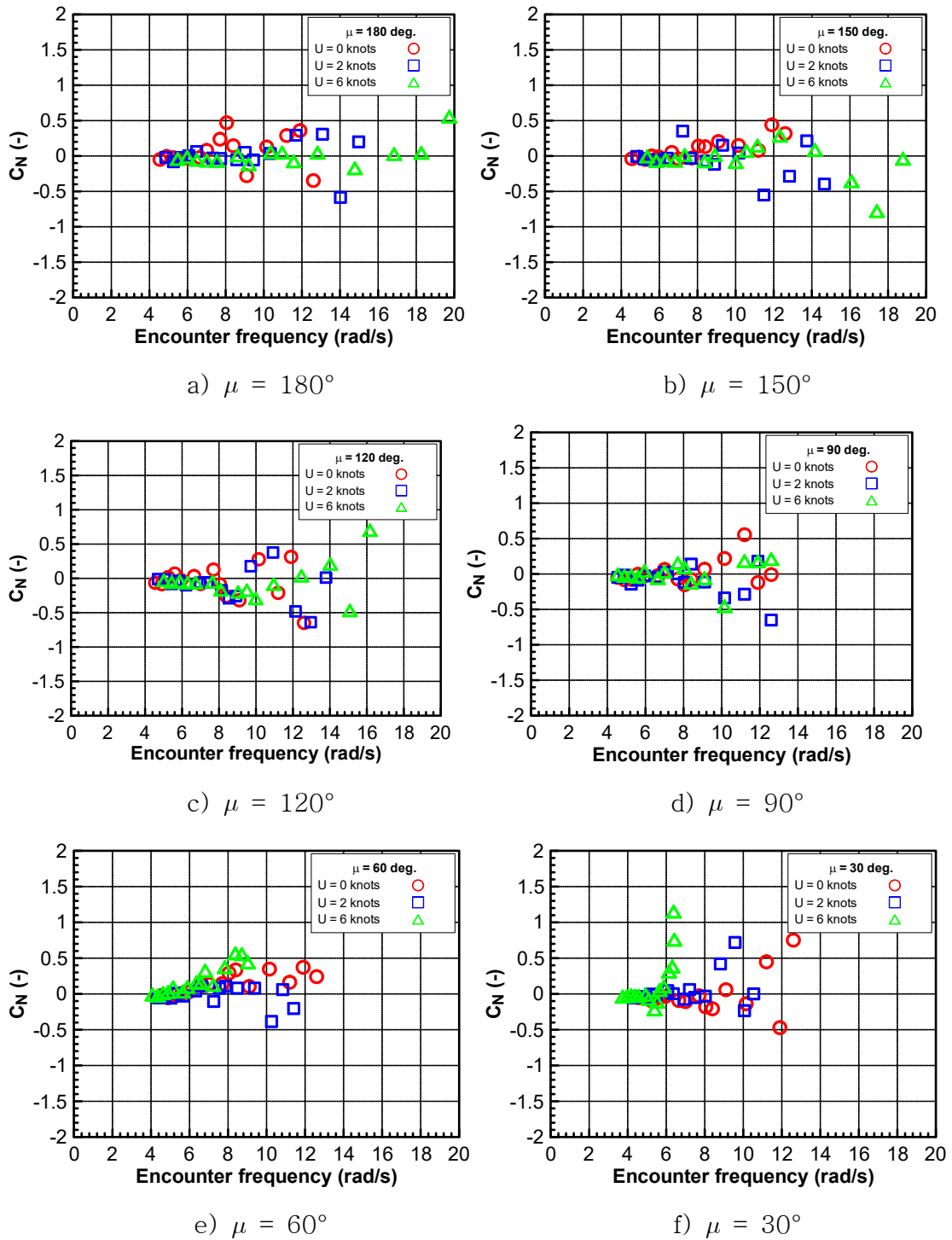
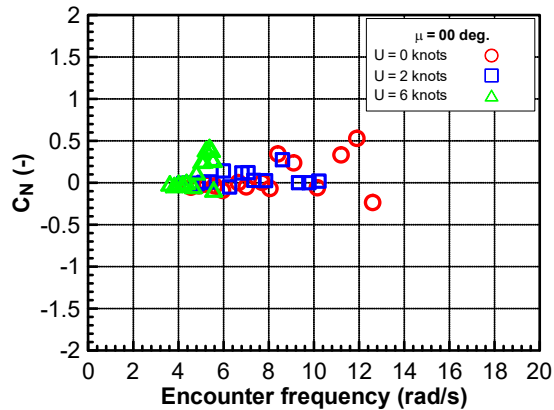


Fig. 3.53 Lateral wave-induced force by speed and incident wave direction



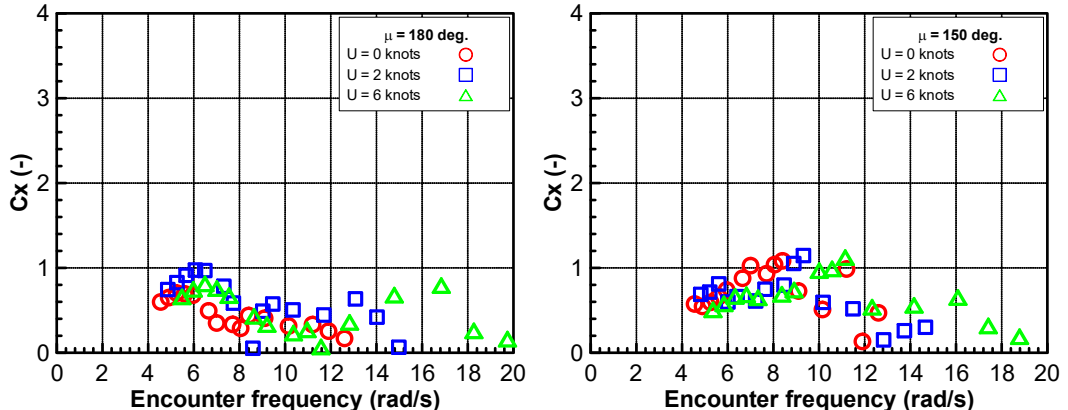


f)  $\mu = 00^\circ$

Fig. 3.54 Yaw wave-induced moment by speed and incident wave direction

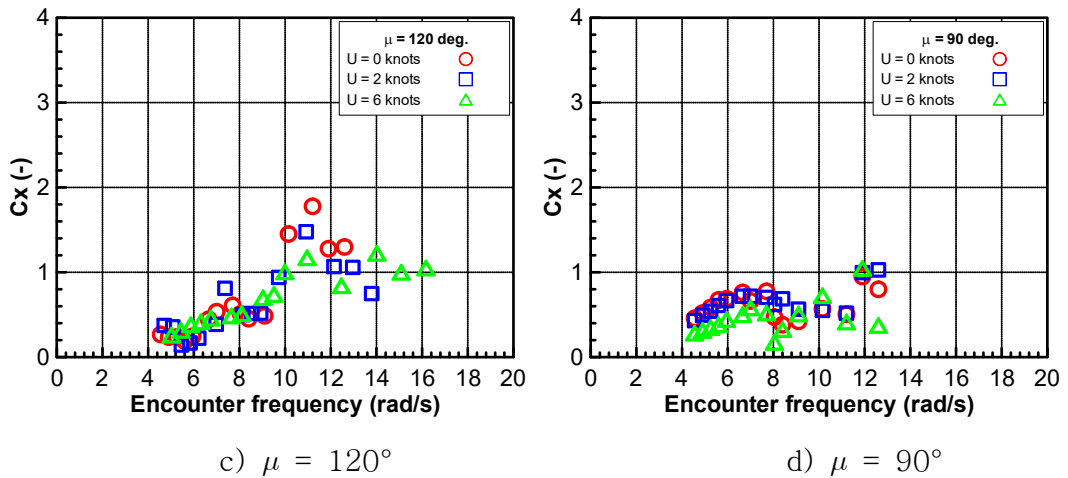
### 3.6.2 First-order wave force

Figs. 3.55~3.57 show the first-order wave force and moment by speed and incident wave direction versus encounter frequency. Speed effect is not clear on the first-order wave force and moment.



a)  $\mu = 180^\circ$

b)  $\mu = 150^\circ$



c)  $\mu = 120^\circ$

d)  $\mu = 90^\circ$

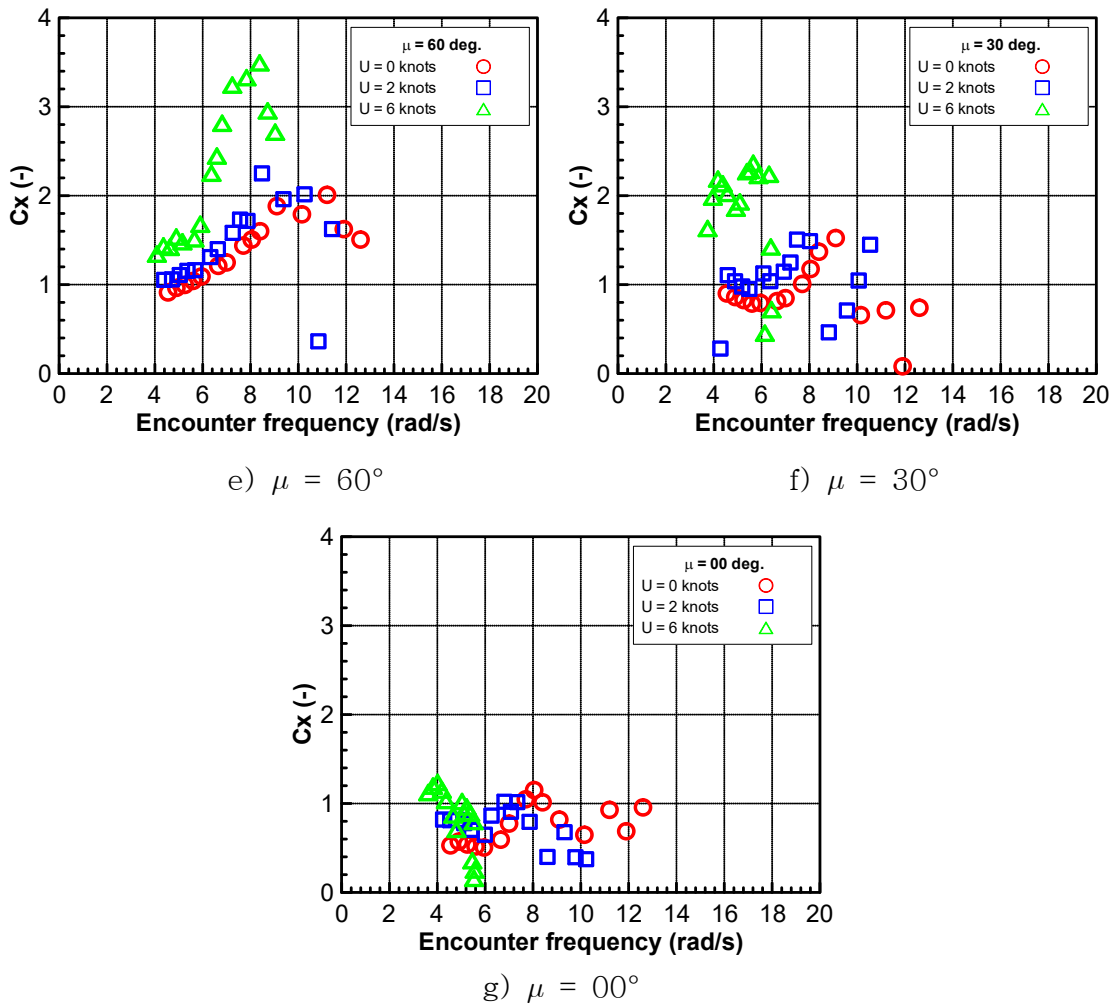
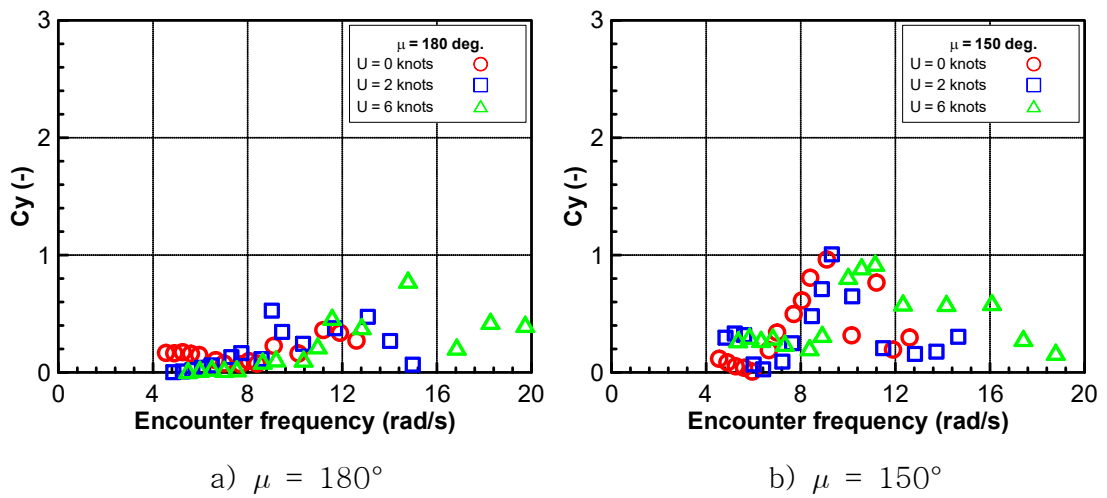


Fig. 3.55 First-order surge force by speed and incident wave direction



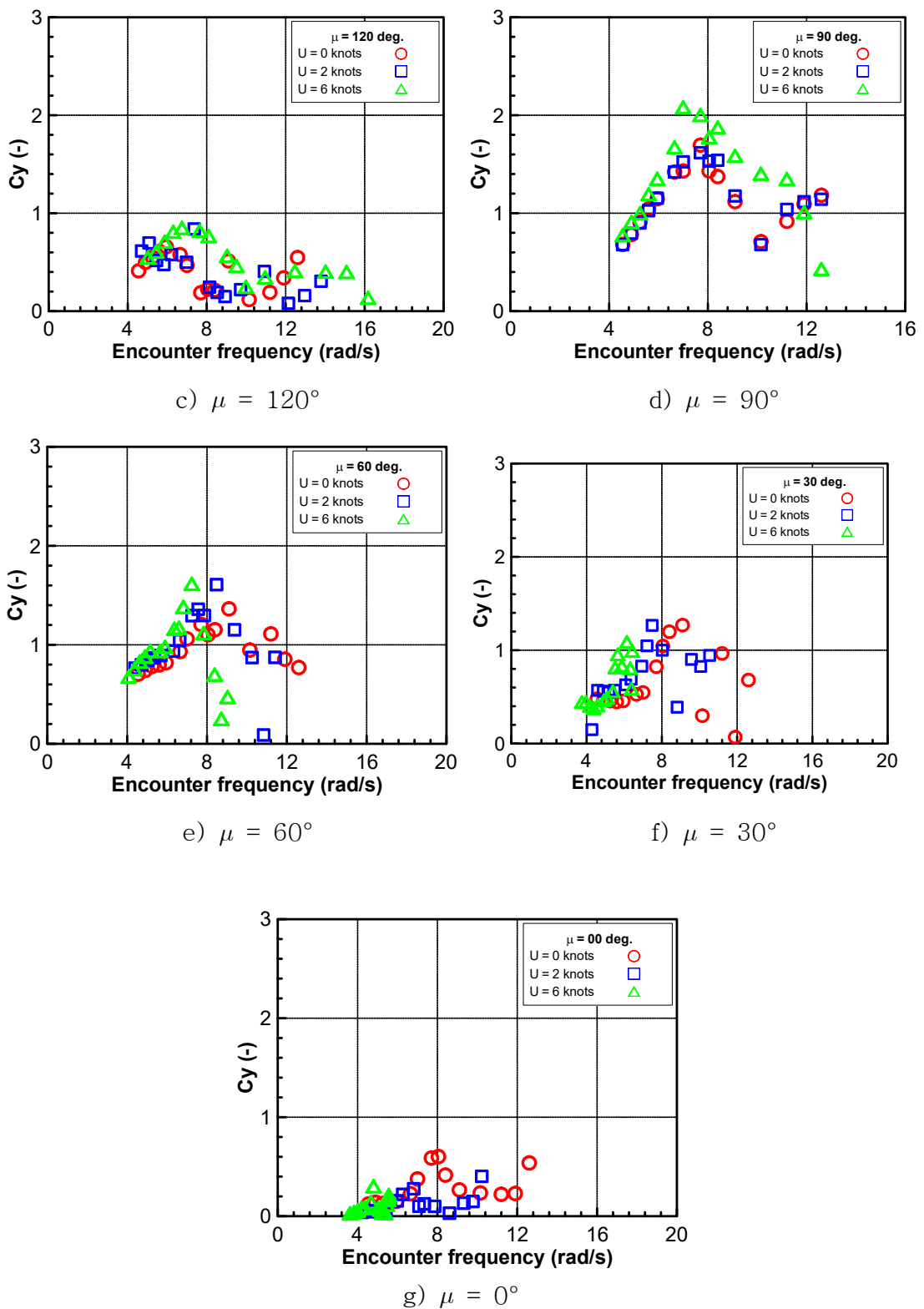
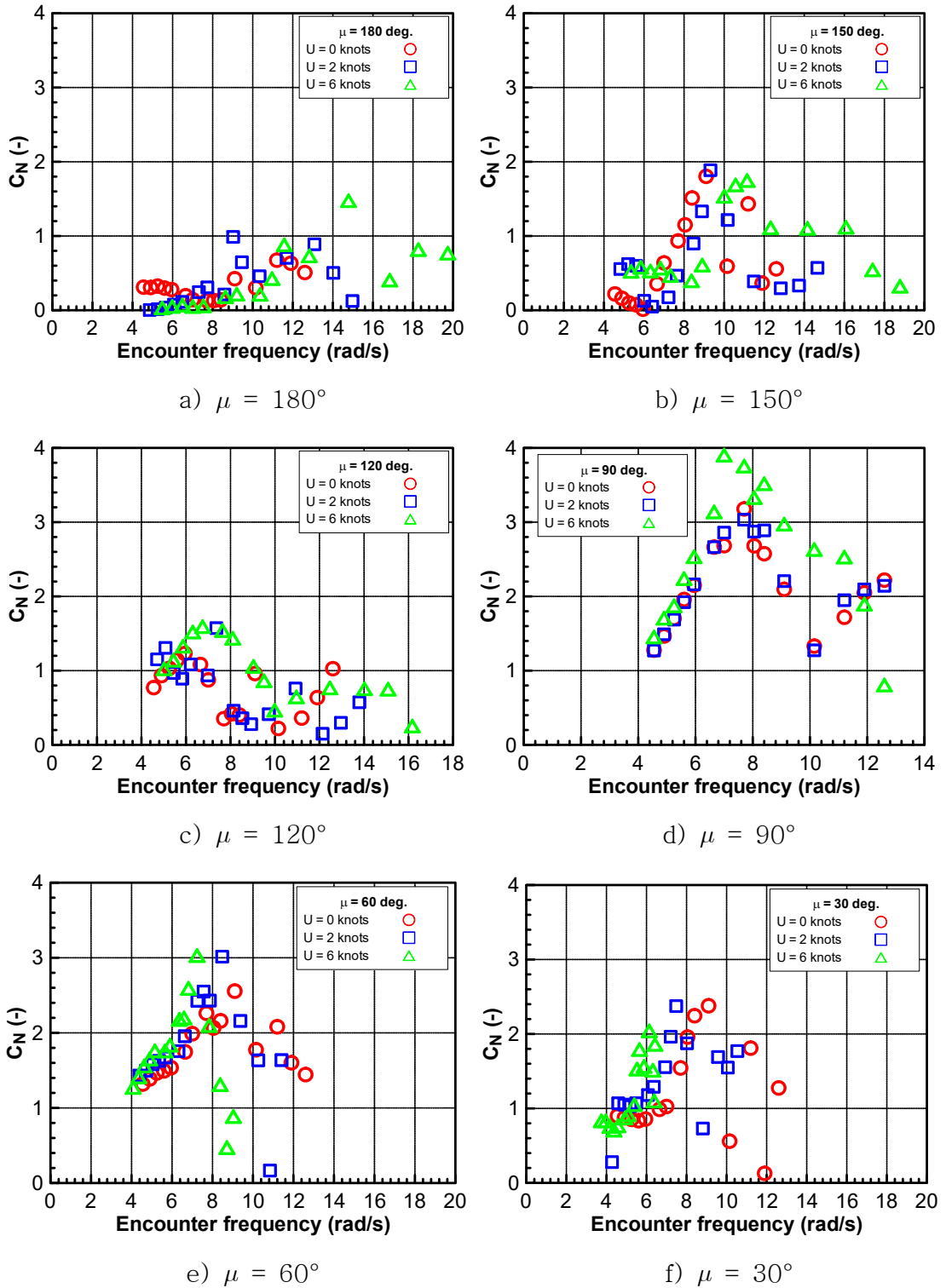
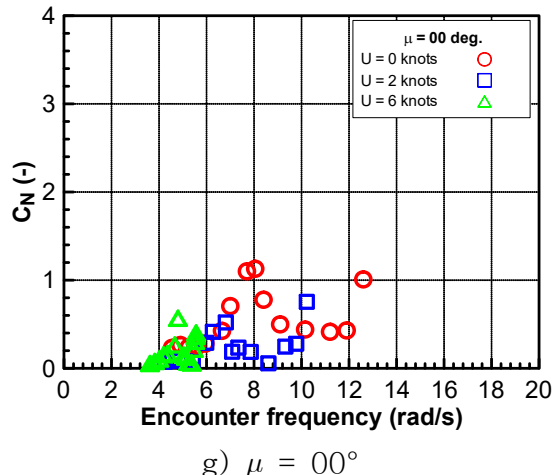


Fig. 3.56 First-order sway force by speed and incident wave direction



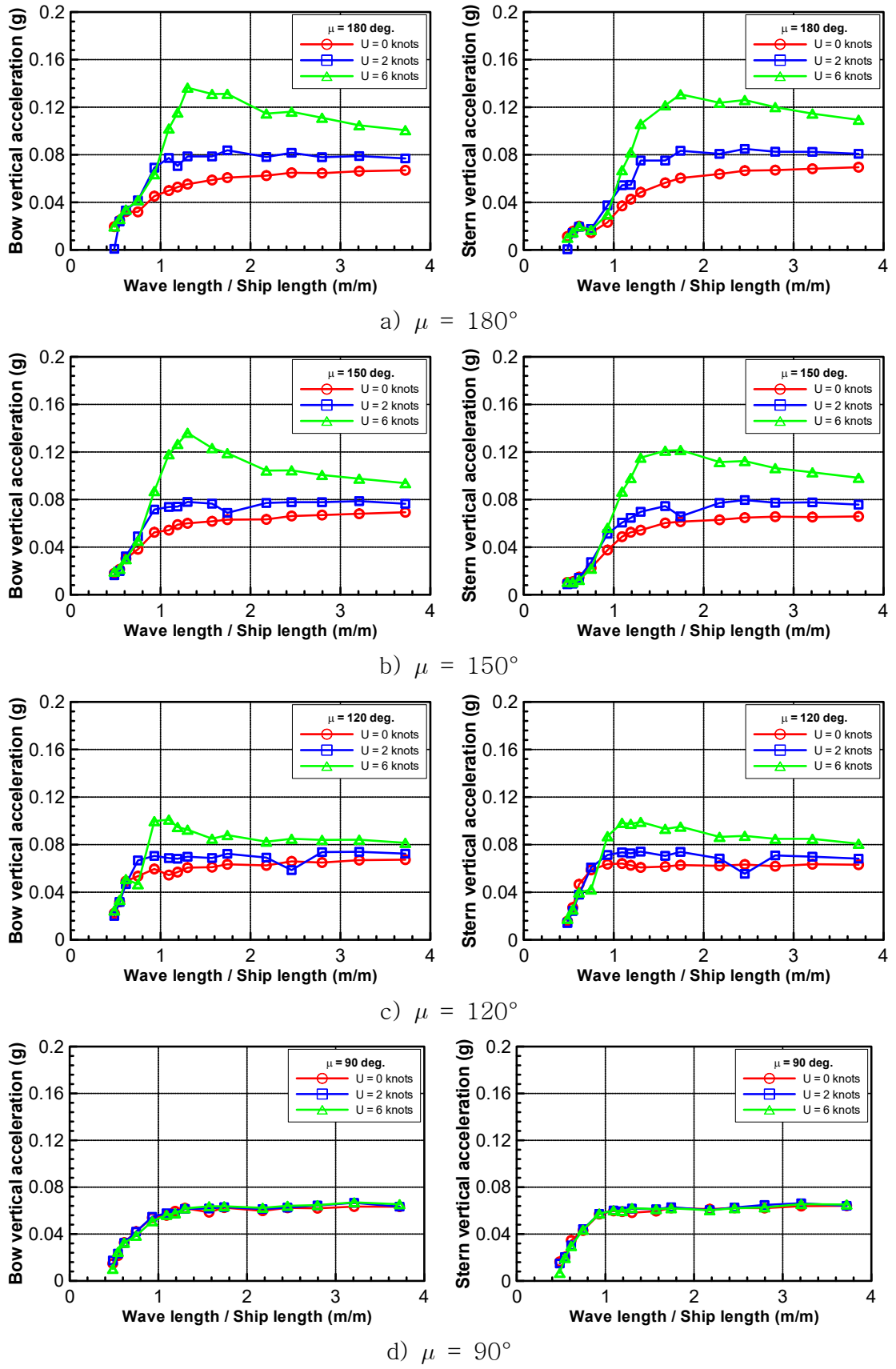


g)  $\mu = 00^\circ$

Fig. 3.57 First-order yaw moment by speed and incident wave direction

### 3.6.3 Vertical acceleration

Vertical acceleration was measured by accelerometers located at bow and stern of model ship. Fig. 3.58 shows results of vertical acceleration response at bow and stern in regular waves by speed and incident wave direction. The horizontal axis of the graph is a dimensionless value by dividing the wavelength to the ship length, and the vertical axis is a dimensionless value by dividing the acceleration to gravitational acceleration ( $9.81 \text{ m/s}^2$ ). As the result, it is confirmed that the magnitude of vertical acceleration increases in head waves and it reduces gradually to beam waves and following waves. This can be clearly observed in 6 knots. In the case of zero speed and 2 knots, the vertical acceleration decreases from head waves to beam waves, and it is almost unchanged at stern quartering waves and following waves. On the other hand, due to the symmetrical shape of the model ship, the vertical acceleration at the bow and stern is similar. According to speed conditions, the vertical acceleration at faster speed increases from head waves to beam waves, however, it decreases from beam waves to following waves. Further, the vertical acceleration at various speed conditions is the same at beam waves.



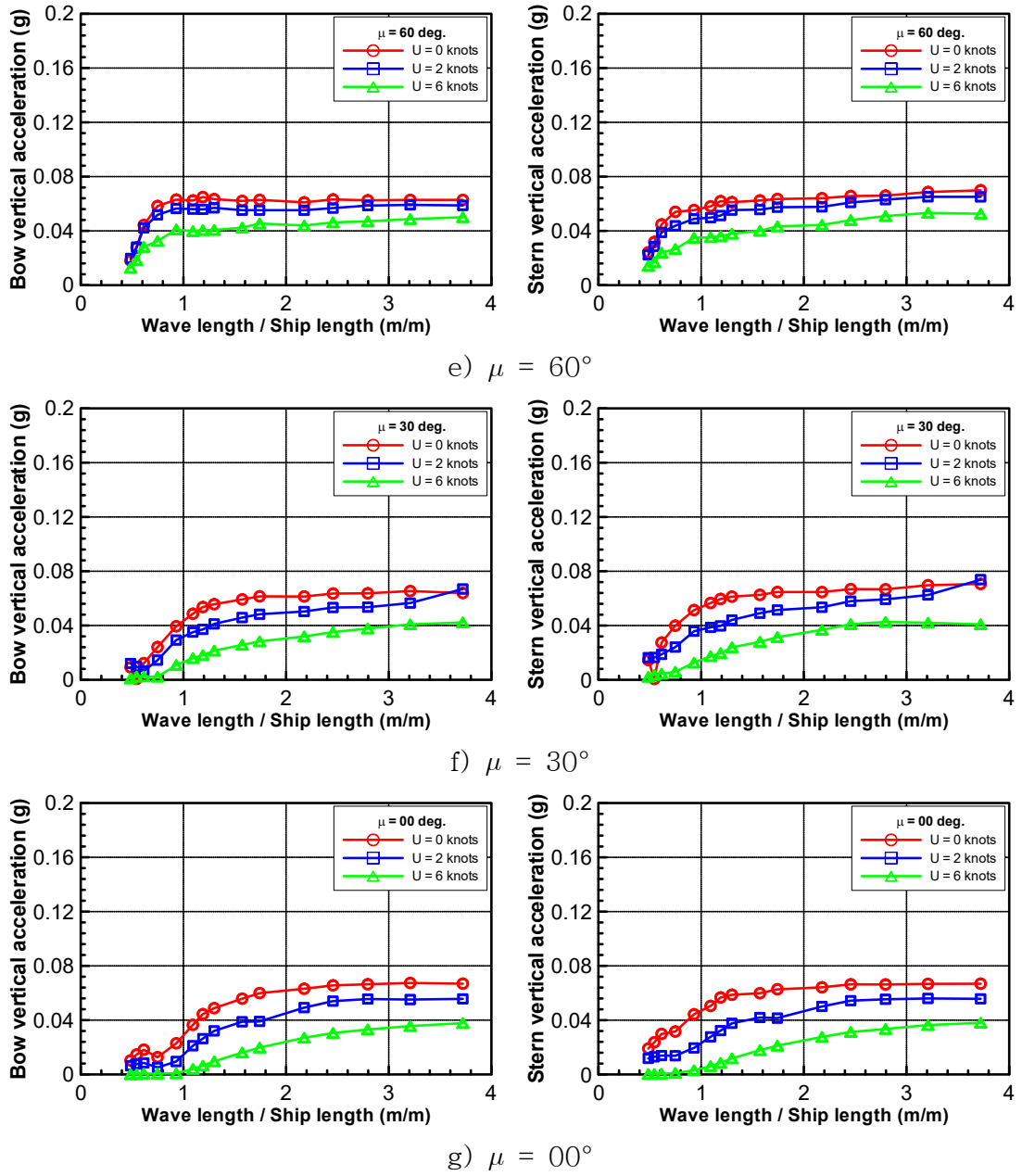


Fig. 3.58 Vertical acceleration

### 3.6.4 RAO and Phase

Model ship motion is measured using OptiTrack and IMU in regular waves. The displacements of the motion are analyzed by Fourier analysis and motion RAO is calculated by Eqs. (2.19) and (2.20) in section 2.1.2 for translational and rotational motion, respectively. As mentioned in section 2.1.3, the phase of motion is defined by the difference from the time when the regular wave and ship motion at the same time. In the experiment, the

phase of wave is estimated by wave probe located far from the center of gravity of the ship, which is a distance  $l_{x_p}$  and  $l_{y_p}$  as shown in Fig. 3.59. Assuming that the Earth-fixed coordinate system is  $O-xy$  and ship-fixed coordinate system is  $o-x_0y_0$ , the ship position and wave probe position with respect to Earth-fixed coordinate system are  $(x_o, y_o)$  and  $(x_w, y_w)$ , respectively, where  $x_w = x_o + \alpha_p$  with  $\alpha_p = l_{x_p} \cos \psi$ .

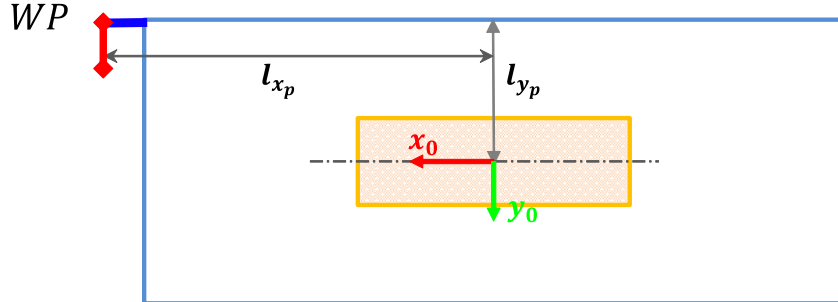


Fig. 3.59 Definition of phase parameter

Set  $t_s$  and  $(x_s, y_s)$  are starting time of valid data of wave time series and the position at the starting time.  $U$  is ship speed and  $\psi$  is the wave direction.

- The wave probe position is defined as,

$$\begin{cases} x_w = x_{ws} + U(t - t_s) \cos \psi \\ y_w = y_{ws} + U(t - t_s) \sin \psi \end{cases} \quad (3.19)$$

- The ship center of gravity position is expressed as,

$$\begin{cases} x_o = x_{os} + U(t - t_s) \cos \psi \\ y_o = y_{os} + U(t - t_s) \sin \psi \end{cases} \quad (3.20)$$

- Therefore,

$$x_{ws} = x_{os} + \alpha_p \quad (3.21)$$

- Wave elevation at the wave probe position for long crested wave is described as,

$$\zeta(x_w, t) = \zeta_a \cos(kx_w - \omega t + \delta) \quad (3.22)$$

- Substituting Eq. (3.19) to Eq. (3.22), the wave elevation is rewritten as,

$$\zeta(x_w, t) = \zeta_a \cos(kU(t - t_s) \cos \psi - \omega t + \delta') = \zeta_a \cos(-\omega_e t + \delta') \quad (3.23)$$

where  $\delta' = k(x_{ws} - Ut_s \cos\psi) + \delta$  and it can be estimated by wave probe's measurement. Then, the wave elevation at the center of the ship is calculated as,

$$\begin{aligned}\zeta(x_o, t) &= \zeta_a \cos(kx_o - \omega t + \delta) \\ &= \zeta_a \cos(-\omega_e t + \delta'')\end{aligned}\quad (3.24)$$

where  $\delta'' = k(x_{os} - Ut_s \cos\psi) + \delta = \delta' - k\alpha_p$ . Finally, the motion phase can be estimated as,

$$\begin{aligned}z(x_0, t) &= z_a \cos(kx_0 - \omega t + \delta + \varepsilon) \\ &= z_a \cos(-\omega_e t + \delta'' + \varepsilon)\end{aligned}\quad (3.25)$$

with  $\varepsilon$  which can be calculated from phase between motion with respect to wave. However, in this experiment, the data acquisition of wave probe and ship motion were done using different software without synchronization, so the measurement timea for wave probe and ship motion were different. It is necessary to synchronize the time of the DAQ (Data AcQuisition) program measuring wave probe and measuring OptiTrack. To do this, we selected the data of vertical acceleration at bow and stern measured by DAQ that motion is expressed clearly especially at high frequency to find the time difference between DAQ and OptiTrack program.

Assuming that

$$t_m = t_w - t_s \quad (3.26)$$

Here,  $t_m$  is the time of motion measured by OptiTrack,  $t_w$  is the time in DAQ program, and  $t_s$  is the time difference between OptiTrack and DAQ. The problem is to find  $t_s$ .

○ The harmonic form for motion and vertical acceleration at bow in regular wave is described as,

$$\text{Motion (OptiTrack): } z = z_a \sin(\omega t_m + \varepsilon_z); \theta = \theta_a \sin(\omega t_m + \varepsilon_z) \quad (3.27)$$

$$\text{Vertical acceleration (DAQ): } a_{bow} = a_a \sin(\omega t_w + \varepsilon_a) \quad (3.28)$$

○ Relationship between  $a$  and  $z$  with accelerometer is located at the center

line

$$a_{bow} = \ddot{z} - x_a \ddot{\theta} \quad (3.29)$$

with

$$\ddot{z} = -\omega^2 z_a \sin(\omega t_m + \varepsilon_z) \quad (3.30)$$

$$\ddot{\theta} = -\omega^2 \theta_a \sin(\omega t_m + \varepsilon_\theta) \quad (3.31)$$

- Substituting Eqs. (3.26), (3.30) and (3.31) to Eq. (3.29), the relationship between  $a$  and  $z$  is rewritten.

$$-a_a \sin(\omega t_w + \varepsilon_a) = -\omega^2 z_a \sin[\omega(t_w - t_s) + \varepsilon_z] + x_a \omega^2 \theta_a \sin[\omega(t_w - t_s) + \varepsilon_\theta] \quad (3.32)$$

- Assuming that  $\sin(\omega_e t_w) = 0$  at the time  $t$

$$-a_a \sin(\varepsilon_a) = -\omega^2 z_a \sin(\omega t_s + \varepsilon_z) + x_a \omega^2 \theta_a \sin(-\omega t_s + \varepsilon_\theta) \quad (3.33)$$

Set  $x_{ab}$  and  $x_{as}$  are  $x$  position of bow and stern accelerometers, respectively. If the results of bow acceleration and stern acceleration are expanded, we have,

$$\begin{cases} a_{ab} \sin(\varepsilon_a) = -\omega^2 z_a \sin(\omega t_s + \varepsilon_z) + x_{ab} \omega^2 \theta_a \sin(-\omega t_s + \varepsilon_\theta) \\ a_{as} \sin(\varepsilon_a) = -\omega^2 z_a \sin(\omega t_s + \varepsilon_z) + x_{ab} \omega^2 \theta_a \sin(-\omega t_s + \varepsilon_\theta) \end{cases} \quad (3.34)$$

It is enough to estimate  $t_s$ , so we can use one of both formulae in Eq. (3.34). But in order to increase statistical significance, we take a mean of both bow and stern acceleration results, which will be the middle position of the vertical acceleration phase at bow and stern.

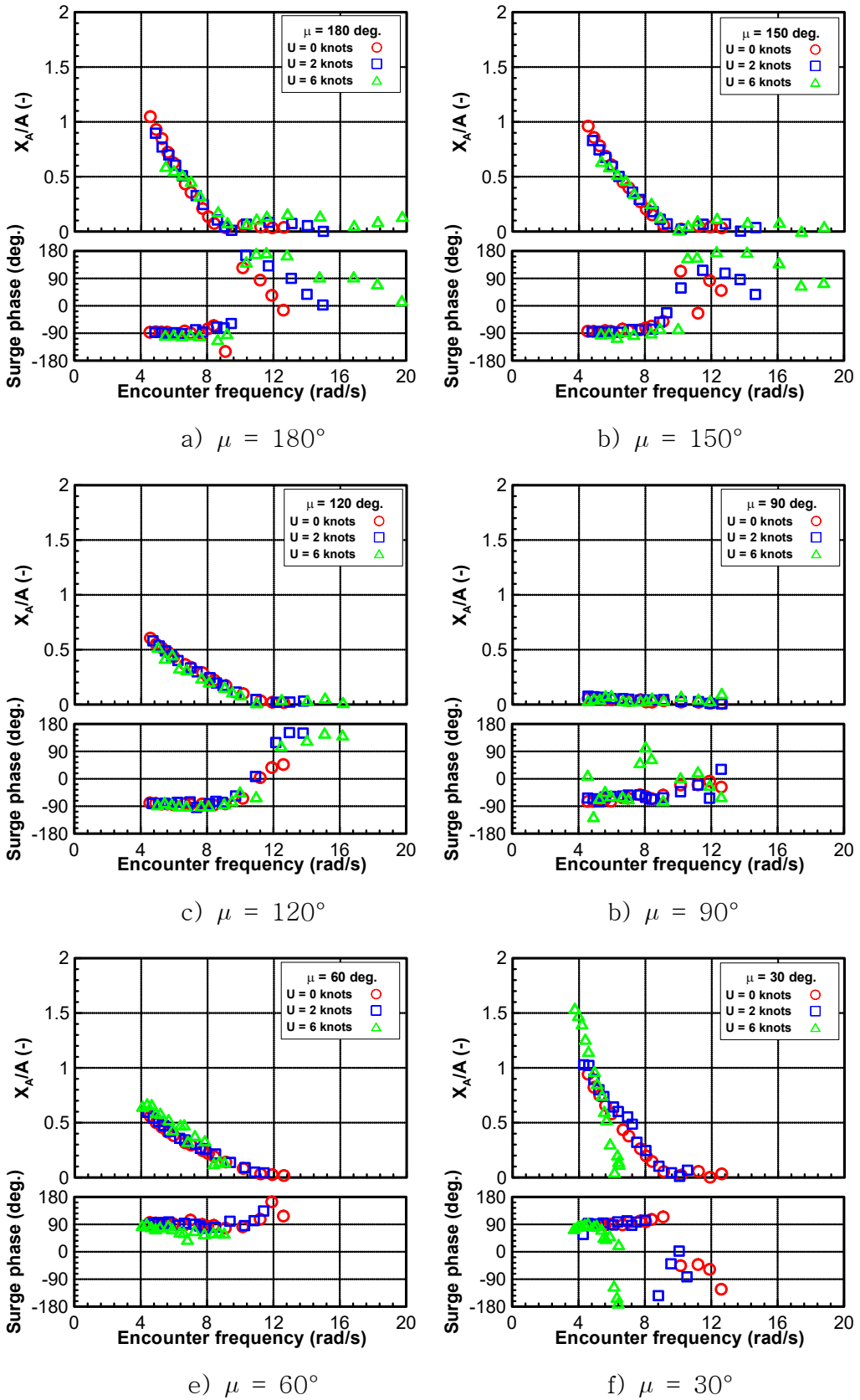
- Therefore the vertical acceleration at midship is expressed as

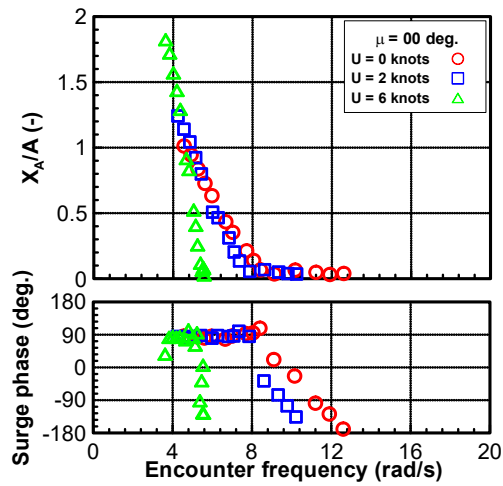
$$\ddot{z}_{mid} = -\omega^2 z_A \sin(\omega t_s + \varepsilon_z) \quad (3.35)$$

- Finally, the difference time between OptiTrack program and DAQ program is defined as Eq. (3.36)

$$t_s = \frac{\varepsilon_{amid} - \varepsilon_z}{\omega} \quad (3.36)$$

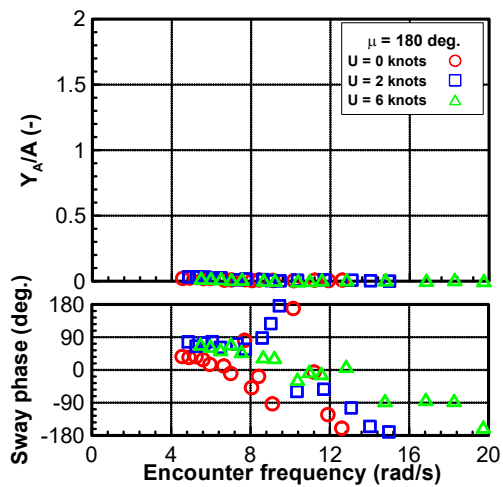
Figs. 3.60~3.65 show the results of motion RAO and motion phase in regular waves for 6-DOF motion according to change speed and incident wave direction with respect to encounter frequency. It can be seen that surge RAO and sway RAO at stern waves is larger than bow waves, it can be observed clearly the big difference at 6 knots. The magnitude of surge RAO is greater at head waves and following waves and it reaches zero at beam waves. Otherwise, the magnitude of sway RAO is greater at beam waves and it becomes zero at head waves and following waves. According to speed conditions, the motion at the higher speed is smaller at the bow waves, while it is greater at the stern waves for both surge and sway RAOs. Heave RAO approximates 1 at low frequency for all incident wave directions because the ship moves along the wave surface as the wave length is long. According to speed conditions, the magnitude of heave RAO is opposite to surge and sway RAOs, which means the motion at higher speed is greater in the bow waves and smaller at the stern waves. Besides, the sway and heave RAOs are almost the same at different speeds in beam waves. The magnitude of roll RAO is dominant at beam waves, and it becomes zero at head waves and following waves. The natural frequency of roll is observed at 9.1 rad/s. According to speed conditions, motion at higher speed is greater at bow waves, while smaller at stern waves, this is seen clearly around the natural frequency area. Opposite with roll RAO, the magnitude of pitch RAO is dominant at head waves and following waves and it reaches zero at beam waves. But the trend of pitch RAO is the same as roll RAO due to speed condition, and it means that motion at higher speed is greater in bow waves and smaller in stern waves. About yaw RAO, it is dominant at quartering waves and approximates zero at head waves, beam waves, and following waves. Motion at higher speed is smaller in bow quartering waves and it increases in stern quartering waves, this is observed clearly at 6 knots.



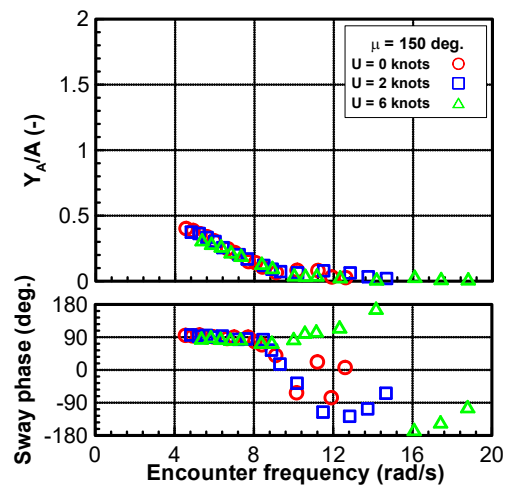


g)  $\mu = 0^\circ$

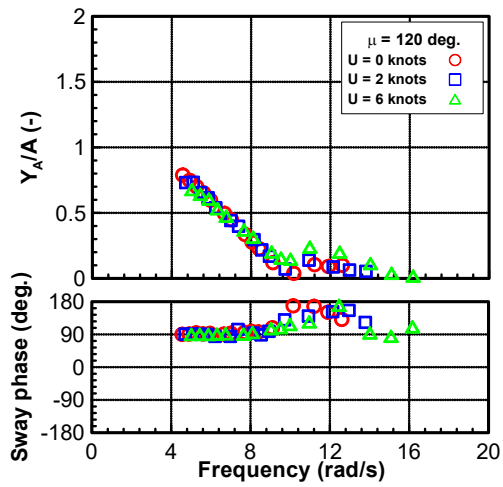
Fig. 3.60 Surge RAO (Experiment)



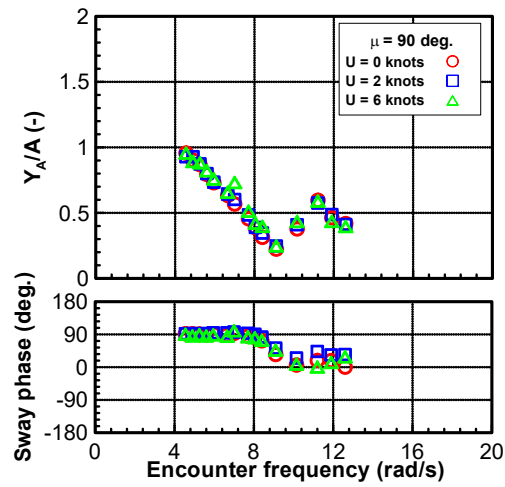
a)  $\mu = 180^\circ$



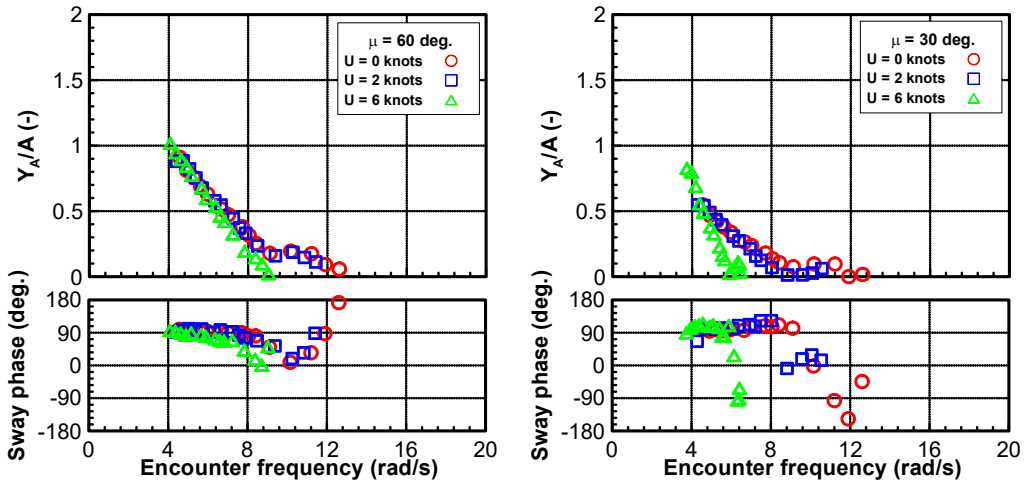
b)  $\mu = 150^\circ$



c)  $\mu = 120^\circ$

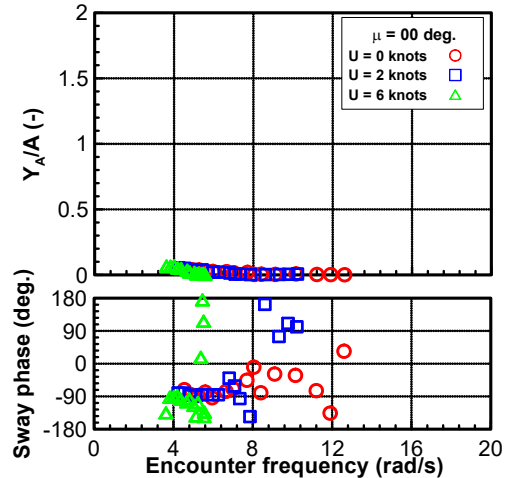


d)  $\mu = 90^\circ$



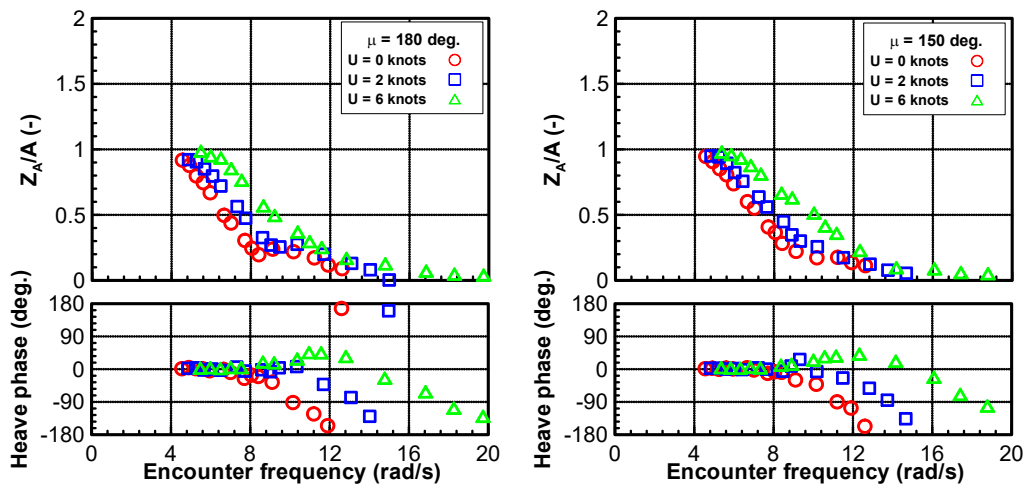
e)  $\mu = 60^\circ$

f)  $\mu = 30^\circ$



g)  $\mu = 0^\circ$

Fig. 3.61 Sway RAO (Experiment)



a)  $\mu = 180^\circ$

b)  $\mu = 150^\circ$

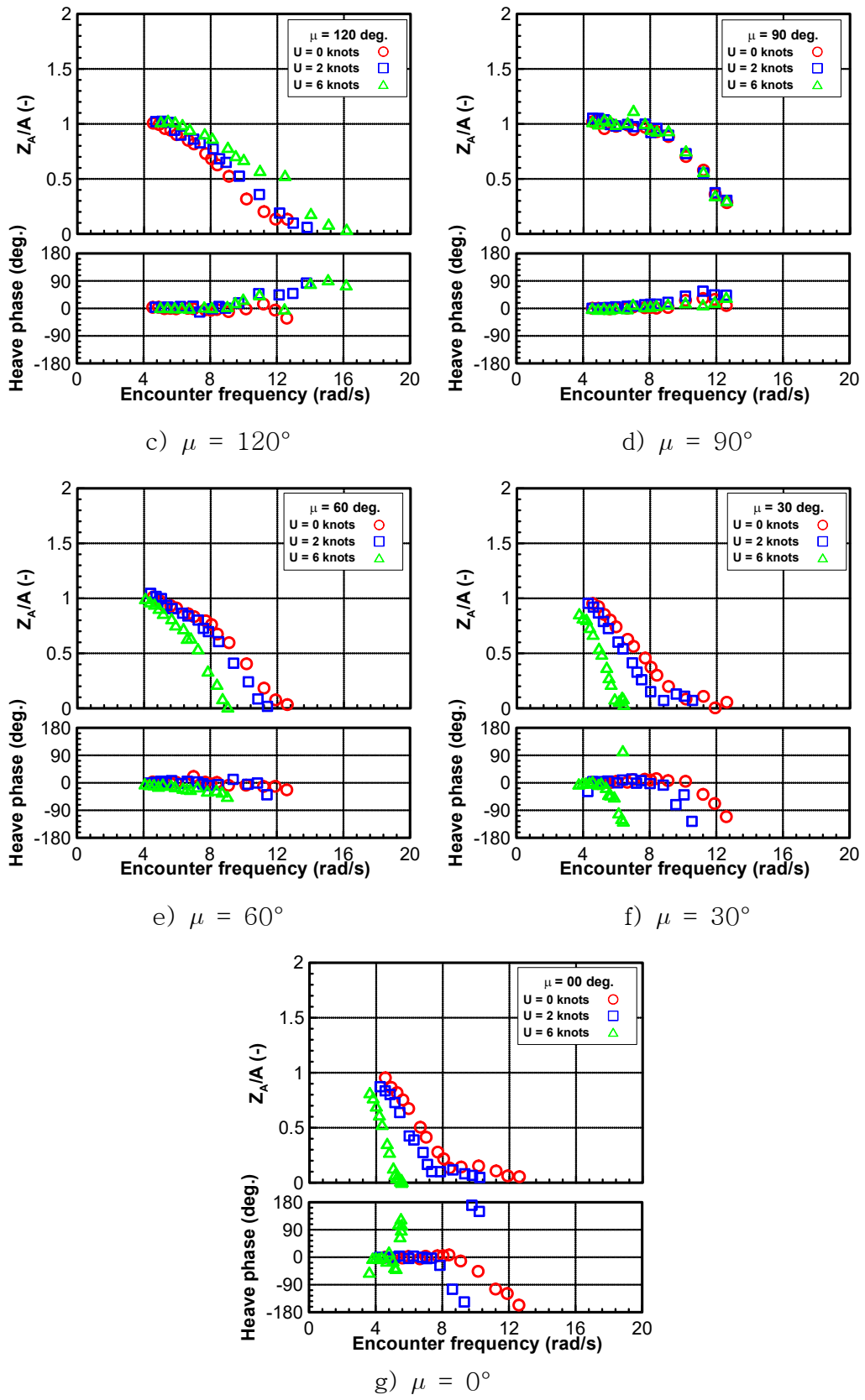
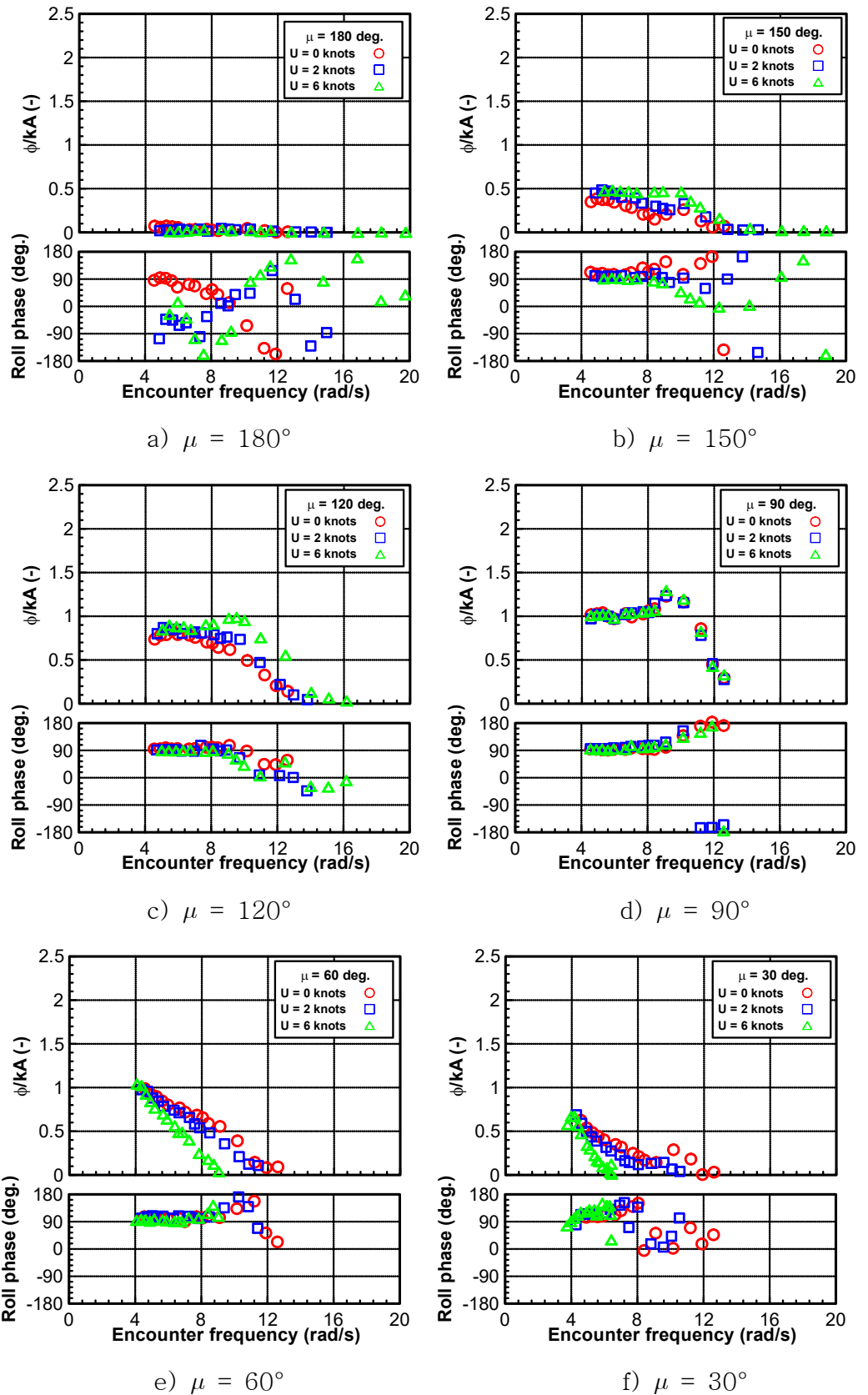
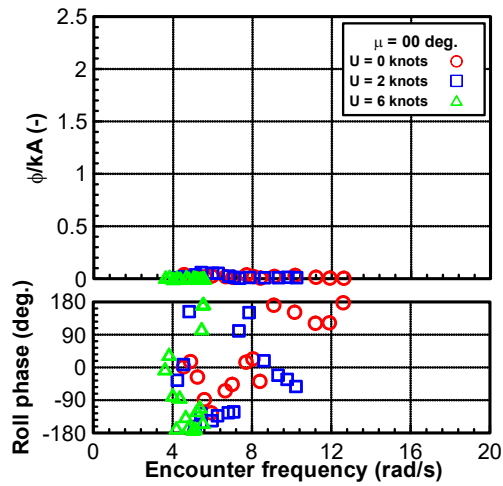


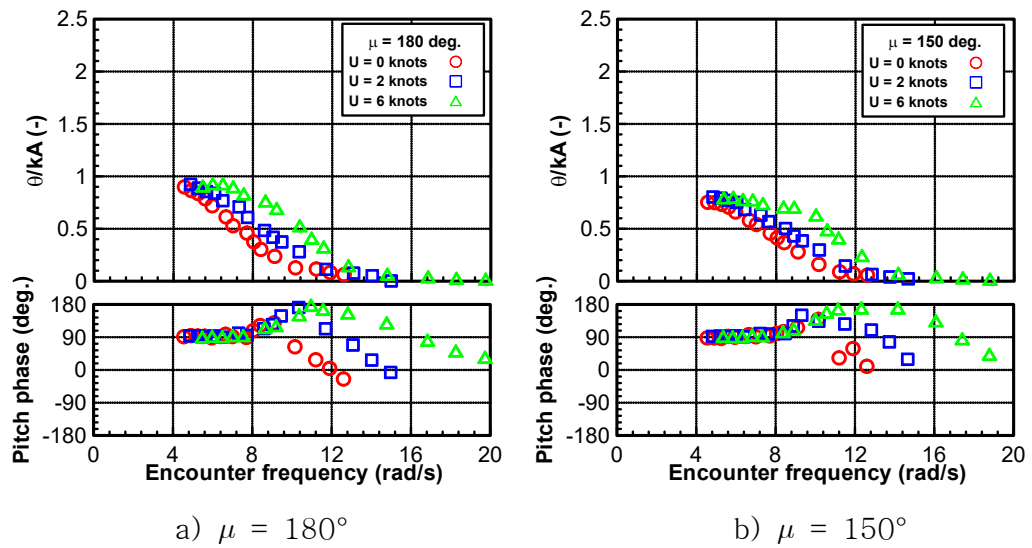
Fig. 3.62 Heave RAO (Experiment)





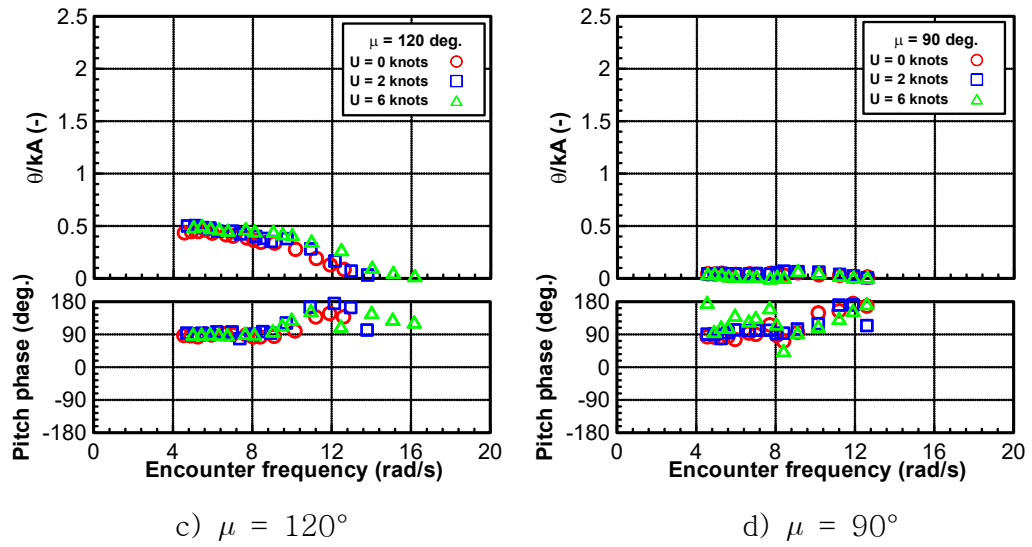
g)  $\mu = 0^\circ$

Fig. 3.63 Roll RAO (Experiment)



a)  $\mu = 180^\circ$

b)  $\mu = 150^\circ$



c)  $\mu = 120^\circ$

d)  $\mu = 90^\circ$

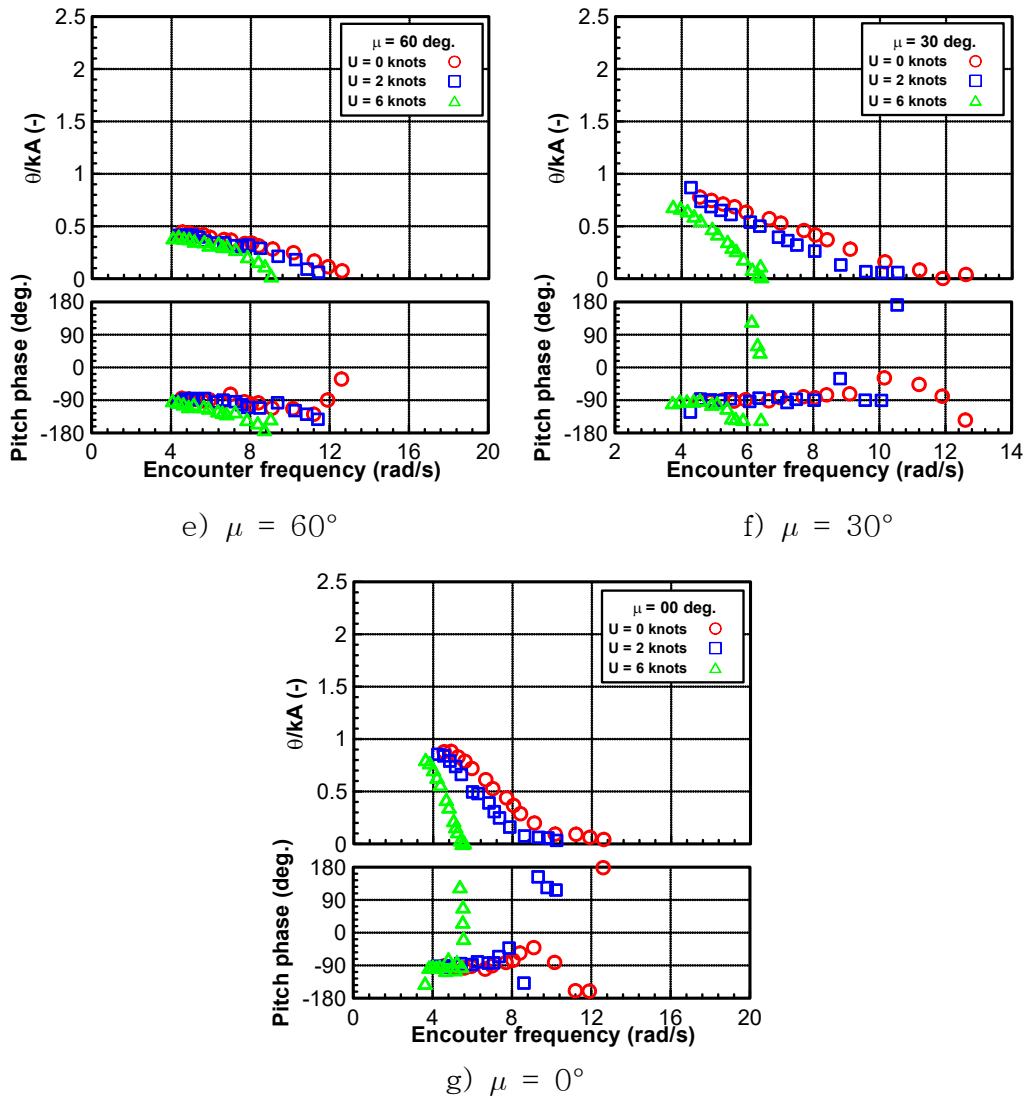
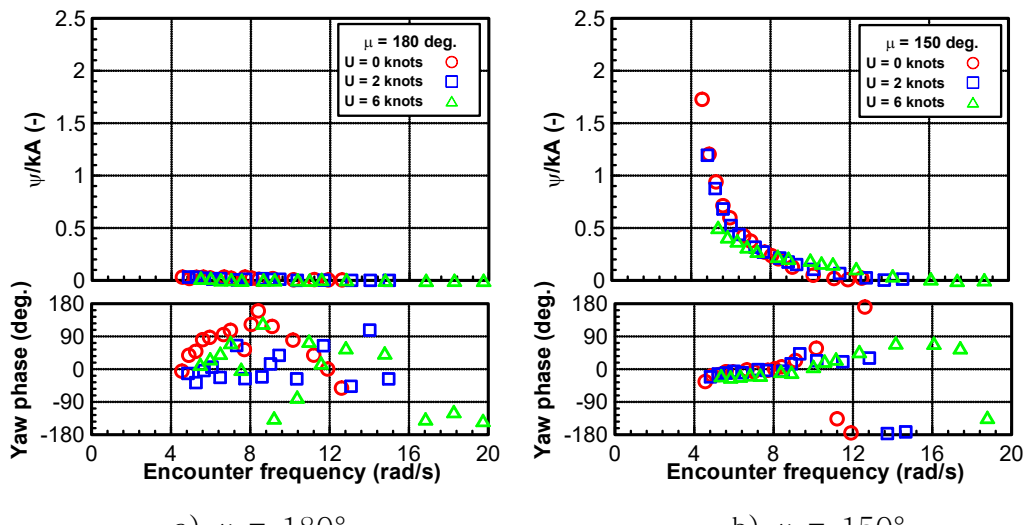


Fig. 3.64 Pitch RAO (Experiment)



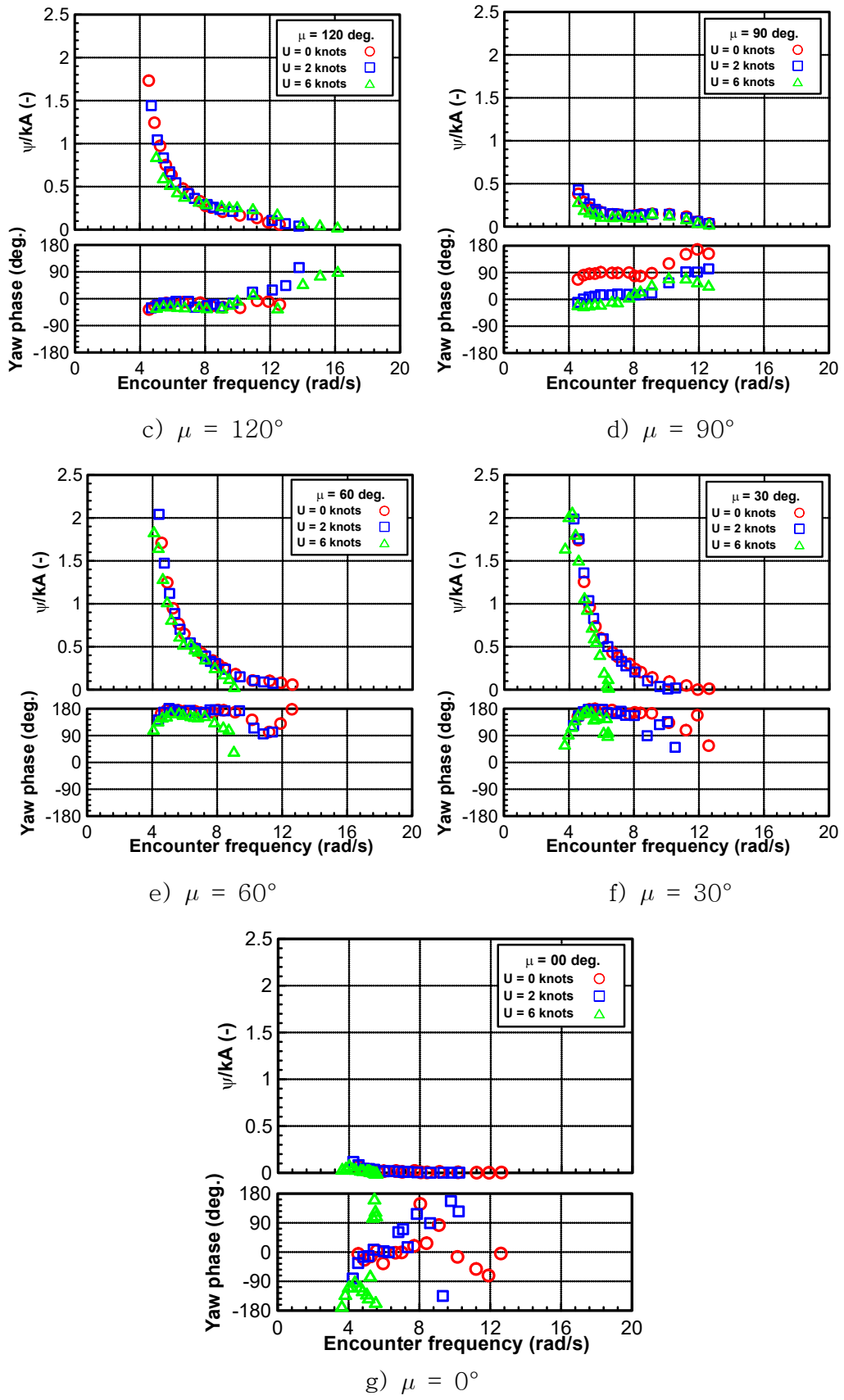
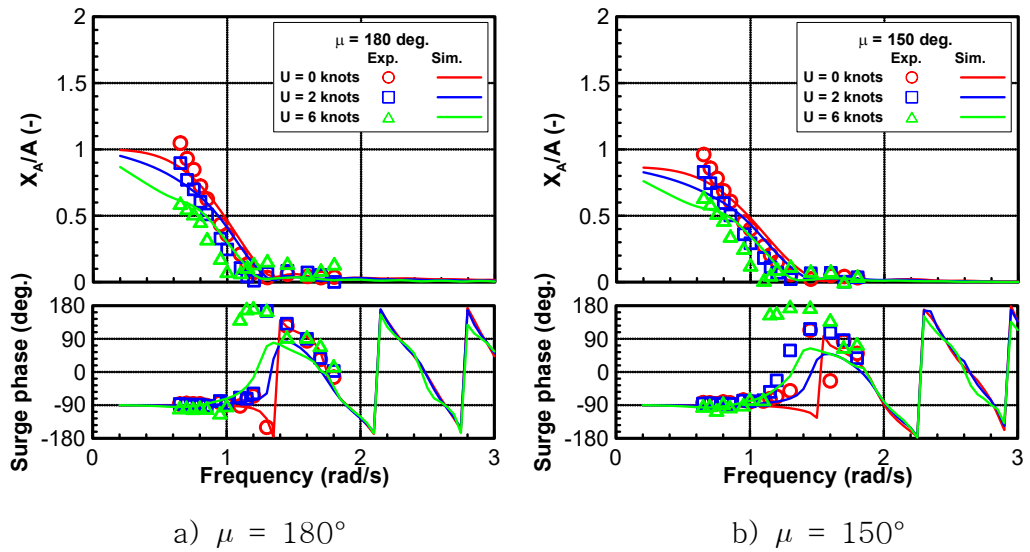


Fig. 3.65 Yaw RAO (Experiment)

### 3.6.5 Comparison of ship motion

Figs. 3.66~3.71 display the comparison results of 6-DOF motion between experiment and numerical simulation according to speed and incident waves with respect to frequency. The frequency of the model ship is converted to the full-scale. It can be seen that the motion RAO and motion phase of the experiment almost give good consistency with numerical results especially according to speed conditions except to yaw RAO. The abnormal points of pitch RAO at forward speed in numerical simulation occur at low frequency and it is out of range of selected frequency condition for the model test. However, we still observe the big difference at beam waves and stern waves for forward speed in numerical simulation results. Those points are obviously not reasonable for viewpoint of seakeeping analysis. Yaw RAO of numerical simulation is seen very large difference bow quartering waves and stern quartering waves compared with experiments. The slopes of numerical simulation occur smaller than slopes of experiment results in the range of frequency. Due to the large differences of pitch RAO and yaw RAO, it is necessary to improve the accuracy of the numerical simulation.



a)  $\mu = 180^\circ$

b)  $\mu = 150^\circ$

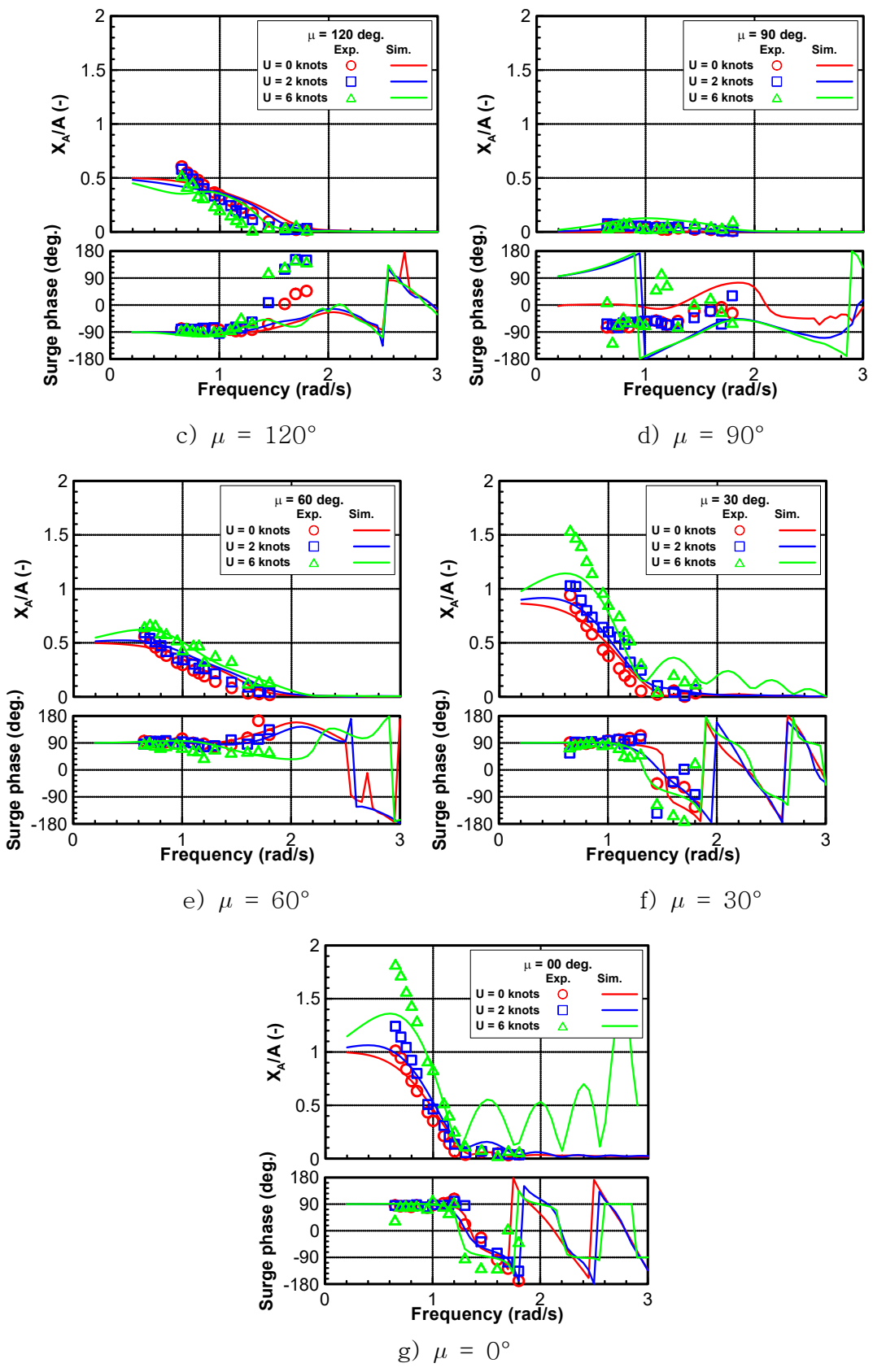
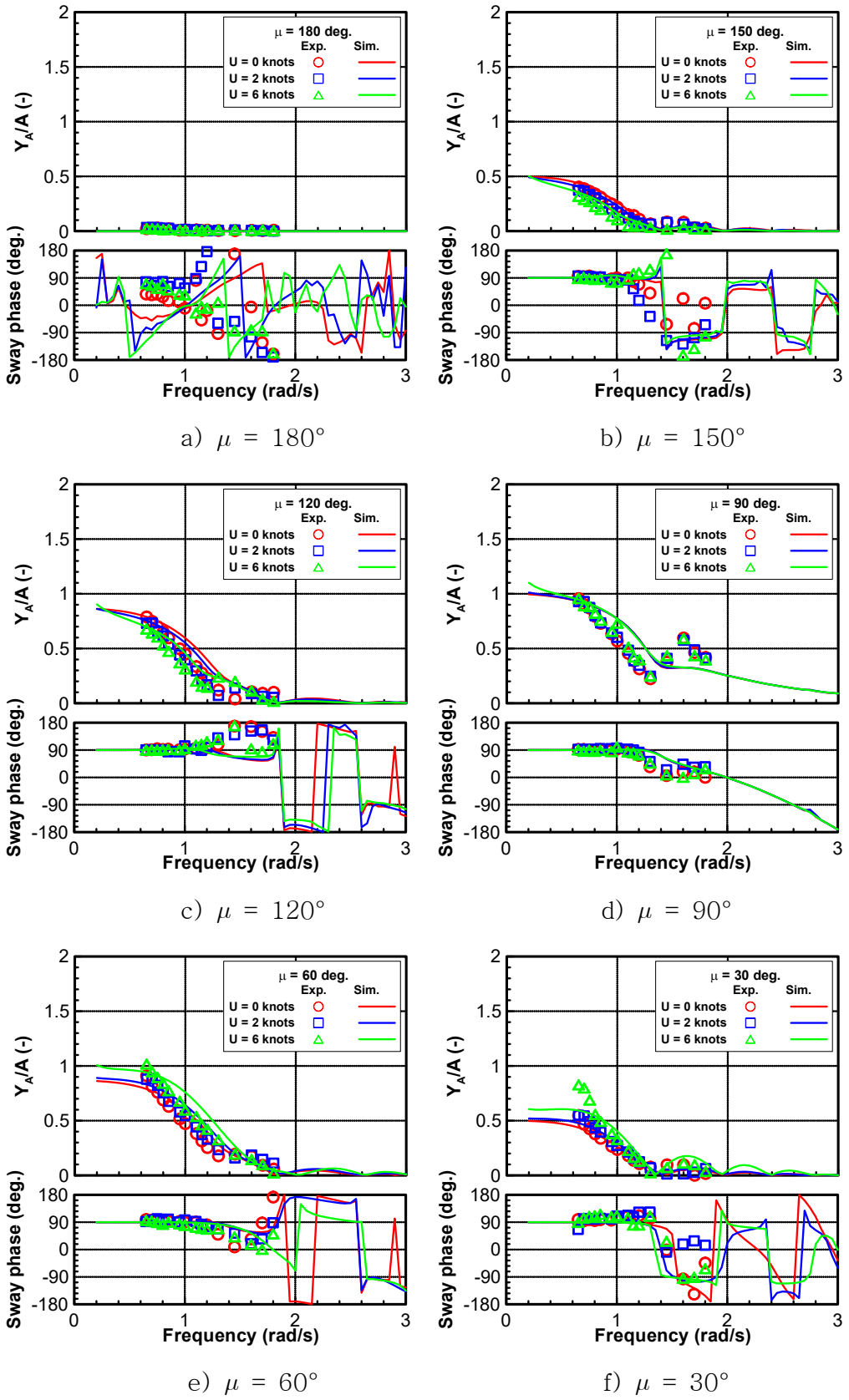
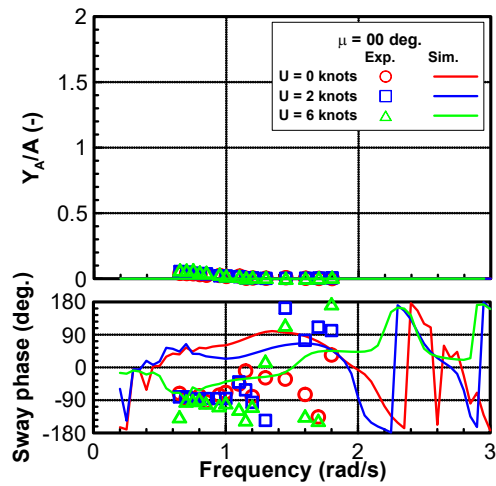


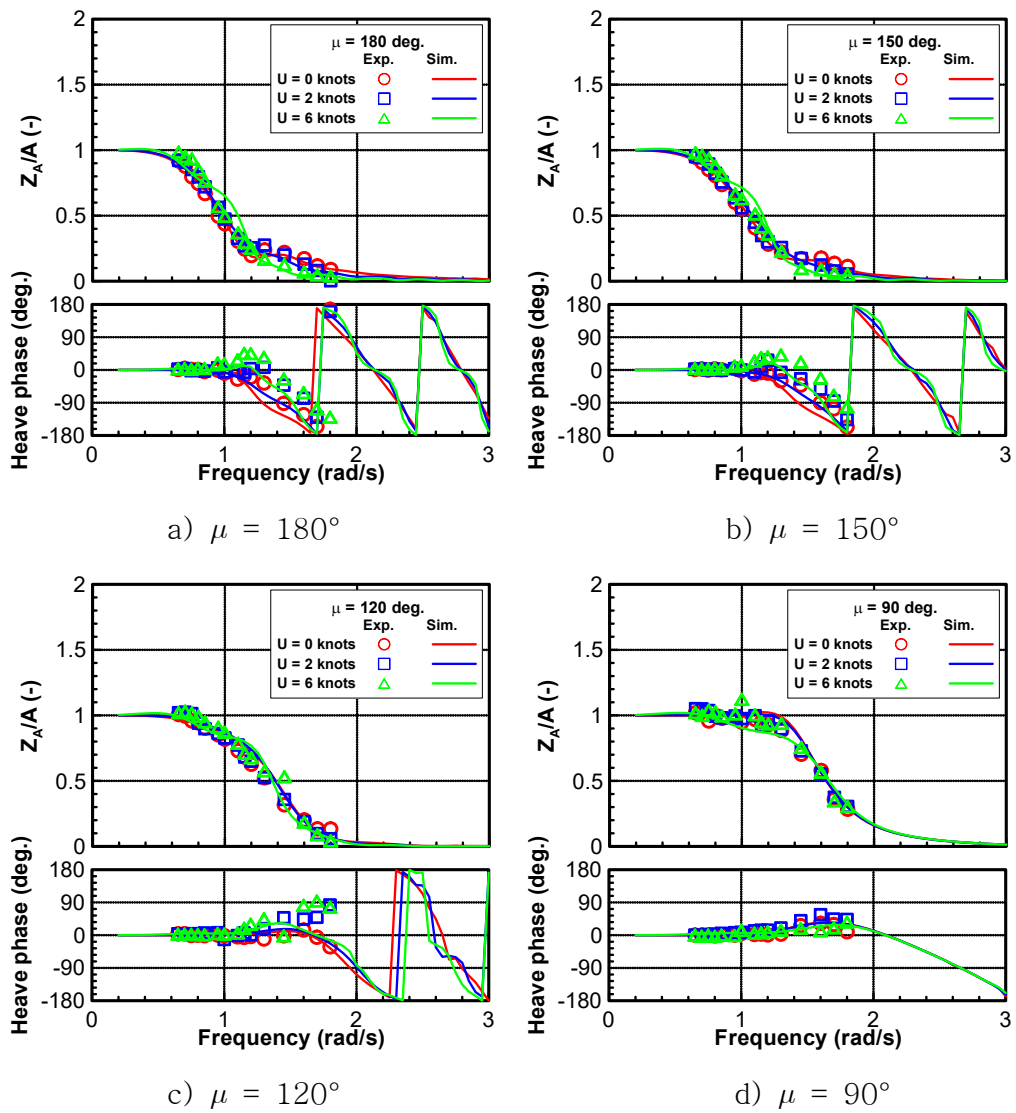
Fig. 3.66 Comparison of surge RAO





g)  $\mu = 0^\circ$

Fig. 3.67 Comparison of sway RAO



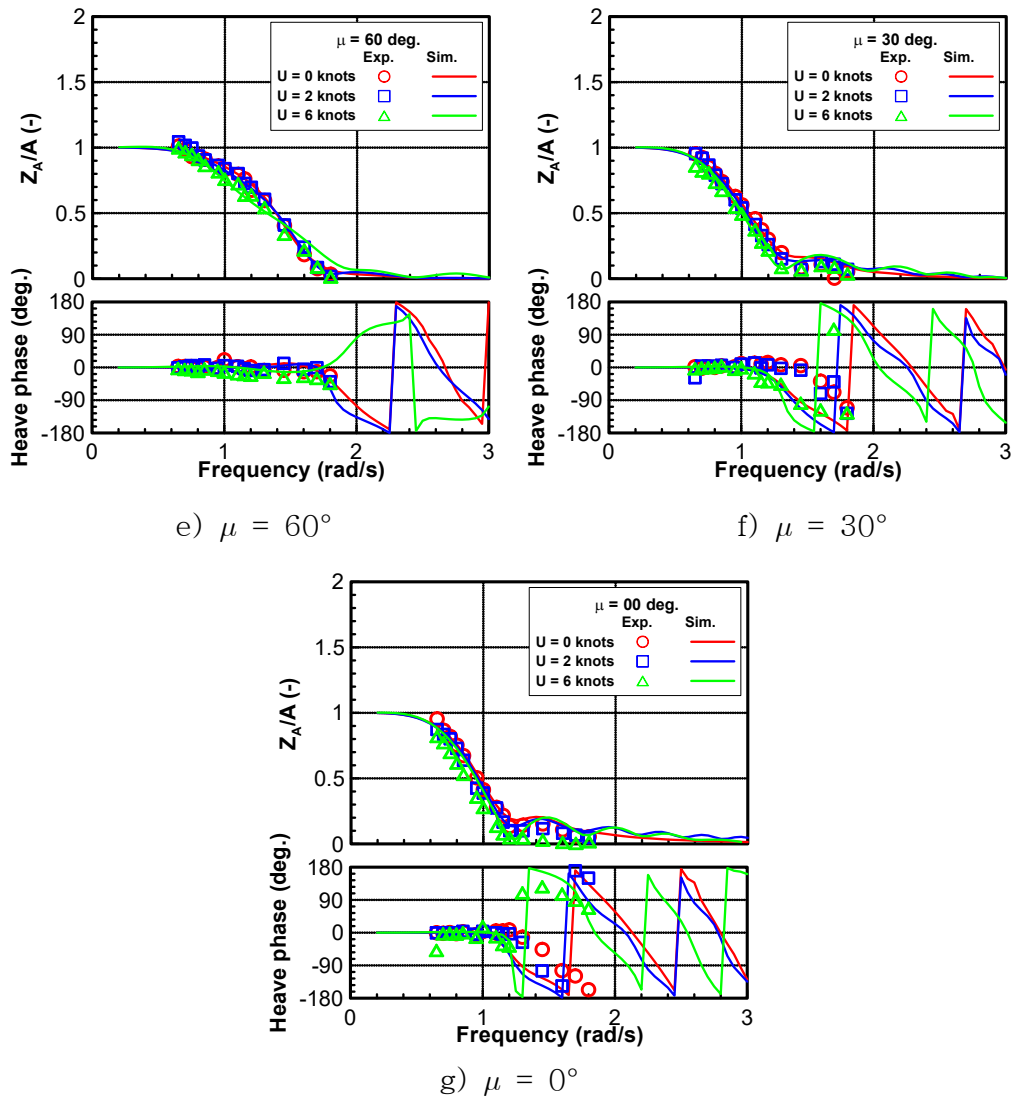
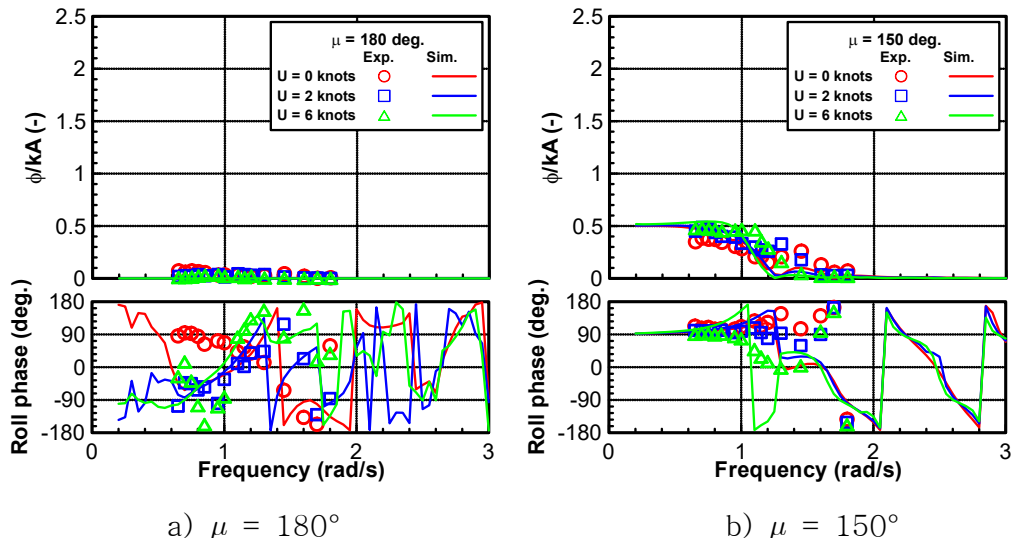


Fig. 3.68 Comparison of heave RAO



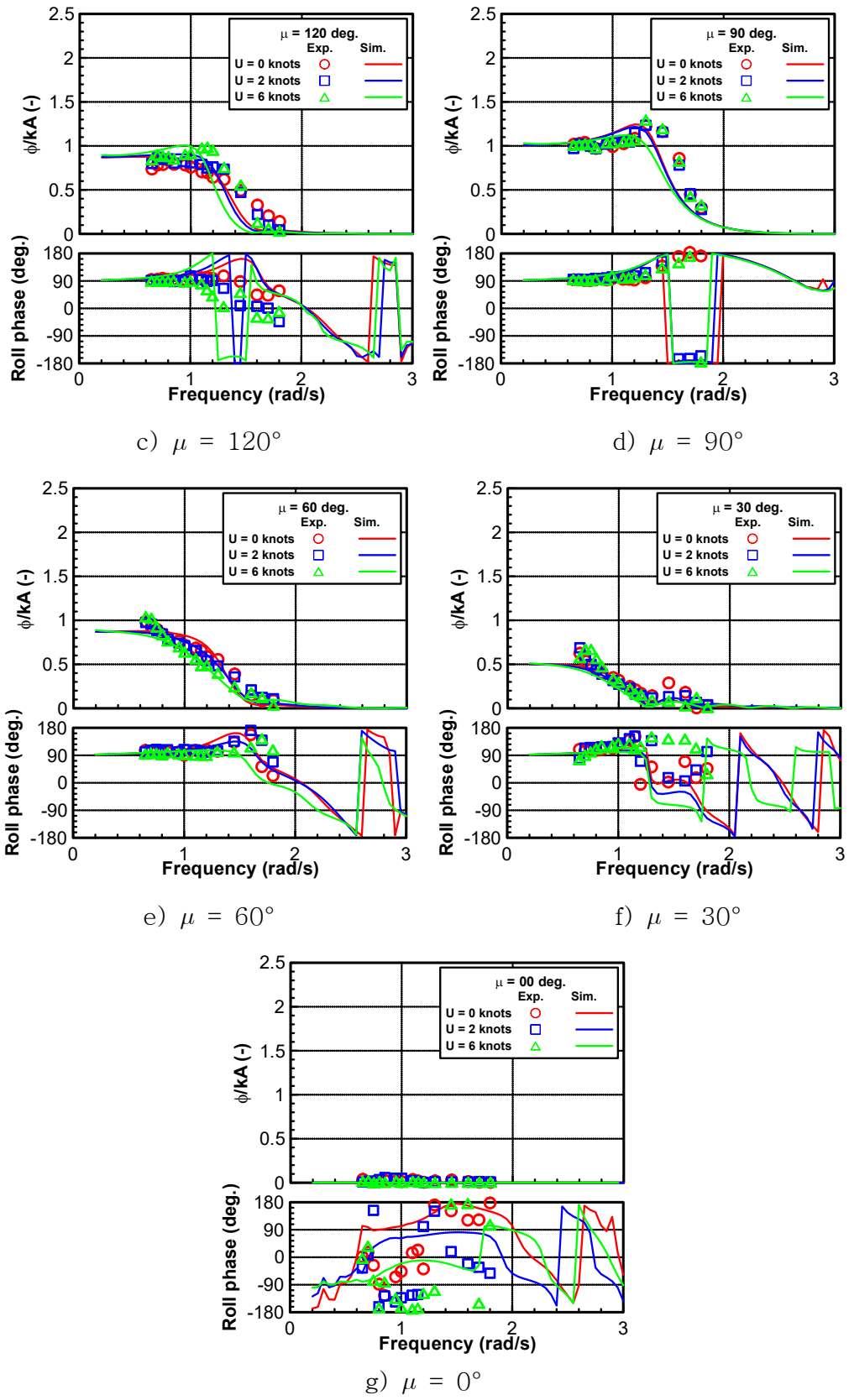
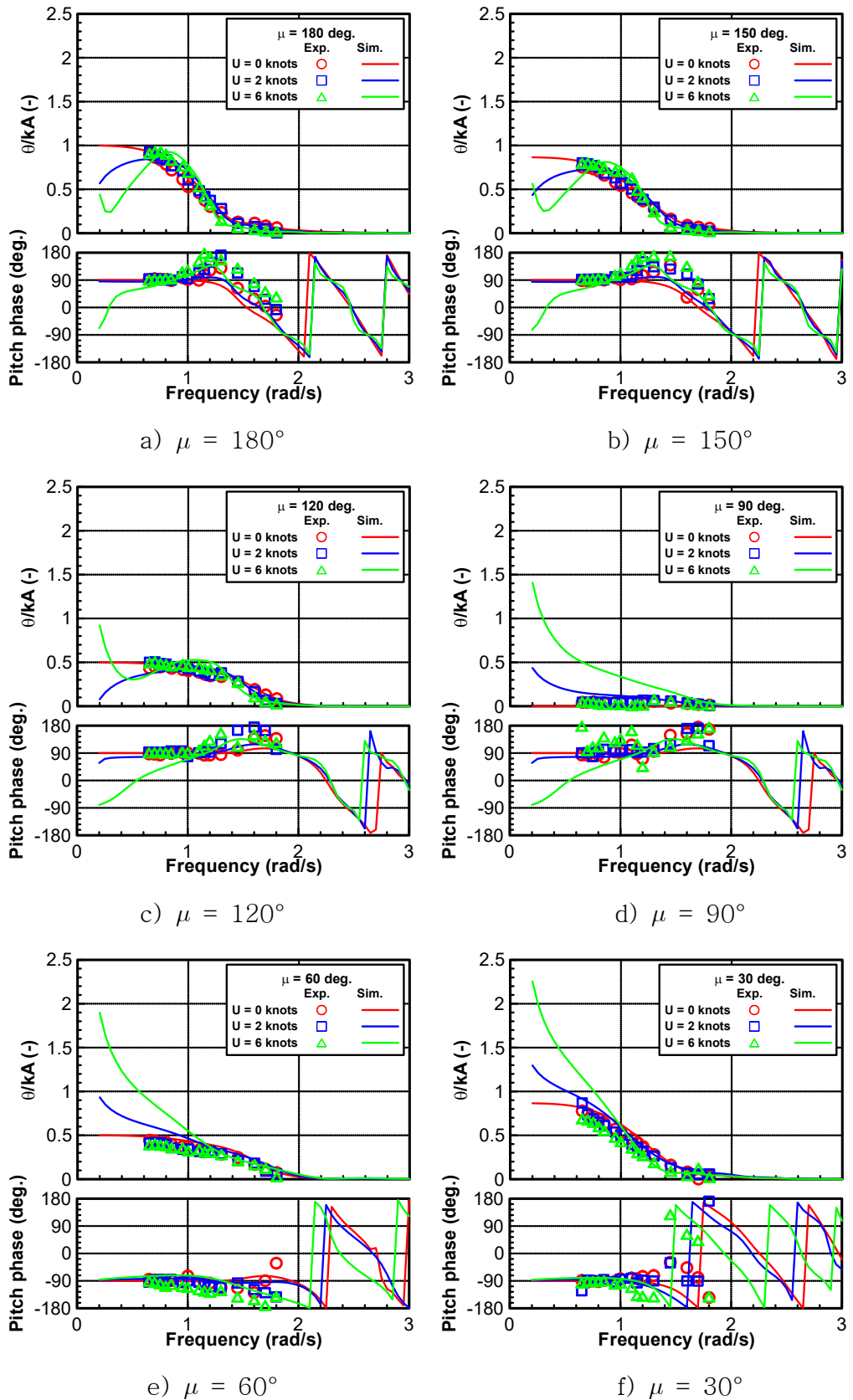
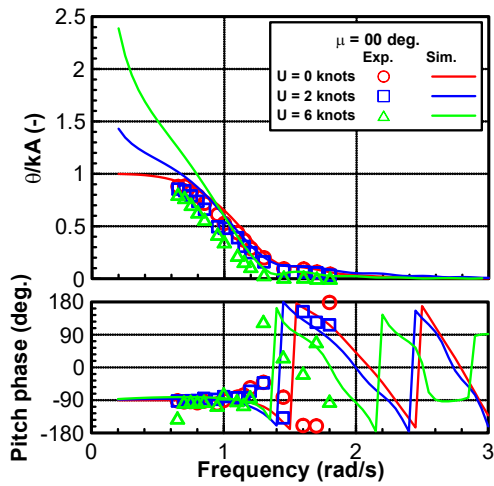


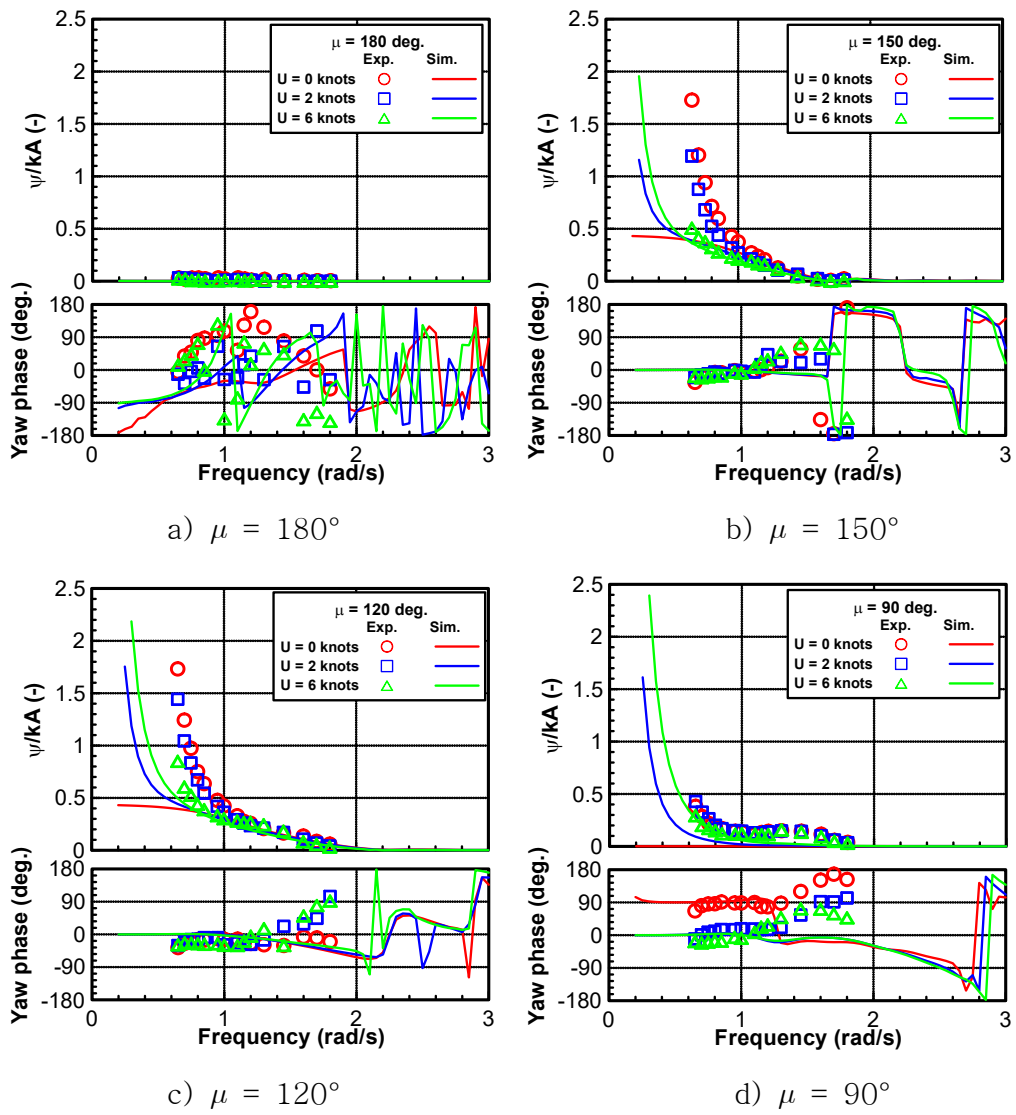
Fig. 3.69 Comparison of roll RAO





g)  $\mu = 0^\circ$

Fig. 3.70 Comparison of pitch RAO



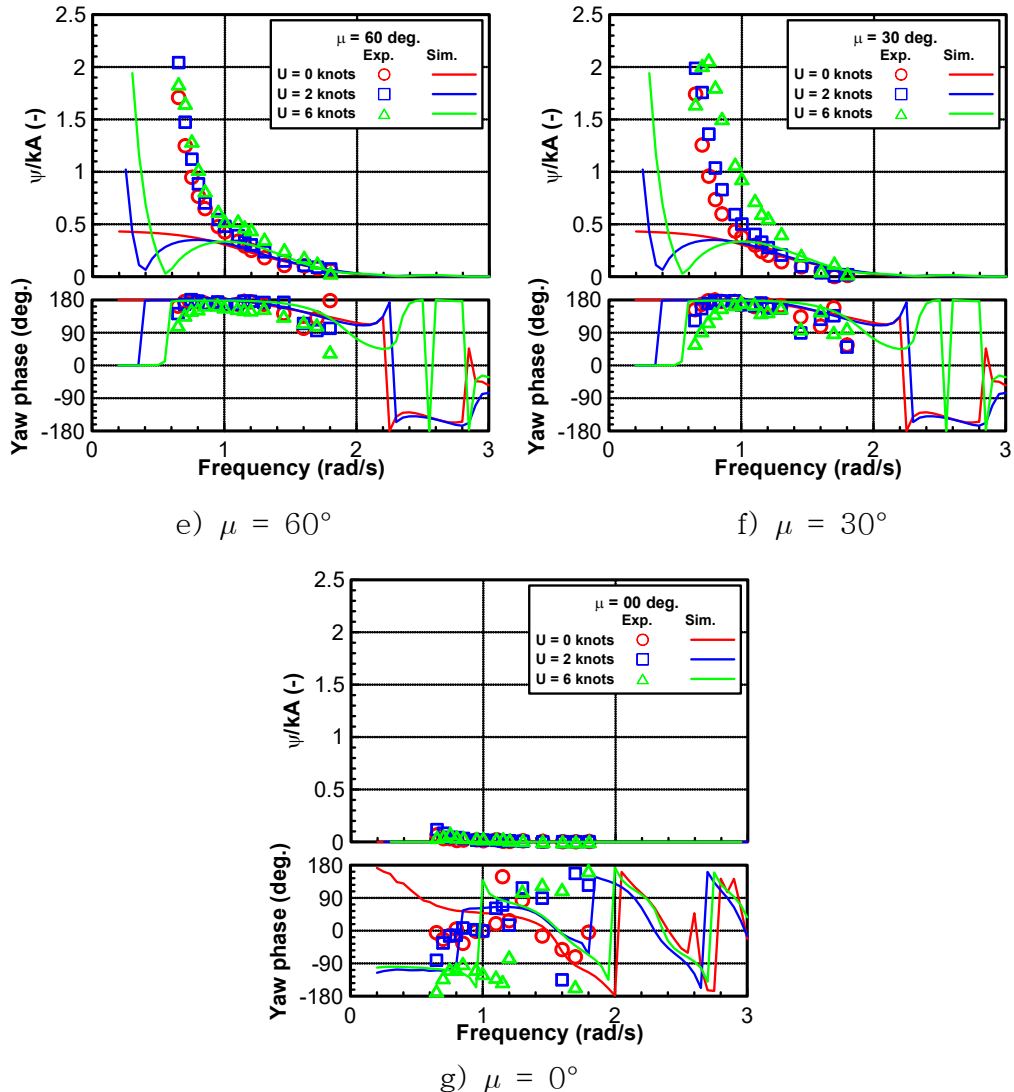


Fig. 3.71 Comparison of yaw RAO

### 3.6.6 Spring effect to ship motion

It is necessary to check the spring effect on the ship motion. In this study, we select three springs that have stiffness 9 N/m, 15 N/m, and 24 N/m, which are available to measure the ship motion at head waves and beam waves. Mooring in bow quartering wave was done with spring stiffness 9 N/m and 15 N/m. Figs. 3.72~3.75 show the results of 6-DOF motion at zero speed for different spring stiffness of wave direction 180°, 150°, 120°, and 90°, respectively. It can be observed that the vertical motions such as heave, roll, and pitch are almost the same with different spring stiffnesses and the difference is not significant. However, spring stiffness clearly affects to horizontal motion such as surge, sway, and yaw

motions. The magnitude of surge RAO is greater at stronger spring stiffness. This occurs similarly for sway RAO as seen at beam waves and yaw RAO.

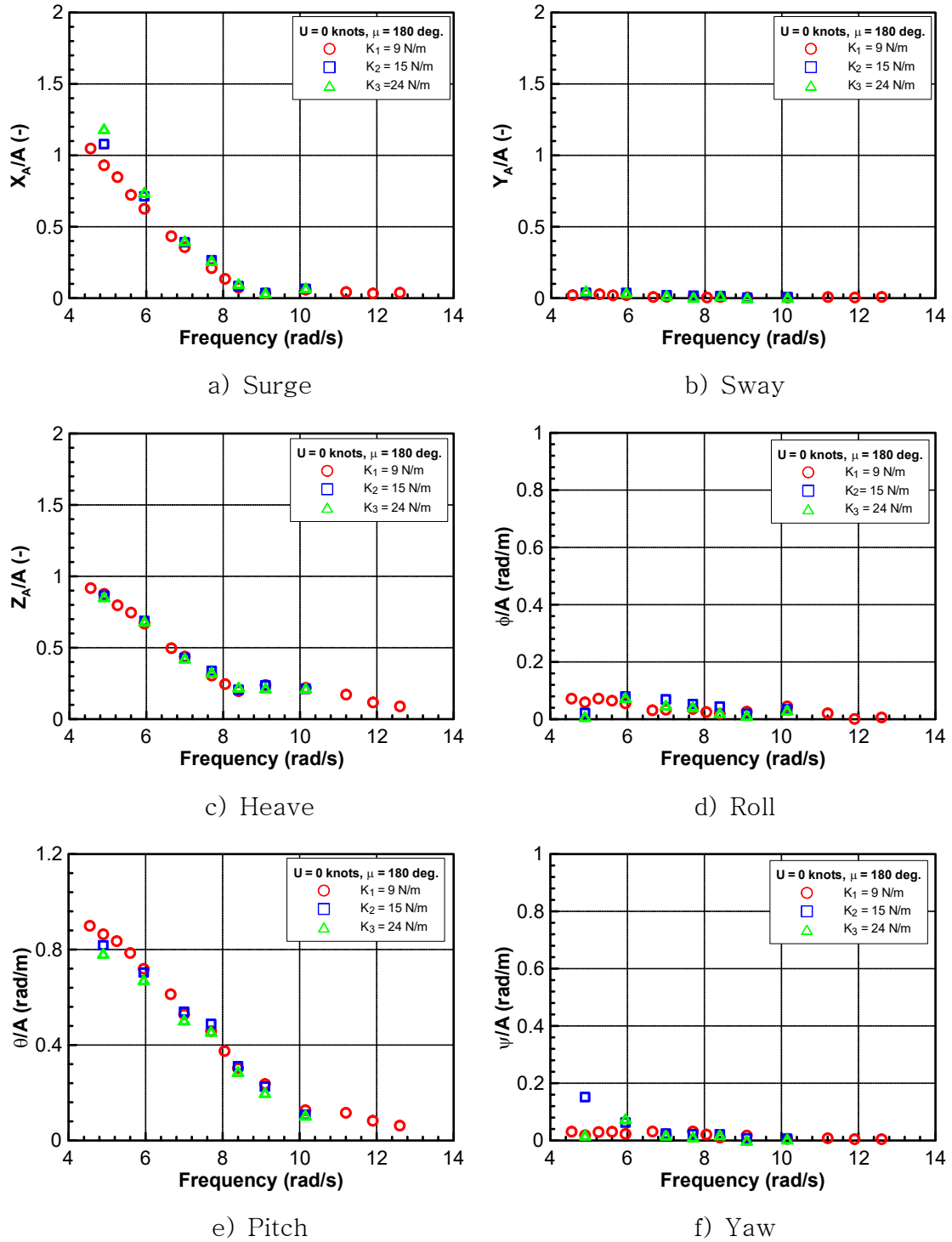


Fig. 3.72 Spring effect of zero speed at wave direction  $180^\circ$

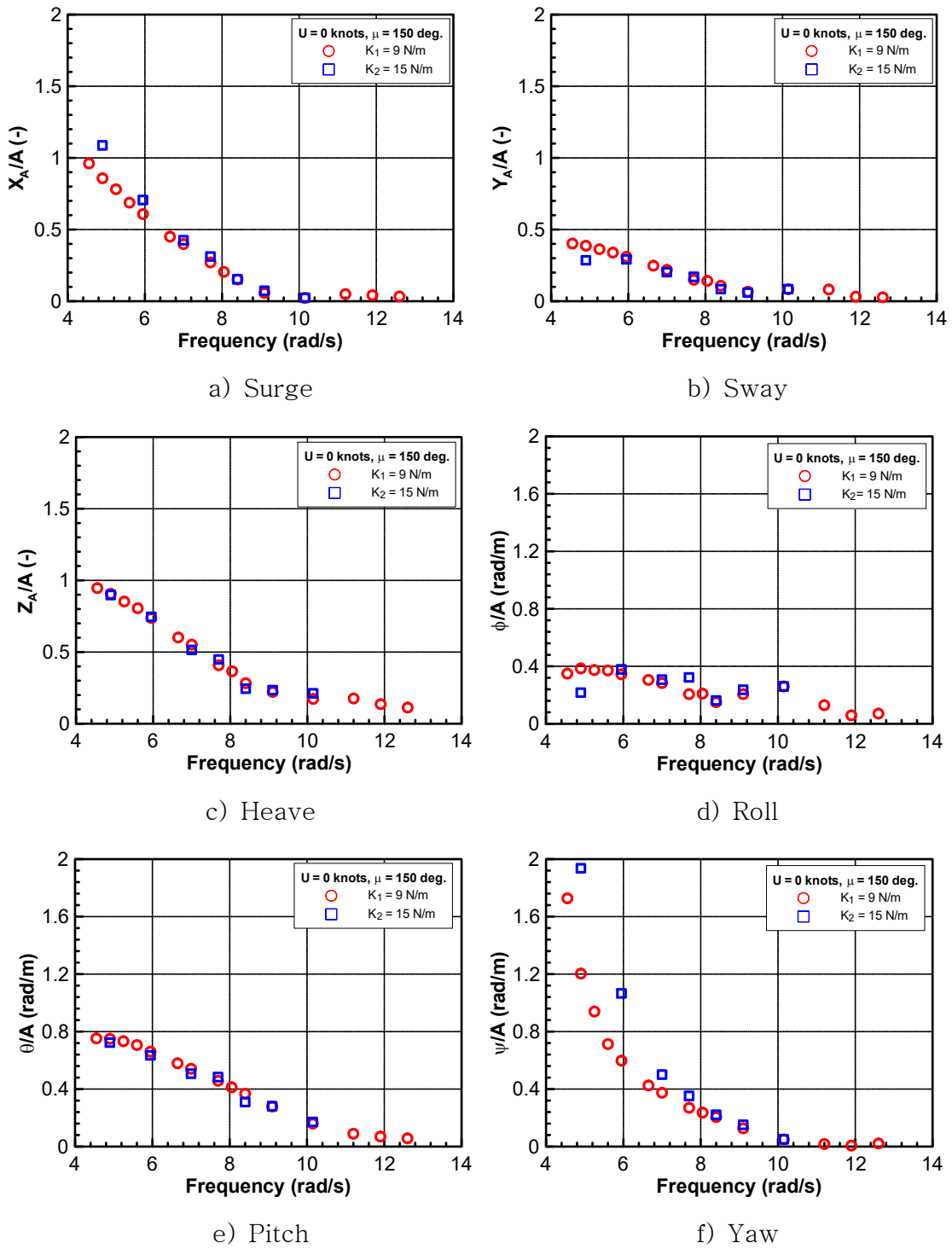


Fig. 3.73 Spring effect of zero speed at wave direction  $150^\circ$

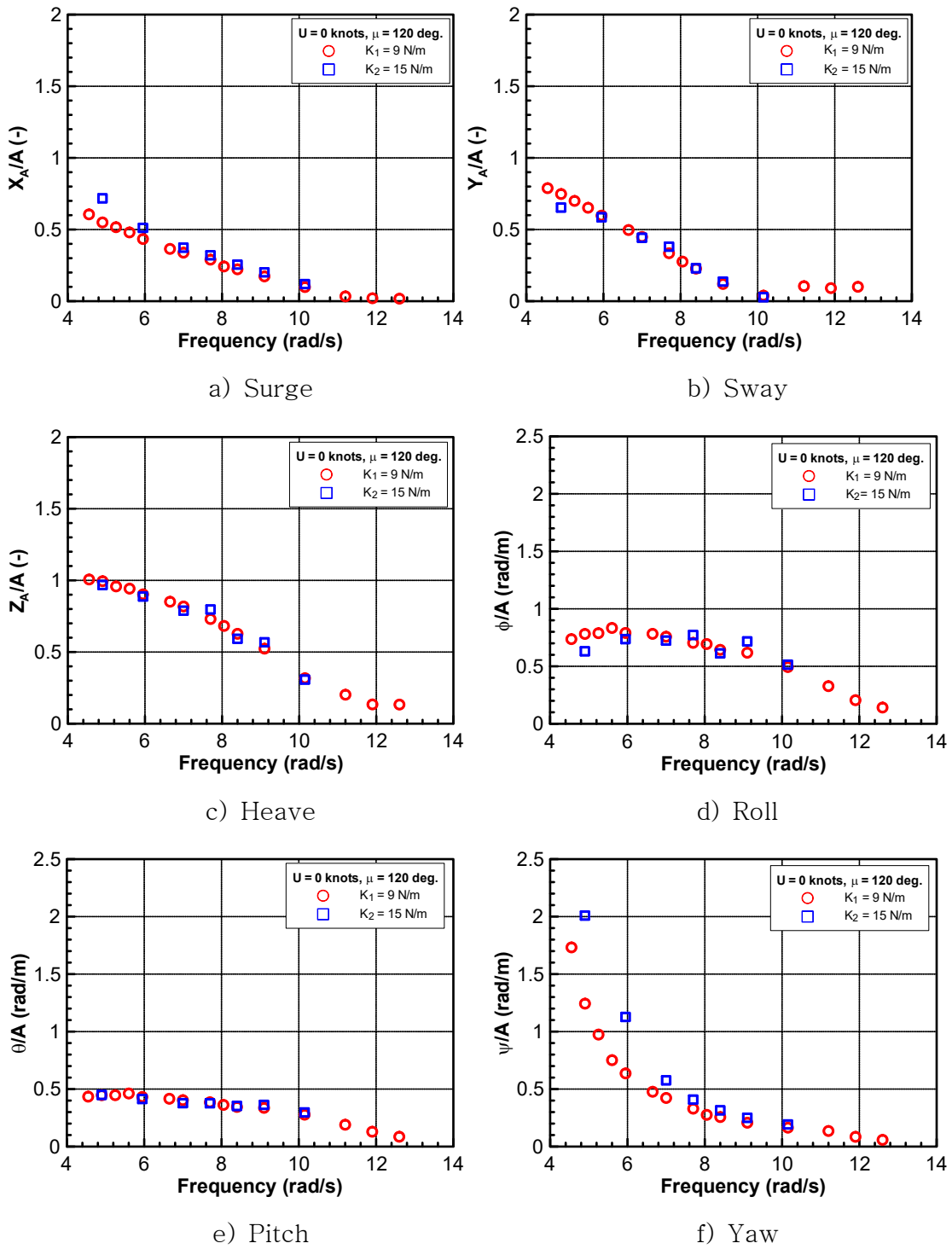


Fig. 3.74 Spring effect of zero speed at wave direction  $120^\circ$

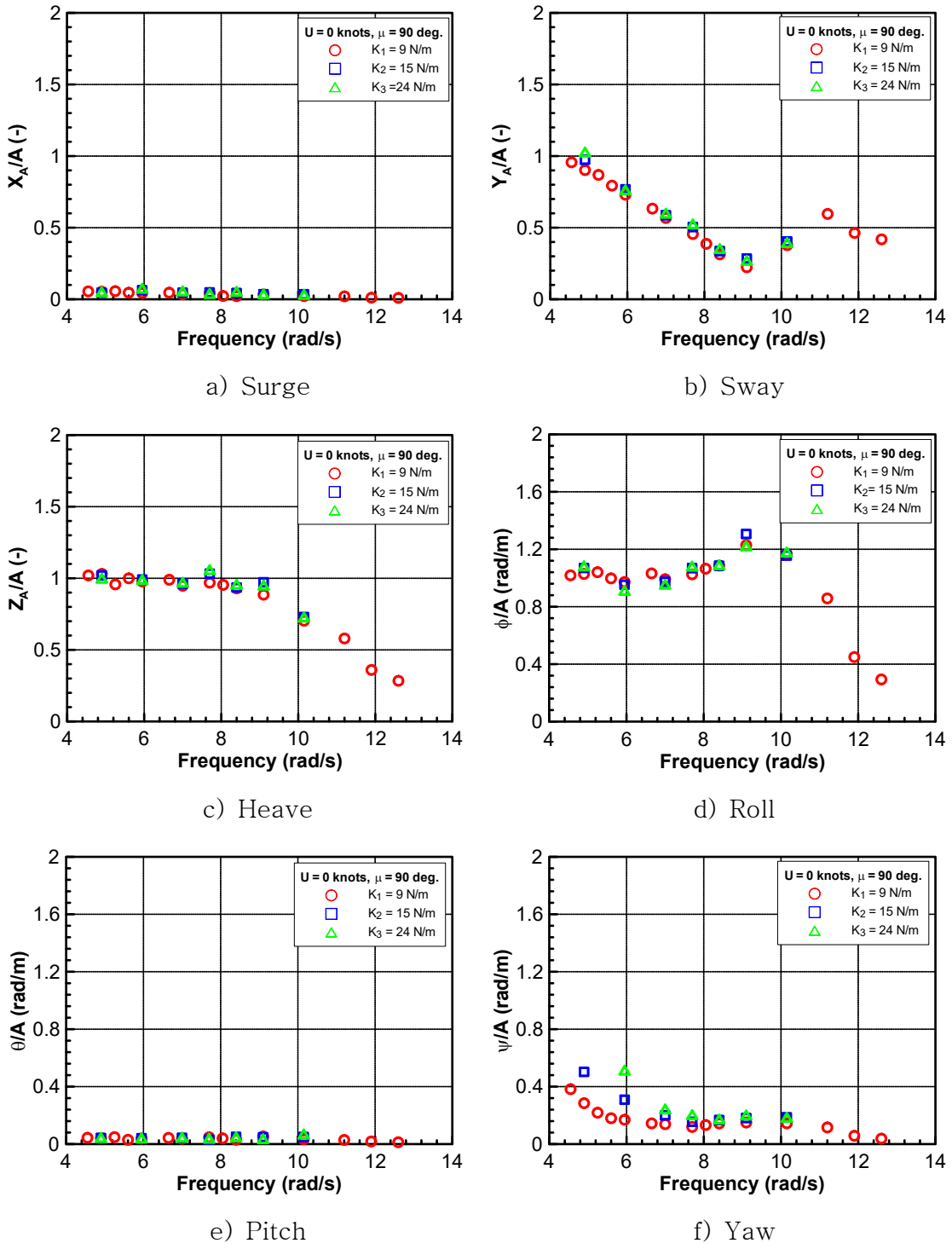


Fig. 3.75 Spring effect of zero speed at wave direction  $90^\circ$

## 4. Seakeeping of the Ship in Irregular Waves

### 4.1 Wave spectrum

In this study, ITTC and TMA spectrum applied for ocean and restricted water, respectively was used to estimate the Root-Mean-Square motion of the ship.

ITTC spectrum is calculated using Eq. (4.1).  $H_s$  is the significant wave height.  $T_1$  is the average period and can be calculated by Eq. (4.2).  $T_z$  is the average zero crossing period.  $\omega$  is the wave frequency.

$$S(\omega) = \frac{A}{\omega^5} e^{-\frac{B}{\omega^4}} \quad (4.1)$$

where,  $A = 173(H_s)^2/T_1^4$ ,  $B = 691/T_1^4$

$$T_1 = 1.073 T_z \quad (4.2)$$

TMA spectrum is usually used for the restricted water depth. Therefore, the definition of the TMA spectrum includes the variable of water depth. TMA spectrum is determined by Eq. (4.3).  $\gamma$  is the peak enhancement factor. The Philips parameter  $\alpha$  depends on the peak enhancement factor  $\gamma$  and can be calculated by Eq. (4.4). The spectral peak period  $T_P$  is estimated by Eq. (4.5).  $h$  is the water depth and  $g$  is gravitational acceleration. The transformation factor  $\phi(\omega_h)$  represents for the effect of water depth and can be determined by Eq. (4.8).

$$S(\omega) = \frac{\alpha H_s^2 \omega_P^4}{\omega^5} \exp\left[-1.25\left(\frac{\omega_P}{\omega}\right)^4\right] \gamma \exp\left[-\frac{(\omega - \omega_P)^2}{2\sigma^2 \omega_P^2}\right] \phi(\omega_h) \quad (4.3)$$

$$\alpha = \frac{0.0624(1.094 - 0.01915 \ln \gamma)}{0.23 + 0.0336\gamma - \frac{0.185}{1.9 + \gamma}} \quad (4.4)$$

$$T_P = \frac{T_z}{\sqrt{\frac{5 + \gamma}{10.89 + \gamma}}} \quad (4.5)$$

$$\begin{cases} \sigma = 0.07 & \text{if } \omega \leq \omega_P \\ \sigma = 0.09 & \text{if } \omega > \omega_P \end{cases} \quad (4.6)$$

$$\omega_h = \omega \sqrt{\frac{h}{g}} \quad (4.7)$$

$$\phi(\omega_h) = \begin{cases} 0.5\left(\omega \sqrt{\frac{h}{g}}\right)^2, & \text{if } \omega \sqrt{\frac{h}{g}} \leq 1 \\ 1 - 0.5\left(2 - \omega \sqrt{\frac{h}{g}}\right)^2, & \text{if } 1 < \omega \sqrt{\frac{h}{g}} < 2 \\ 1, & \text{if } \omega \sqrt{\frac{h}{g}} \geq 2 \end{cases} \quad (4.8)$$

In this study, the operation area of the ship is Sinan and Tongyeong. Therefore, the irregular wave conditions were investigated based on the database. The irregular wave conditions were investigated in sea state 2, sea state 3 and sea state 4. Irregular wave conditions of Sinan and Tongyeong are listed in Tables 4.1~4.2. The comparison of ITTC spectrum and TMA spectrum in various sea states in Sinan and Tongyeong are shown in Fig. 4.1.

Table 4.1 Irregular wave conditions in Sinan

Item	Unit	Sea state		
		SS2	SS3	SS4
$H_s$	m	0.5	1.0	1.3
$T_z$	s	3.5	4.0	4.5
$\gamma$	-	1.0	1.0	1.0
$h$	m	20	20	20

Table 4.2 Irregular wave conditions in Tongyeong

Item	Unit	Sea state		
		SS2	SS3	SS4
$H_s$	m	0.5	1.2	2.2
$T_z$	s	3.5	3.5	4.5
$\gamma$	-	2.16	2.16	2.16
$h$	m	20	20	20

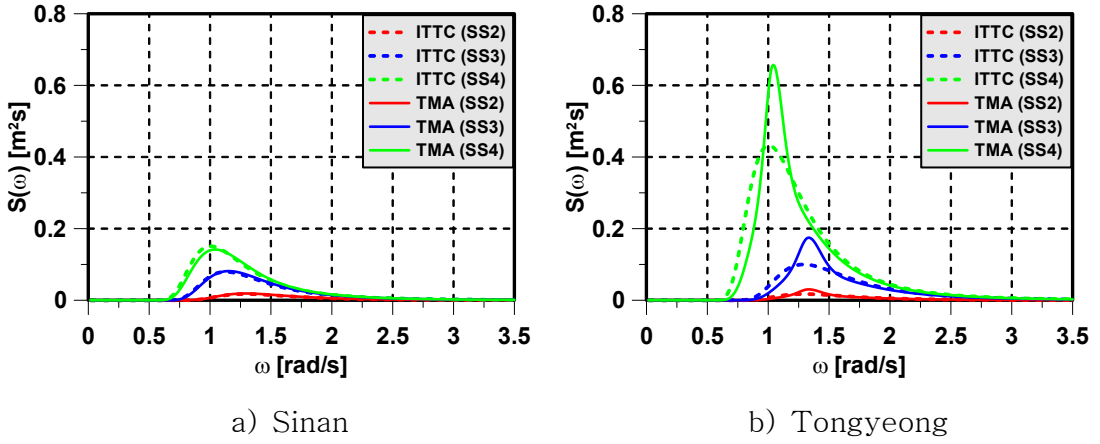


Fig. 4.1 Comparison of ITTC and TMA spectrum in various sea states

Surge, sway, and heave motion energy spectrums can be estimated by Eqs. (4.9)~(4.11). To find the roll, pitch and yaw motion energy spectrum, we need to add the wave slope energy spectrum by Eq. (4.12). Then, roll, pitch and yaw motion energy spectrum can be estimated by Eqs. (4.13)~(4.15).

$$S_x(\omega_e)d\omega_e = \left[ \frac{x_A}{A} \right]^2 S_\zeta(\omega_e)d\omega_e = RAO_x^2 S_\zeta(\omega_e)d\omega_e \quad (4.9)$$

$$S_y(\omega_e)d\omega_e = \left[ \frac{y_A}{A} \right]^2 S_\zeta(\omega_e)d\omega_e = RAO_y^2 S_\zeta(\omega_e)d\omega_e \quad (4.10)$$

$$S_z(\omega_e)d\omega_e = \left[ \frac{z_A}{A} \right]^2 S_\zeta(\omega_e)d\omega_e = RAO_z^2 S_\zeta(\omega_e)d\omega_e \quad (4.11)$$

$$S_\alpha(\omega_e) = \frac{\omega^2}{g} S_\zeta(\omega_e) = k^2 S_\zeta(\omega_e) \quad (4.12)$$

$$S_\phi(\omega_e)d\omega_e = \left[ \frac{\phi_A}{kA} \right]^2 k^2 S_\zeta(\omega_e)d\omega_e = RAO_\phi^2 S_\alpha(\omega_e)d\omega_e \quad (4.13)$$

$$S_\theta(\omega_e)d\omega_e = \left[ \frac{\theta_A}{kA} \right]^2 k^2 S_\zeta(\omega_e)d\omega_e = RAO_\theta^2 S_\alpha(\omega_e)d\omega_e \quad (4.14)$$

$$S_\psi(\omega_e)d\omega_e = \left[ \frac{\psi_A}{kA} \right]^2 k^2 S_\zeta(\omega_e)d\omega_e = RAO_\psi^2 S_\alpha(\omega_e)d\omega_e \quad (4.15)$$

The variances of surge, sway, heave, roll, pitch and yaw can be estimated by Eqs. (4.16)~(4.21). The root-mean-square (RMS) motion value are equal to the square-root of the variances. So, the RMS values for surge, sway, heave, roll, pitch and yaw amplitude can be estimated by Eqs. (4.22)~(4.27).

$$m_{0x} = \int_0^{\infty} S_x(\omega_e) d\omega_e \quad (4.16)$$

$$m_{0y} = \int_0^{\infty} S_y(\omega_e) d\omega_e \quad (4.17)$$

$$m_{0z} = \int_0^{\infty} S_z(\omega_e) d\omega_e \quad (4.18)$$

$$m_{0\phi} = \int_0^{\infty} S_{\phi}(\omega_e) d\omega_e \quad (4.19)$$

$$m_{0\theta} = \int_0^{\infty} S_{\theta}(\omega_e) d\omega_e \quad (4.20)$$

$$m_{0\psi} = \int_0^{\infty} S_{\psi}(\omega_e) d\omega_e \quad (4.21)$$

$$\sigma_x = \sqrt{m_{0x}} \quad (4.22)$$

$$\sigma_y = \sqrt{m_{0y}} \quad (4.23)$$

$$\sigma_z = \sqrt{m_{0z}} \quad (4.24)$$

$$\sigma_{\phi} = \sqrt{m_{0\phi}} \quad (4.25)$$

$$\sigma_{\theta} = \sqrt{m_{0\theta}} \quad (4.26)$$

$$\sigma_{\psi} = \sqrt{m_{0\psi}} \quad (4.27)$$

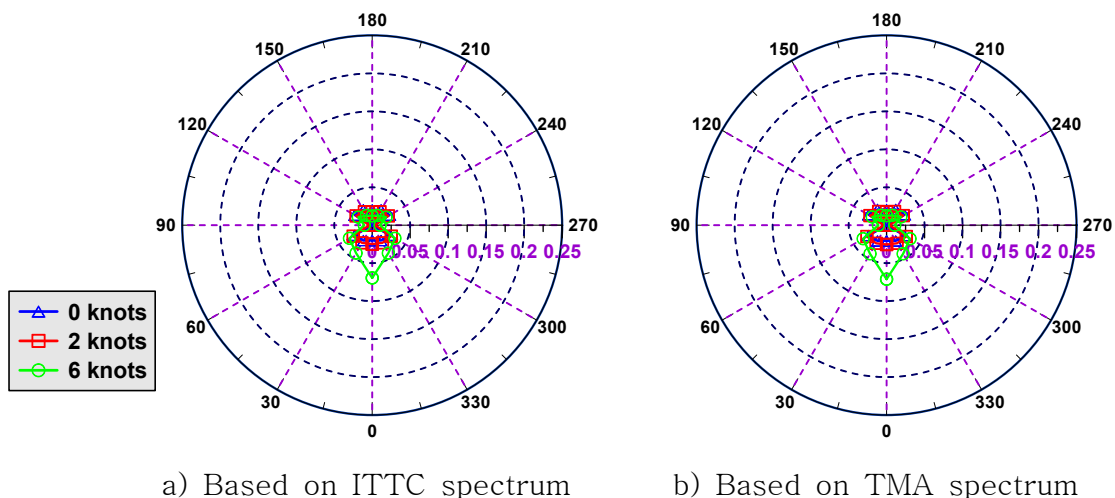
## 4.2 Root-Mean-Square (RMS) motion

In this study, the irregular wave conditions are considered in Sinan and Tongyeong area. The significant wave height and average zero crossing period were calculated based on the database of sea states in Sinan and Tongyeong. The RMS value for 6-DOF motion was estimated in sea state 2, sea state 3 and sea state 4 for various ship speeds and wave directions. The RMS motion changes dramatically in various wave directions and sea states. The RMS motion which is calculated based on ITTC spectrum and TMA spectrum are compared.

### 4.2.1 Sinan

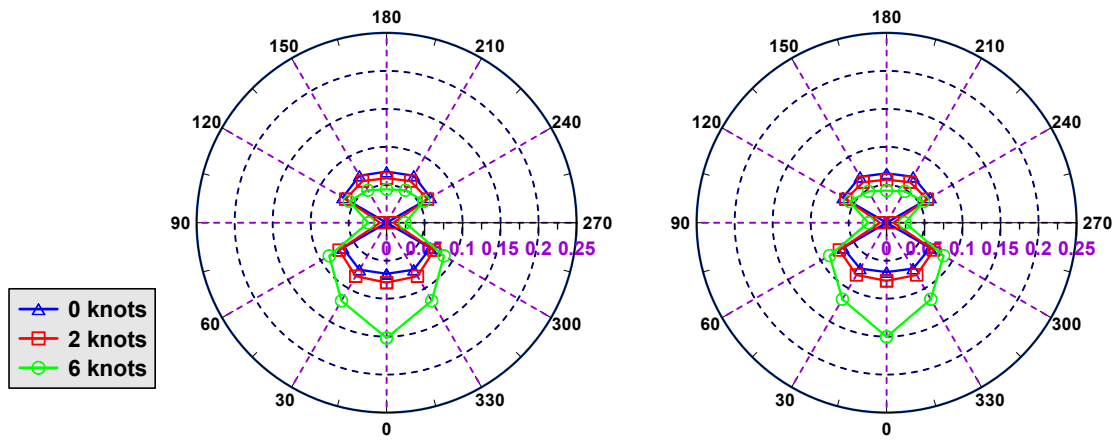
This part investigates RMS motion in Sinan. Because the wave spectrums in Sinan show the same results when the ITTC and TMA spectrum were applied, RMS motion is almost same. Figs. 4.2~4.4 show the comparison of RMS surge which is estimated based on ITTC and TMA spectrum. RMS

motion increases significantly when the sea state increases. RMS surge is greatest when the wave direction reaches to 0 degree and 180 degrees. RMS surge is the smallest in beam sea. In addition, RMS surge changes dramatically in various ship speed, especially in case of 6 knots. Figs. 4.5~4.7 show the comparison of RMS sway which is estimated based on ITTC and TMA spectrum. In case of RMS sway, it is dominant at beam sea and reduces when the wave direction reaches to head sea and following sea. RMS sway increases slightly when the ship speed increases. Tables 4.3~4.6 list the results of RMS surge and RMS sway in various wave directions and various ship speeds at sea state 2, sea state 3 and sea state 4 based on ITTC and TMA spectrum. Figs. 4.8~4.10 show the comparison of RMS heave which is estimated based on ITTC and TMA spectrum. The RMS heave changes slightly in various wave directions and it is the largest in beam sea. RMS heave changes slightly in various ship speeds. Figs. 4.11~4.13 show the comparison of RMS roll which is estimated based on ITTC and TMA spectrum. RMS roll is dominant in case of beam sea due to wave exciting in y direction. As the same as RMS sway, RMS roll reduces when the wave direction reaches head sea and following sea. RMS roll is the largest in zero speed and reduces when the ship speed increases. Tables 4.7~4.10 list the results of RMS heave and RMS roll in various wave directions and various ship speeds at sea state 2, sea state 3 and sea state 4 based on ITTC and TMA spectrum. Figs. 4.14~4.16 show the comparison of RMS pitch which is estimated based on ITTC and TMA spectrum. RMS pitch is the greatest in head sea and following sea. In addition, when the wave direction reaches to 90 degrees, RMS pitch becomes zero. Figs. 4.17~4.19 show the comparison of RMS yaw which is estimated based on ITTC and TMA spectrum. RMS yaw is dominant in oblique wave and it is the smallest when the wave direction reaches to 0 degree, 90 degrees and 180 degrees. Tables 4.20~4.24 list the results of RMS pitch and RMS yaw in various wave directions and various ship speeds at sea state 2, sea state 3 and sea state 4 based on ITTC and TMA spectrum.



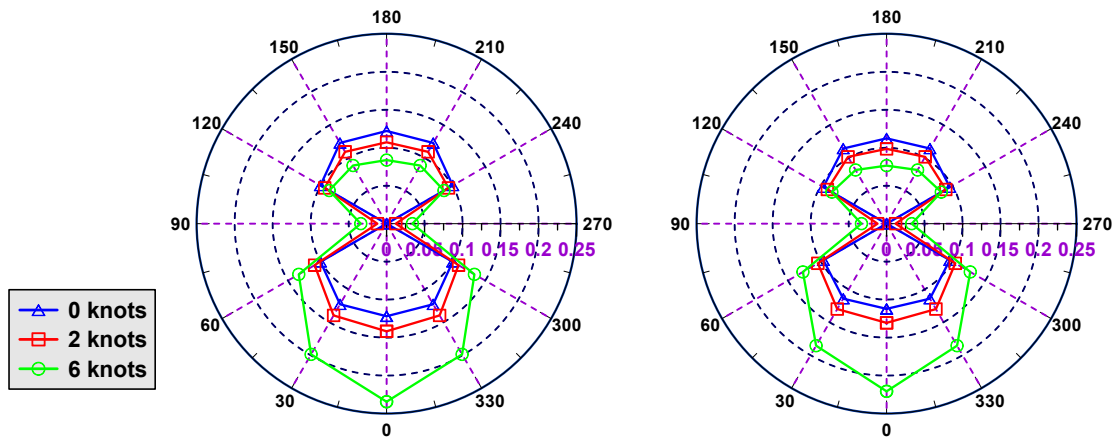
a) Based on ITTC spectrum      b) Based on TMA spectrum

Fig. 4.2 RMS surge in case of sea state 2 in Sinan (m)



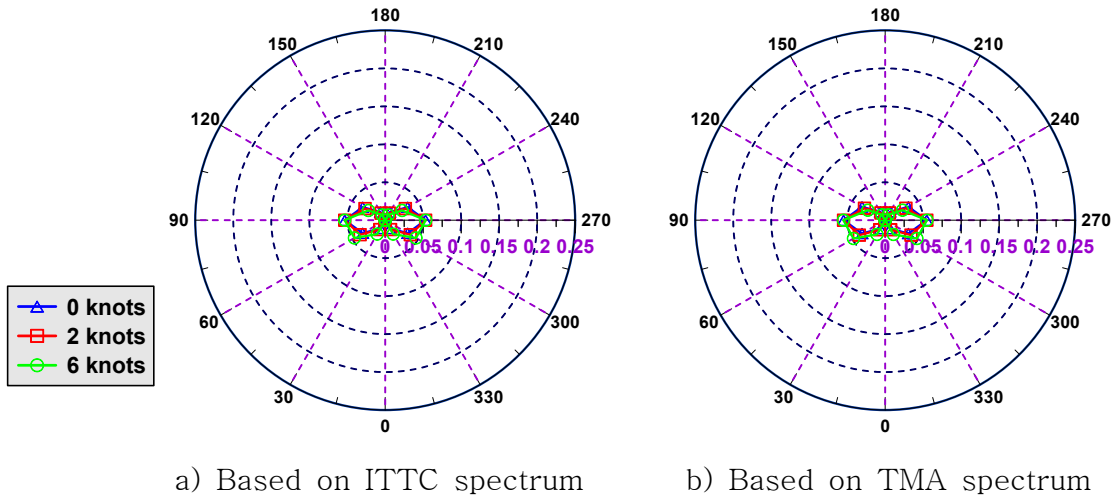
a) Based on ITTC spectrum      b) Based on TMA spectrum

Fig. 4.3 RMS surge in case of sea state 3 in Sinan (m)



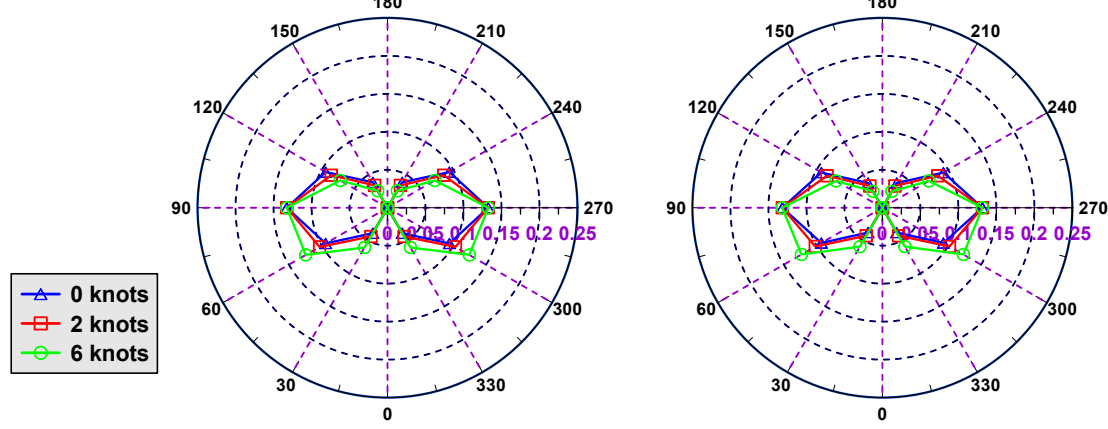
a) Based on ITTC spectrum      b) Based on TMA spectrum

Fig. 4.4 RMS surge in case of sea state 4 in Sinan (m)



a) Based on ITTC spectrum      b) Based on TMA spectrum

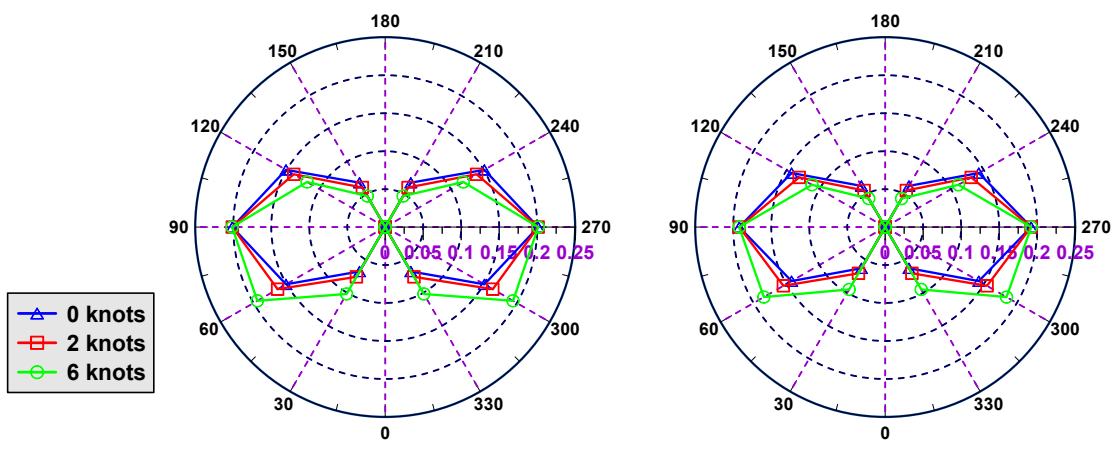
Fig. 4.5 RMS sway in case of sea state 2 in Sinan (m)



a) Based on ITTC spectrum

b) Based on TMA spectrum

Fig. 4.6 RMS sway in case of sea state 3 in Sinan (m)



a) Based on ITTC spectrum

b) Based on TMA spectrum

Fig. 4.7 RMS sway in case of sea state 4 in Sinan (m)

Table 4.3 RMS value for surge based on ITTC spectrum in Sinan (m)

Wave direction [deg.]	0 knots			2 knots			6 knots		
	SS2	SS3	SS4	SS2	SS3	SS4	SS2	SS3	SS4
0	0.020	0.067	0.122	0.025	0.079	0.142	0.069	0.152	0.234
30	0.023	0.071	0.123	0.027	0.081	0.140	0.042	0.119	0.199
60	0.026	0.066	0.100	0.029	0.072	0.109	0.035	0.087	0.133
90	0.000	0.000	0.000	0.004	0.009	0.012	0.010	0.024	0.034
120	0.027	0.067	0.101	0.024	0.062	0.094	0.021	0.057	0.087
150	0.023	0.072	0.123	0.020	0.063	0.109	0.015	0.049	0.088
180	0.020	0.067	0.122	0.017	0.059	0.107	0.012	0.044	0.084

Table 4.4 RMS value for surge based on TMA spectrum in Sinan (m)

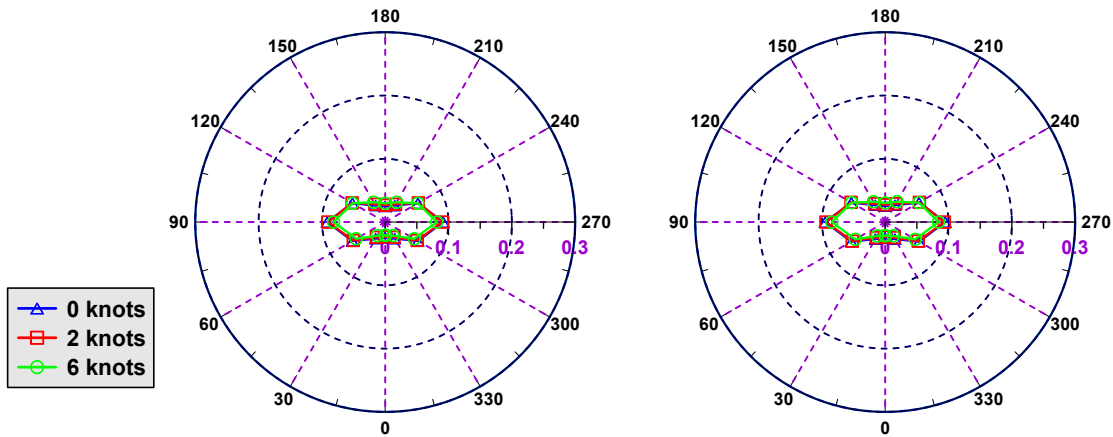
Wave direction [deg.]	0 knots			2 knots			6 knots		
	SS2	SS3	SS4	SS2	SS3	SS4	SS2	SS3	SS4
0	0.021	0.065	0.112	0.025	0.076	0.131	0.071	0.150	0.221
30	0.024	0.070	0.114	0.028	0.079	0.130	0.044	0.116	0.186
60	0.027	0.066	0.096	0.030	0.072	0.104	0.036	0.087	0.127
90	0.000	0.000	0.000	0.004	0.009	0.012	0.011	0.024	0.033
120	0.027	0.066	0.096	0.025	0.062	0.090	0.022	0.056	0.083
150	0.024	0.070	0.114	0.021	0.062	0.102	0.015	0.048	0.082
180	0.021	0.065	0.112	0.018	0.057	0.098	0.012	0.042	0.076

Table 4.5 RMS value for sway based on ITTC spectrum in Sinan (m)

Wave direction [deg.]	0 knots			2 knots			6 knots		
	SS2	SS3	SS4	SS2	SS3	SS4	SS2	SS3	SS4
0	0.000	0.000	0.000	0.000	0.000	0.000	0.000	0.000	0.000
30	0.012	0.039	0.068	0.014	0.044	0.076	0.021	0.060	0.102
60	0.034	0.094	0.151	0.038	0.103	0.164	0.047	0.124	0.194
90	0.053	0.133	0.201	0.053	0.132	0.201	0.053	0.133	0.201
120	0.034	0.094	0.151	0.031	0.086	0.139	0.026	0.072	0.119
150	0.012	0.039	0.067	0.011	0.034	0.060	0.008	0.026	0.047
180	0.000	0.000	0.000	0.000	0.000	0.000	0.000	0.000	0.000

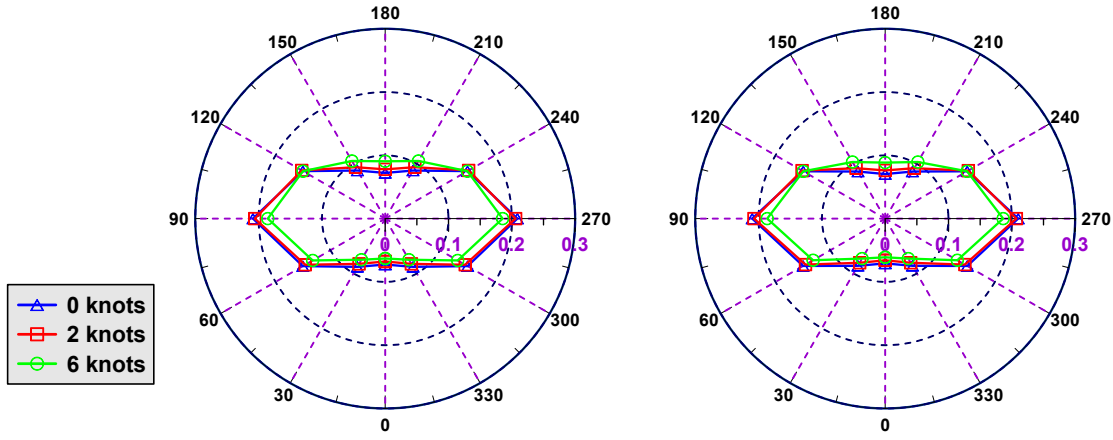
Table 4.6 RMS value for sway based on TMA spectrum in Sinan (m)

Wave direction [deg.]	0 knots			2 knots			6 knots		
	SS2	SS3	SS4	SS2	SS3	SS4	SS2	SS3	SS4
0	0.000	0.000	0.000	0.000	0.000	0.000	0.000	0.000	0.000
30	0.013	0.038	0.063	0.015	0.043	0.070	0.022	0.059	0.095
60	0.035	0.093	0.142	0.039	0.102	0.155	0.048	0.123	0.184
90	0.055	0.132	0.192	0.055	0.132	0.192	0.055	0.132	0.192
120	0.035	0.093	0.142	0.032	0.084	0.131	0.026	0.071	0.111
150	0.013	0.038	0.063	0.011	0.033	0.056	0.008	0.025	0.043
180	0.000	0.000	0.000	0.000	0.000	0.000	0.000	0.000	0.000



a) Based on ITTC spectrum      b) Based on TMA spectrum

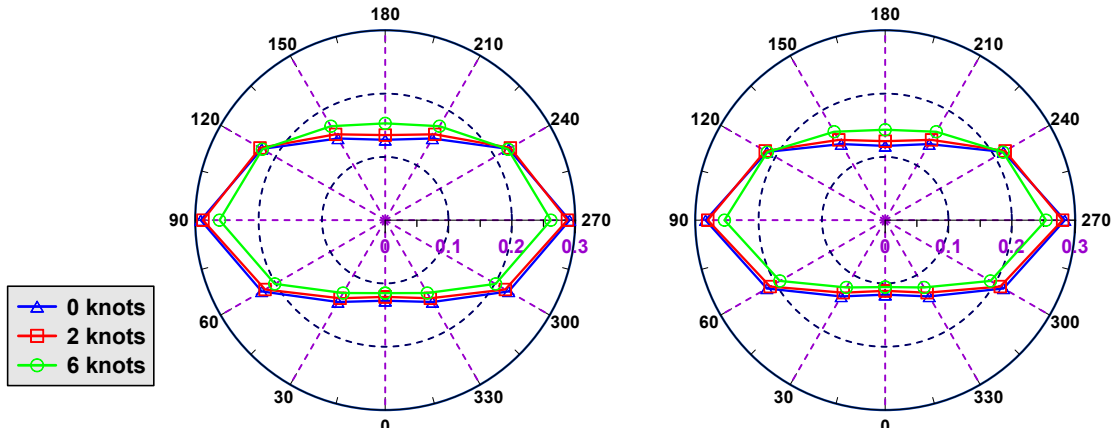
Fig. 4.8 RMS heave in case of sea state 2 in Sinan (m)



a) Based on ITTC spectrum

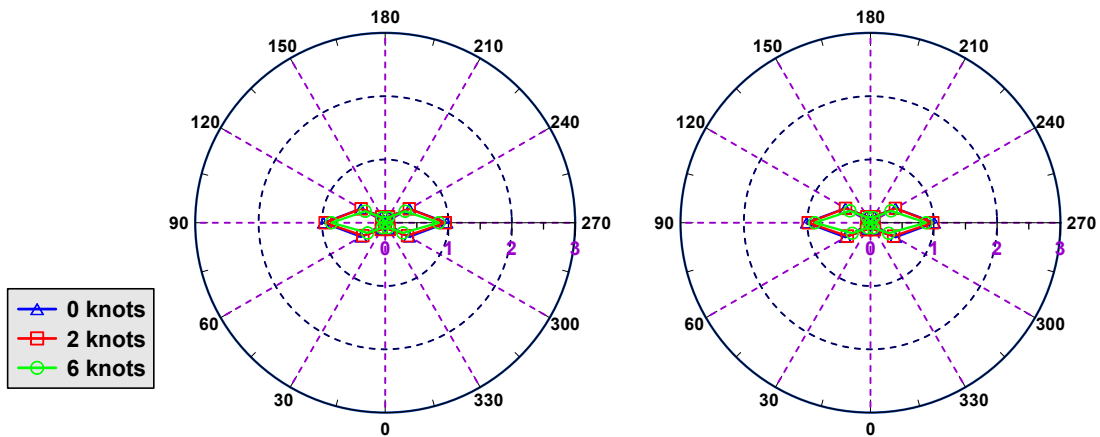
b) Based on TMA spectrum

Fig. 4.9 RMS heave in case of sea state 3 in Sinan (m)



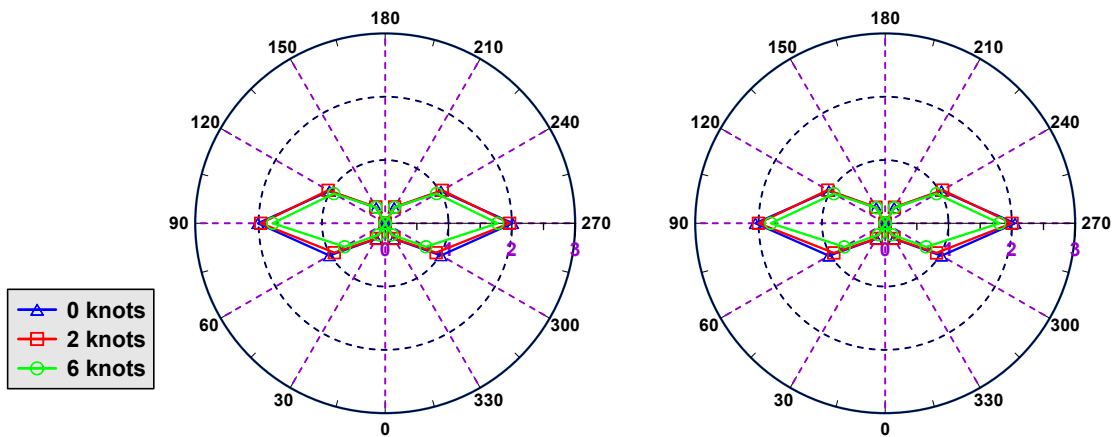
a) Based on ITTC spectrum      b) Based on TMA spectrum

Fig. 4.10 RMS heave in case of sea state 4 in Sinan (m)



a) Based on ITTC spectrum      b) Based on TMA spectrum

Fig. 4.11 RMS roll in case of sea state 2 in Sinan (°)



a) Based on ITTC spectrum      b) Based on TMA spectrum

Fig. 4.12 RMS roll in case of sea state 3 in Sinan (°)

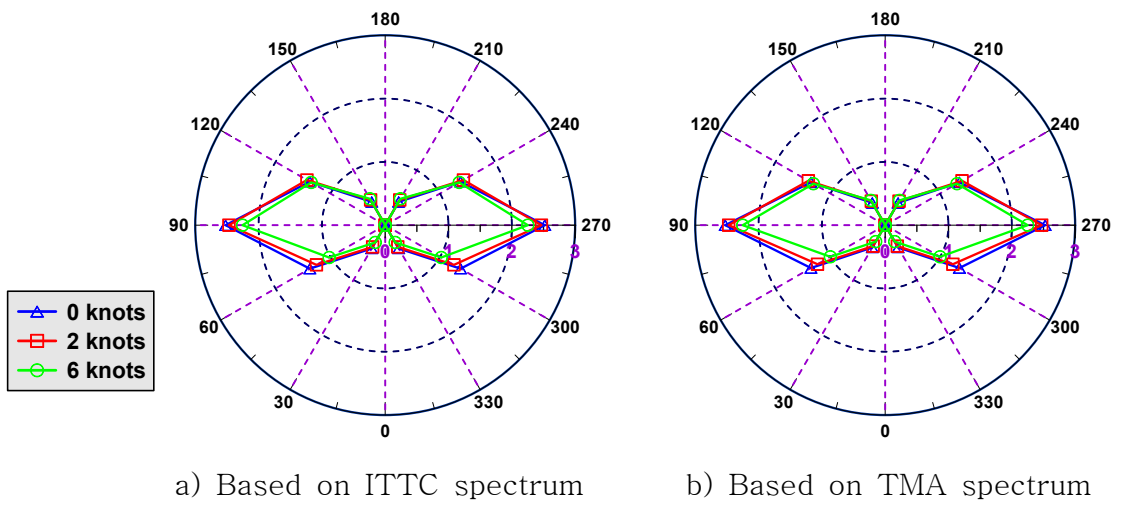


Fig. 4.13 RMS roll in case of sea state 4 in Sinan ( $^{\circ}$ )

Table 4.7 RMS value for heave based on ITTC spectrum in Sinan (m)

Wave direction [deg.]	0 knots			2 knots			6 knots		
	SS2	SS3	SS4	SS2	SS3	SS4	SS2	SS3	SS4
0	0.025	0.073	0.127	0.023	0.068	0.121	0.021	0.063	0.115
30	0.030	0.088	0.149	0.028	0.083	0.143	0.025	0.075	0.133
60	0.060	0.150	0.225	0.058	0.146	0.219	0.053	0.132	0.201
90	0.092	0.209	0.291	0.090	0.206	0.288	0.081	0.185	0.262
120	0.060	0.150	0.225	0.060	0.152	0.228	0.059	0.150	0.224
150	0.030	0.088	0.149	0.033	0.094	0.157	0.036	0.105	0.171
180	0.025	0.072	0.127	0.027	0.078	0.134	0.030	0.091	0.153

Table 4.8 RMS value for heave based on TMA spectrum in Sinan (m)

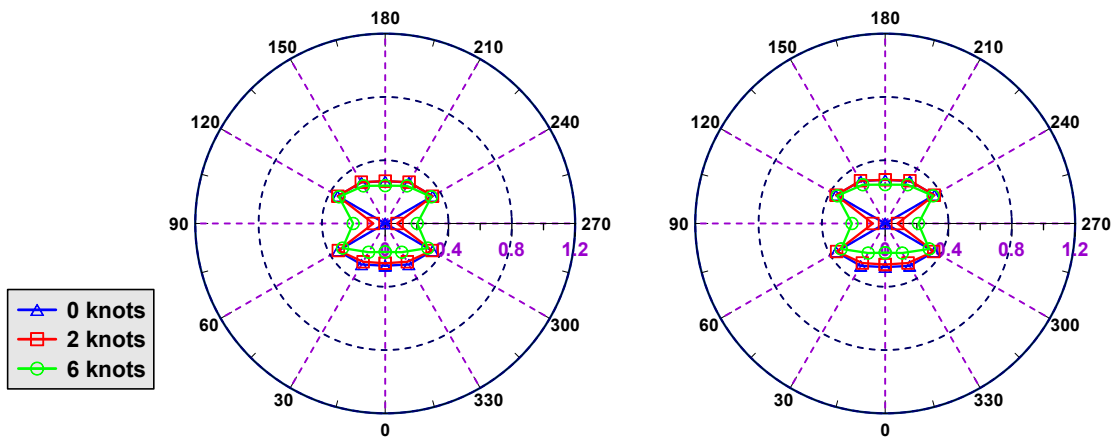
Wave direction [deg.]	0 knots			2 knots			6 knots		
	SS2	SS3	SS4	SS2	SS3	SS4	SS2	SS3	SS4
0	0.026	0.071	0.118	0.023	0.066	0.112	0.021	0.061	0.106
30	0.031	0.086	0.139	0.028	0.081	0.132	0.025	0.073	0.123
60	0.062	0.150	0.216	0.060	0.145	0.210	0.055	0.132	0.192
90	0.095	0.210	0.284	0.093	0.207	0.280	0.084	0.186	0.254
120	0.062	0.149	0.216	0.062	0.152	0.219	0.061	0.149	0.215
150	0.031	0.086	0.139	0.033	0.092	0.146	0.037	0.103	0.161
180	0.025	0.070	0.117	0.027	0.076	0.125	0.030	0.088	0.143

Table 4.9 RMS value for roll based on ITTC spectrum in Sinan (°)

Wave direction [deg.]	0 knots			2 knots			6 knots		
	SS2	SS3	SS4	SS2	SS3	SS4	SS2	SS3	SS4
0	0.000	0.000	0.000	0.000	0.000	0.000	0.000	0.000	0.000
30	0.114	0.284	0.425	0.124	0.277	0.397	0.090	0.210	0.315
60	0.442	1.018	1.374	0.407	0.928	1.254	0.322	0.742	1.022
90	0.973	2.012	2.520	0.948	1.965	2.467	0.847	1.775	2.252
120	0.442	1.017	1.374	0.439	1.042	1.427	0.364	0.938	1.350
150	0.114	0.285	0.425	0.108	0.298	0.460	0.092	0.292	0.481
180	0.000	0.000	0.000	0.000	0.000	0.000	0.000	0.000	0.000

Table 4.10 RMS value for roll based on TMA spectrum in Sinan (°)

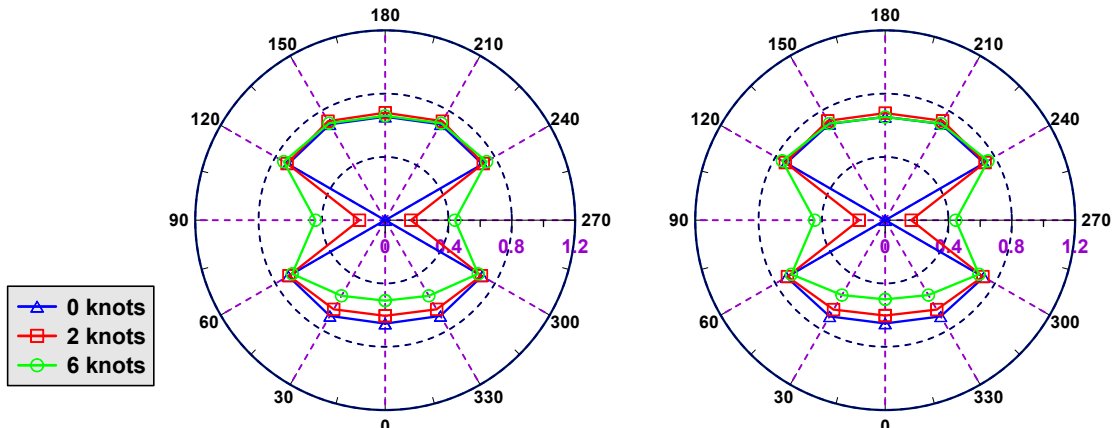
Wave direction [deg.]	0 knots			2 knots			6 knots		
	SS2	SS3	SS4	SS2	SS3	SS4	SS2	SS3	SS4
0	0.000	0.000	0.000	0.000	0.000	0.000	0.000	0.000	0.000
30	0.117	0.282	0.407	0.127	0.277	0.382	0.092	0.209	0.300
60	0.458	1.026	1.354	0.422	0.937	1.234	0.333	0.746	1.000
90	1.010	2.050	2.526	0.984	2.002	2.472	0.879	1.806	2.250
120	0.458	1.026	1.354	0.454	1.048	1.401	0.375	0.935	1.310
150	0.117	0.283	0.407	0.110	0.293	0.438	0.094	0.284	0.452
180	0.000	0.000	0.000	0.000	0.000	0.000	0.000	0.000	0.000



a) Based on ITTC spectrum

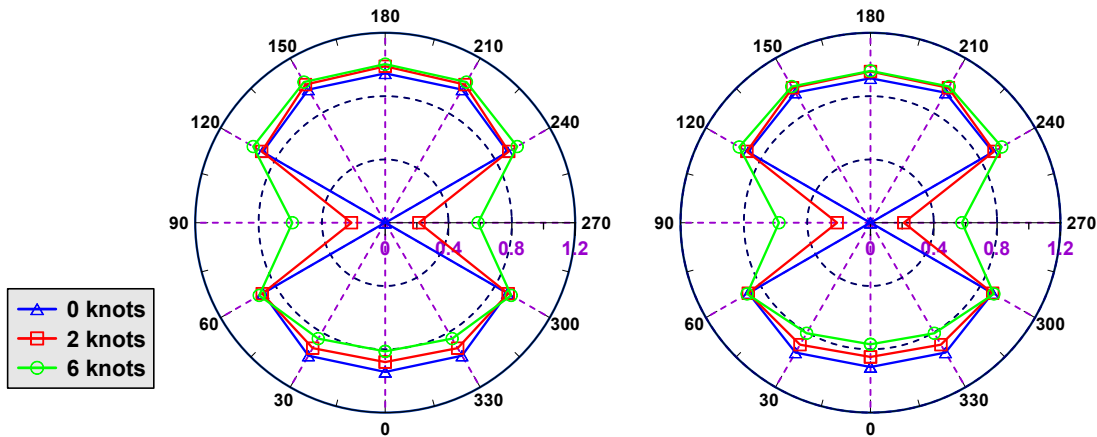
b) Based on TMA spectrum

Fig. 4.14 RMS pitch in case of sea state 2 in Sinan (°)



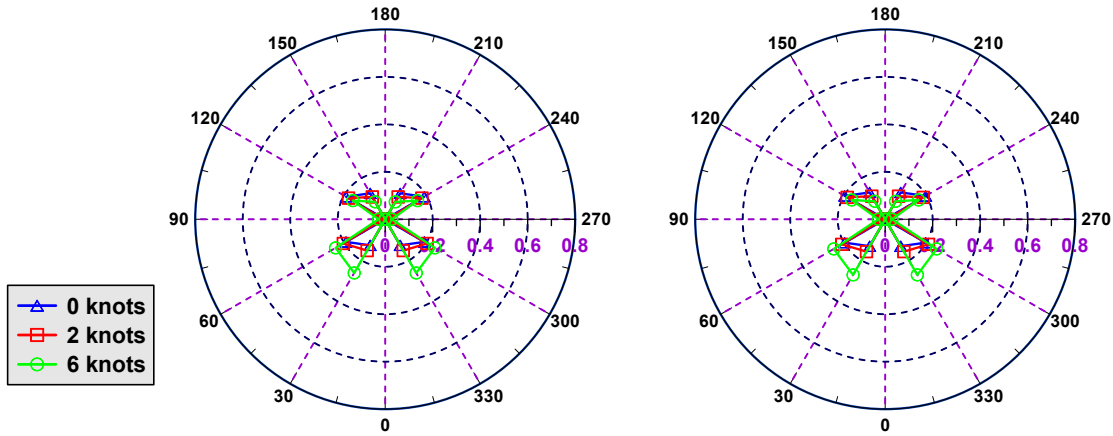
a) Based on ITTC spectrum      b) Based on TMA spectrum

Fig. 4.15 RMS pitch in case of sea state 3 in Sinan ( $^{\circ}$ )



a) Based on ITTC spectrum      b) Based on TMA spectrum

Fig. 4.16 RMS pitch in case of sea state 4 in Sinan ( $^{\circ}$ )



a) Based on ITTC spectrum      b) Based on TMA spectrum

Fig. 4.17 RMS yaw in case of sea state 2 in Sinan ( $^{\circ}$ )

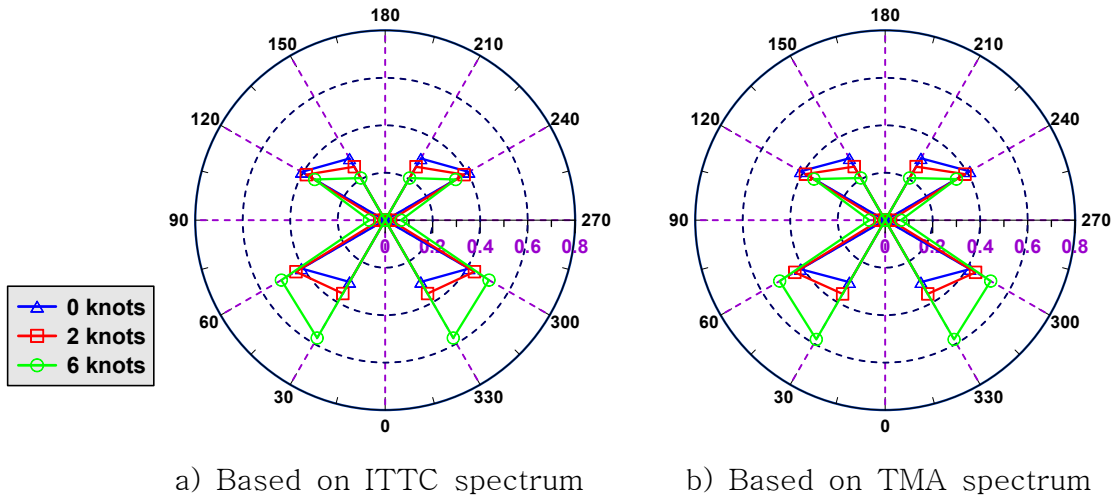


Fig. 4.18 RMS yaw in case of sea state 3 in Sinan ( $^{\circ}$ )

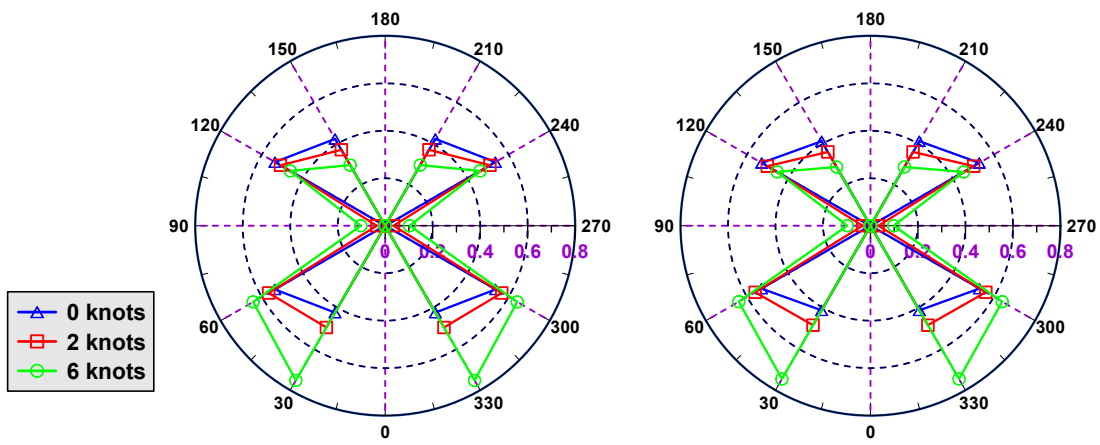


Fig. 4.19 RMS yaw in case of sea state 4 in Sinan ( $^{\circ}$ )

Table 4.11 RMS value for pitch based on ITTC spectrum in Sinan ( $^{\circ}$ )

Wave direction [deg.]	0 knots			2 knots			6 knots		
	SS2	SS3	SS4	SS2	SS3	SS4	SS2	SS3	SS4
0	0.267	0.654	0.943	0.252	0.604	0.881	0.180	0.509	0.813
30	0.299	0.699	0.970	0.279	0.650	0.916	0.210	0.552	0.846
60	0.345	0.707	0.892	0.342	0.702	0.897	0.311	0.678	0.919
90	0.001	0.001	0.001	0.075	0.162	0.213	0.202	0.441	0.586
120	0.346	0.709	0.894	0.345	0.715	0.901	0.337	0.740	0.963
150	0.300	0.700	0.971	0.302	0.723	1.008	0.274	0.708	1.026
180	0.267	0.654	0.944	0.268	0.679	0.989	0.239	0.660	1.002

Table 4.12 RMS value for pitch based on TMA spectrum in Sinan (°)

Wave direction [deg.]	0 knots			2 knots			6 knots		
	SS2	SS3	SS4	SS2	SS3	SS4	SS2	SS3	SS4
0	0.275	0.653	0.912	0.259	0.603	0.848	0.185	0.500	0.769
30	0.309	0.702	0.948	0.289	0.652	0.890	0.216	0.547	0.807
60	0.358	0.719	0.890	0.354	0.713	0.891	0.321	0.684	0.900
90	0.001	0.001	0.001	0.078	0.164	0.211	0.210	0.445	0.578
120	0.359	0.721	0.892	0.358	0.728	0.902	0.349	0.750	0.957
150	0.310	0.703	0.949	0.312	0.725	0.984	0.283	0.705	0.994
180	0.276	0.653	0.913	0.276	0.677	0.956	0.246	0.652	0.960

Table 4.13 RMS value for yaw based on ITTC spectrum in Sinan (°)

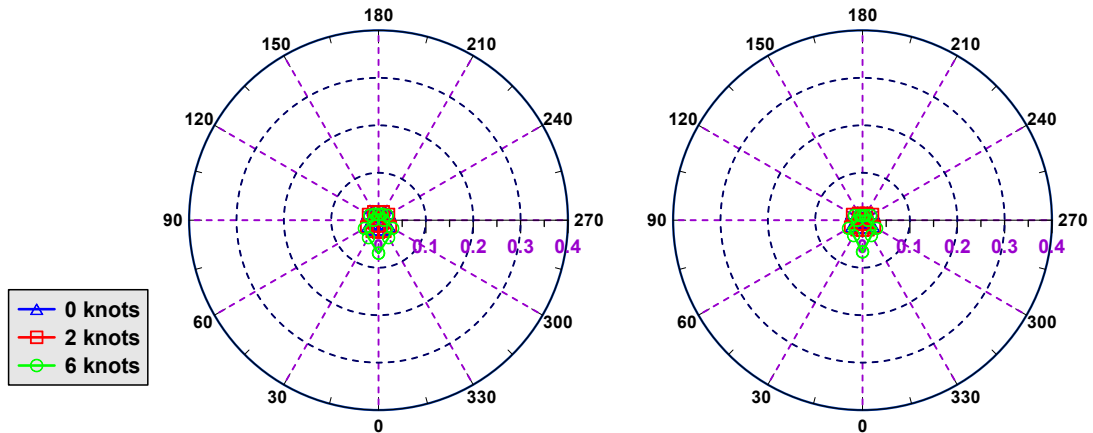
Wave direction [deg.]	0 knots			2 knots			6 knots		
	SS2	SS3	SS4	SS2	SS3	SS4	SS2	SS3	SS4
0	0.000	0.000	0.000	0.000	0.000	0.000	0.000	0.000	0.000
30	0.127	0.300	0.423	0.152	0.357	0.495	0.261	0.573	0.753
60	0.190	0.407	0.537	0.204	0.434	0.567	0.241	0.505	0.642
90	0.001	0.001	0.002	0.010	0.023	0.035	0.028	0.067	0.103
120	0.190	0.407	0.536	0.178	0.384	0.509	0.157	0.343	0.461
150	0.126	0.300	0.422	0.109	0.260	0.369	0.085	0.205	0.295
180	0.000	0.000	0.000	0.000	0.000	0.000	0.000	0.000	0.000

Table 4.14 RMS value for yaw based on TMA spectrum in Sinan (°)

Wave direction [deg.]	0 knots			2 knots			6 knots		
	SS2	SS3	SS4	SS2	SS3	SS4	SS2	SS3	SS4
0	0.000	0.000	0.000	0.000	0.000	0.000	0.000	0.000	0.000
30	0.131	0.301	0.412	0.157	0.359	0.484	0.271	0.580	0.746
60	0.197	0.412	0.530	0.211	0.439	0.561	0.250	0.513	0.641
90	0.001	0.001	0.002	0.010	0.023	0.033	0.029	0.067	0.098
120	0.197	0.411	0.529	0.185	0.388	0.502	0.163	0.346	0.453
150	0.131	0.301	0.411	0.113	0.261	0.359	0.088	0.205	0.286
180	0.000	0.000	0.000	0.000	0.000	0.000	0.000	0.000	0.000

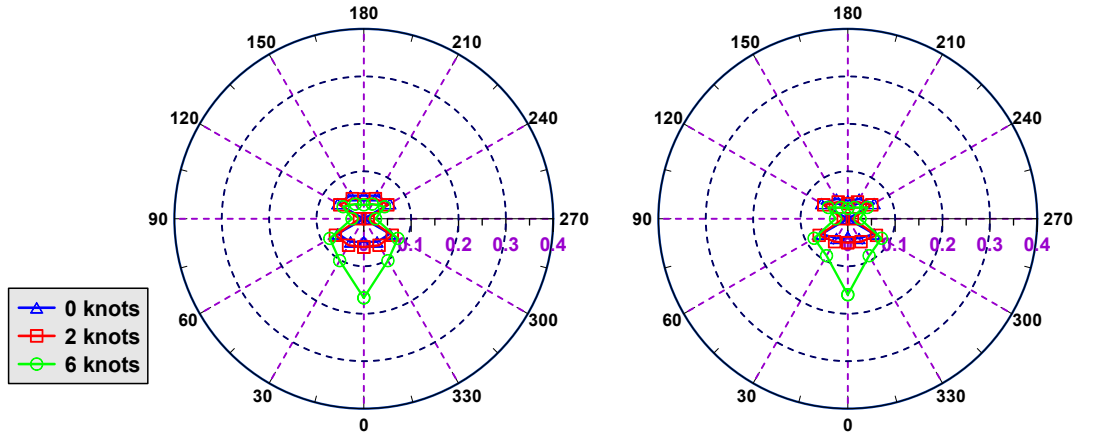
#### 4.2.2 Tongyeong

This part investigates the RMS motion in Tongyeong. Although the amplitude of TMA spectrum is higher than the amplitude of ITTC spectrum, the range of frequency of ITTC spectrum is larger than range of frequency of TMA spectrum. Therefore, the area under wave spectrum based on TMA and ITTC spectrum are the same. Figs. 4.20~4.22 show the comparison of RMS surge which is estimated based on ITTC and TMA spectrum. The RMS motion increases significantly following the larger sea state. The RMS surge is the greatest when the wave direction reaches 0 degree due to the speed effect especially in case of 6 knots. Figs. 4.23~4.25 show the comparison of RMS sway which is estimated based on ITTC spectrum and TMA spectrum. In case of RMS sway, it is dominant at beam sea and reduces when the wave direction reaches to head sea and following sea. The RMS of sway increases slightly when the ship speed increases. Tables 4.15~4.18 list the results of the RMS surge and RMS sway in various wave directions and various ship speeds at various sea states based on ITTC and TMA spectrum. Figs. 4.26~4.28 show the comparison of RMS heave which is estimated based on ITTC and TMA spectrum. The RMS heave changes slightly in various wave directions and it is the largest in beam sea. Figs. 4.29~4.31 show the comparison of RMS roll which is estimated based on ITTC and TMA spectrum. The RMS roll is dominant in case of beam sea due to wave exciting in y direction. As the same as RMS sway, RMS roll reduces when the wave direction reaches head sea and following sea. Tables 4.17~4.20 list the results of the RMS heave and RMS roll in various wave directions, various ship speeds and various sea states based on ITTC and TMA spectrum. Figs. 4.32~4.34 show the comparison of RMS pitch which is estimated based on ITTC and TMA spectrum. The RMS pitch is the greatest in head sea and following sea. Figs. 4.35~4.37 show the comparison of RMS yaw which is estimated based on ITTC and TMA spectrum. The RMS yaw is dominant in oblique wave and it is the smallest when the wave direction reaches to 0 degree, 90 degrees and 180 degrees. Tables 4.21~4.24 list the results of the RMS pitch and RMS yaw in various wave directions and various ship speeds at various sea states based on ITTC and TMA spectrum.



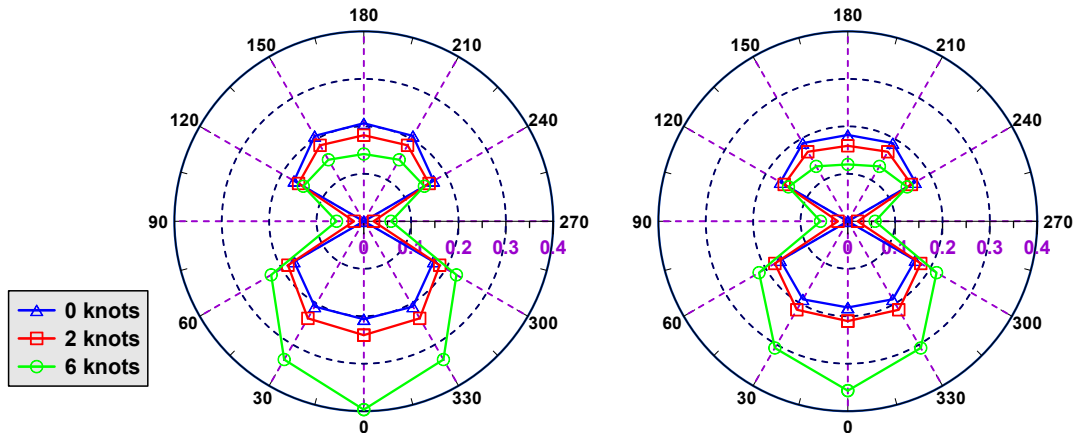
a) Based on ITTC spectrum      b) Based on TMA spectrum

Fig. 4.20 RMS surge in case of sea state 2 in Tongyeong (m)



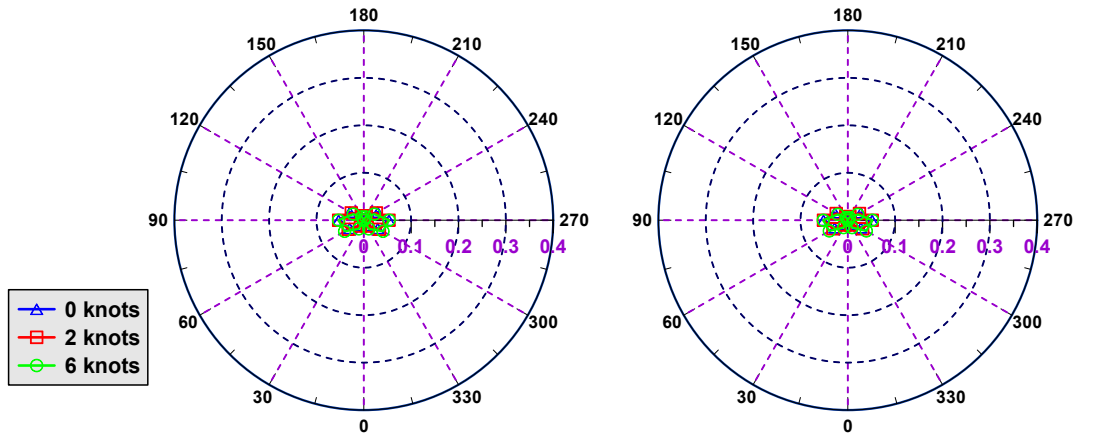
a) Based on ITTC spectrum      b) Based on TMA spectrum

Fig. 4.21 RMS surge in case of sea state 3 in Tongyeong (m)



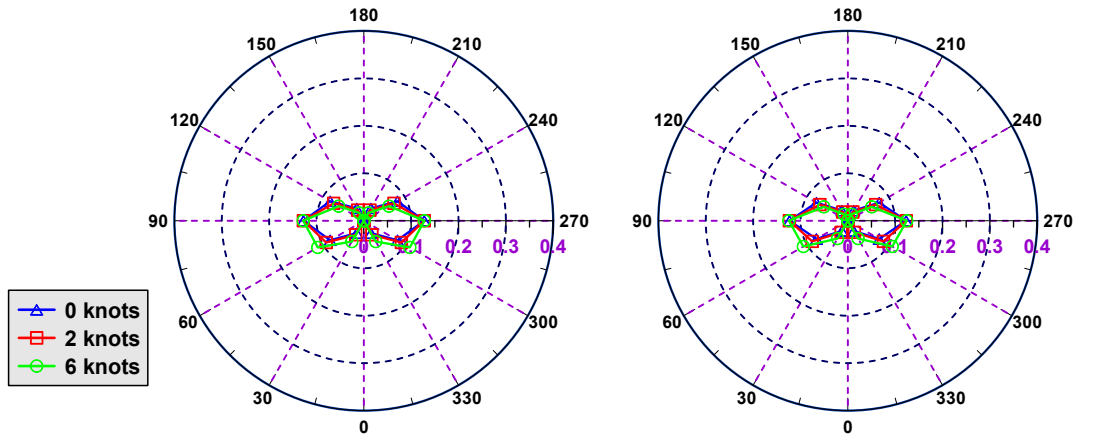
a) Based on ITTC spectrum      b) Based on TMA spectrum

Fig. 4.22 RMS surge in case of sea state 4 in Tongyeong (m)



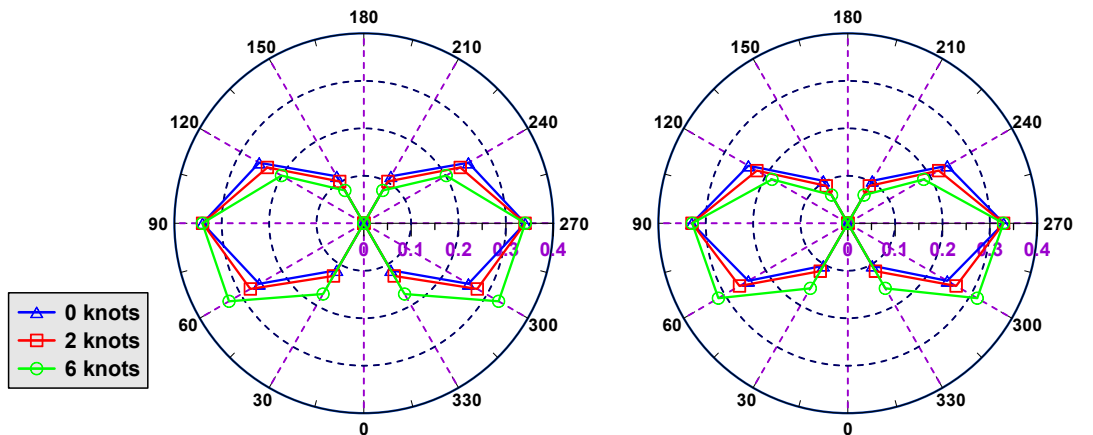
a) Based on ITTC spectrum      b) Based on TMA spectrum

Fig. 4.23 RMS sway in case of sea state 2 in Tongyeong (m)



a) Based on ITTC spectrum      b) Based on TMA spectrum

Fig. 4.24 RMS sway in case of sea state 3 in Tongyeong (m)



a) Based on ITTC spectrum      b) Based on TMA spectrum

Fig. 4.25 RMS sway in case of sea state 3 in Tongyeong (m)

Table 4.15 RMS value for surge based on ITTC spectrum in Tongyeong (m)

Wave direction [deg.]	0 knots			2 knots			6 knots		
	SS2	SS3	SS4	SS2	SS3	SS4	SS2	SS3	SS4
0	0.020	0.049	0.206	0.025	0.060	0.240	0.069	0.167	0.397
30	0.023	0.056	0.207	0.027	0.064	0.236	0.042	0.102	0.336
60	0.026	0.063	0.170	0.029	0.069	0.185	0.035	0.083	0.226
90	0.000	0.000	0.000	0.004	0.009	0.021	0.010	0.025	0.058
120	0.027	0.064	0.170	0.024	0.059	0.159	0.021	0.051	0.148
150	0.023	0.056	0.208	0.020	0.049	0.185	0.015	0.036	0.150
180	0.020	0.049	0.206	0.017	0.041	0.181	0.012	0.029	0.142

Table 4.16 RMS value for surge based on TMA spectrum in Tongyeong (m)

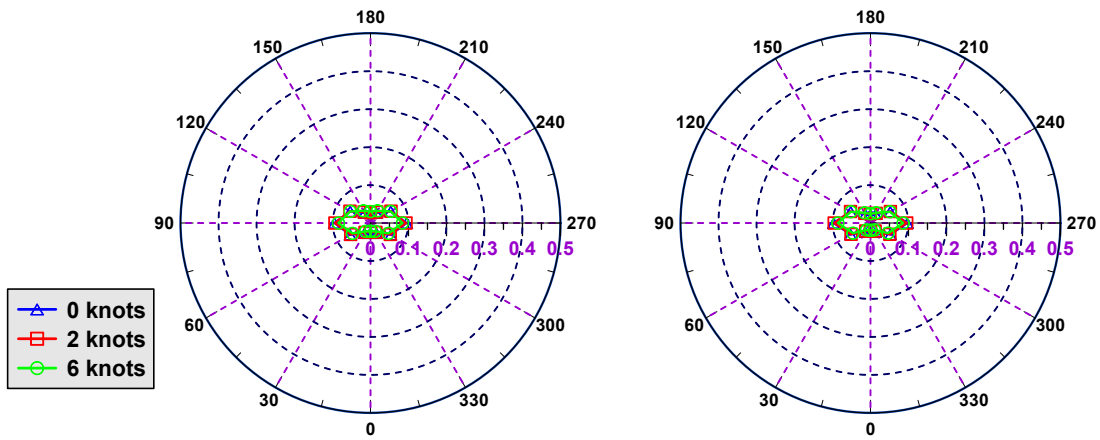
Wave direction [deg.]	0 knots			2 knots			6 knots		
	SS2	SS3	SS4	SS2	SS3	SS4	SS2	SS3	SS4
0	0.016	0.038	0.182	0.021	0.050	0.210	0.067	0.160	0.357
30	0.020	0.048	0.190	0.023	0.056	0.215	0.037	0.090	0.308
60	0.027	0.064	0.164	0.029	0.070	0.178	0.034	0.082	0.216
90	0.000	0.000	0.000	0.004	0.010	0.021	0.011	0.026	0.058
120	0.027	0.064	0.165	0.024	0.059	0.155	0.020	0.048	0.145
150	0.020	0.048	0.190	0.017	0.041	0.169	0.011	0.028	0.134
180	0.016	0.038	0.182	0.013	0.032	0.159	0.009	0.022	0.120

Table 4.17 RMS value for sway based on ITTC spectrum in Tongyeong (m)

Wave direction [deg.]	0 knots			2 knots			6 knots		
	SS2	SS3	SS4	SS2	SS3	SS4	SS2	SS3	SS4
0	0.000	0.000	0.000	0.000	0.000	0.000	0.000	0.000	0.000
30	0.012	0.030	0.114	0.014	0.034	0.128	0.021	0.051	0.172
60	0.034	0.082	0.255	0.038	0.092	0.277	0.047	0.112	0.329
90	0.053	0.128	0.341	0.053	0.128	0.340	0.053	0.128	0.341
120	0.034	0.082	0.255	0.031	0.074	0.235	0.026	0.061	0.201
150	0.012	0.030	0.114	0.011	0.026	0.102	0.008	0.019	0.080
180	0.000	0.000	0.000	0.000	0.000	0.000	0.000	0.000	0.000

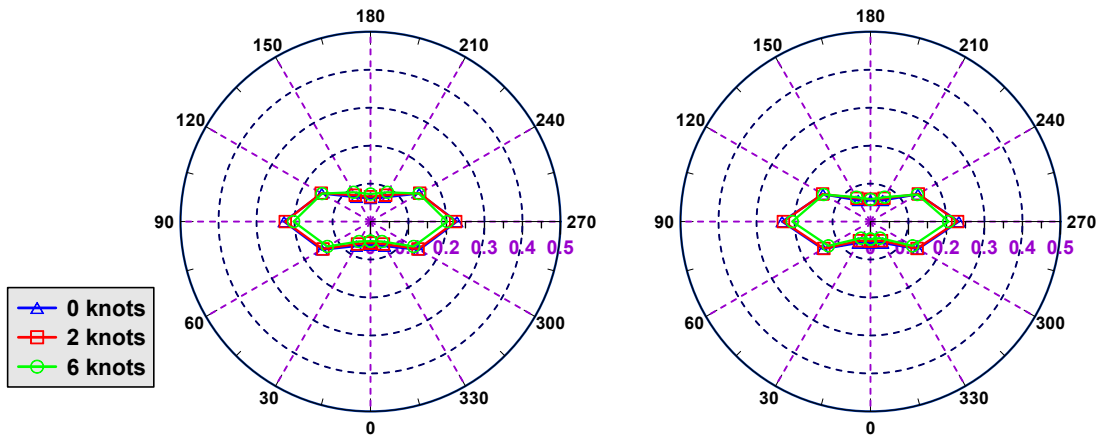
Table 4.18 RMS value for sway based on TMA spectrum in Tongyeong (m)

Wave direction [deg.]	0 knots			2 knots			6 knots		
	SS2	SS3	SS4	SS2	SS3	SS4	SS2	SS3	SS4
0	0.000	0.000	0.000	0.000	0.000	0.000	0.000	0.000	0.000
30	0.010	0.025	0.103	0.012	0.028	0.117	0.018	0.043	0.158
60	0.032	0.077	0.242	0.036	0.087	0.264	0.045	0.108	0.316
90	0.051	0.123	0.329	0.051	0.123	0.329	0.052	0.124	0.329
120	0.032	0.076	0.242	0.028	0.068	0.222	0.024	0.059	0.185
150	0.010	0.025	0.103	0.009	0.021	0.091	0.007	0.016	0.069
180	0.000	0.000	0.000	0.000	0.000	0.000	0.000	0.000	0.000



a) Based on ITTC spectrum      b) Based on TMA spectrum

Fig. 4.26 RMS heave in case of sea state 2 in Tongyeong (m)



a) Based on ITTC spectrum      b) Based on TMA spectrum

Fig. 4.27 RMS heave in case of sea state 3 in Tongyeong (m)

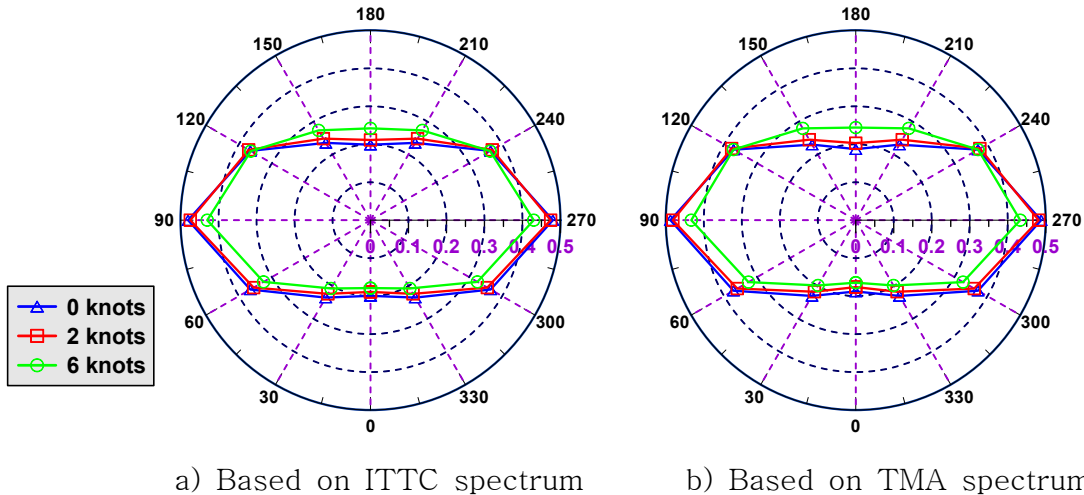


Fig. 4.28 RMS heave in case of sea state 4 in Tongyeong (m)

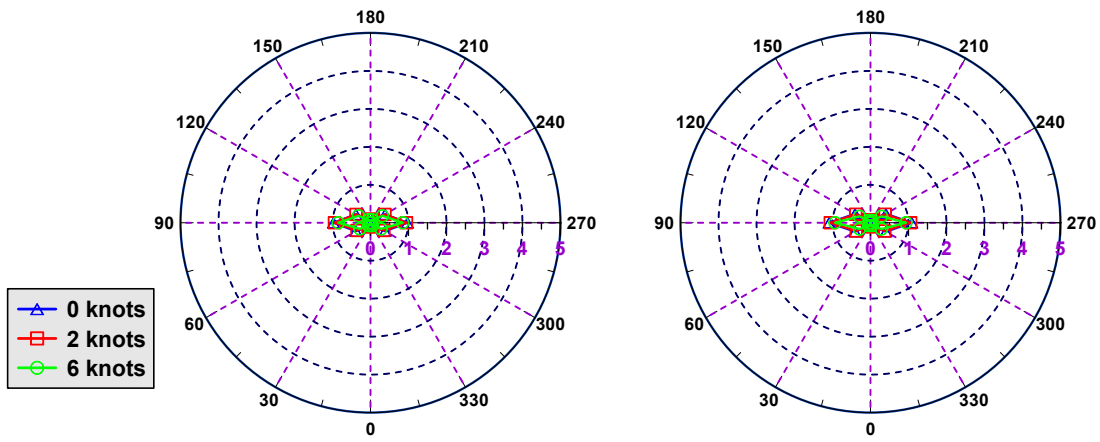


Fig. 4.29 RMS roll in case of sea state 2 in Tongyeong (°)

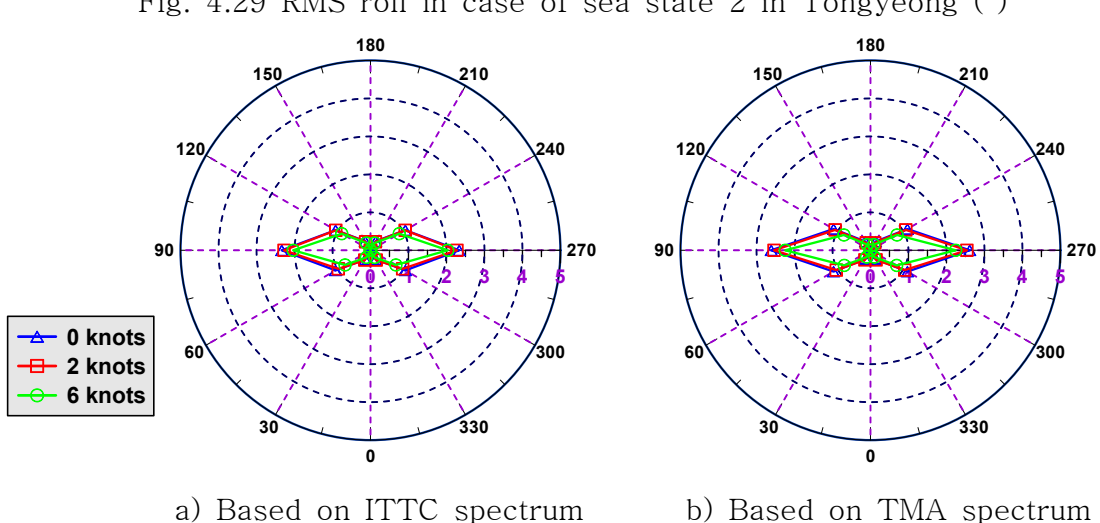


Fig. 4.30 RMS roll in case of sea state 3 in Tongyeong (°)

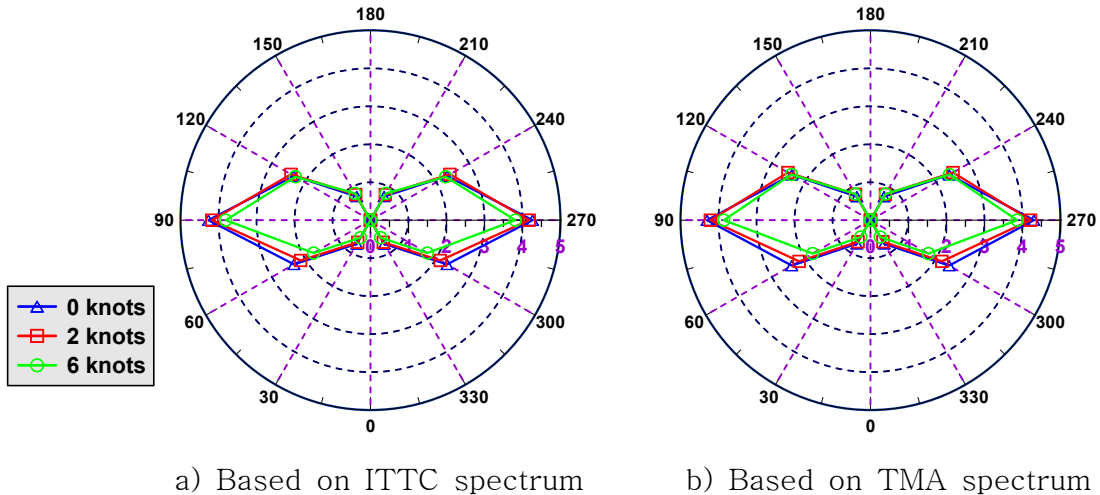


Fig. 4.31 RMS roll in case of sea state 4 in Tongyeong (°)

Table 4.19 RMS value for heave based on ITTC spectrum in Tongyeong (m)

Wave direction [deg.]	0 knots			2 knots			6 knots		
	SS2	SS3	SS4	SS2	SS3	SS4	SS2	SS3	SS4
0	0.026	0.061	0.199	0.023	0.056	0.189	0.021	0.051	0.179
30	0.031	0.074	0.236	0.028	0.068	0.224	0.025	0.061	0.208
60	0.062	0.148	0.365	0.060	0.144	0.355	0.055	0.131	0.325
90	0.095	0.227	0.480	0.093	0.224	0.474	0.084	0.202	0.430
120	0.062	0.148	0.365	0.062	0.150	0.370	0.061	0.147	0.364
150	0.031	0.074	0.235	0.033	0.080	0.248	0.037	0.089	0.273
180	0.025	0.061	0.199	0.027	0.066	0.211	0.030	0.073	0.242

Table 4.20 RMS value for heave based on TMA spectrum in Tongyeong (m)

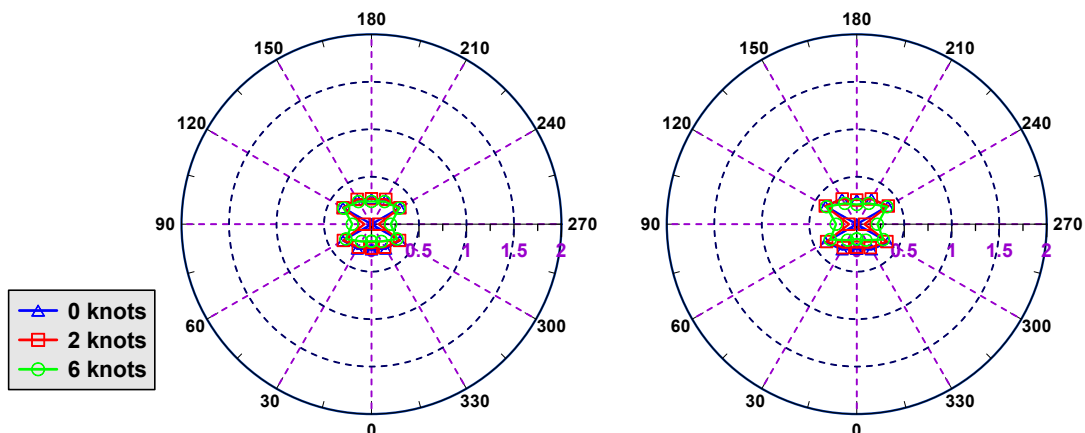
Wave direction [deg.]	0 knots			2 knots			6 knots		
	SS2	SS3	SS4	SS2	SS3	SS4	SS2	SS3	SS4
0	0.023	0.056	0.188	0.021	0.051	0.176	0.019	0.046	0.165
30	0.027	0.065	0.230	0.024	0.058	0.218	0.021	0.050	0.199
60	0.060	0.145	0.372	0.059	0.142	0.360	0.053	0.128	0.326
90	0.097	0.233	0.488	0.096	0.229	0.481	0.086	0.206	0.433
120	0.060	0.144	0.371	0.061	0.145	0.377	0.059	0.142	0.372
150	0.027	0.064	0.230	0.030	0.071	0.245	0.031	0.074	0.279
180	0.023	0.056	0.187	0.025	0.059	0.203	0.024	0.059	0.244

Table 4.21 RMS value for roll based on ITTC spectrum in Tongyeong (°)

Wave direction [deg.]	0 knots			2 knots			6 knots		
	SS2	SS3	SS4	SS2	SS3	SS4	SS2	SS3	SS4
0	0.000	0.000	0.000	0.000	0.000	0.000	0.000	0.000	0.000
30	0.114	0.273	0.719	0.124	0.297	0.672	0.090	0.215	0.533
60	0.442	1.060	2.326	0.407	0.977	2.122	0.322	0.772	1.730
90	0.973	2.335	4.265	0.948	2.275	4.176	0.847	2.033	3.812
120	0.442	1.060	2.326	0.439	1.054	2.414	0.364	0.874	2.284
150	0.114	0.274	0.720	0.108	0.258	0.779	0.092	0.221	0.814
180	0.000	0.000	0.000	0.000	0.000	0.000	0.000	0.000	0.000

Table 4.22 RMS value for roll based on TMA spectrum in Tongyeong (°)

Wave direction [deg.]	0 knots			2 knots			6 knots		
	SS2	SS3	SS4	SS2	SS3	SS4	SS2	SS3	SS4
0	0.000	0.000	0.000	0.000	0.000	0.000	0.000	0.000	0.000
30	0.109	0.262	0.716	0.122	0.292	0.657	0.086	0.206	0.512
60	0.467	1.122	2.392	0.434	1.041	2.169	0.332	0.796	1.760
90	1.088	2.612	4.301	1.058	2.538	4.215	0.935	2.244	3.861
120	0.467	1.122	2.392	0.448	1.074	2.508	0.336	0.806	2.402
150	0.110	0.263	0.717	0.094	0.225	0.787	0.071	0.171	0.796
180	0.000	0.000	0.000	0.000	0.000	0.000	0.000	0.000	0.000



a) Based on ITTC spectrum

b) Based on TMA spectrum

Fig. 4.32 RMS pitch in case of sea state 2 in Tongyeong (°)

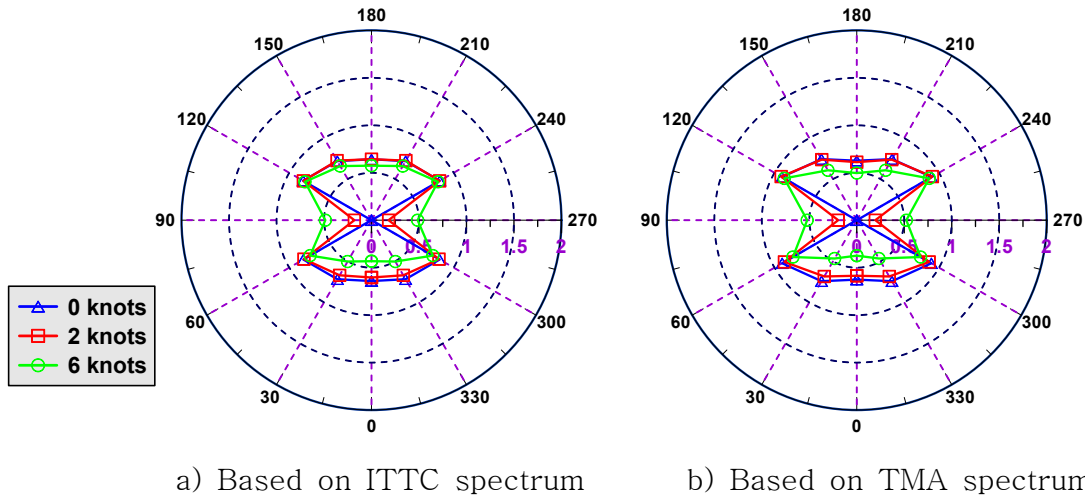


Fig. 4.33 RMS pitch in case of sea state 3 in Tongyeong ( $^{\circ}$ )

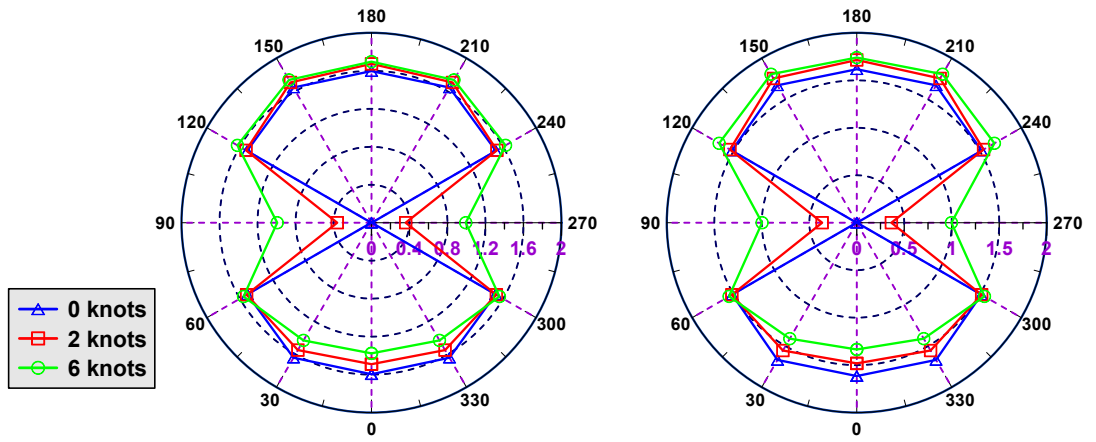


Fig. 4.34 RMS pitch in case of sea state 4 in Tongyeong ( $^{\circ}$ )

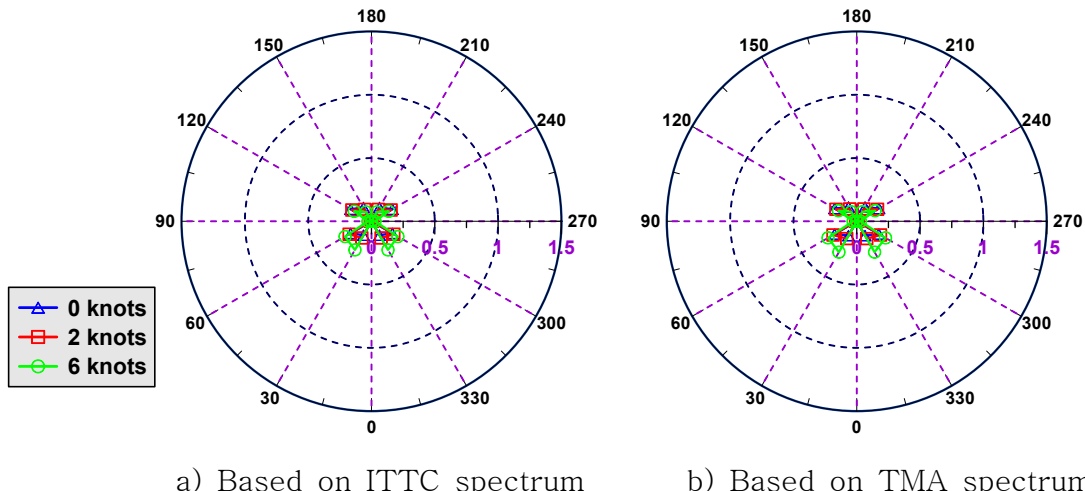


Fig. 4.35 RMS yaw in case of sea state 2 in Tongyeon ( $^{\circ}$ )

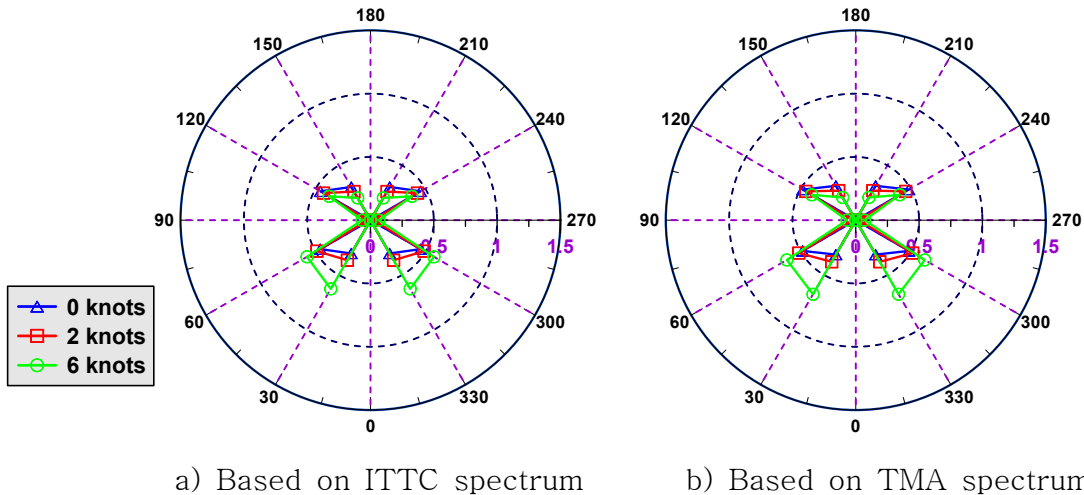


Fig. 4.36 RMS yaw in case of sea state 3 in Tongyeong ( $^{\circ}$ )

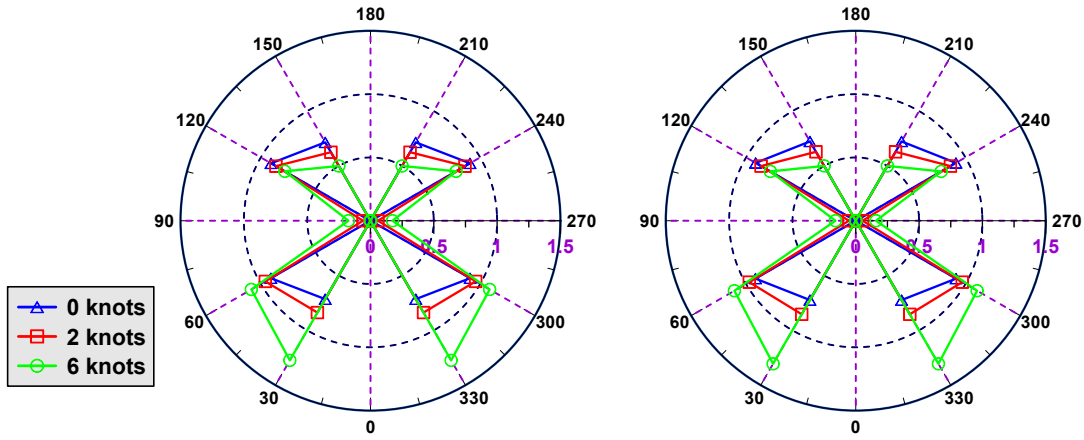


Fig. 4.37 RMS yaw in case of sea state 4 in Tongyeong ( $^{\circ}$ )

Table 4.23 RMS value for pitch based on ITTC spectrum in Tongyeong ( $^{\circ}$ )

Wave direction [deg.]	0 knots			2 knots			6 knots		
	SS2	SS3	SS4	SS2	SS3	SS4	SS2	SS3	SS4
0	0.267	0.641	1.596	0.252	0.604	1.490	0.180	0.432	1.376
30	0.299	0.718	1.642	0.279	0.670	1.549	0.210	0.503	1.431
60	0.345	0.829	1.509	0.342	0.821	1.518	0.311	0.746	1.555
90	0.001	0.001	0.002	0.075	0.180	0.360	0.202	0.486	0.992
120	0.346	0.831	1.513	0.345	0.828	1.525	0.337	0.809	1.630
150	0.300	0.719	1.644	0.302	0.725	1.706	0.274	0.659	1.737
180	0.267	0.642	1.597	0.268	0.643	1.673	0.239	0.574	1.696

Table 4.24 RMS value for pitch based on TMA spectrum in Tongyeong (°)

Wave direction [deg.]	0 knots			2 knots			6 knots		
	SS2	SS3	SS4	SS2	SS3	SS4	SS2	SS3	SS4
0	0.261	0.626	1.615	0.244	0.585	1.482	0.156	0.373	1.335
30	0.309	0.742	1.669	0.285	0.685	1.555	0.194	0.466	1.410
60	0.378	0.907	1.515	0.366	0.879	1.518	0.323	0.776	1.552
90	0.001	0.002	0.002	0.082	0.196	0.364	0.218	0.522	0.997
120	0.379	0.910	1.518	0.383	0.919	1.542	0.367	0.882	1.673
150	0.310	0.744	1.671	0.307	0.737	1.755	0.253	0.607	1.806
180	0.261	0.627	1.616	0.255	0.612	1.714	0.207	0.497	1.739

Table 4.25 RMS value for yaw based on ITTC spectrum in Tongyeong (°)

Wave direction [deg.]	0 knots			2 knots			6 knots		
	SS2	SS3	SS4	SS2	SS3	SS4	SS2	SS3	SS4
0	0.000	0.000	0.000	0.000	0.000	0.000	0.000	0.000	0.000
30	0.127	0.304	0.715	0.152	0.365	0.838	0.261	0.627	1.274
60	0.190	0.457	0.908	0.204	0.489	0.959	0.241	0.579	1.087
90	0.001	0.002	0.003	0.010	0.023	0.059	0.028	0.067	0.174
120	0.190	0.456	0.907	0.178	0.428	0.862	0.157	0.378	0.781
150	0.126	0.303	0.715	0.109	0.261	0.625	0.085	0.203	0.499
180	0.000	0.000	0.000	0.000	0.000	0.000	0.000	0.000	0.000

Table 4.26 RMS value for yaw based on TMA spectrum in Tongyeong (°)

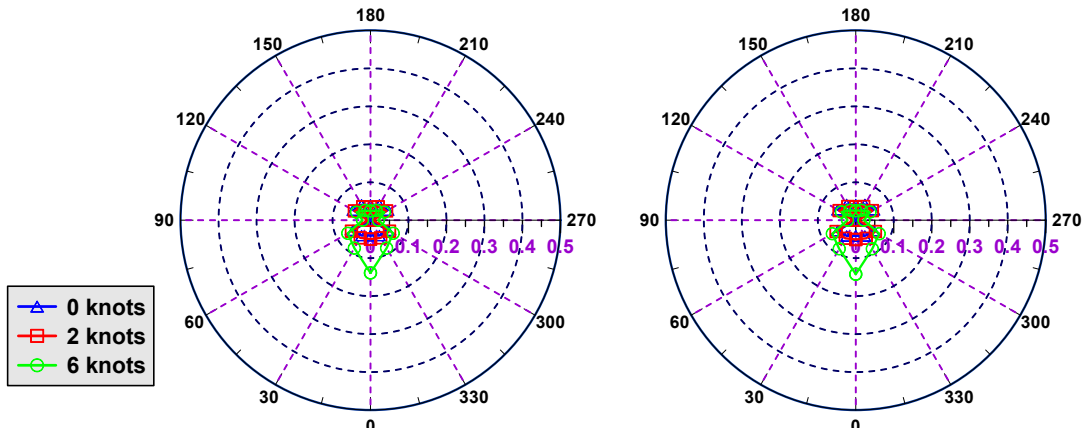
Wave direction [deg.]	0 knots			2 knots			6 knots		
	SS2	SS3	SS4	SS2	SS3	SS4	SS2	SS3	SS4
0	0.000	0.000	0.000	0.000	0.000	0.000	0.000	0.000	0.000
30	0.131	0.314	0.724	0.158	0.380	0.854	0.281	0.675	1.306
60	0.202	0.485	0.914	0.216	0.520	0.971	0.262	0.628	1.107
90	0.001	0.002	0.003	0.010	0.024	0.054	0.029	0.069	0.160
120	0.202	0.484	0.913	0.190	0.455	0.863	0.167	0.401	0.779
150	0.131	0.314	0.723	0.112	0.270	0.628	0.086	0.207	0.500
180	0.000	0.000	0.000	0.000	0.000	0.000	0.000	0.000	0.000

### 4.3 Significant Single Amplitude (SSA)

In order to check the seakeeping criteria, the Significant Single Amplitude (SSA) is calculated by two times of RMS motion. The SSA for 6-DOF motion is estimated in sea state 2, sea state 3 and sea state 4 in various ship speeds and various wave directions. The SSA motion changes dramatically in various wave directions and sea states. The SSA motion which is calculated based on ITTC and TMA spectrum are compared.

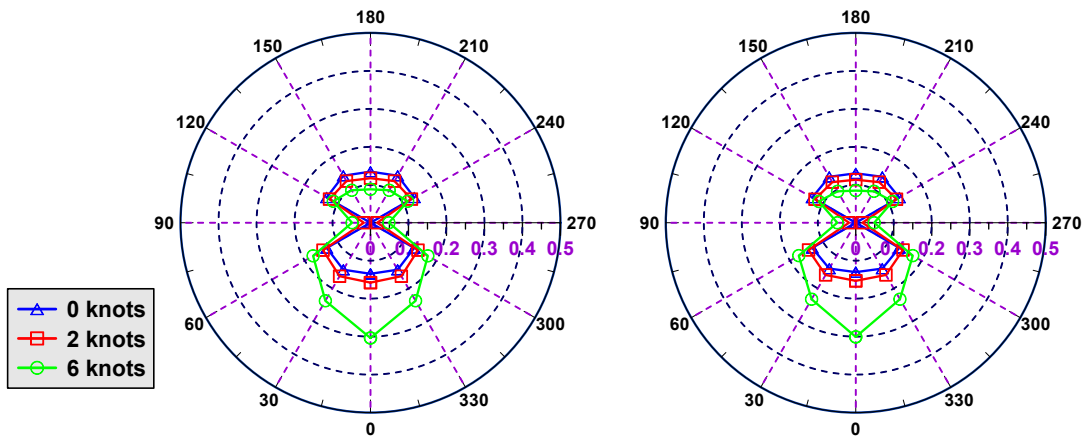
#### 4.3.1 Sinan

This part investigates the SSA motion in Sinan. The SSA motion equals two times of RMS motion. Therefore, the trend of SSA motion and RMS motion are the same. Figs. 4.38~4.40 show the comparison of SSA surge. The SSA motion increases significantly in various irregular wave conditions. The SSA surge is the greatest when the wave direction reaches 0 degree due to the speed effect especially in case of 6 knots. Figs. 4.41~4.43 show the comparison of SSA sway. In case of SSA sway, it is dominant at beam sea and reduces when the wave direction reaches to head sea and following sea. The SSA sway increases slightly when the ship speed increases. Tables 4.27~4.30 list the results of the SSA surge and SSA sway in various wave directions and various ship speeds at various sea states based on ITTC and TMA spectrum. Figs. 4.44~4.46 show the comparison of SSA heave. The SSA heave changes slightly in various wave directions and it is the largest in beam sea. Figs. 4.47~4.49 show the comparison of SSA roll. The SSA roll is dominant in case of beam sea due to wave exciting in y direction. As the same as RMS sway, SSA roll reduces when the wave direction reaches head sea and following sea. Tables 4.31~4.34 list the results of SSA heave and SSA roll in various wave directions, various ship speeds and various sea states based on ITTC spectrum and TMA spectrum. Figs. 4.50~4.52 show the comparison of SSA pitch. The SSA pitch is the greatest in head sea and following sea. Figs. 4.53~4.55 show the comparison of SSA yaw. The SSA yaw is dominant in oblique wave and it is the smallest when the wave direction reaches to 0 degree, 90 degrees and 180 degrees. Tables 4.35~4.38 list the results of the SSA pitch and SSA yaw in various wave directions and various ship speeds at various sea states based on ITTC and TMA spectrum.



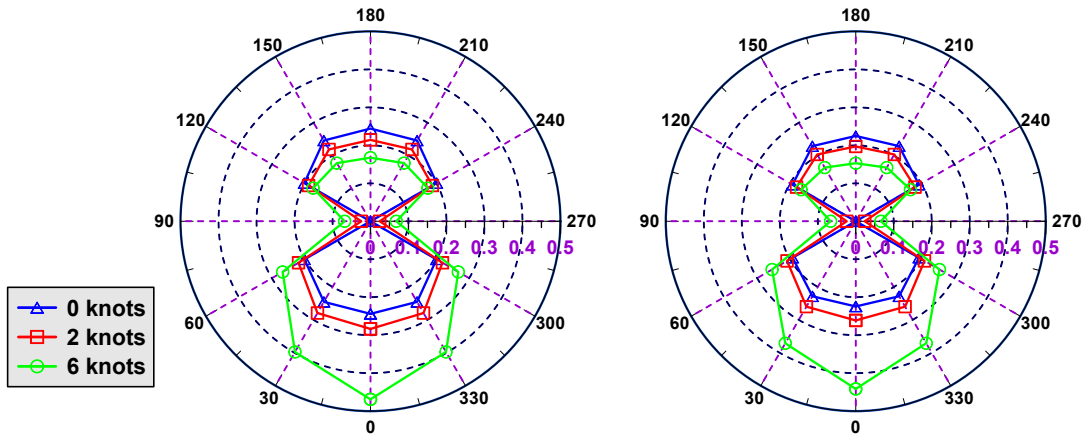
a) Based on ITTC spectrum      b) Based on TMA spectrum

Fig. 4.38 SSA surge in case of sea state 2 in Sinan (m)



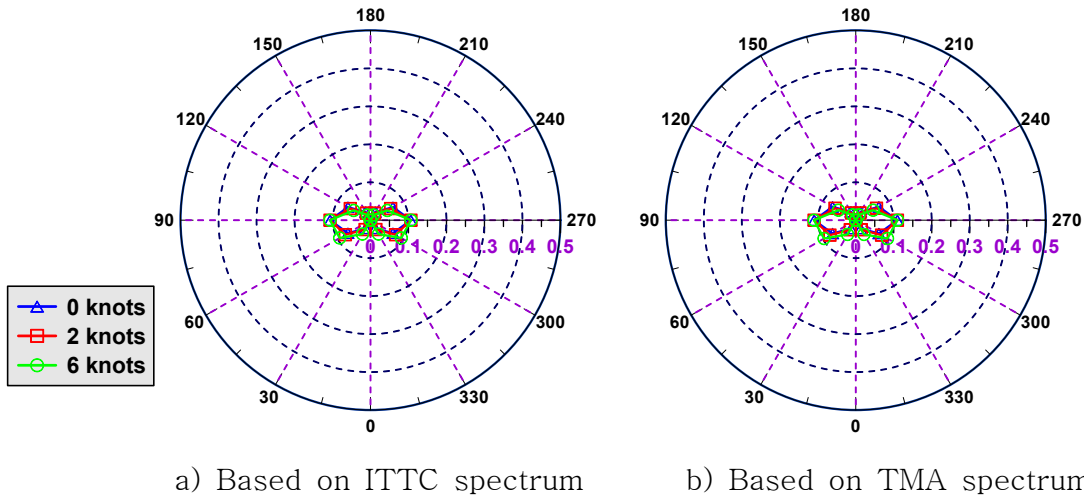
a) Based on ITTC spectrum      b) Based on TMA spectrum

Fig. 4.39 SSA surge in case of sea state 3 in Sinan (m)

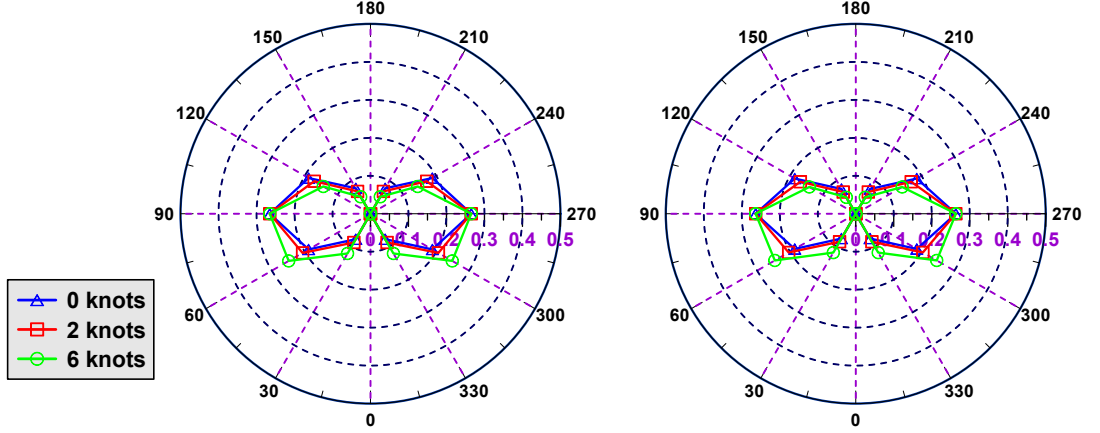


a) Based on ITTC spectrum      b) Based on TMA spectrum

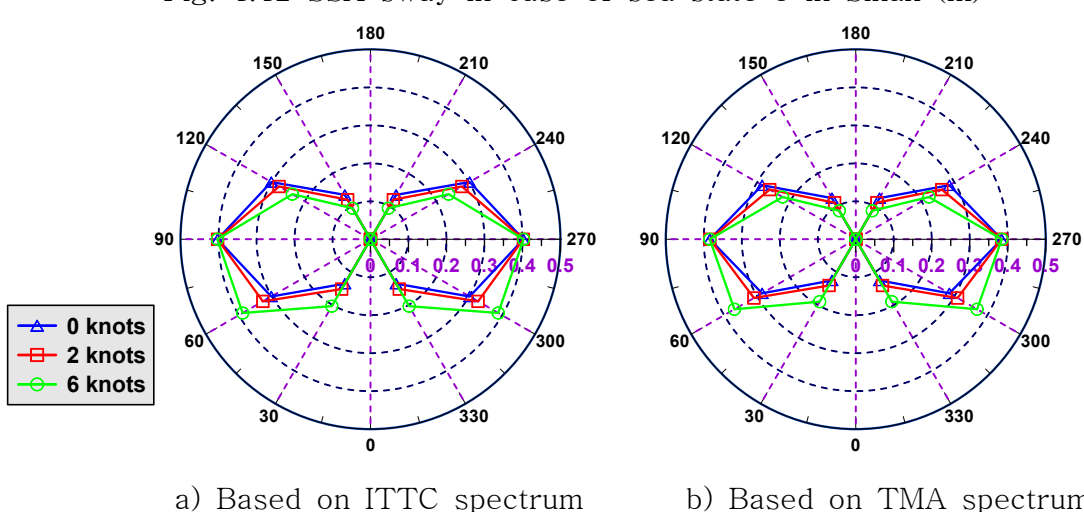
Fig. 4.40 SSA surge in case of sea state 4 in Sinan (m)



a) Based on ITTC spectrum      b) Based on TMA spectrum  
Fig. 4.41 SSA sway in case of sea state 2 in Sinan (m)



a) Based on ITTC spectrum      b) Based on TMA spectrum  
Fig. 4.42 SSA sway in case of sea state 3 in Sinan (m)



a) Based on ITTC spectrum      b) Based on TMA spectrum  
Fig. 4.43 SSA sway in case of sea state 4 in Sinan (m)

Table 4.27 SSA value for surge based on ITTC spectrum in Sinan (m)

Wave direction [deg.]	0 knots			2 knots			6 knots		
	SS2	SS3	SS4	SS2	SS3	SS4	SS2	SS3	SS4
0	0.040	0.134	0.244	0.050	0.158	0.284	0.139	0.304	0.469
30	0.047	0.143	0.245	0.054	0.163	0.279	0.085	0.237	0.397
60	0.053	0.133	0.201	0.058	0.144	0.219	0.069	0.174	0.267
90	0.000	0.000	0.000	0.008	0.018	0.024	0.021	0.048	0.068
120	0.053	0.133	0.201	0.049	0.124	0.188	0.042	0.113	0.174
150	0.047	0.143	0.245	0.041	0.127	0.218	0.030	0.099	0.177
180	0.040	0.135	0.244	0.035	0.117	0.214	0.024	0.088	0.167

Table 4.28 SSA value for surge based on TMA spectrum in Sinan (m)

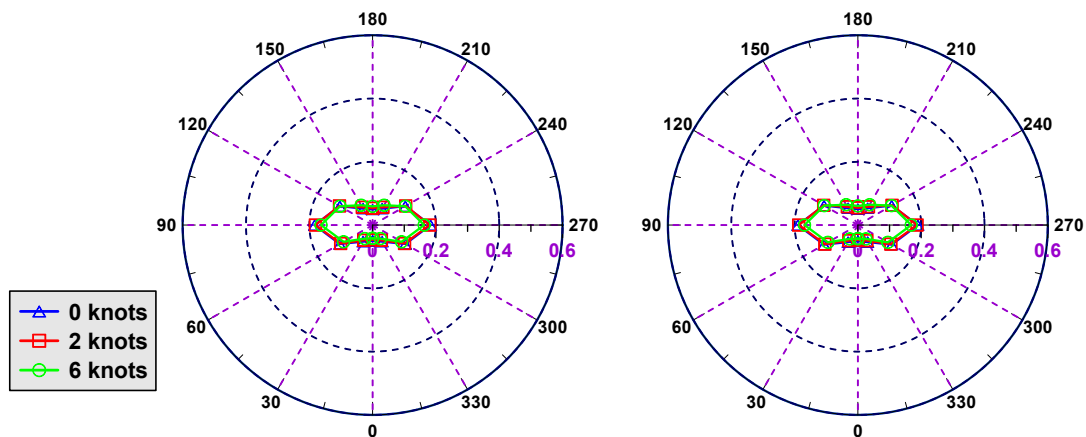
Wave direction [deg.]	0 knots			2 knots			6 knots		
	SS2	SS3	SS4	SS2	SS3	SS4	SS2	SS3	SS4
0	0.041	0.130	0.224	0.051	0.153	0.261	0.142	0.301	0.442
30	0.048	0.139	0.228	0.055	0.159	0.260	0.087	0.233	0.371
60	0.055	0.132	0.192	0.060	0.144	0.209	0.071	0.173	0.254
90	0.000	0.000	0.000	0.008	0.018	0.024	0.022	0.049	0.066
120	0.055	0.133	0.192	0.050	0.124	0.180	0.043	0.112	0.166
150	0.048	0.140	0.228	0.042	0.123	0.203	0.030	0.096	0.163
180	0.041	0.130	0.225	0.035	0.113	0.197	0.025	0.085	0.153

Table 4.29 SSA value for sway based on ITTC spectrum in Sinan (m)

Wave direction [deg.]	0 knots			2 knots			6 knots		
	SS2	SS3	SS4	SS2	SS3	SS4	SS2	SS3	SS4
0	0.000	0.000	0.000	0.000	0.000	0.000	0.000	0.000	0.000
30	0.025	0.077	0.135	0.028	0.087	0.151	0.042	0.121	0.203
60	0.068	0.188	0.301	0.076	0.206	0.327	0.094	0.249	0.388
90	0.106	0.265	0.403	0.106	0.265	0.402	0.107	0.265	0.403
120	0.068	0.188	0.301	0.061	0.171	0.278	0.051	0.144	0.237
150	0.025	0.077	0.135	0.022	0.068	0.120	0.016	0.052	0.094
180	0.000	0.000	0.000	0.000	0.000	0.000	0.000	0.000	0.000

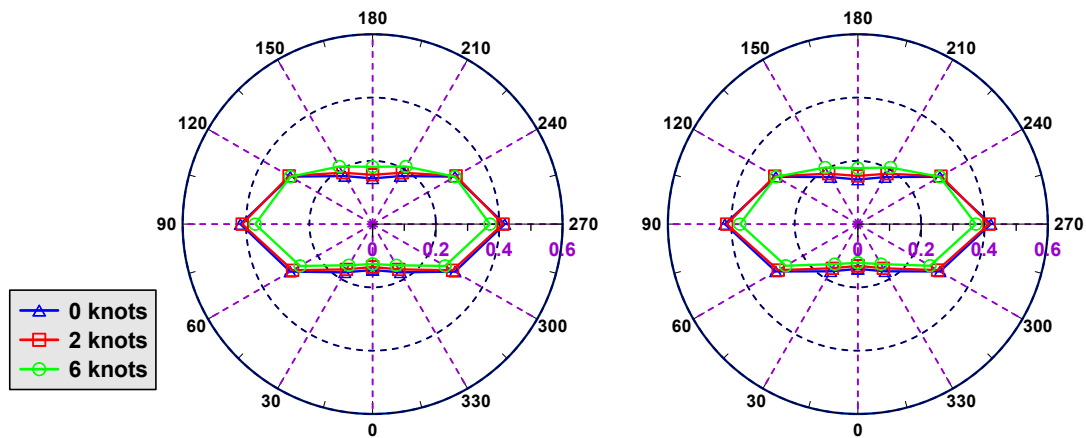
Table 4.30 SSA value for sway based on TMA spectrum in Sinan (m)

Wave direction [deg.]	0 knots			2 knots			6 knots		
	SS2	SS3	SS4	SS2	SS3	SS4	SS2	SS3	SS4
0	0.000	0.000	0.000	0.000	0.000	0.000	0.000	0.000	0.000
30	0.025	0.075	0.125	0.029	0.085	0.141	0.043	0.118	0.190
60	0.070	0.185	0.285	0.079	0.204	0.309	0.096	0.246	0.369
90	0.110	0.263	0.384	0.110	0.263	0.384	0.110	0.264	0.384
120	0.070	0.185	0.285	0.063	0.168	0.262	0.053	0.141	0.222
150	0.025	0.075	0.125	0.022	0.066	0.111	0.016	0.050	0.087
180	0.000	0.000	0.000	0.000	0.000	0.000	0.000	0.000	0.000



a) Based on ITTC spectrum      b) Based on TMA spectrum

Fig. 4.44 SSA heave in case of sea state 2 in Sinan (m)



a) Based on ITTC spectrum      b) Based on TMA spectrum

Fig. 4.45 SSA heave in case of sea state 3 in Sinan (m)

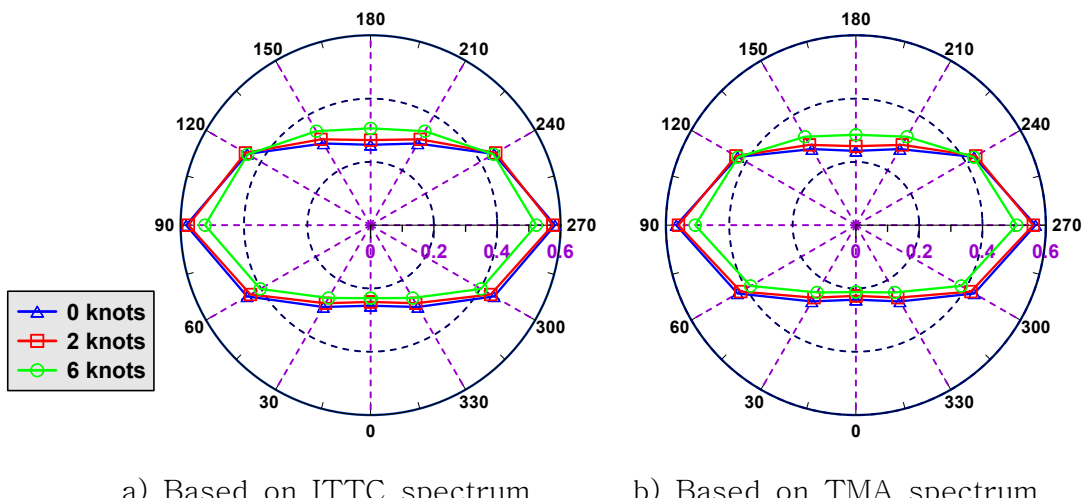


Fig. 4.46 SSA heave in case of sea state 4 in Sinan (m)

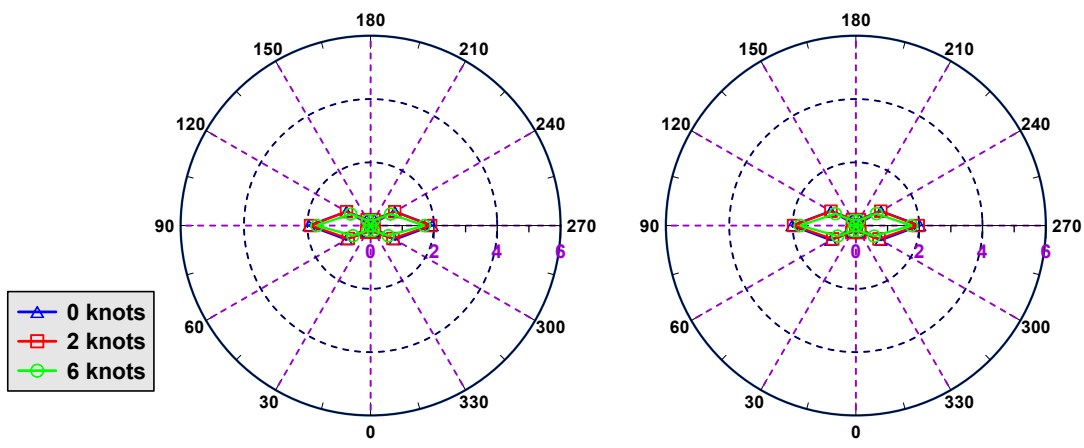


Fig. 4.47 SSA roll in case of sea state 2 in Sinan (°)

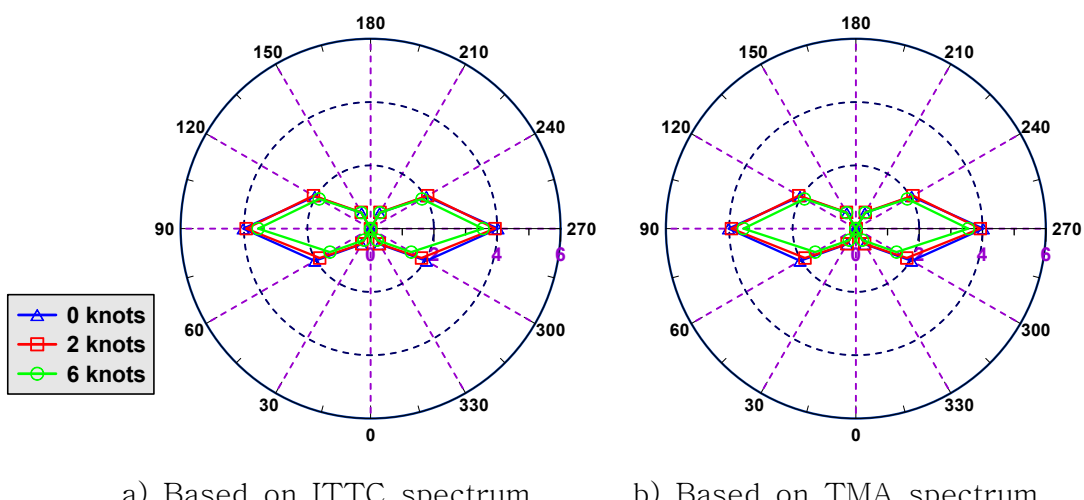
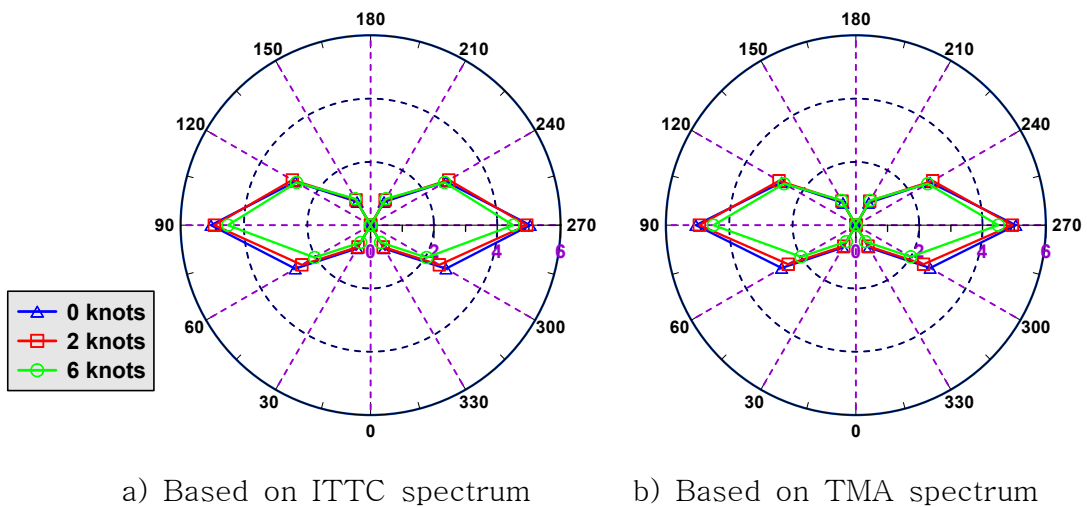


Fig. 4.48 SSA roll in case of sea state 3 in Sinan (°)



a) Based on ITTC spectrum      b) Based on TMA spectrum

Fig. 4.49 SSA roll in case of sea state 4 in Sinan (°)

Table 4.31 SSA value for heave based on ITTC spectrum in Sinan (m)

Wave direction [deg.]	0 knots			2 knots			6 knots		
	SS2	SS3	SS4	SS2	SS3	SS4	SS2	SS3	SS4
0	0.050	0.145	0.255	0.046	0.136	0.243	0.042	0.126	0.231
30	0.060	0.176	0.299	0.055	0.165	0.285	0.049	0.150	0.266
60	0.120	0.300	0.450	0.117	0.292	0.438	0.106	0.265	0.403
90	0.183	0.418	0.583	0.181	0.412	0.576	0.163	0.371	0.523
120	0.119	0.300	0.450	0.121	0.304	0.457	0.119	0.300	0.448
150	0.060	0.175	0.298	0.065	0.188	0.313	0.072	0.210	0.343
180	0.050	0.144	0.254	0.053	0.156	0.269	0.059	0.181	0.306

Table 4.32 SSA value for heave based on TMA spectrum in Sinan (m)

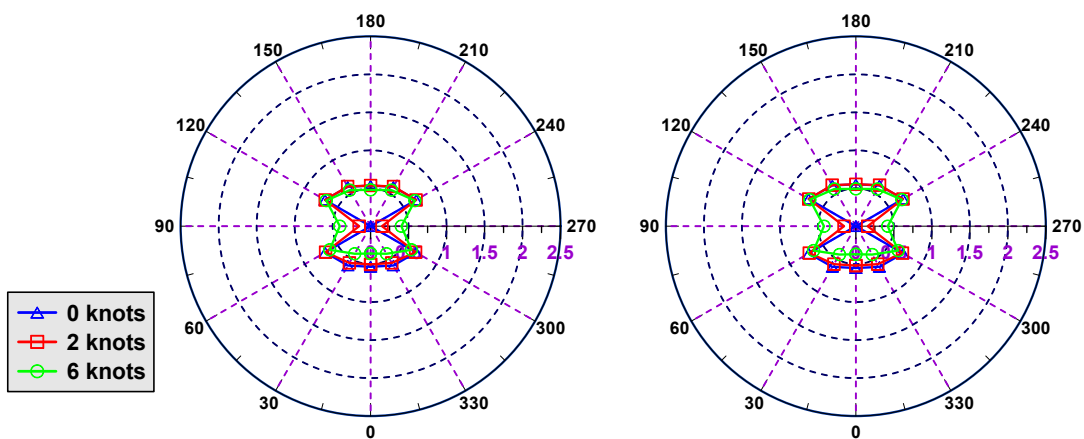
Wave direction [deg.]	0 knots			2 knots			6 knots		
	SS2	SS3	SS4	SS2	SS3	SS4	SS2	SS3	SS4
0	0.051	0.142	0.235	0.047	0.132	0.223	0.043	0.122	0.211
30	0.062	0.172	0.278	0.057	0.161	0.265	0.050	0.146	0.246
60	0.123	0.299	0.432	0.120	0.291	0.420	0.109	0.263	0.384
90	0.190	0.420	0.567	0.187	0.414	0.560	0.169	0.373	0.508
120	0.123	0.299	0.431	0.125	0.303	0.437	0.123	0.299	0.430
150	0.062	0.172	0.278	0.067	0.184	0.293	0.074	0.207	0.323
180	0.051	0.141	0.235	0.055	0.152	0.250	0.061	0.177	0.286

Table 4.33 SSA value for roll based on ITTC spectrum in Sinan (°)

Wave direction [deg.]	0 knots			2 knots			6 knots		
	SS2	SS3	SS4	SS2	SS3	SS4	SS2	SS3	SS4
0	0.000	0.000	0.000	0.000	0.000	0.000	0.000	0.000	0.000
30	0.228	0.569	0.850	0.247	0.554	0.794	0.180	0.421	0.630
60	0.883	2.035	2.749	0.814	1.857	2.508	0.644	1.483	2.044
90	1.946	4.024	5.041	1.896	3.930	4.935	1.695	3.550	4.505
120	0.883	2.035	2.749	0.878	2.083	2.853	0.728	1.875	2.700
150	0.228	0.569	0.850	0.215	0.595	0.920	0.184	0.583	0.962
180	0.000	0.000	0.000	0.000	0.000	0.000	0.000	0.000	0.000

Table 4.34 SSA value for roll based on TMA spectrum in Sinan (°)

Wave direction [deg.]	0 knots			2 knots			6 knots		
	SS2	SS3	SS4	SS2	SS3	SS4	SS2	SS3	SS4
0	0.000	0.000	0.000	0.000	0.000	0.000	0.000	0.000	0.000
30	0.234	0.564	0.814	0.255	0.554	0.765	0.185	0.418	0.601
60	0.915	2.053	2.708	0.844	1.873	2.469	0.666	1.491	1.999
90	2.020	4.100	5.052	1.968	4.004	4.943	1.758	3.611	4.500
120	0.915	2.053	2.708	0.909	2.096	2.802	0.750	1.870	2.620
150	0.235	0.565	0.815	0.221	0.587	0.877	0.187	0.568	0.904
180	0.000	0.000	0.000	0.000	0.000	0.000	0.000	0.000	0.000



a) Based on ITTC spectrum      b) Based on TMA spectrum

Fig. 4.50 SSA pitch in case of sea state 2 in Sinan (°)

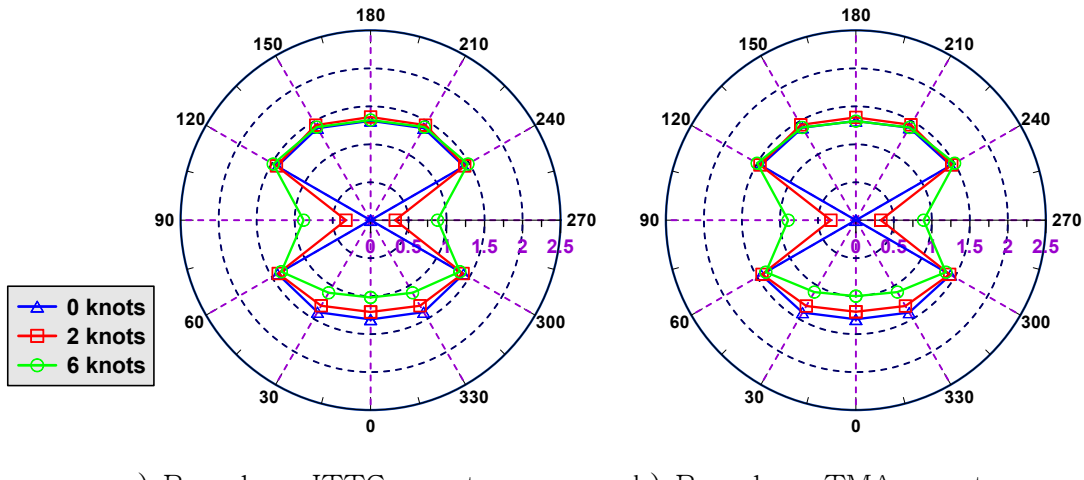


Fig. 4.51 SSA pitch in case of sea state 3 in Sinan ( $^{\circ}$ )

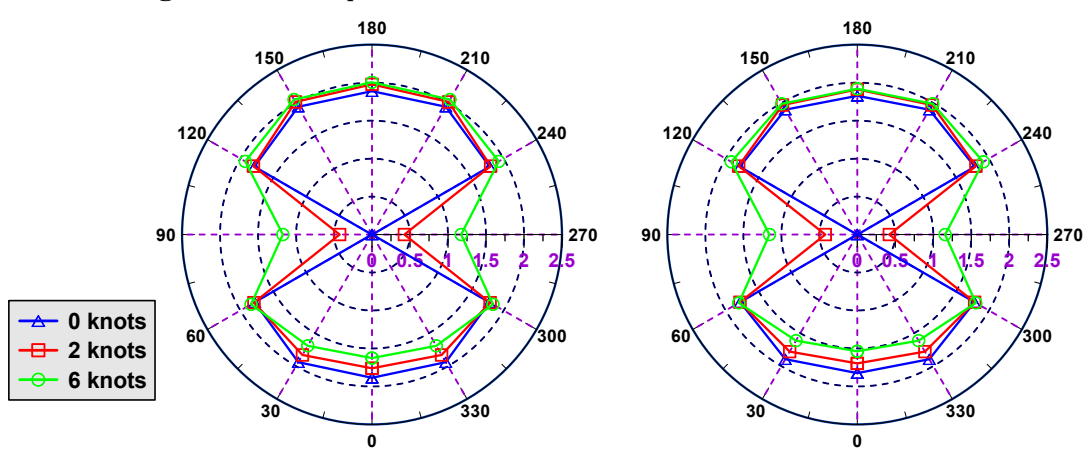


Fig. 4.52 SSA pitch in case of sea state 4 in Sinan (deg.)

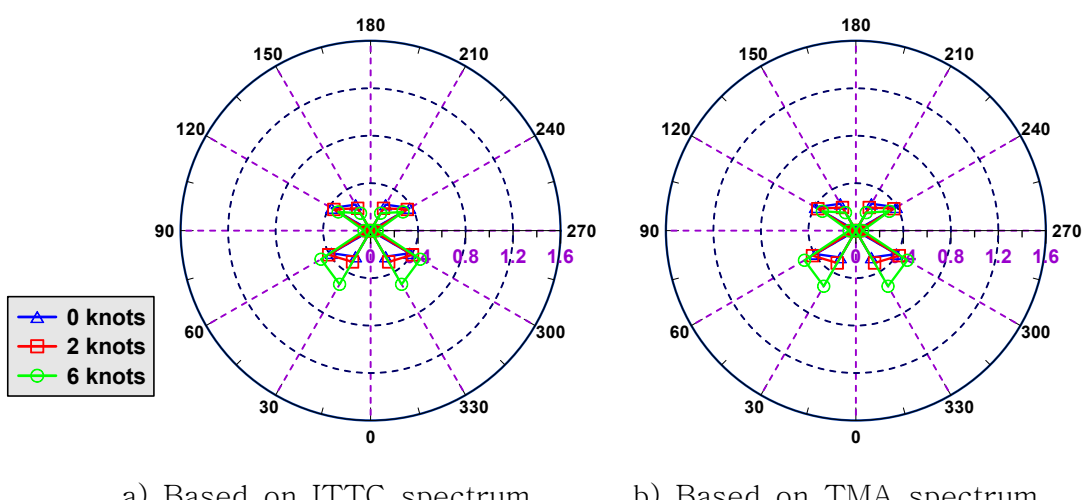


Fig. 4.53 SSA yaw in case of sea state 2 in Sinan ( $^{\circ}$ )

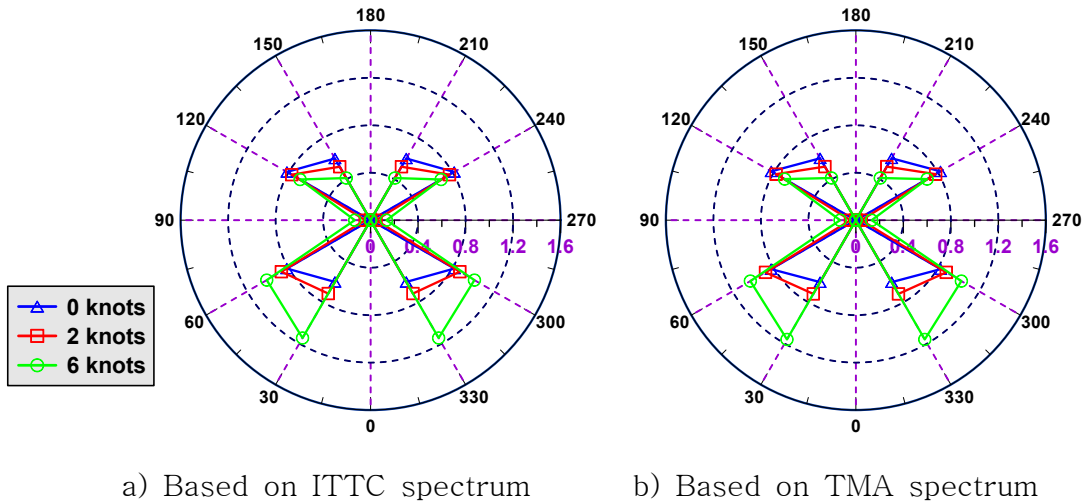
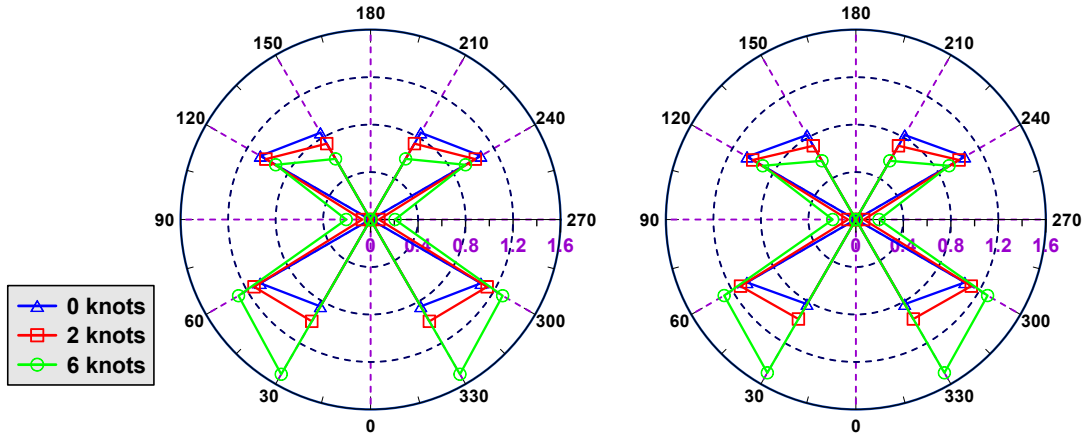


Fig. 4.54 SSA yaw in case of sea state 3 in Sinan (°)



a) Based on ITTC spectrum      b) Based on TMA spectrum

Fig. 4.55 SSA yaw in case of sea state 4 in Sinan (°)

Table 4.35 SSA value for pitch based on ITTC spectrum in Sinan (°)

Wave direction [deg.]	0 knots			2 knots			6 knots		
	SS2	SS3	SS4	SS2	SS3	SS4	SS2	SS3	SS4
0	0.534	1.307	1.886	0.503	1.209	1.761	0.360	1.017	1.626
30	0.598	1.397	1.941	0.559	1.301	1.831	0.419	1.104	1.692
60	0.691	1.414	1.783	0.684	1.404	1.794	0.622	1.357	1.838
90	0.001	0.002	0.002	0.150	0.325	0.426	0.405	0.881	1.173
120	0.693	1.418	1.788	0.690	1.431	1.802	0.674	1.480	1.926
150	0.599	1.399	1.943	0.604	1.445	2.016	0.549	1.416	2.053
180	0.535	1.308	1.888	0.536	1.359	1.978	0.478	1.320	2.005

Table 4.36 SSA value for pitch based on TMA spectrum in Sinan (°)

Wave direction [deg.]	0 knots			2 knots			6 knots		
	SS2	SS3	SS4	SS2	SS3	SS4	SS2	SS3	SS4
0	0.551	1.305	1.825	0.518	1.206	1.697	0.369	1.000	1.537
30	0.619	1.404	1.896	0.577	1.305	1.780	0.431	1.093	1.613
60	0.716	1.439	1.781	0.708	1.426	1.783	0.643	1.368	1.800
90	0.001	0.002	0.002	0.156	0.329	0.422	0.419	0.891	1.156
120	0.718	1.443	1.785	0.716	1.457	1.803	0.699	1.500	1.915
150	0.620	1.406	1.898	0.624	1.450	1.969	0.565	1.410	1.988
180	0.552	1.306	1.826	0.552	1.354	1.911	0.491	1.304	1.919

Table 4.37 SSA value for yaw based on ITTC spectrum in Sinan (°)

Wave direction [deg.]	0 knots			2 knots			6 knots		
	SS2	SS3	SS4	SS2	SS3	SS4	SS2	SS3	SS4
0	0.000	0.000	0.000	0.000	0.000	0.000	0.000	0.000	0.000
30	0.253	0.601	0.845	0.304	0.714	0.990	0.522	1.146	1.505
60	0.381	0.815	1.073	0.407	0.868	1.133	0.482	1.010	1.284
90	0.002	0.003	0.003	0.019	0.046	0.070	0.055	0.134	0.206
120	0.380	0.813	1.072	0.357	0.767	1.018	0.315	0.686	0.923
150	0.253	0.600	0.845	0.218	0.520	0.739	0.169	0.410	0.590
180	0.000	0.000	0.000	0.000	0.000	0.000	0.000	0.000	0.000

Table 4.38 SSA value for yaw based on TMA spectrum in Sinan (°)

Wave direction [deg.]	0 knots			2 knots			6 knots		
	SS2	SS3	SS4	SS2	SS3	SS4	SS2	SS3	SS4
0	0.000	0.000	0.000	0.000	0.000	0.000	0.000	0.000	0.000
30	0.262	0.603	0.823	0.315	0.717	0.968	0.541	1.160	1.491
60	0.394	0.824	1.060	0.422	0.879	1.122	0.500	1.026	1.281
90	0.002	0.003	0.003	0.020	0.046	0.066	0.057	0.133	0.195
120	0.393	0.823	1.058	0.370	0.776	1.003	0.326	0.693	0.906
150	0.261	0.602	0.823	0.225	0.522	0.718	0.175	0.411	0.571
180	0.000	0.000	0.000	0.000	0.000	0.000	0.000	0.000	0.000

### 4.3.2 Tongyeong

This part investigates the SSA motion in Tongyeong. The SSA motion equals two times of RMS motion. Therefore, the trend of SSA motion and RMS motion are the same. Figs. 4.56~4.58 show the comparison of SSA surge motion which is estimated based on ITTC and TMA spectrum. The SSA motion increases significantly in various irregular wave conditions. The SSA surge motion is the greatest when the wave direction reaches 0 degree due to the speed effect especially in case of 6 knots. Figs. 4.59~4.61 show the comparison of SSA sway which is estimated based on ITTC spectrum and TMA spectrum. In case of sway, motion is dominant at beam sea and reduces when the wave direction reaches to head sea and following sea. The SSA sway increases slightly when the ship speed increases. Tables 4.39~4.42 list the results of the SSA surge and SSA sway in various wave directions and various ship speeds at various sea states based on ITTC spectrum and TMA spectrum. Figs. 4.62~4.64 show the comparison of SSA heave which is estimated based on ITTC and TMA spectrum. The SSA heave changes slightly in various wave directions and it is the largest in beam sea. Figs. 4.65~4.67 show the comparison of SSA roll which is estimated based on ITTC and TMA spectrum. The SSA roll is dominant in case of beam sea due to wave exciting in y direction. As the same as RMS sway, SSA roll reduces when the wave direction reaches head sea and following sea. Tables 4.43~4.46 list the results of the SSA heave and SSA roll in various wave directions, various ship speeds and various sea states based on ITTC and TMA spectrum. Figs. 4.68~4.70 show the comparison of SSA pitch which is estimated based on ITTC and TMA spectrum. SSA pitch is the greatest in head sea and following sea. Figs. 4.71~4.73 show the comparison of SSA yaw which is estimated based on ITTC spectrum and TMA spectrum. The SSA yaw is dominant in oblique wave and it is the smallest when the wave direction reaches to 0 degree, 90 degrees and 180 degrees. Tables 4.47~4.50 list the results of the SSA pitch and SSA yaw in various wave directions and various ship speeds at various sea states based on ITTC and TMA spectrum.

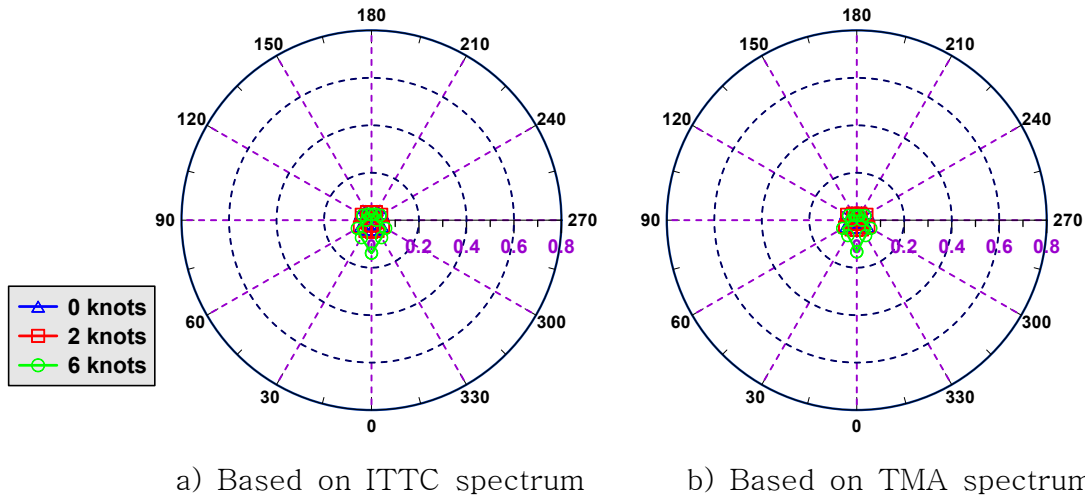


Fig. 4.56 SSA surge in case of sea state 2 in Tongyeong (m)

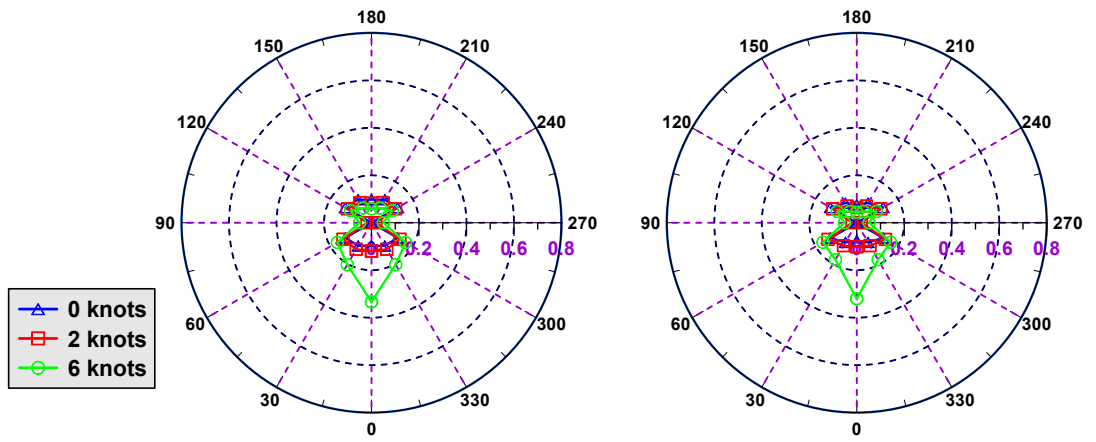


Fig. 4.57 SSA surge in case of sea state 3 in Tongyeong (m)

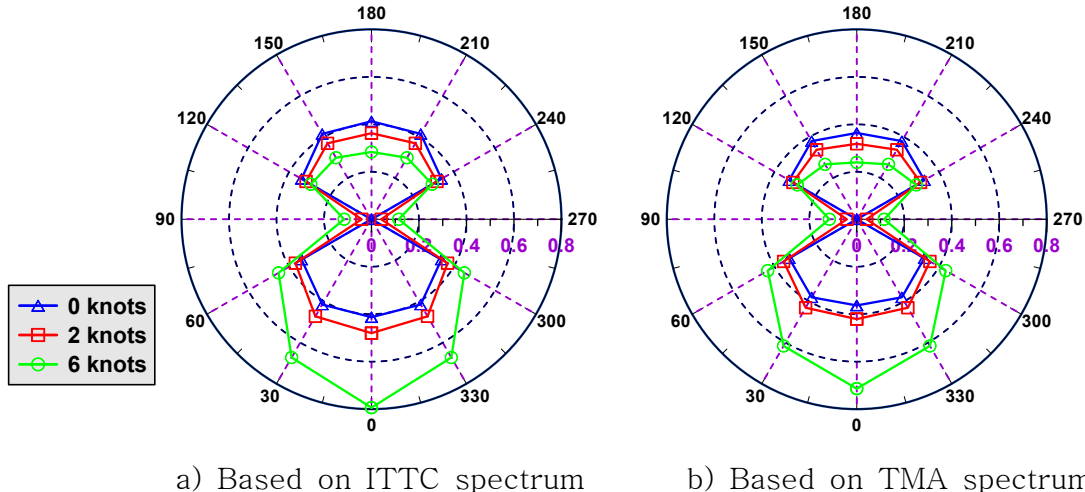


Fig. 4.58 SSA surge in case of sea state 4 in Tongyeong (m)

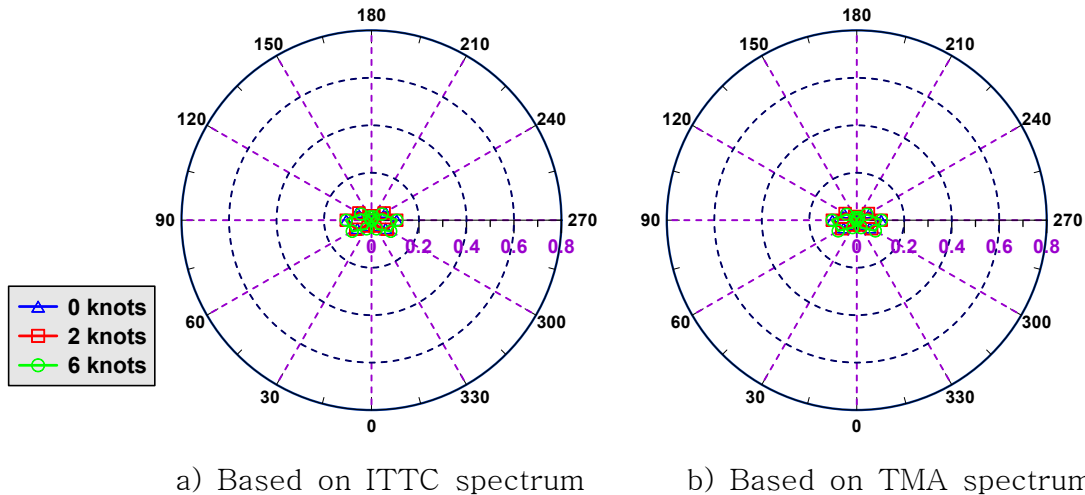


Fig. 4.59 SSA sway in case of sea state 2 in Tongyeong (m)

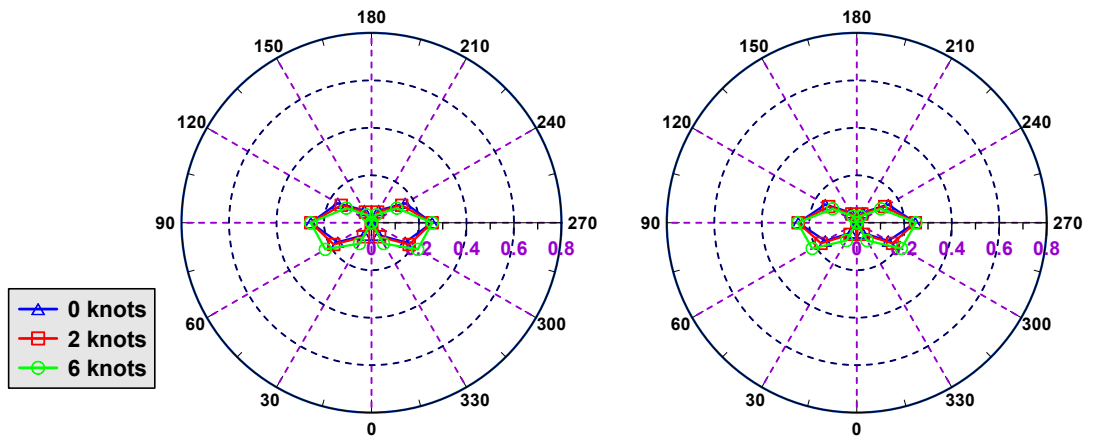


Fig. 4.60 SSA sway in case of sea state 3 in Tongyeong (m)

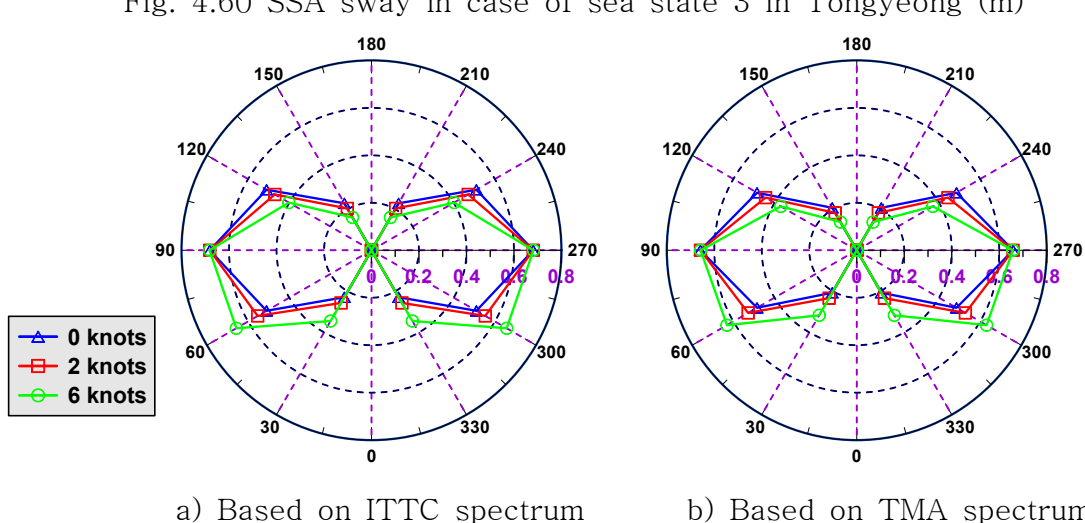


Fig. 4.61 SSA sway in case of sea state 4 in Tongyeong (m)

Table 4.39 SSA value for surge based on ITTC spectrum in Tongyeong (m)

Wave direction [deg.]	0 knots			2 knots			6 knots		
	SS2	SS3	SS4	SS2	SS3	SS4	SS2	SS3	SS4
0	0.040	0.097	0.413	0.050	0.119	0.480	0.139	0.333	0.794
30	0.047	0.112	0.415	0.054	0.129	0.472	0.085	0.204	0.673
60	0.053	0.127	0.340	0.058	0.139	0.370	0.069	0.166	0.452
90	0.000	0.000	0.000	0.008	0.018	0.041	0.021	0.050	0.115
120	0.053	0.127	0.340	0.049	0.117	0.318	0.042	0.101	0.295
150	0.047	0.113	0.415	0.041	0.098	0.370	0.030	0.071	0.299
180	0.040	0.097	0.413	0.035	0.083	0.363	0.024	0.059	0.283

Table 4.40 SSA value for surge based on TMA spectrum in Tongyeong (m)

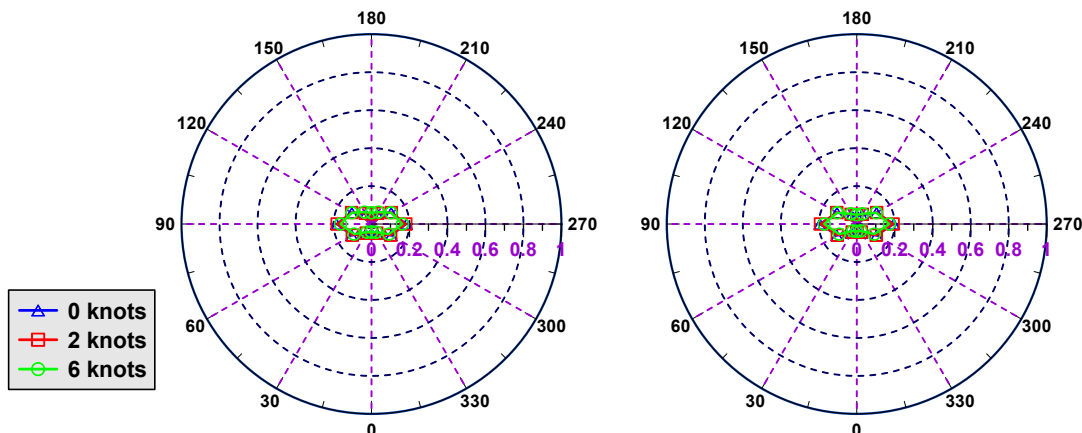
Wave direction [deg.]	0 knots			2 knots			6 knots		
	SS2	SS3	SS4	SS2	SS3	SS4	SS2	SS3	SS4
0	0.032	0.076	0.363	0.042	0.101	0.421	0.133	0.320	0.713
30	0.040	0.095	0.380	0.046	0.112	0.431	0.075	0.180	0.616
60	0.053	0.128	0.329	0.058	0.140	0.356	0.069	0.164	0.433
90	0.000	0.000	0.000	0.008	0.019	0.042	0.022	0.052	0.115
120	0.054	0.128	0.329	0.049	0.117	0.310	0.040	0.095	0.290
150	0.040	0.096	0.380	0.034	0.082	0.338	0.023	0.055	0.267
180	0.032	0.076	0.364	0.027	0.064	0.318	0.018	0.044	0.240

Table 4.41 SSA value for sway based on ITTC spectrum in Tongyeong (m)

Wave direction [deg.]	0 knots			2 knots			6 knots		
	SS2	SS3	SS4	SS2	SS3	SS4	SS2	SS3	SS4
0	0.000	0.000	0.000	0.000	0.000	0.000	0.000	0.000	0.000
30	0.025	0.060	0.228	0.028	0.068	0.256	0.042	0.101	0.344
60	0.068	0.164	0.510	0.076	0.183	0.553	0.094	0.225	0.657
90	0.106	0.255	0.681	0.106	0.255	0.681	0.107	0.256	0.682
120	0.068	0.164	0.510	0.061	0.147	0.470	0.051	0.123	0.402
150	0.025	0.060	0.228	0.022	0.052	0.204	0.016	0.038	0.160
180	0.000	0.000	0.000	0.000	0.000	0.000	0.000	0.000	0.000

Table 4.42 SSA value for sway based on TMA spectrum in Tongyeong (m)

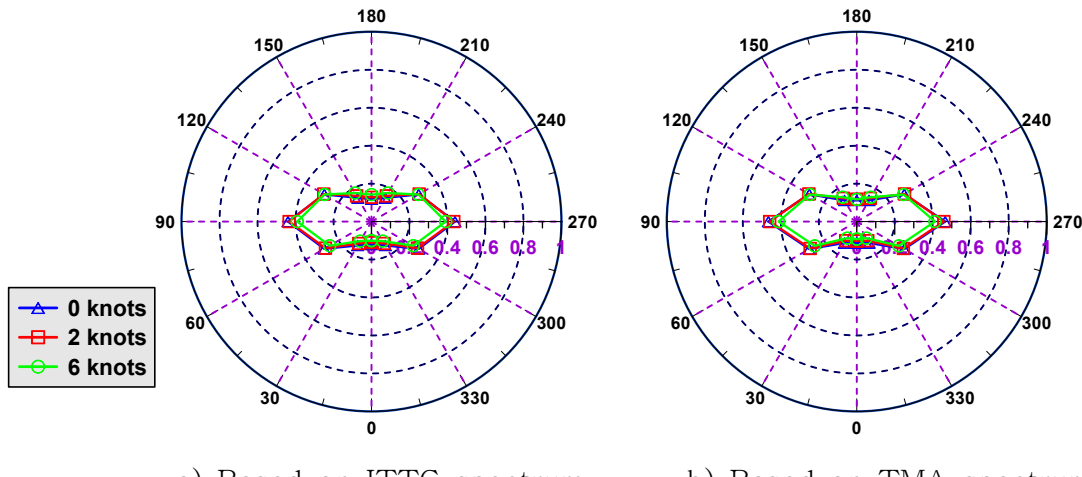
Wave direction [deg.]	0 knots			2 knots			6 knots		
	SS2	SS3	SS4	SS2	SS3	SS4	SS2	SS3	SS4
0	0.000	0.000	0.000	0.000	0.000	0.000	0.000	0.000	0.000
30	0.021	0.049	0.207	0.023	0.056	0.233	0.036	0.087	0.317
60	0.064	0.153	0.485	0.072	0.174	0.528	0.090	0.217	0.631
90	0.103	0.246	0.659	0.103	0.247	0.658	0.104	0.249	0.657
120	0.064	0.153	0.485	0.057	0.136	0.444	0.049	0.117	0.370
150	0.021	0.049	0.206	0.018	0.043	0.182	0.013	0.031	0.137
180	0.000	0.000	0.000	0.000	0.000	0.000	0.000	0.000	0.000



a) Based on ITTC spectrum

b) Based on TMA spectrum

Fig. 4.62 SSA heave in case of sea state 2 in Tongyeong (m)



a) Based on ITTC spectrum

b) Based on TMA spectrum

Fig. 4.63 SSA heave in case of sea state 3 in Tongyeong (m)

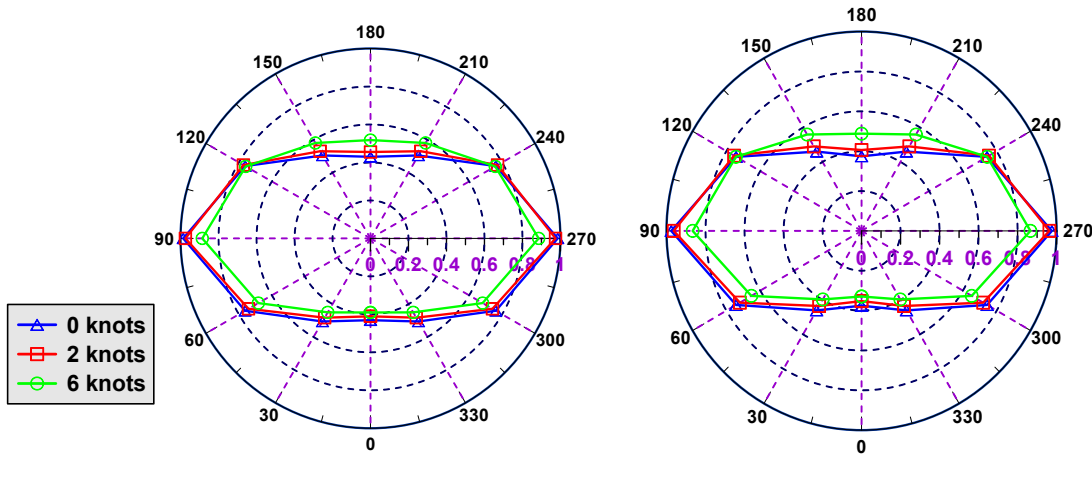


Fig. 4.64 SSA heave in case of sea state 4 in Tongyeong (m)

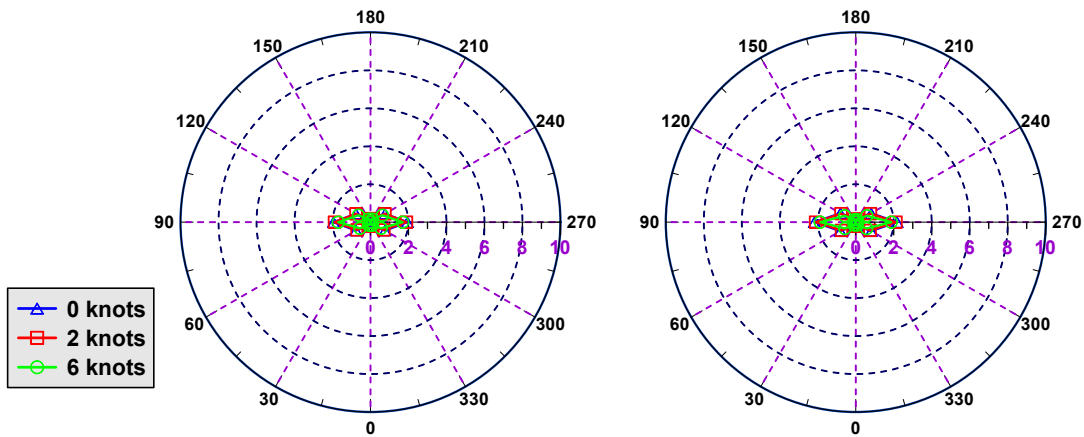


Fig. 4.65 SSA roll in case of sea state 2 in Tongyeong (°)

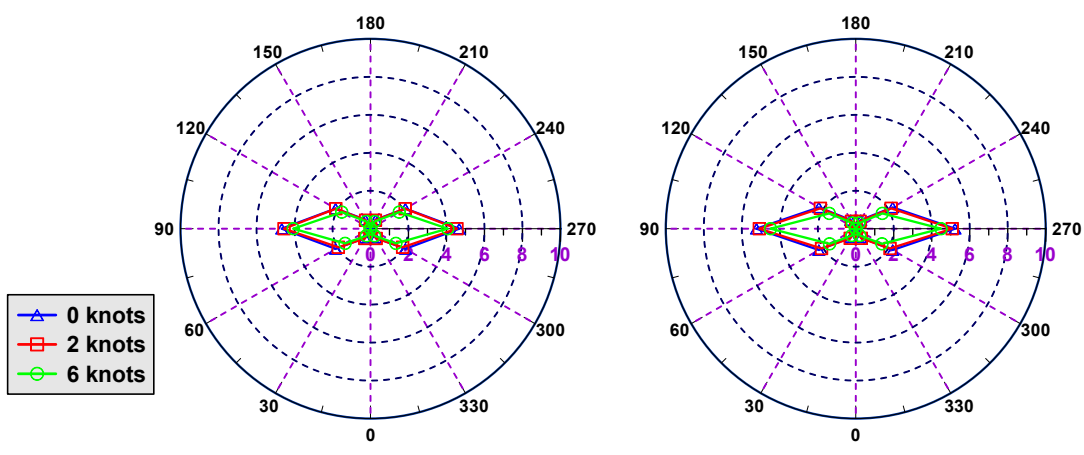


Fig. 4.66 SSA roll in case of sea state 3 in Tongyeong (°)

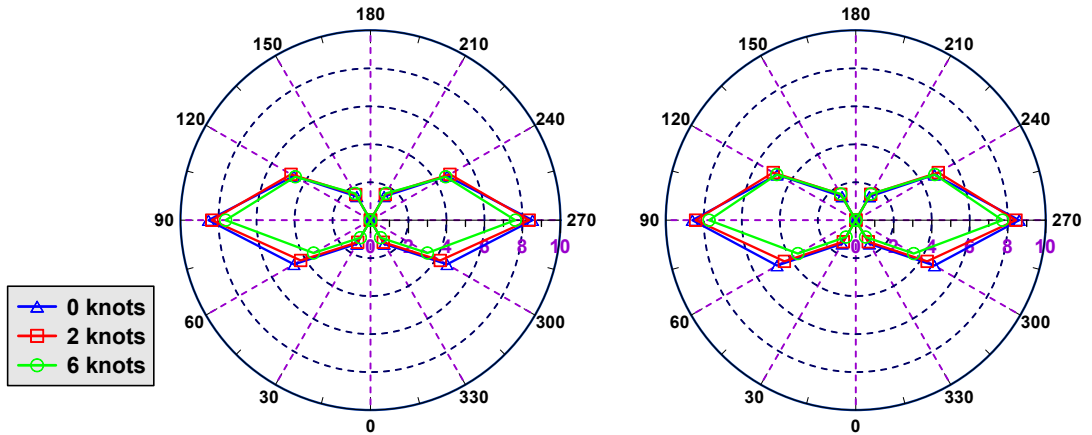


Fig. 4.67 SSA roll in case of sea state 4 in Tongyeong (°)

Table 4.43 SSA value for heave based on ITTC spectrum in Tongyeong (m)

Wave direction [deg.]	0 knots			2 knots			6 knots		
	SS2	SS3	SS4	SS2	SS3	SS4	SS2	SS3	SS4
0	0.050	0.120	0.431	0.046	0.110	0.410	0.042	0.101	0.390
30	0.060	0.145	0.505	0.055	0.133	0.482	0.049	0.119	0.450
60	0.120	0.287	0.762	0.117	0.280	0.742	0.106	0.254	0.681
90	0.183	0.440	0.986	0.181	0.433	0.974	0.163	0.391	0.885
120	0.119	0.287	0.762	0.121	0.290	0.773	0.119	0.285	0.758
150	0.060	0.144	0.504	0.065	0.156	0.530	0.072	0.174	0.580
180	0.050	0.119	0.430	0.053	0.128	0.455	0.059	0.142	0.518

Table 4.44 SSA value for heave based on TMA spectrum in Tongyeong (m)

Wave direction [deg.]	0 knots			2 knots			6 knots		
	SS2	SS3	SS4	SS2	SS3	SS4	SS2	SS3	SS4
0	0.047	0.113	0.376	0.042	0.102	0.352	0.038	0.092	0.329
30	0.054	0.130	0.461	0.048	0.116	0.435	0.042	0.101	0.397
60	0.120	0.289	0.743	0.118	0.283	0.720	0.107	0.256	0.652
90	0.194	0.465	0.976	0.191	0.459	0.963	0.172	0.412	0.866
120	0.120	0.289	0.743	0.121	0.291	0.755	0.119	0.285	0.744
150	0.054	0.129	0.460	0.059	0.142	0.489	0.062	0.148	0.558
180	0.046	0.112	0.374	0.049	0.118	0.406	0.049	0.117	0.488

Table 4.45 SSA value for roll based on ITTC spectrum in Tongyeong (°)

Wave direction [deg.]	0 knots			2 knots			6 knots		
	SS2	SS3	SS4	SS2	SS3	SS4	SS2	SS3	SS4
0	0.000	0.001	0.001	0.000	0.000	0.001	0.000	0.000	0.000
30	0.228	0.546	1.439	0.247	0.594	1.343	0.180	0.431	1.066
60	0.883	2.120	4.652	0.814	1.955	4.244	0.644	1.545	3.459
90	1.946	4.670	8.530	1.896	4.550	8.351	1.695	4.067	7.624
120	0.883	2.120	4.652	0.878	2.108	4.829	0.728	1.747	4.569
150	0.228	0.548	1.439	0.215	0.516	1.557	0.184	0.441	1.629
180	0.000	0.000	0.000	0.000	0.000	0.000	0.000	0.000	0.001

Table 4.46 SSA value for roll based on TMA spectrum in Tongyeong (°)

Wave direction [deg.]	0 knots			2 knots			6 knots		
	SS2	SS3	SS4	SS2	SS3	SS4	SS2	SS3	SS4
0	0.000	0.001	0.001	0.000	0.000	0.000	0.000	0.000	0.000
30	0.218	0.524	1.433	0.244	0.585	1.314	0.172	0.413	1.024
60	0.935	2.244	4.784	0.867	2.082	4.339	0.663	1.592	3.520
90	2.177	5.224	8.603	2.115	5.076	8.430	1.870	4.487	7.722
120	0.935	2.244	4.784	0.895	2.149	5.016	0.672	1.613	4.803
150	0.219	0.526	1.433	0.188	0.451	1.574	0.143	0.343	1.593
180	0.000	0.000	0.000	0.000	0.000	0.000	0.000	0.000	0.001

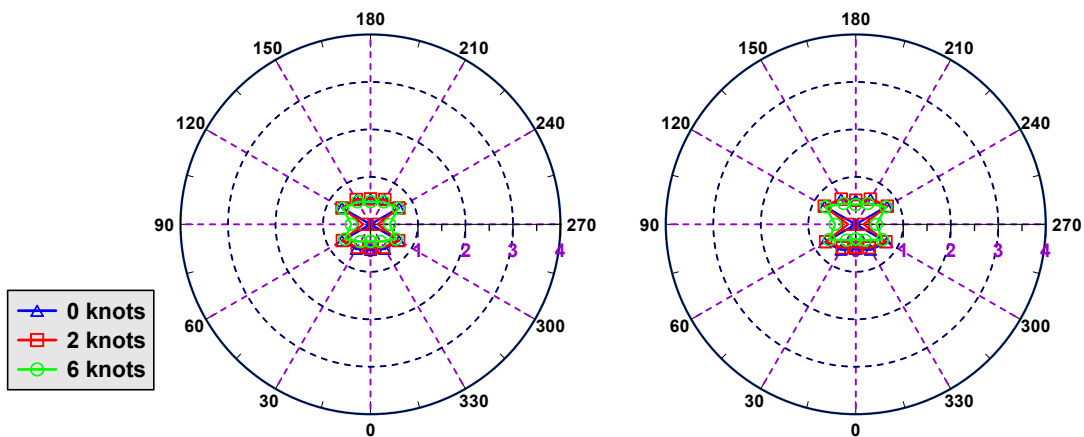
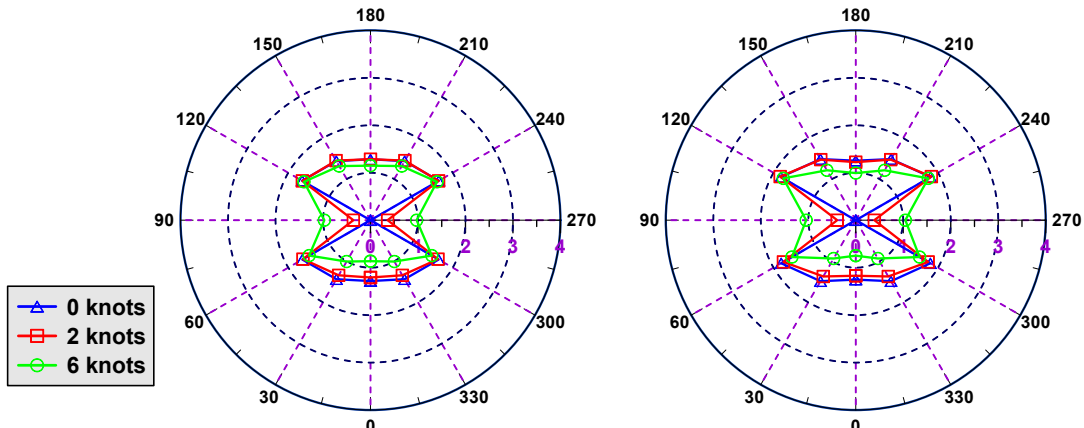
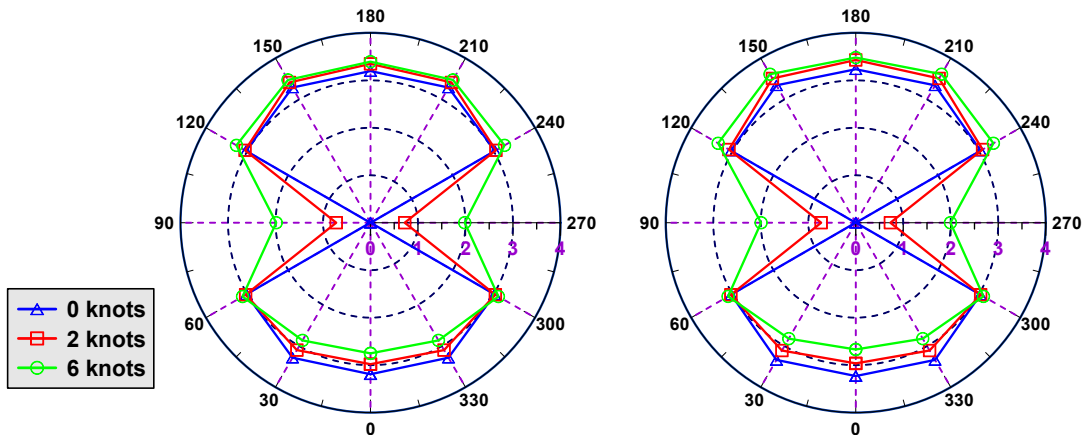


Fig. 4.68 SSA pitch in case of sea state 2 in Tongyeong (°)



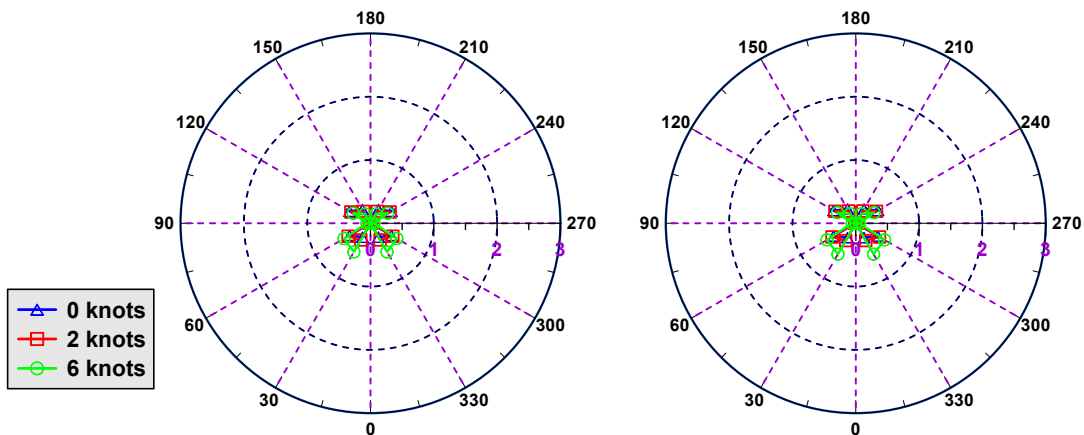
a) Based on ITTC spectrum      b) Based on TMA spectrum

Fig. 4.69 SSA pitch in case of sea state 3 in Tongyeong ( $^{\circ}$ )



a) Based on ITTC spectrum      b) Based on TMA spectrum

Fig. 4.70 SSA pitch in case of sea state 4 in Tongyeong ( $^{\circ}$ )



a) Based on ITTC spectrum      b) Based on TMA spectrum

Fig. 4.71 SSA yaw in case of sea state 2 in Tongyeong ( $^{\circ}$ )

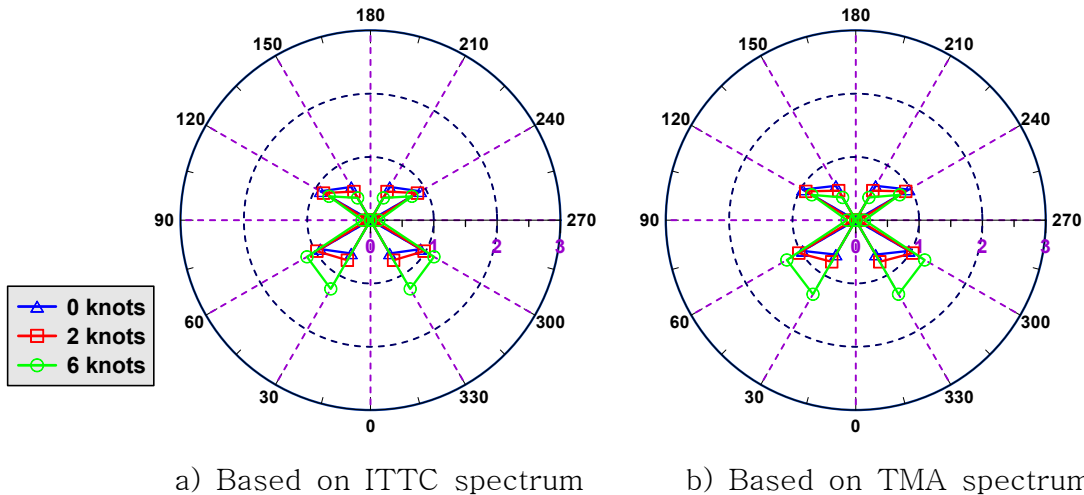


Fig. 4.72 SSA yaw in case of sea state 3 in Tongyeong ( $^{\circ}$ )

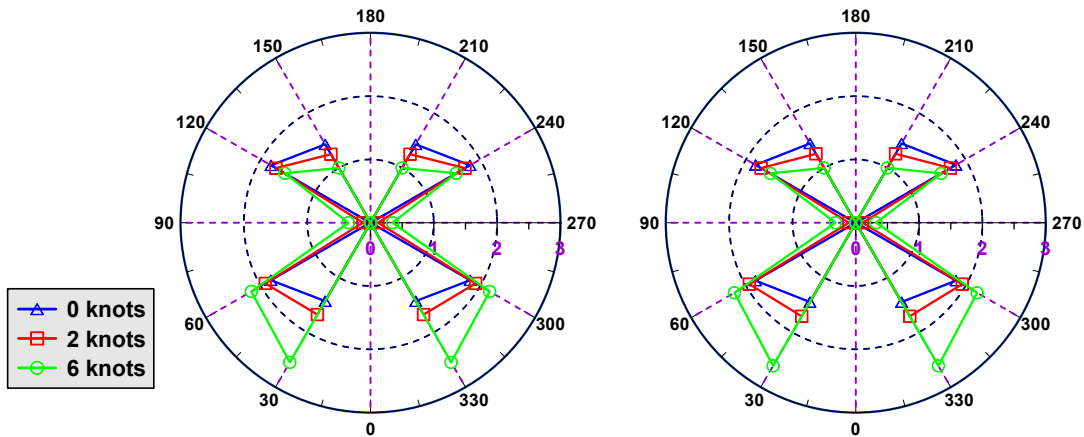


Fig. 4.73 SSA yaw in case of sea state 4 in Tongyeong ( $^{\circ}$ )

Table 4.47 SSA value for pitch based on ITTC spectrum in Tongyeong ( $^{\circ}$ )

Wave direction [deg.]	0 knots			2 knots			6 knots		
	SS2	SS3	SS4	SS2	SS3	SS4	SS2	SS3	SS4
0	0.534	1.282	3.192	0.503	1.208	2.981	0.360	0.864	2.752
30	0.598	1.436	3.284	0.559	1.340	3.099	0.419	1.006	2.863
60	0.691	1.657	3.018	0.684	1.641	3.036	0.622	1.492	3.110
90	0.001	0.003	0.004	0.150	0.361	0.721	0.405	0.972	1.985
120	0.693	1.663	3.025	0.690	1.656	3.050	0.674	1.617	3.259
150	0.599	1.438	3.288	0.604	1.450	3.412	0.549	1.317	3.474
180	0.535	1.284	3.195	0.536	1.286	3.347	0.478	1.148	3.392

Table 4.48 SSA value for pitch based on TMA spectrum in Tongyeong (°)

Wave direction [deg.]	0 knots			2 knots			6 knots		
	SS2	SS3	SS4	SS2	SS3	SS4	SS2	SS3	SS4
0	0.521	1.251	3.230	0.488	1.171	2.964	0.311	0.747	2.671
30	0.618	1.484	3.338	0.570	1.369	3.109	0.388	0.932	2.820
60	0.756	1.813	3.029	0.733	1.759	3.036	0.647	1.552	3.105
90	0.001	0.003	0.004	0.163	0.391	0.729	0.435	1.044	1.994
120	0.758	1.819	3.036	0.766	1.838	3.083	0.735	1.763	3.346
150	0.620	1.487	3.342	0.614	1.473	3.509	0.506	1.214	3.612
180	0.522	1.253	3.233	0.510	1.223	3.428	0.414	0.993	3.479

Table 4.49 SSA value for yaw based on ITTC spectrum in Tongyeong (°)

Wave direction [deg.]	0 knots			2 knots			6 knots		
	SS2	SS3	SS4	SS2	SS3	SS4	SS2	SS3	SS4
0	0.000	0.000	0.000	0.000	0.000	0.000	0.000	0.000	0.000
30	0.253	0.607	1.431	0.304	0.730	1.676	0.522	1.254	2.548
60	0.381	0.914	1.817	0.407	0.978	1.918	0.482	1.158	2.173
90	0.002	0.004	0.005	0.019	0.046	0.118	0.055	0.133	0.348
120	0.380	0.912	1.814	0.357	0.857	1.724	0.315	0.755	1.562
150	0.253	0.607	1.430	0.218	0.522	1.250	0.169	0.406	0.999
180	0.000	0.000	0.000	0.000	0.000	0.000	0.000	0.000	0.000

Table 4.50 SSA value for yaw based on TMA spectrum in Tongyeong (°)

Wave direction [deg.]	0 knots			2 knots			6 knots		
	SS2	SS3	SS4	SS2	SS3	SS4	SS2	SS3	SS4
0	0.000	0.000	0.000	0.000	0.000	0.000	0.000	0.000	0.000
30	0.262	0.628	1.448	0.316	0.759	1.707	0.563	1.351	2.611
60	0.404	0.969	1.829	0.433	1.039	1.942	0.524	1.257	2.213
90	0.001	0.004	0.005	0.020	0.049	0.108	0.058	0.138	0.321
120	0.403	0.967	1.826	0.379	0.911	1.727	0.334	0.802	1.557
150	0.261	0.627	1.446	0.225	0.540	1.257	0.173	0.415	1.000
180	0.000	0.000	0.000	0.000	0.000	0.000	0.000	0.000	0.000

## 5. Conclusion

This study performed seakeeping analysis of the garbage barge in waves using numerical simulation and experiment method. The concluding remarks as follows:

- The numerical simulation was performed to predict motion RAO and phase of the full-scale vessel in regular waves using 3D panel method of Ansys AQWA at various wave directions and speed conditions. The roll damping coefficients were estimated using roll decay test results at various ship speed conditions to correct the roll amplitude at the resonance frequency. The effects of wave direction and ship speed on ship motion were examined.
- The model test in the 3D wave tank was performed in regular waves to evaluate the seakeeping performance. Based on the pre-test, it was confirmed that the mass distribution of the model ship was reasonably adjusted to the required value. Then, decay test was conducted for different spring stiffnesses to select a reasonable spring for the model test. In addition, decay tests with mooring system for various speed conditions were performed to analyze the effect of unnecessary spring effect due to the speed. Moreover, the model test was conducted to measure the wave force, vertical acceleration, and ship motion. The analysis method for wave force, vertical acceleration, and ship motion was summarized from the model test data. Then, the effect of wave direction and ship speed to wave force, vertical accelerations and ship motion were discussed. The comparison of the ship motion between numerical simulation and experiment method proved the accuracy of the model test. The effect of spring stiffness was investigated after implementing various kinds of spring. It proved that the spring stiffness significantly affects on horizontal motion, and slightly affects on vertical motion.
- The seakeeping performance in irregular waves was estimated for sea state 2, 3, and 4 considering ITTC and TMA spectrum at Sinan and Tongyeong based on motion RAO results in regular waves. The RMS and SSA were calculated at various wave directions and speed conditions.

The similarity between ITTC and TMA spectrum at Sinan area gives similar results of RMS and SSA values for each sea state, wave direction and ship speed. However, TMA spectrum is smaller than ITTC spectrum at Tongyeong. This means RMS and SSA calculated by TMA spectrum is smaller than calculated by ITTC spectrum for each sea state, wave direction and ship speed.

## 6. Reference

- [1] ITTC. (2014). ITTC – Recommended Procedures and Guidelines–Seakeeping Experiments. 27th ITTC Seakeeping Committee, 1–22.
- [2] Irkal, M.A.R., Nallayarasu, S., Bhattacharyya, S.K. (2019). Numerical prediction of roll damping of ships with and without bilge keel. Ocean Engineering, 179(August 2018), 226–245. <https://doi.org/10.1016/j.oceaneng.2019.03.027>
- [3] Rodríguez, C.A., Ramos, I.S., Esperança, P.T.T., Oliveira, M.C. (2020). Realistic estimation of roll damping coefficients in waves based on model tests and numerical simulations. Ocean Engineering, 213(July), 107664. <https://doi.org/10.1016/j.oceaneng.2020.107664>.
- [4] Igbadumhe, J.F., Sallam, O., Fürth, M., Feng, R. (2020). Experimental Determination of Non-Linear Roll Damping of an FPSO Pure Roll Coupled with Liquid Sloshing in Two-Row Tanks. Journal of Marine Science and Engineering, 8(8). <https://doi.org/10.3390/JMSE8080582>
- [5] Jeon, M., Mai, T.L., Yoon, H.K., Kim, D.J. (2021). Estimation of wave-induced steady force using system identification , model tests , and numerical approach. Ocean Engineering, 233(April), 109207. <https://doi.org/10.1016/j.oceaneng.2021.109207>
- [6] Seo, M.G., Nam, B.W., Kim, Y.G. (2018). Numerical evaluation of ship maneuvering performance in waves. Proceedings of the International Conference on Offshore Mechanics and Arctic Engineering – OMAE, 7A, 1–10. <https://doi.org/10.1115/OMAE201877208>
- [7] Kim, D.J., Yun, K., Park, J.Y., Yeo, D.J., Kim, Y.G. (2019). Experimental investigation on turning characteristics of KVLCC2 tanker in regular waves. Ocean Engineering, 175(February), 197–206. <https://doi.org/10.1016/j.oceaneng.2019.02.011>
- [8] Lloyd, A.R.J.M. (1998). Seakeeping Ship Behaviour in Rough Weather
- [9] Goda, Y. (2010). Random Seas and Design of Maritime Structures, World Scientific
- [10] Lewis, E.V. (1988). Principle of Naval Architecture, vol-I, Stability and Strength 1988, Published by The society of Naval Architects and Marine Engineers, Editor.